ADVANCES IN MOLECULAR TARGETED THERAPIES OF UROLOGIC CANCERS

EDITED BY: Bianca Nitzsche, Friedemann Zengerling and Michael Höpfner
PUBLISHED IN: Frontiers in Oncology

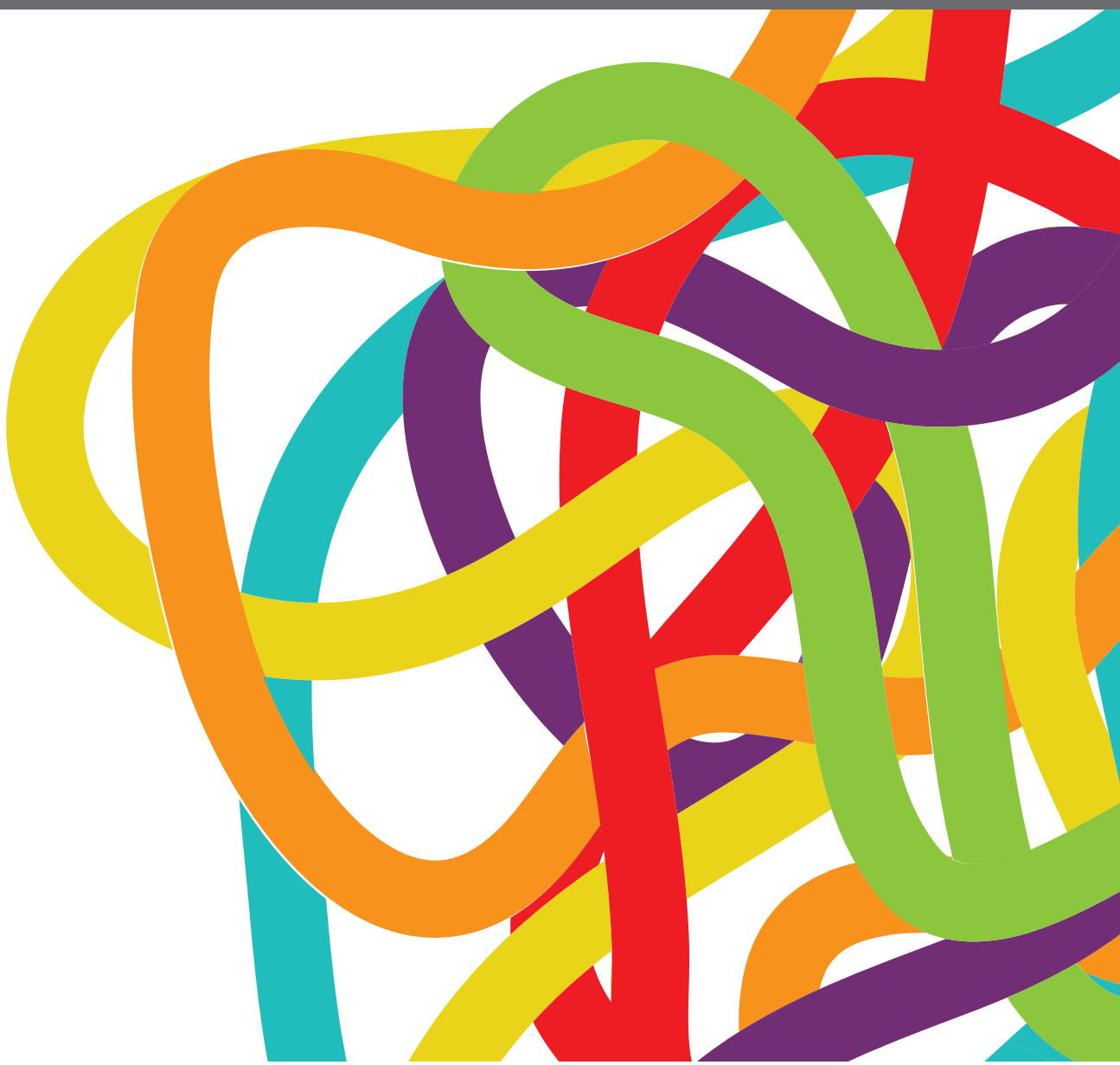

frontiers Research Topics

ISSN 1664-8714
ISBN 978-2-83250-699-8
DOI 10.3389/978-2-83250-699-8

About Frontiers

Frontiers is more than just an open-access publisher of scholarly articles: it is a pioneering approach to the world of academia, radically improving the way scholarly research is managed. The grand vision of Frontiers is a world where all people have an equal opportunity to seek, share and generate knowledge. Frontiers provides immediate and permanent online open access to all its publications, but this alone is not enough to realize our grand goals.

Frontiers Journal Series

The Frontiers Journal Series is a multi-tier and interdisciplinary set of open-access, online journals, promising a paradigm shift from the current review, selection and dissemination processes in academic publishing. All Frontiers journals are driven by researchers for researchers; therefore, they constitute a service to the scholarly community. At the same time, the Frontiers Journal Series operates on a revolutionary invention, the tiered publishing system, initially addressing specific communities of scholars, and gradually climbing up to broader public understanding, thus serving the interests of the lay society, too.

Dedication to Quality

Each Frontiers article is a landmark of the highest quality, thanks to genuinely collaborative interactions between authors and review editors, who include some of the world's best academicians. Research must be certified by peers before entering a stream of knowledge that may eventually reach the public - and shape society; therefore, Frontiers only applies the most rigorous and unbiased reviews.
Frontiers revolutionizes research publishing by freely delivering the most outstanding research, evaluated with no bias from both the academic and social point of view. By applying the most advanced information technologies, Frontiers is catapulting scholarly publishing into a new generation.

What are Frontiers Research Topics?

Frontiers Research Topics are very popular trademarks of the Frontiers Journals Series: they are collections of at least ten articles, all centered on a particular subject. With their unique mix of varied contributions from Original Research to Review Articles, Frontiers Research Topics unify the most influential researchers, the latest key findings and historical advances in a hot research area! Find out more on how to host your own Frontiers Research Topic or contribute to one as an author by contacting the Frontiers Editorial Office: frontiersin.org/about/contact

ADVANCES IN MOLECULAR TARGETED THERAPIES OF UROLOGIC CANCERS

Topic Editors:
Bianca Nitzsche, Charité Universitätsmedizin Berlin, Germany
Friedemann Zengerling, Ulm University Medical Center, Germany
Michael Höpfner, Charité Universitätsmedizin Berlin, Germany

The authors declare that the research was conducted in the absence of any commercial or financial relationships that could be construed as a potential conflict of interest.

Citation: Nitzsche, B., Zengerling, F., Höpfner, M., eds. (2022). Advances in Molecular Targeted Therapies of Urologic Cancers. Lausanne: Frontiers Media SA. doi: 10.3389/978-2-83250-699-8

Table of Contents

frontiers | Frontiers in Oncology

TYPE Editorial
PUBLISHED 19 October 2022
DOI 10.3389/fonc.2022.1062015

OPEN ACCESS

EDITED AND REVIEWED BY
Ronald M Bukowski,
Cleveland Clinic, United States

*CORRESPONDENCE
Bianca Nitzsche
bianca.nitzsche@charite.de
Michael Höpfner
michael.hoepfner@charite.de

SPECIALTY SECTION
This article was submitted to Genitourinary Oncology, a section of the journal Frontiers in Oncology

RECEIVED 05 October 2022
ACCEPTED 06 October 2022
PUBLISHED 19 October 2022

CITATION
Nitzsche B and Höpfner M (2022) Editorial: Advances in molecular targeted therapies of urologic cancers. *Front. Oncol.* 12:1062015. doi: 10.3389/fonc.2022.1062015

Editorial: Advances in molecular targeted therapies of urologic cancers

Bianca Nitzsche[1,2*] and Michael Höpfner[1,2*]

[1]Charité – Universitätsmedizin Berlin, Berlin, Germany, [2]HumboldtUniversität zu Berlin, Institute for Physiology, Berlin, Germany

KEYWORDS

molecular targeted therapy, bladder cancer (BCa), prostate cancer, circRNA, kidney cancer

Editorial on the Research Topic
Advances in molecular targeted therapies of urologic cancers

Urologic cancer is a generic term for distinct malignancies of the urogenital tract comprising of solid tumors of different organs such as bladder, prostate, kidney, urothelium and testicles. Except for testicular cancer rather showing an increased prevalence and incidence in younger adults, most urologic cancers develop in the older male population. All types of urologic cancers represent a problem of major concern and some of them (e.g. prostate cancer) rank among the three most frequent cancers, worldwide and account for a large number of cancer related deaths per year (1). And even more alarming the incidence of urologic cancer is rising due to demographic reasons such as population growth and aging but also due to environmental factors, which have been linked to the development and growth of single urologic cancers, too (e.g. kidney, prostate, bladder) (2).

In the past decade, the understanding of dysregulated pathways in urologic cancers as well as the identification of potential biomarkers helped to identify new targets and pathways for novel therapeutic approaches. In this respect new immunomodulatory substances, antiangiogenic agents, growth factor receptor inhibitors or the targeting of epigenetically modulated signaling pathways have become interesting and promising starting points for future medical treatment of urologic cancer. Besides being more effective, targeted approaches also aim at reducing the severe short- and long-term side effects known for conventional chemo- and radiotherapies.

The idea of the Research Topic "*Advances in molecular targeted therapies of urologic cancers*" was to bring together experts in the field reporting on recent (pre-)clinical findings and achievements and to give an overview on possible therapeutic developments and biomarker analysis in urologic cancer research.

Prostate cancer

Prostate Cancer (PCa) is the 2nd most diagnosed cancer in men over the last years with more than 1.4 million new cases worldwide in the year 2020 and it is also the 2nd leading cause of cancer death in men for incidence (1, 3). Usually, radical prostatectomy is the main treatment option for localized PCa, and the prognosis is generally favorable. However, in metastatic diseases and in case of a postoperative biochemical recurrence or the development of castration-resistant PCa the outcome for patients remains to be poor (4). The Gleason score is the main criteria for histological staging and for the prediction of outcomes in PCA patients. The main biomarker currently used for the diagnosis of PCa is prostate-specific antigen (PSA) but there is no consensus about the optimal concentration to assess patients prognosis (5). Here novel marker may help to improve the treatment strategy and survival in the affected patients. Circular RNAs (circRNAs) are a novel class of non-coding RNAs (ncRNAs) which have been found to show extensive dysregulation in a handful of human diseases including cancers and their role and their potential has been intensively reviewed and discussed by Taheri et al.. In their review they listed relevant findings about circRNAs that are up- or downregulated and with diagnostic or prognostic values in PCa. Here for circRNA such as circ-ITCH and circMBOAT2, a correlation has been recognized between circRNA expression levels and prognosis in PCa patients. Further studies are needed to determine precisely which circRNA or which set of circRNAs could be used for PCa diagnosis and prognosis.

More targeted treatment options and the improvement of early detection and prognostic values would facilitate reductions in prostate cancer related deaths. Thereby the need to update existing therapy options and invest in the search for novel alternative therapies remains to be a challenge in the future. In line with that, the review "*From Therapy Resistance to Targeted Therapies in Prostate Cancer*" of Moreira-Silva et al. summarized the current state of targeted therapies in PCa and discussed the role and the mechanisms underlying therapy resistance in PCa. They also suggest that selective drug targeting, either alone or in combination with standard treatment options, might improve therapeutic sensitivity of resistant PCa. For castration resistant prostate cancer in non-metastatic or metastatic variants, the therapy options are limited, and further improvements are urgently needed. Taken into account that histone deacetylases are upregulated in many cancer cell types including prostate cancer, molecules that inhibits these epigenetic enzymes have the potential to overcome drug resistance in prostate cancer and promising clinical trials are currently ongoing (6).

Bladder cancer

Bladder cancer is a common type of cancer that originates in the urinary tract. According to Global Cancer Risk, this cancer caused a total of 570,000 new cases and 200,000 deaths worldwide in 2020 (1). Clinically, 30% of bladder cancer patients present with invasive tumors when initially diagnosed. Even if curative surgery is available, these patients have a 5-year survival rate of only 50%. Therefore, new efforts are needed to investigate the biological causes of bladder cancer progression, and further develop better diagnostic and therapeutic modalities. The study by Dong et al. explored the role of the transmembrane glycoprotein receptor neuropilin.1 (NRP1) in bladder cancer and provided evidence for specific NRP1 expression patterns and could show that inhibiting NRP1 expression could promote apoptosis and suppress proliferation, angiogenesis, migration, and invasion of BC cells, implying the NRP1 as an potential target in BD therapy. In the last years various novel antitumor treatments have been developed for various cancer entities as well as bladder cancer and immunotherapeutic approaches are among the most promising. Immunotherapy aims to activate the immune system to target uncontrolled cancer cell proliferation within the body. Accordingly, two articles in the present Research Topic deal with the immune characteristics of bladder cancer cells as well as the evaluation of important side effects of immunotherapy for bladder cancer. Both adding new and intriguing aspects and information on this emerging topic (Zhu et al.; Lou et al.).

In conclusion, several pathways have been explored as potential targets for enhanced urologic cancer treatment in the future. The present Research Topic aimed adding new aspects to the developmental status of targeted therapies, especially in prostate and bladder cancer and brought forth a Research Topic of intriguing studies on the suitability of novel single agents or combination therapies to fight urologic cancers.

Author contributions

Both authors have made a substantial, direct, and intellectual contribution to the work and approved it for publication.

Conflict of interest

The authors declare that the research was conducted in the absence of any commercial or financial relationships that could be construed as a potential conflict of interest.

Publisher's note

References

1. Sung H, Ferlay J, Siegel RL, Laversanne M, Soerjomataram I, Jemal A, et al. Global cancer statistics 2020: GLOBOCAN estimates of incidence and mortality worldwide for 36 cancers in 185 countries. *CA Cancer J Clin* (2021) 71:209–49. doi: 10.3322/caac.21660

2. Dy GW, Gore JL, Forouzanfar MH, Naghavi M, Fitzmaurice C. Global burden of urologic cancers, 1990–2013. *Eur Urol* (2017) 71:437–46. doi: 10.1016/j.eururo.2016.10.008

3. Siegel RL, Miller KD, Fuchs HE, Jemal A. Cancer statistics, 2022. *CA Cancer J Clin* (2022) 72:7–33. doi: 10.3322/caac.21708

4. Hull GW, Rabbani F, Abbas F, Wheeler TM, Kattan MW, Scardino PT. Cancer control with radical prostatectomy alone in 1,000 consecutive patients. *J Urol* (2002) 167:528–34. doi: 10.1016/S0022-5347(01)69079-7

5. Asso RN, Degrande FAM, Fernandes da Silva JL, Leite ETT. Postoperative radiotherapy in prostate cancer: When and how? – an update review. *Cancer* (2022) 26:742–8. doi: 10.1016/j.canrad.2021.10.009

6. Biersack B, Nitzsche B, Höpfner M. HDAC inhibitors with potential to overcome drug resistance in castration-resistant prostate cancer. *Cancer Drug Resist Alhambra Calif* (2022) 5:64–79. doi: 10.20517/cdr.2021.105

frontiers in Oncology

ORIGINAL RESEARCH
published: 19 May 2021
doi: 10.3389/fonc.2021.661431

LINC00467 Promotes Prostate Cancer Progression *via* M2 Macrophage Polarization and the miR-494-3p/STAT3 Axis

Hao Jiang[1,2], *Wen Deng*[1,2], *Ke Zhu*[1,2], *Zhenhao Zeng*[1,2], *Bing Hu*[1,2], *Zhengtao Zhou*[2], *An Xie*[2], *Cheng Zhang*[1], *Bin Fu*[1,2], *Xiaochen Zhou*[1,2*] and *Gongxian Wang*[1,2*]

[1] *Department of Urology, The First Affiliated Hospital of Nanchang University, Nanchang, China,* [2] *Jiangxi Institute of Urology, Nanchang, China*

OPEN ACCESS

Edited by:
Bianca Nitzsche, Charité—Universitätsmedizin Berlin, Germany

Reviewed by:
Alessandro Tafuri, University of Verona, Italy
Russell Pachynski, Washington University School of Medicine in St. Louis, United States

***Correspondence:**
Gongxian Wang
wanggx-mr@126.com
Xiaochen Zhou
mo_disc@126.com

Specialty section:
This article was submitted to Genitourinary Oncology, a section of the journal Frontiers in Oncology

Received: *30 January 2021*
Accepted: *23 April 2021*
Published: *19 May 2021*

Citation:
Jiang H, Deng W, Zhu K, Zeng Z, Hu B, Zhou Z, Xie A, Zhang C, Fu B, Zhou X and Wang G (2021) LINC00467 Promotes Prostate Cancer Progression via M2 Macrophage Polarization and the miR-494-3p/STAT3 Axis. Front. Oncol. 11:661431. doi: 10.3389/fonc.2021.661431

Background: The long non-coding RNA LINC00467 plays a vital role in many malignancies. Nevertheless, the role of LINC00467 in prostate carcinoma (PC) is unknown. Herein, we aimed to explore the mechanism by which LINC00467 regulates PC progression.

Methods: We used bioinformatics analyses and RT-qPCR to investigate the expression of LINC00467 in PC tissues and cells. The function of LINC00467 in the progression of PC was confirmed by loss-of-function experiments. PC cell proliferation was assessed by CCK-8 and EdU assays. The cell cycle progression of PC cells was examined by flow cytometry. Moreover, Transwell assays were used to investigate the migration and invasion of PC cells. Western blot assays were used to detect the expression of factors associated with epithelial–mesenchymal transition. The interactions of LINC00467 with prostate cancer progression and M2 macrophage polarization were confirmed by RT-qPCR. The subcellular localization of LINC00467 was investigated *via* the fractionation of nuclear and cytoplasmic RNA. Bioinformatics data analysis was used to predict the correlation of LINC00467 expression with miR-494-3p expression. LINC00467/miR-494-3p/STAT3 interactions were identified by using a dual-luciferase reporter system. Finally, the influence of LINC00467 expression on PC progression was investigated with an *in vivo* nude mouse model of tumorigenesis.

Results: We established that LINC00467 expression was upregulated in PC tissues and cells. Downregulated LINC00467 expression inhibited PC cell growth, cell cycle progression, migration, and invasion. Downregulated LINC00467 expression similarly inhibited PC cell migration *via* M2 macrophage polarization. Western blot analysis showed that LINC00467 could regulate the STAT3 pathway. We established that LINC00467 is mainly localized to the cytoplasm. Bioinformatics analysis and rescue experiments indicated that LINC00467 promotes PC progression *via* the miR-494-3p/STAT3 axis. Downregulated LINC00467 expression was also able to suppress PC tumor growth *in vivo*.

Conclusions: Our study reveals that LINC00467 promotes prostate cancer progression *via* M2 macrophage polarization and the miR-494-3p/STAT3 axis.

Keywords: LINC00467, prostate cancer, M2 macrophage polarization, miR-494-3p, STAT3

INTRODUCTION

Prostate cancer (PC) is one of the most common tumors of the urinary system. According to the latest statistics from the National Center for Health Statistics (NCHS), the incidence and mortality of prostate cancer in the United States are predicted to be 191,930 and 33,330, respectively, in 2020 (1). Despite the rapid development of approaches for the diagnosis and treatment of prostate cancer, the poor treatment effect and high prevalence rate are still serious challenges in the clinic (2). Therefore, the identification of new potential biomarkers and therapeutic targets is crucial for the improvement of alternative therapies.

Recently, a large number of ncRNAs (non-coding RNAs) have been identified, and these ncRNAs are important components of the complex regulatory network of the body. LncRNAs (long non-coding RNAs), a class of RNAs with lengths greater than 200 nts, do not encode proteins but regulate the expression of genes at the RNA level in a variety of ways (3). Researchers have recognized that functional lncRNAs participate in a variety of physiological and pathological processes (4, 5), particularly oncogenesis, because these lncRNAs can affect gene expression by sponging microRNAs and mRNAs in various tumor types (6). For example, PCA3 (7), PCGEM1 (8) and PlncRNA-1 (9) are known to be overexpressed in prostate cancer and to promote cancer progression.

In the present study, we showed that LINC00467 expression was upregulated in human prostate cancer tissues and cell lines. However, the function of LINC00467 in PC, as well as the underlying mechanism, remains unknown. Therefore, we investigated the function of LINC00467 in PC progression and its underlying mechanism, providing a new theoretical basis for the treatment of PC.

MATERIALS AND METHODS

Prostate Cancer Cell Lines and Clinical Tissues

The human prostate cancer (PC) cell lines VCaP, LNCaP, 22RV1, PC3, and DU145 and the normal human prostate epithelial cell lines HrPEC and RWPE-1 were purchased from American Type Culture Collection (ATCC, www.atcc.rog, USA). LNCaP, 22RV1, DU145 and THP-1 cells were cultured in RPMI-1640 (Gibco, USA), PC3 cells were cultured in F12K medium (Gibco), VCaP and RWPE1 cells were cultured in DMEM (Gibco, USA), and HrPEC cells were cultured in ATCC prostatic primary epithelial cell culture medium. Ten percent fetal bovine serum (FBS, Gibco) and 1% penicillin streptomycin (Solarbio, China) were added to the medium, and the cells were cultured in a humidified environment at 37°C and 5% CO_2. THP-1 monocytes were treated with 100 nM phorbol 12-myristate 13-acetate (PMA) (Sigma-Aldrich, USA) for 24 h to induce their differentiation into macrophages. To obtain conditioned media (CM) from the PC cells, the indicated PC cells were grown to 70–80% confluence, washed three times with FBS-free medium, and cultured in fresh FBS-free medium for another 72 h. Next, the supernatants were filtered through 0.22-μm filters and collected for use as CM.

From September 2017 to June 2019, we collected clinical tissues from 22 PC patients undergoing prostatectomy in the urology department of the First Affiliated Hospital of Nanchang University. Prostate tumor tissues and paired adjacent normal tissues were collected. After collection, all the samples were immediately stored in a −80°C freezer until further treatment.

Cell Transfection

LINC00467 siRNA, miR-494-3p inhibitor and miR-494-3p mimics were designed and synthesized by RiboBio (Guangzhou, China). The sequences of the siRNAs were as follows: siLINC00467-1#: 5'-ACACTAAGTTCAGACTCAT-3'; siLINC00467-2#: 5'-TCAGACTCATGAAACCAAT-3'. The siRNAs were transfected into THP-1, 22RV1 and DU145 cells using Lipofectamine 3000 according to the manufacturer's instructions. The sequence of siLINC00467-2# was used for lentivirus transfection. shLINC00467 and shNC (negative control) vectors were transfected with lentivirus (Hanbio, Shanghai, China). The lentiviral vectors were added to 22RV1 and DU145 culture media. After 72 h, 22RV1 and DU145 cells carrying the constructs were selected using puromycin (selection concentration, 6 μg/ml; maintenance concentration, 2 μg/ml).

RNA Extraction and Real-Time Quantitative RT-PCR (RT-qPCR) Analysis

Total RNA was extracted and reverse transcribed into cDNA using the RNeasy Mini kit (Qiagen, USA) and the First-Strand cDNA Synthesis kit (Qiagen, USA) according to the manufacturer's instructions. RT-qPCR was performed using a SYBR Real-Time PCR kit (Qiagen, USA) under the following conditions: 95°C for 2 min, followed by 40 cycles of 95°C for 5 s and 60°C for 10 s. Relative fold expression was calculated using the $2-\Delta\Delta Ct$ method. Each analysis was performed in triplicate. In addition, β-actin was used as an internal reference gene. The primers used in the study are listed in **Table 1**.

CCK8 Assay

Cell Counting Kit 8 (CCK-8) assays were used to analyse the proliferation of lentivirus-transfected DU145 and 22RV1 cells. After transfection, the cells in the logarithmic stage of growth (DU145 cells, 6×10^3 cells/well; 22RV1 cells, 5×10^4 cells/well) were seeded in a 96-well culture plate. After 1 day, 2 days, 3 days, and 4 days, 100 μl RPMI-1640 medium and 10 μl CCK8 solution

TABLE 1 | Primers used for RT-qPCR.

Genes	Forward (5′-3′)	Reverse (5′-3′)
β-actin	CATGTACGTTGCTATCCAGGC	CTCCTTAATGTCACGCACGAT
LINC00467	TTCGGTCCGGTTGAGGTTGT	AAACCTCCCTGCCATGTTGGA
STAT3	ACCAGCAGTATAGCCGCTTC	GCCACAATCCGGGCAATCT
U6	AAAGCAAATCATCGGACGACC	GGGGTCGTTGATGGCAACA
MALAT1	GCCAAATTGAGACAATTTCAGC	CGAATTCAGGGTGAGGAAGTA
CD86	CTGCTCATCTATACACGGTTACC	GGAAACGTCGTACAGTTCTGTG
INOS	TCATCCGCTATGCTGGCTAC	CCCGAAACCACTCGTATTTGG
CD163	TTTGTCAACTTGAGTCCCTTCAC	TCCCGCTACACTTGTTTTCAC
MRC1	GGGTTGCTATCACTCTCTATGC	TTTCTTGTCTGTTGCCGTAGTT
ARG1	TGGACAGACTAGGAATTGGCA	CCAGTCCGTCAACATCAAAACT
IL10	TCAAGGCGCATGTGAACTCC	GATGTCAAACTCACTCATGGCT
VEGF	AGGGCAGAATCATCACGAAGT	AGGGTCTCGATTGGATGGCA

were added to each well. After the cells were incubated at 37°C for 2 h, the OD value was measured at 450 nm by a microplate system. Each experiment was repeated three times.

Ethynyl Deoxyuridine (EdU) Assay

A 5-ethynyl-2'-deoxyuridine (EdU) detection kit (RiboBio, Guangzhou, China) was used to assess the proliferation of lentivirus-transfected DU145 and 22RV1 cells according to the manufacturer's guidelines. Transfected DU145 and 22RV1 cells in the logarithmic stage of growth (DU145 cells, 1×10^4 cells/well; 22RV1 cells, 3×10^4 cells/well) were seeded in a 96-well culture plate. After the cells were cultured for 24 h, the cells were treated with 50 μM EdU for 2 h at 37°C, fixed with 4% paraformaldehyde for 30 min, incubated with 2 mg/ml glycin for 5 min, incubated with PBS containing 0.5% Triton X-100 for 10 min, stained with 1× Apollo staining reaction solution for 30 min, incubated with PBS containing 0.5% Triton X-100 for 10 min, and finally incubated with 100 μl of 1× Hoechst 33342 for 30 min. The percentage of EdU-positive cells was examined using a fluorescence microscope. Each experiment was repeated three times.

Transwell Assay

For the cell migration and invasion assays, the transfected cells (DU145 cells, 4 × 104 cells/well; 22RV1 cells, 1 × 105 cells/well) were cultured in an upper Transwell chamber coated with FBS-free RPMI-1640 medium (without Matrigel added; 8-μm pores, Corning, USA), and 600 μl RPMI-1640 medium containing 20% foetal bovine serum was added to the lower chamber. The 22RV1 cells were incubated for 48 h, and the DU145 cells were incubated for 24 h. The cells in the lower chamber were fixed with 4% paraformaldehyde for 20 min and stained crystal violet staining solution for 30 min, and the excess cells in the upper chamber were removed. Then, the chambers were dried. Three fields were randomly selected for each sample to capture the penetrating cells and take pictures. All the assays were conducted three independent times.

Cell Cycle Assay

DU145 and 22RV1 cells were harvested 48 h after transfection and washed with ice-cold PBS solution. Then, the cells were fixed with 75% ethanol overnight at 4°C, resuspended in propidium iodide (PI)/RNase A solution (5 μg/ml PI and 100 mg/ml RNase A) and incubated for 15 min at room temperature in the dark. Then, a flow cytometer (Millipore, Guava) was utilized to analyse cell cycle progression. All the assays were conducted three independent times.

Subcellular Fractionation

Nuclear and cytoplasmic RNA were extracted using the NE-PER nuclear and cytoplasm extraction reagent kit (Thermo Scientific, USA) following the manufacturer's protocol. Then, the relative RNA levels in the nucleus and cytoplasm were measured by RT-qPCR. MALAT1 served as a positive nuclear control, U6 served as a nuclear control transcript, and β-actin served as a cytoplasmic control.

Western Blotting

Transfected DU145 and 22RV1 cells were collected and lysed on ice with RIPA lysis buffer (Applygen, Beijing, China) containing protease inhibitors and phosphatase inhibitors for 30 min and centrifuged at 12,000*g* for 15 min, and the supernatants were collected. The extracted proteins were quantified by a BCA Protein Assay Kit (Trans, China). Then, the total cellular proteins were subjected to SD-PAGE (10%) for Western blot analysis. After transferring the proteins to polyvinylidene difluoride (PVDF) membranes, the membranes were blocked with 5% BSA in Tris-buffered saline with Tween for 60 min and incubated overnight at 4°C on a rocker with the following primary antibodies: β-Actin (CST, 4970, 1:1,000), STAT3 (CST, 9139, 1:1,000), pSTAT3 (CST, 9145, 1:1,000), E-cadherin (CST, 3195, 1:1,000), N-cadherin(CST, 13116, 1:1,000) and Vimentin (CST, 5741, 1:1,000). After washing three times with TBST for 10 min, the membranes were incubated with a horseradish peroxidase (HRP)-labeled goat anti-rabbit (CST, 7074, 1:4,000) or anti-mouse (CST, 7076, 1:4,000) secondary antibody for 1 h at room temperature (RT) and washed six times with TBST for 5 min. The protein bands were visualized by enhanced chemiluminescence (ECL).

Tumor Xenograft Model in Nude Mice

DU145 cells transfected with shLINC00467 or shNC were subcutaneously inoculated with Matrigel into 6-week-old male BALB/c nude mice. The tumor weights and volumes were

measured once a week, and of the tumor volumes were calculated as follows: V = 3.14/6Ddd (D = tumor length, d = tumor width). Finally, the mice were sacrificed, the tumors were removed, and the tumor weights were recorded.

Hematoxylin Eosin (HE) Staining

Xenograft tissues from nude mice were paraffin embedded, sliced, and dried at 65°C. After drying, the sections were dewaxed with xylene for 20 min, dehydrated with gradient ethanol of 100, 95, 85 and 75% for 5 min, and washed with tap water for 2 min. Then, the sections were stained with haematoxylin for 10 min and washed with tap water for 2 min, hydrochloric acid and ethanol for 10 s, and ammonia antiblue for 10 s. The sections were stained with eosin for 3 min and then rinsed with distilled water. The sections were dehydrated with gradient ethanol and then cleared with xylene. The HE staining results were observed and photographed under an optical microscope.

Immunohistochemistry

Xenograft tissues from nude mice were paraffin embedded, sliced, and dried at 65°C. After drying, the sections were dewaxed with xylene for 20 min and dehydrated with gradient ethanol solutions of 100, 95, 85 and 75% for 5 min. Then, the sections were incubated with citric acid buffer for 10 min for antigen repair, with peroxidase for 15 min, and with 10% goat serum for 30 min. The primary antibody was added and incubated at 4 °C overnight. The secondary antibody was added and incubated at room temperature for 30 min, and diaminobenzidine (DAB) staining was used to adjust the chrominance under the microscope. The sections were washed with tap water for 5 min, stained with haematoxylin for 5 min, differentiated with 1% hydrochloric acid and ethanol for 5 s, stained with reverse blue for 5 s with ammonia, sealed with neutral glue, and observed and photographed with light microscopy.

Statistical Analysis

All the data are expressed as the means ± SD with at least three replicates in each group. Statistical analysis was performed to determine the significance of the difference between groups using ANOVA or Student's t test. All the statistical analyses were performed using GraphPad/Prism software for Windows. Differences were considered to be statistically significant when $p < 0.05$.

RESULTS

High Expression of LINC00467 in PC Tissues and Cells

First, the RNA-seq data obtained from the GTEx and TCGA databases were analysed. The results showed that there were higher LINC00467 levels in most cancer samples (**Figure 1A**). Then, we analysed 49 pairs of PC tissues obtained from the GTEx and TCGA databases. The level of LINC00467 was markedly higher in PC tissues than in neighboring nonmalignant tissues (**Figure 1B**). RT-qPCR analysis showed that LINC00467 was overexpressed in 24 PC tissues compared with neighbouring nonmalignant tissues (**Figure 1C**). ROC curves revealed the sensitivity and specificity of LINC00467 expression in prostate cancer samples (**Figure 1D**). Furthermore, we analysed the RNA-seq data obtained from the Cancer Cell Line Encyclopedia (CCLE) database and found that LINC00467 was overexpressed in PC cell lines compared with other cancer cell lines (**Figure 1E**). RT-qPCR analysis demonstrated that LINC00467 was highly expressed in PC cell lines compared with nonmalignant prostate cell lines (**Figure 1F**).

Effects of LINC00467 Downregulation on Prostate Cancer Cell Proliferation, Cell Cycle Progression, Migration and Infiltration

To investigate the physiological effects of LINC00467, LINC00467 expression was silenced in the DU45 and 22RV1 cell lines (**Figure 2A**). With CCK-8 and EdU assays, we found that knockdown of LINC00467 expression inhibited the proliferation of DU145 and 22RV1 cells (**Figures 2B–D**). Abnormal cell cycle progression may lead to decreased cell proliferation. Therefore, we measured the effect of LINC00467 knockdown on cell cycle progression. Based on flow cytometry analysis, we found that LINC00467 knockdown resulted in increased DU45 and 22RV1 cell numbers in the G0/G1 phase and decreased cell numbers in the S and G2/M phase (**Figures 2E, F**). The Transwell assay data demonstrated that LINC00467 silencing inhibited the migration and infiltration of DU45 and 22RV1 cells (**Figures 2G, H**). Epithelial–mesenchymal transition (EMT) is a basic process by which epithelial cells lose their epithelial characteristics and transform into mesenchymal cells, thereby reducing intercellular adhesion and increasing cell motility (10). Western blotting analysis showed that knockdown of LINC00467 expression inhibited the expression of EMT-related proteins (**Figure 2I**), suggesting that LINC00467 may plays a role in the process of EMT.

LINC00467 Downregulation Inhibits PC Cell Migration and Invasion by Decreasing M2 Macrophage Polarization *Via* the STAT3 Pathway

Previous investigations documented that TAMs (tumor-associated macrophages) with an M2-like phenotype are the most predominant immune-associated cells in the TME (tumor microenvironment) and are involved in tumor development by inducing angiogenesis, metastasis, and immune escape. To investigate whether LINC00467 participates in M2 polarization, we assessed the expression of LINC00467, M1 biomarkers, and M2 biomarkers in IL-4/IL-13-treated M2 macrophages, unpolarized macrophages, and LPS/IFN-γ-treated M1 macrophages. Consequently, the expression levels of M1-associated genes (iNOS and CD86) were markedly higher in M1 macrophages, while those of M2-associated genes (CD163, MRC-1, ARG1 and IL10) were markedly higher in M2 macrophages (**Figure 3A**); these results suggested successful monocyte

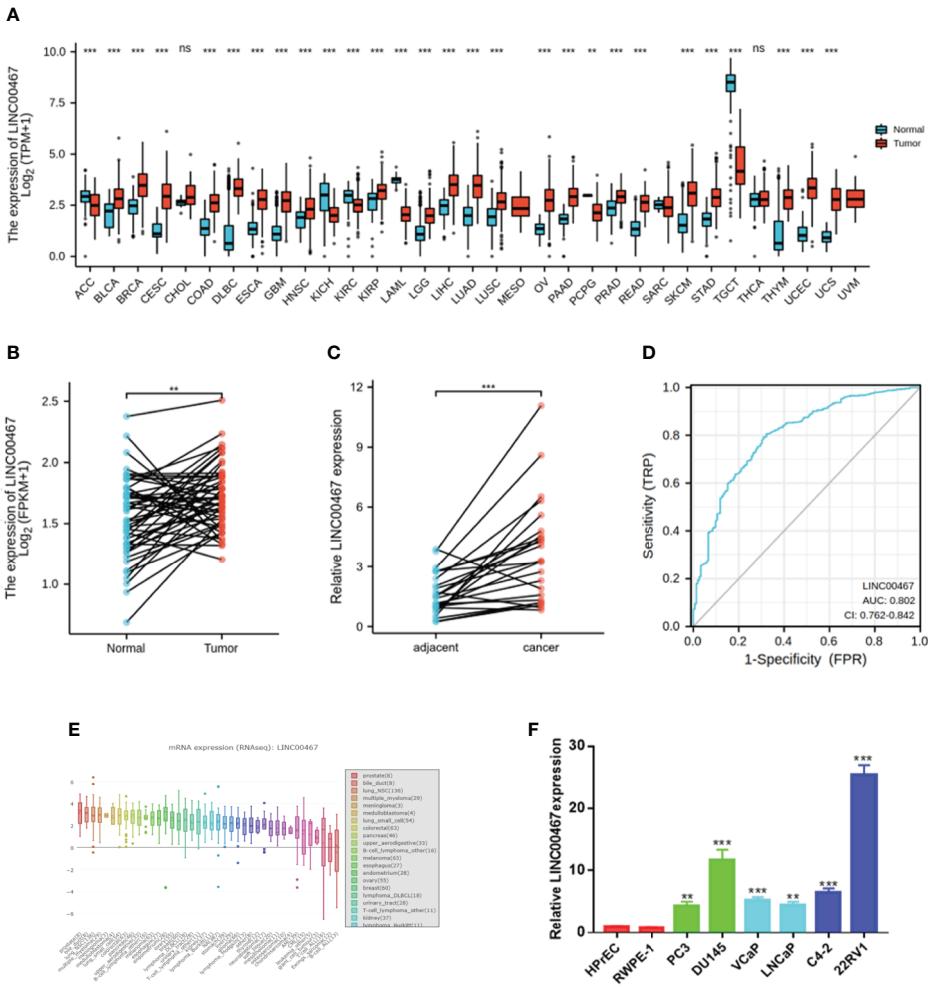

FIGURE 1 | LINC00467 expression was markedly higher in human prostate cancer tissues and cell lines. **(A)** TCGA and GTEx databases showed LINC00467 expression in most human cancers. **(B)** TCGA and GTEx database analysis showing LINC00467 expression in 49 pairs of prostate cancer samples. **(C)** RT-qPCR analysis showing LINC00467 expression in 22 pairs of prostate cancer samples. **(D)** CCLE database showed LINC00467 expression in different cancer cell lines. **(E)** RT-qPCR analysis showing LINC00467 expression in prostate cancer cell lines and nonmalignant cell lines. **(F)** ROC curves indicating the sensitivity and specificity of LINC00467 expression in prostate cancer samples. $^{**}p < 0.01$, $^{***}p < 0.001$; the data are presented as the means ± SD, n = 3. ns, not statistically significant (p>0.05).

polarization. In addition, there was higher LINC00467 content in M2 macrophages than in M1 macrophages (**Figure 3B**), suggesting that LINC00467 may be related to the polarization of M2 macrophages. After treatment with PMA for 24 h, we transfected THP-1 cells with siNC (negative control) or siLINC00467, added IL-4 and IL-13 and incubated the cells for 24 h to stimulate polarization toward the M2 phenotype. Consequently, the expression of M2 signature genes was markedly decreased in the siLINC00467 groups (**Figure 3C**). Moreover, the supernatants from LINC00467-knockdown DU145 and 22RV1 cells exhibited lower M2 biomarker levels than those from control DU145 and 22RV1 cells, as shown in **Figure 3D**. Then, we explored the mechanism responsible for the crosstalk between macrophages and PC cells. To further assess whether LINC00467-mediated M2 macrophages enhance tumor development, macrophages were treated with the supernatants obtained from LINC00467-silenced or control cells. Then, we collected the conditioned medium from treated macrophages and used it to treat DU145 cells. The results showed that the macrophages treated with supernatants from LINC00467-silenced cells markedly inhibited cell migration, as indicated in **Figures 3E, F**. Furthermore, a large number of studies have shown that M2 macrophage polarization promotes PC progression (11–13). Taken together, these results suggested that LINC00467 could enhance polarization toward the M2 phenotype and promote the tumor-enhancing role of these M2 macrophages.

In our investigation of the molecular mechanism by which LINC00467 promotes PC cell development, we found that

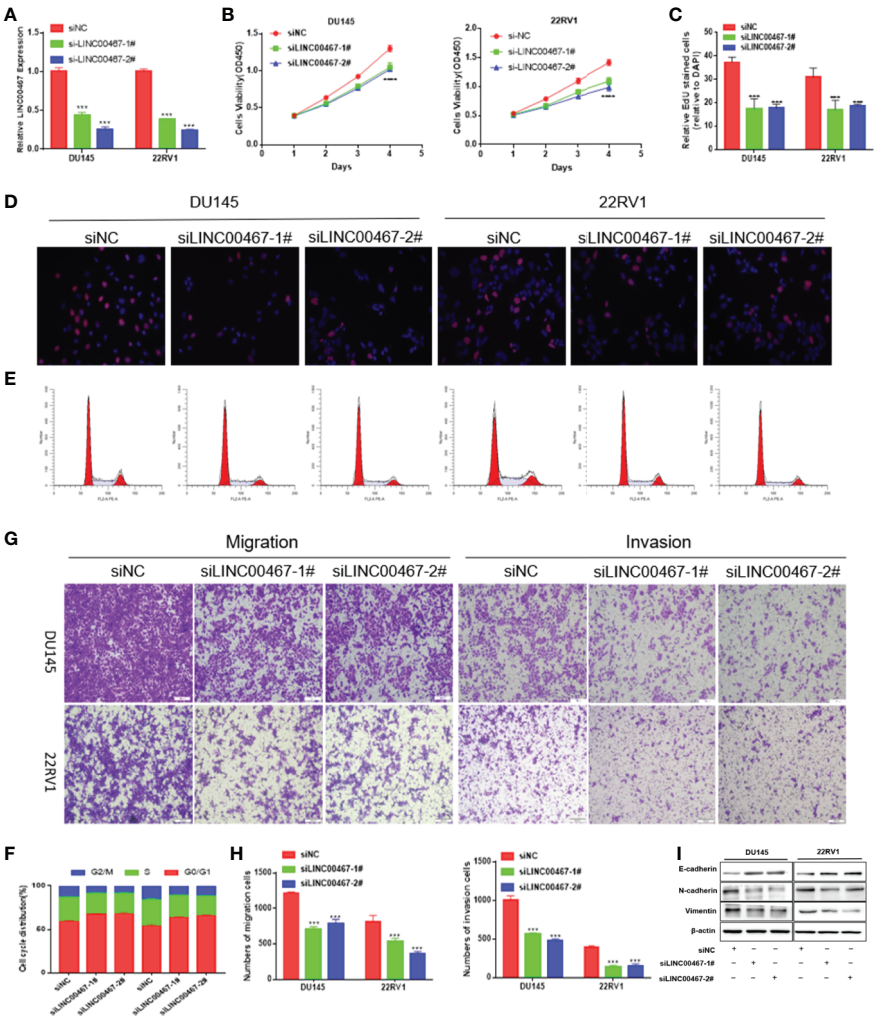

FIGURE 2 | LINC00467 downregulation inhibits cell growth, cell cycle progression, migration, and infiltration. **(A)** RT-qPCR assessment of LINC00467 expression levels in DU145 and 22RV1 cells after transfection with siLINC00467 or the negative control. **(B, D)** CCK-8 and EdU assay data indicating proliferation of DU145 and 22RV1 cells transfected with siLINC00467 or the negative control. **(E, F)** Cell cycle progression results indicating that DU145 and 22RV1 cells were arrested in the G0/G1 phase after treatment with siLINC00467. **(G, H)** Cell migration and invasion results indicating that the downregulation of LINC00467 expression inhibits the migration and invasion of DU145 and 22RV1 cells. **(I)** Western blot analysis showed that the EMT protein was decreased after treatment with siLINC00467. ***$p < 0.001$, ****$p < 0.0001$; the data are presented as the means ± SD, n = 3.

LINC00467 can induce M2 macrophage polarization and that M2 macrophage polarization can activate the STAT3 pathway. Thus, we hypothesized that LINC00467 can influence the expression of pSTAT3 and tSTAT3 in PC cells. RT-qPCR analysis showed that downregulated LINC00467 expression decreased the mRNA expression of STAT3 in PC cells (**Figure 3G**). Western blot indicating that the downregulation of LINC00467 expression decreased the expression of tSTAT3 (total STAT3), pSTAT3 (phosphorylated STAT3) and the ratio of p/t STAT3 (phosphorylated STAT3/total STAT3) in PC cells (**Figure 3H**), suggesting that LINC00467 could directly inhibit pSTAT3 expression and indirectly inhibited pSTAT3 expression through tSTAT3.

miR-494-3p Acts as a Medium of LINC00467 and STAT3 in PC

A series of lncRNAs have been found to be able to competitively bind to miRNAs as endogenous RNAs, thus preventing miRNAs from binding to target genes (14). Given that LINC00467 was mainly located in the cytoplasm (**Figure 4A**), we evaluated whether LINC00467 could serve as miRNAs sponge or ceRNAs (competing endogenous RNAs).

The LncBase and starBase databases were used to predict the interaction between miRNA and LINC00467, and starBase and TargetScan were used to predict the interaction between miRNA and STAT3. Venn diagram analysis was used to combine all the predicted miRNAs, and only two miRNAs (miR-1252 and

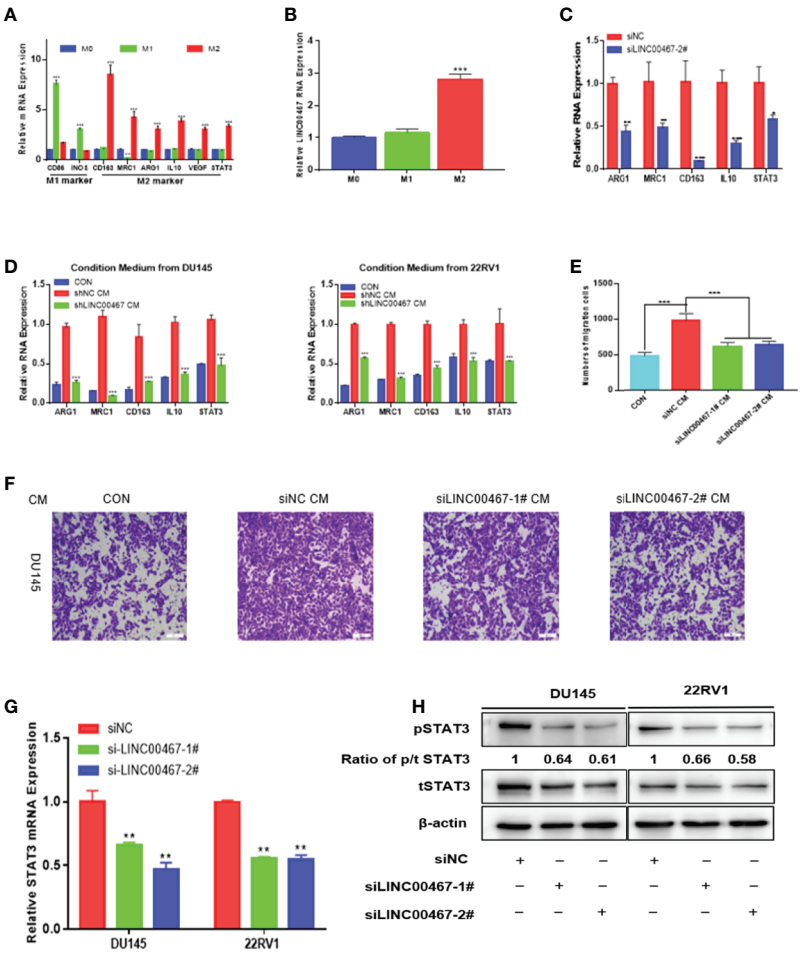

FIGURE 3 | LINC00467 downregulation inhibits PC cell migration and invasion by decreasing M2 macrophage polarization *via* the STAT3 pathway. **(A)** RT-qPCR was used to assess the expression of M1 markers and M2 markers after treatment with LPS/INF-γ or IL-4/IL-13. **(B)** The expression of LINC00467 was higher in M2 macrophages. **(C)** M2 biomarker expression was markedly decreased in the LINC00467-silenced M2 macrophage group. **(D)** Conditioned medium derived from LINC00467-knockdown cells further decreased the expression of M2 biomarkers and LINC00467 in macrophages. **(E, F)** Downregulation of LINC00467 expression in macrophages inhibited the migration of DU145 cells. **(G)** RT-qPCR showing that STAT3 mRNA expression was decreased in LINC00467-knockdown PC cells. **(H)** Western blot indicating that the downregulation of LINC00467 expression decreased the expression of tSTAT3, pSTAT3 and the ratio of p/t STAT3 in PC cells. *$p < 0.05$, **$p < 0.01$, ***$p < 0.001$; the data are presented as the means ± SD, n = 3.

miR-494-3p) could bind to LINC00467 and STAT3 (**Figure 4B**). RT-qPCR was used to assess miR-494-3p expression in LINC00467-knockdown DU145 and 22RV1 cells (**Figures 4C, D**). We found that the binding sites of miR-494-3p were complementary to the sequence of LINC00467 and the 3'UTR of STAT3. A luciferase reporter assay was used to evaluate the crosstalk between miR-494-3p and STAT3 and between miR-494-3p and LINC00467. In the cells transfected with the miR-494-3p mimic, the luciferase activities of the wild-type LINC00467 and STAT3 vectors were markedly lower than that of the reporter vector mutated at the LINC00467 and STAT3 binding sites (**Figures 4E–H**). Then, we used Western blotting to determine how miR-494-3p affects the STAT3 pathway. The miR-494-3p mimic inhibited the expression of pSTAT3 and tSTAT3 in 22RV1 cells, and the miR-494-3p inhibitor enhanced the expression of pSTAT3 and tSTAT3 in DU145 cells (**Figure 4I**). But miR-494-3p could only regulate the expression of tSTAT3 and pSTAT3, not change the ratio of p/t STAT3, indicating that miR-494-3p only indirectly inhibited phosphorylated STAT3 expression through total STAT3. These results suggest that miR-494-3p directly targets STAT3 in PC cells.

miR-494-3p Inhibition Affects Prostate Cancer Cell Proliferation and Infiltration by Targeting STAT3

To investigate the expression level of miR-494-3p in PC and its effect on the malignant phenotype, we first analysed the expression of miR-494-3p in 20 pairs of PC tissues and PC cell lines using RT-qPCR and found that miR-494-3p expression was downregulated in PC tissues and PC cell lines compared to normal tissues and cell lines (**Figures 5A, C**). miR-494-3p expression was negatively correlated with LINC00467 expression (**Figure 5B**). Then, we

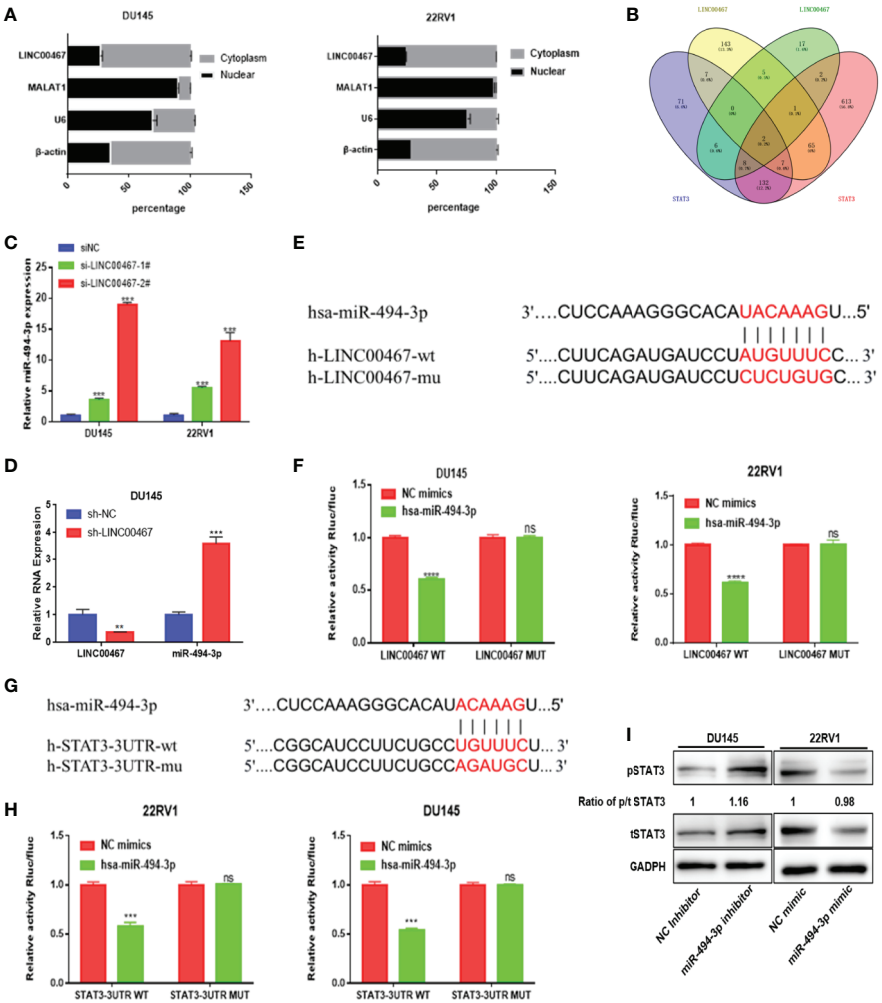

FIGURE 4 | miR-494-3p acts as a medium of LINC00467 and STAT3 in PC. **(A)** Subcellular fractionation indicating that LINC00467 is located mainly in the cytoplasm. **(B)** Venn analysis showing the bioinformatics prediction of miRNAs that target LINC00467 and STAT3. **(C, D)** RT-qPCR analysis showing that miR-494-3p expression is upregulated in LINC00467-knockdown DU145 and 22RV1 cells. **(E, F)** Dual-luciferase reporter assay confirmed the interaction between miR-494-3p and LINC00467. **(G, H)** A dual-luciferase reporter system confirmed the interaction between miR-494-3p and STAT3. **(I)** Western blotting analysis showing that the miR-494-3p inhibitor increased the expression of pSTAT3 and tSTAT3, while the miR-494-3p mimic decreased the expression of pSTAT3 and tSTAT3. $^{**}p < 0.01$, $^{***}p < 0.001$; the data are presented as the means ± SD, n = 3. ns, not statistically significant (p>0.05).

transfected 22RV1 cells with a miRNA mimic (**Figure 5D**) and DU145 cells with a miRNA inhibitor (**Figure 5E**). Elevated expression of miR-494-3p markedly inhibited cell viability, migration, and infiltration (**Figures 5F–H**). Knockdown of miR-494-3p expression markedly promoted cell viability, migration and infiltration, but these events were alleviated by siSTAT3 (**Figures 5I–K**). These data demonstrated that miR-494-3p inhibited PC development by targeting STAT3 *in vitro*.

LINC00467 Regulates the Proliferation, Migration and Invasion of Prostate Cancer Cells by Modulating the miR-494-3p/STAT3 Pathway

To further investigate whether LINC00467 functions by modulating the miR-494-3p/STAT3 cascade, we conducted rescue experiments in DU145 and 22RV1 cells by transfecting these cells with a miR-494-3p inhibitor. We first verified the transfection efficiency by analysing the miR-494-3p levels (**Figure 6A**) and then performed CCK-8 and Transwell assays. LINC00467 gene knockout reduced the proliferation, migration and invasion of DU145 cells. However, miR-494-3p inhibition increased the proliferation, migration, and invasion of prostate cancer cells (**Figures 6C–E**). These findings suggest that LINC00467 plays a tumor-promoting role in prostate cancer, while miR-494-3p plays an inhibitory role in prostate cancer. The downregulated of LINC00467 reduced the expression of tSTAT3, pSTAT3 and the ratio of p/t STAT3, but miR-494-3p could only rescue the expression of tSTAT3 and pSTAT3, suggesting that LINC00467 may regulate the expression of STAT3 pathway through other pathways (**Figure 6B**). Hence, LINC00467 plays a role by regulating the miR-494-3p/STAT3 signaling pathway.

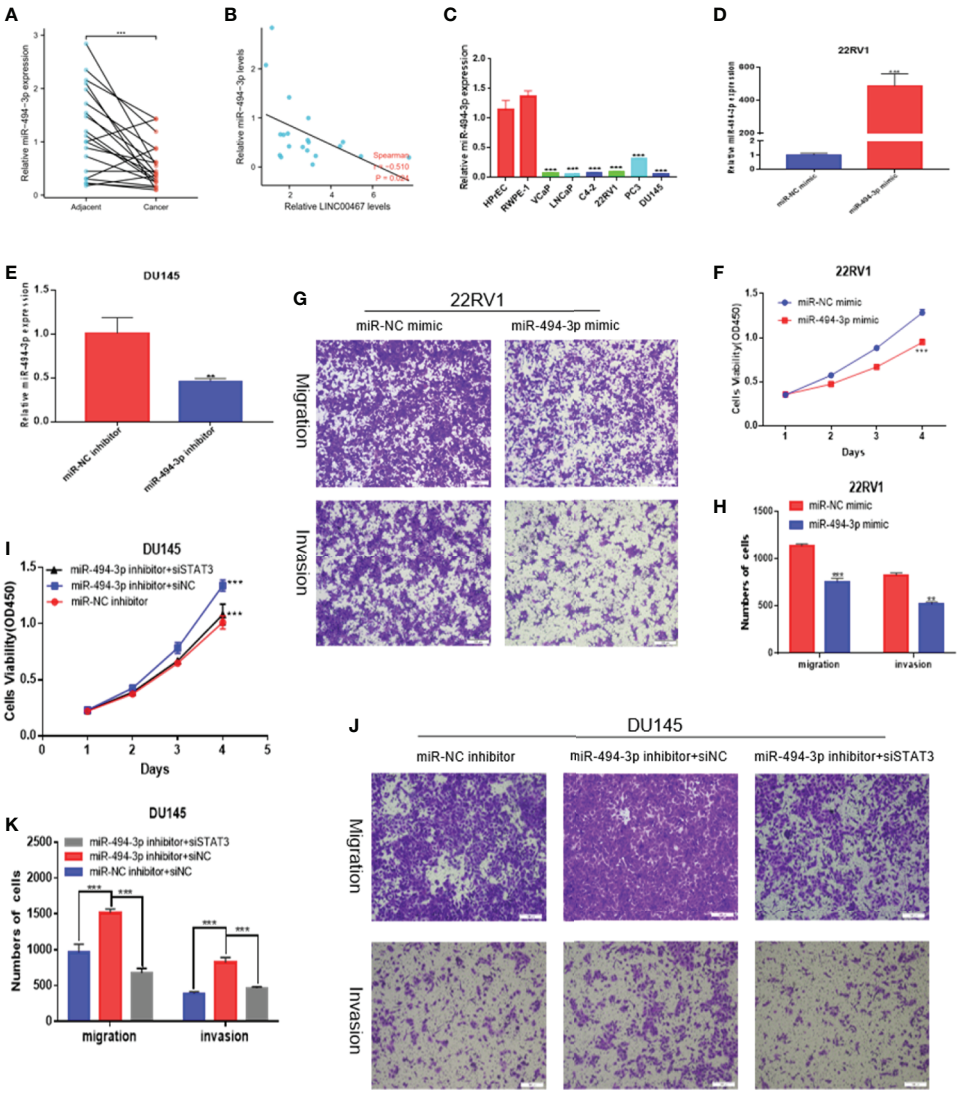

FIGURE 5 | miR-494-3p inhibits prostate cancer progression by targeting STAT3. **(A, C)** RT-qPCR indicating that miR-494-3p expression was downregulated in PC tissues and cell lines compared to nonmalignant tissues and cell lines. **(B)** A negative correlation between the expression of LINC00467 and miR-494-3p was showed using Spearman correlation analysis. **(D, E)** RT-qPCR was used to assess the efficiency of the miR-494-3p inhibitor and mimic in PC cells. **(F–H)** CCK-8 and Transwell assays showing that the miR-494-3p mimic repressed the proliferation, migration and invasion of 22RV1 cells. **(I–K)** CCK-8 and Transwell assays indicating that the miR-494-3p inhibitor promoted the proliferation, migration and invasion of DU145 cells, which could be reversed by siSTAT3. $^{**}p < 0.01$, $^{***}p < 0.001$; the data are presented as the means ± SD, n = 3.

Downregulation of LINC00467 Expression Represses Tumor Growth in Nude Mouse Xenografts

To investigate whether LINC00467 participates in the progression of prostate cancer *in vivo*, we used lentivirus to construct a stable strain LINC00467-knockdown DU145 cells and implanted these cells in nude mice to induce subcutaneous tumor formation. The results showed that LINC00467 knockdown inhibited tumor growth and weight, as well as volume, compared with the lentivirus-mediated stable control vector (**Figures 7A–D**). Therefore, we believe that downregulation of LINC00467 expression can inhibit the formation of xenograft tumors in nude mice. RT-qPCR showed that silencing LINC00467 expression could promote miR-494-3p expression and inhibit STAT3 expression (**Figures 7E, F**). These results suggest that LINC00467 plays a role through its functions in the LINC00467/miR-494-3p/STAT3 axis.

DISCUSSION

Despite significant advances in diagnosis and treatment, prostate cancer remains the primary cause of morbidity and mortality among men in the United States. Therefore, exploring new

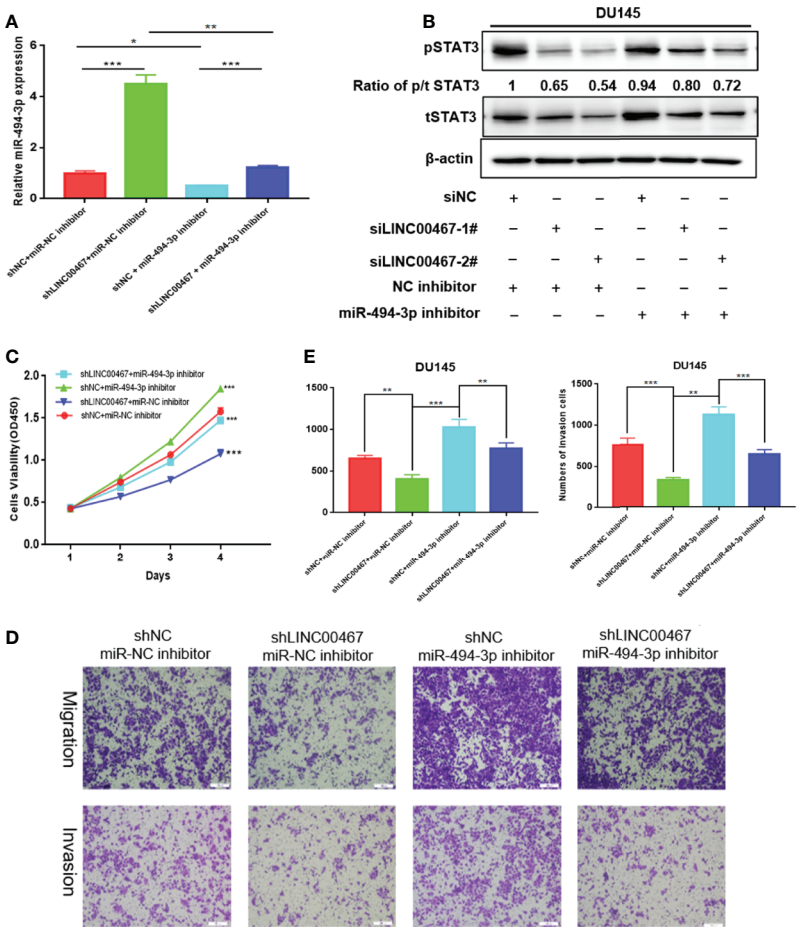

FIGURE 6 | LINC00467 enhances prostate cancer progression by targeting the miR-494-3p/STAT3 axis. **(A)** qPCR analysis indicating miR-494-3p expression. **(C–E)** CCK-8 and Transwell assays showing that shLINC00467 inhibited the proliferation, migration and infiltration abilities of DU145 and 22RV1 cells, and when co-transfected with miR-494-3p inhibitor, the effect was reversed. **(B)** Western blotting analysis indicating that miR-494-3p could partially increase the protein levels of tSTAT3 and pSTAT3, which were decreased by LINC00467, but not rescue the ratio of p/t STAT3. *p < 0.05, **p < 0.01, ***p < 0.001; the data are presented as the means ± SD, n = 3.

therapeutic markers has important clinical significance for prostate cancer patients. In our study, the GTEx and TCGA databases screening and analysis showed that LINC00467 was overexpressed in most human cancers, including prostate cancer. Then analyzed 49 pairs of PC tissues from the GTEx and TCGA databases and qRT-PCR analysis detected 24 pairs of PC tissues, results showed that the level of LINC00467 was markedly higher in PC tissues than in neighbouring nonmalignant tissues, suggesting that LINC00467 may function as a cancer-promoting gene.

LINC00467 expression is aberrantly upregulated in multiple tumor tissues and can enhance cell proliferation in neuroblastoma (15), lung cancer (16), and glioma cells (17). LINC00467 expression is closely associated with worse prognosis of these tumors. The first study about LINC00467 revealed its carcinogenic functions in neuroblastoma; LINC00467 silencing decreased the proliferation of tumor cells but enhanced apoptosis, indicating that LINC00467 functions as a tumor repressor (15). A previous study revealed that LINC00467 promoted proliferation and invasion, inhibited apoptosis, and contributed to axitinib resistance in hepatocellular carcinoma through miR-509-3p/PDGFRA (18). Another study demonstrated that LINC00467 enhances the progression of non-small cell lung cancer through the AKT signaling cascade, and TDG-induced acetylation is the pivotal factor that modulates the expression of LINC00467 (16). Hence, to investigate the physiological effects of LINC00467, downregulated LINC00467 expression inhibited PC cell growth, cell cycle progression, migration, and invasion.

Recently, attention has been focused on the importance of the tumor microenvironment in the progression of tumors. The tumor microenvironment is a complex system consisting of cancer cells, cancer-related fibroblasts, and immune inflammatory cells (19). The crosstalk of cancer cells with TAMs (tumor-associated macrophages), one of the most predominant immune cells in many solid cancers, was linked to cancer progression, drugs resistance and worse prognosis in individuals with cancer (20). On the basis of their biological characteristics, macrophages are

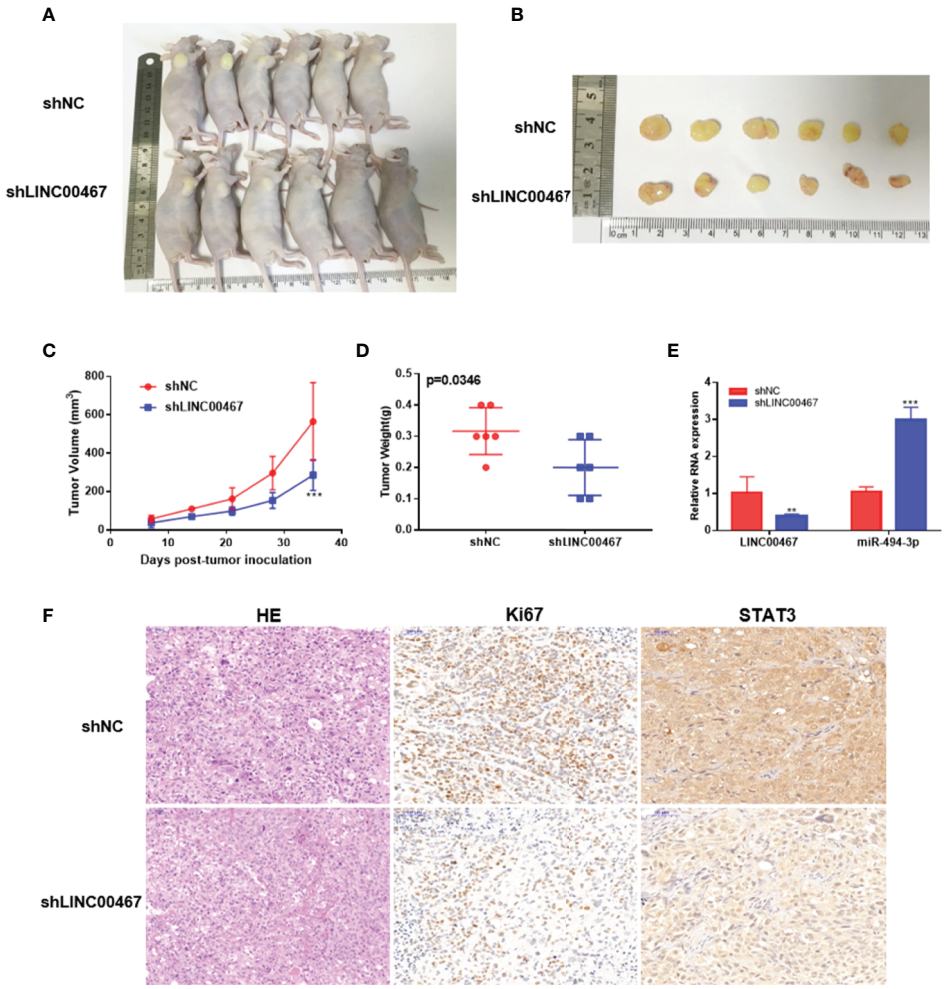

FIGURE 7 | LINC00467 promotes the growth of prostate cancer tumors *in vivo*. **(A)** Subcutaneous administration of DU145 cells stably transfected with shLINC00467 or control vector into nude mice. (n = six per group). **(B)** Image illustrating xenograft tumor formation in nude mice. **(C, D)** The rate of tumor growth and weight were markedly reduced in the shLINC00467 group. **(E)** RT-qPCR analysis indicating the LINC00467 and miR-494-3p levels in tumor tissues. **(F)** HE and IHC staining indicating the expression of Ki67 and STAT3 in tumor tissues. $^{**}p < 0.01$, $^{***}p < 0.001$; the data are presented as the means ± SD, n = 3.

grouped into two main phenotypes, namely, proinflammatory (M1) and anti-inflammatory (M2) macrophages. Numerous studies have documented that TAMs are recognized as M2-like macrophages, which are strongly linked to the progression of cancer (21–24). Herein, we established that the LINC00467 levels were markedly higher in M2-like macrophages than in M1-like macrophages and unpolarized macrophages. In addition, LINC00467 knockdown markedly inhibited the expression of M2-like macrophage biomarkers, indicating that LINC00467 promotes the polarization of M2 macrophages. Conditioned medium from prostate cancer cells affected macrophage polarization, reflecting the existence of a transferred mediator. Downregulation of LINC00467 expression in macrophages decreased the migration of PC cells.

A previous study showed that macrophage polarization can increase the migration of pancreatic cancer cells *via* activated STAT3 (25). STAT3 plays a core role in the progression of multiple cancers. STAT3 is a pivotal oncogenic protein that is constitutively activated in PC (26). After activation by phosphorylation, STAT3 translocates into the nucleus and modulates the transcription of numerous genes that participate in antiapoptosis, proliferation, and metastasis processes. In our study, we found that downregulated LINC00467 can inhibit the activated of STAT3 pathway.

The biological roles of lncRNAs primarily depend on their subcellular localization. Growing research evidence has documented that lncRNAs located in the cytoplasm are involved in gene regulation at the posttranscriptional level, such as by functioning as ceRNAs and protecting target mRNAs from suppression (14, 27). Our cell cytoplasmic/nuclear fractionation data demonstrated that LINC00467 was preferentially localized to the cytoplasm, suggesting that it sponges miRNAs.

Therefore, we used the LncBase, StarBase and TargetScan databases to predict the miRNAs that can interact with LINC00467 and STAT3. Venn analysis showed that only two miRNAs were identified, miR-494-3p and miR-1252. miRNA-494-3p has been documented to inhibit the proliferation, infiltration, and migration of prostate cancer cells (28). Herein, miR-494-3p expression was reported to be downregulated in prostate cancer, suggesting a tumor suppressive effect of miR-494-3p, which was consistent with previous studies. The miR-494-3p inhibitor increased tSTAT3 expression and increased the pSTAT3 levels, which confirmed that miR-494-3p regulated the progression of prostate cancer by targeting STAT3. Rescue experiments confirmed that STAT3 is involved in the regulation of miR-494-3p to inhibit the progression of prostate cancer, and miR-494-3p participates in the modulation of LINC00467 to promote the progression of prostate cancer. miR-494-3p is considered to be negatively regulated by LINC00467 *in vivo* and *in vitro*. All the evidence showed that LINC00467 regulated STAT3 to promote the progression of prostate cancer by sponging miR-494-3p.

CONCLUSIONS

Our data revealed that LINC00467 was overexpressed in prostate cancer tissues and cell lines. LINC00467 served as an oncogene in prostate cancer progression. LINC00467 promoted M2 macrophage polarization. The repression of LINC00467 inhibited proliferation and infiltration by regulating the miR-494-3p/STAT3 cascade. Hence, inhibiting LINC00467 could be a prospective therapeutic target for patients with early stage prostate cancer.

DATA AVAILABILITY STATEMENT

The raw data supporting the conclusions of this article will be made available by the authors, without undue reservation.

ETHICS STATEMENT

The studies involving human participants were reviewed and approved by the First Affiliated Hospital of Nanchang University. The patients/participants provided their written informed consent to participate in this study. The animal study was reviewed and approved by the First Affiliated Hospital of Nanchang University.

AUTHOR CONTRIBUTIONS

HJ and XZ performed the experiments and generated data. HJ, WD, KZ, ZZe, BH, ZZh, CZ, and AX analyzed data. XZ, GW, and BF designed the experiments. HJ, XZ, and GW wrote the manuscript. All authors contributed to the article and approved the submitted version.

FUNDING

This work was supported by the National Natural Science Foundation of P.R. China (Grant Nos. 82060467 and 81760457) and the Natural Science Foundation of Jiangxi (Grant No. S2017ZRZDB0212).

REFERENCES

1. Siegel RL, Miller KD, Jemal A. Cancer Statistics, 2020. *CA Cancer J Clin* (2020) 70(1):7–30. doi: 10.3322/caac.21590
2. Litwin MS, Tan HJ. The Diagnosis and Treatment of Prostate Cancer: A Review. *JAMA* (2017) 317(24):2532–42. doi: 10.1001/jama.2017.7248
3. Wang KC, Chang HY. Molecular Mechanisms of Long Noncoding Rnas. *Mol Cell* (2011) 43(6):904–14. doi: 10.1016/j.molcel.2011.08.018
4. Cabili MN, Trapnell C, Goff L, Koziol M, Tazon-Vega B, Regev A, et al. Integrative Annotation of Human Large Intergenic Noncoding RNAs Reveals Global Properties and Specific Subclasses. *Genes Dev* (2011) 25(18):1915–27. doi: 10.1101/gad.17446611
5. Huang Y, Liu N, Wang JP, Wang YQ, Yu XL, Wang ZB, et al. Regulatory Long non-Coding RNA and its Functions. *J Physiol Biochem* (2012) 68(4):611–8. doi: 10.1007/s13105-012-0166-y
6. Liao Q, Liu C, Yuan X, Kang S, Miao R, Xiao H, et al. Large-Scale Prediction of Long non-Coding RNA Functions in a Coding-non-Coding Gene Co-Expression Network. *Nucleic Acids Res* (2011) 39(9):3864–78. doi: 10.1093/nar/gkq1348
7. de Kok JB, Verhaegh GW, Roelofs RW, Hessels D, Kiemeney LA, Aalders TW, et al. DD3(PCA3), a Very Sensitive and Specific Marker to Detect Prostate Tumors. *Cancer Res* (2002) 62(9):2695–8.
8. Petrovics G, Zhang W, Makarem M, Street JP, Connelly R, Sun L, et al. Elevated Expression of PCGEM1, a Prostate-Specific Gene With Cell Growth-Promoting Function, is Associated With High-Risk Prostate Cancer Patients. *Oncogene* (2004) 23(2):605–11. doi: 10.1038/sj.onc.1207069
9. Cui Z, Ren S, Lu J, Wang F, Xu W, Sun Y, et al. The Prostate Cancer-Up-Regulated Long Noncoding RNA PlncRNA-1 Modulates Apoptosis and Proliferation Through Reciprocal Regulation of Androgen Receptor. *Urol Oncol* (2013) 31(7):1117–23. doi: 10.1016/j.urolonc.2011.11.030
10. Nieszporek A, Skrzypek K, Adamek G, Majka M. Molecular Mechanisms of Epithelial to Mesenchymal Transition in Tumor Metastasis. *Acta Biochim Pol* (2019) 66(4):509–20. doi: 10.18388/abp.2019_2899
11. Sousa S, Maatta J. The Role of Tumour-Associated Macrophages in Bone Metastasis. *J Bone Oncol* (2016) 5(3):135–8. doi: 10.1016/j.jbo.2016.03.004
12. Mazalova L, Sladek Z, Raudenska M, Balvan J, Gumulec J, Masarik M. Effect of Prostate Cancer Cell Line Supernatant on Functional Polarization in Macrophages. *Bratisl Lek Listy* (2018) 119(8):516–21. doi: 10.4149/BLL_2018_095
13. Baig MS, Roy A, Rajpoot S, Liu D, Savai R, Banerjee S, et al. Tumor-Derived Exosomes in the Regulation of Macrophage Polarization. *Inflammation Res* (2020) 69(5):435–51. doi: 10.1007/s00011-020-01318-0
14. Salmena L, Poliseno L, Tay Y, Kats L, Pandolfi PP. A ceRNA Hypothesis: The Rosetta Stone of a Hidden RNA Language? *Cell* (2011) 146(3):353–8. doi: 10.1016/j.cell.2011.07.014
15. Atmadibrata B, Liu PY, Sokolowski N, Zhang L, Wong M, Tee AE, et al. The Novel Long Noncoding RNA linc00467 Promotes Cell Survival But is Down-Regulated by N-Myc. *PloS One* (2014) 9(2):e88112. doi: 10.1371/journal.pone.0088112
16. Zhu Y, Li J, Bo H, He D, Xiao M, Xiang L, et al. LINC00467 Is Up-Regulated by TDG-mediated Acetylation in non-Small Cell Lung Cancer and Promotes Tumor Progression. *Oncogene* (2020) 39(38):6071–84. doi: 10.1038/s41388-020-01421-w

17. Gao S, Duan H, An D, Yi X, Li J, Liao C. Knockdown of Long non-Coding RNA LINC00467 Inhibits Glioma Cell Progression Via Modulation of E2F3 Targeted by Mir-200a. *Cell Cycle* (2020) 19(16):2040–53. doi: 10.1080/15384101.2020.1792127
18. Li W, He Y, Chen W, Man W, Fu Q, Tan H, et al. Knockdown of LINC00467 Contributed to Axitinib Sensitivity in Hepatocellular Carcinoma Through miR-509-3p/PDGFRA Axis. *Gene Ther* (2020). doi: 10.1038/s41434-020-0137-9
19. Chen X, Zhou J, Li X, Wang X, Lin Y, Wang X. Exosomes Derived From Hypoxic Epithelial Ovarian Cancer Cells Deliver microRNAs to Macrophages and Elicit a Tumor-Promoted Phenotype. *Cancer Lett* (2018) 435:80–91. doi: 10.1016/j.canlet.2018.08.001
20. Tang X, Mo C, Wang Y, Wei D, Xiao H. Anti-Tumour Strategies Aiming to Target Tumour-Associated Macrophages. *Immunology* (2013) 138(2):93–104. doi: 10.1111/imm.12023
21. Binnemars-Postma K, Storm G, Prakash J. Nanomedicine Strategies to Target Tumor-Associated Macrophages. *Int J Mol Sci* (2017) 18(5):979. doi: 10.3390/ijms18050979
22. Anfray C, Ummarino A, Andon FT, Allavena P. Current Strategies to Target Tumor-Associated-Macrophages to Improve Anti-Tumor Immune Responses. *Cells* (2019) 9(1):46. doi: 10.3390/cells9010046
23. Liang Y, Song X, Li Y, Chen B, Zhao W, Wang L, et al. Lncrna BCRT1 Promotes Breast Cancer Progression by Targeting miR-1303/PTBP3 Axis. *Mol Cancer* (2020) 19(1):85. doi: 10.1186/s12943-020-01206-5
24. Tian X, Wu Y, Yang Y, Wang J, Niu M, Gao S, et al. Long Noncoding RNA LINC00662 Promotes M2 Macrophage Polarization and Hepatocellular Carcinoma Progression Via Activating Wnt/beta-catenin Signaling. *Mol Oncol* (2020) 14(2):462–83. doi: 10.1002/1878-0261.12606
25. Salmiheimo A, Mustonen H, Vainionpaa S, Shen Z, Kemppainen E, Puolakkainen P, et al. Tumour-Associated Macrophages Activate Migration and STAT3 in Pancreatic Ductal Adenocarcinoma Cells in Co-Cultures. *Pancreatology* (2017) 17(4):635–41. doi: 10.1016/j.pan.2017.04.013
26. Don-Doncow N, Marginean F, Coleman I, Nelson PS, Ehrnstrom R, Krzyzanowska A, et al. Expression of STAT3 in Prostate Cancer Metastases. *Eur Urol* (2017) 71(3):313–6. doi: 10.1016/j.eururo.2016.06.018
27. Yang S, Ning Q, Zhang G, Sun H, Wang Z, Li Y. Construction of Differential mRNA-lncRNA Crosstalk Networks Based on ceRNA Hypothesis Uncover Key Roles of lncRNAs Implicated in Esophageal Squamous Cell Carcinoma. *Oncotarget* (2016) 7(52):85728–40. doi: 10.18632/oncotarget.13828
28. Shen PF, Chen XQ, Liao YC, Chen N, Zhou Q, Wei Q, et al. MicroRNA-494-3p Targets CXCR4 to Suppress the Proliferation, Invasion, and Migration of Prostate Cancer. *Prostate* (2014) 74(7):756–67. doi: 10.1002/pros.22795

Conflict of Interest: The authors declare that the research was conducted in the absence of any commercial or financial relationships that could be construed as a potential conflict of interest.

frontiers in Oncology

ORIGINAL RESEARCH
published: 23 June 2021
doi: 10.3389/fonc.2021.685980

Role of NRP1 in Bladder Cancer Pathogenesis and Progression

Yang Dong[1,2,3†], Wei-ming Ma[1,2†], Zhen-duo Shi[1,3†], Zhi-guo Zhang[1,2,3†], Jia-he Zhou[1], Yang Li[4], Shao-qi Zhang[2], Kun Pang[1,2], Bi-bo Li[5], Wen-da Zhang[1], Tao Fan[1], Guang-yuan Zhu[1], Liang Xue[1], Rui Li[4], Ying Liu[4], Lin Hao[1,2,3] and Cong-hui Han[1,2,3,5*]*

[1] Department of Urology, Xuzhou Central Hospital, Xuzhou, China, [2] Medical College of Soochow University, Suzhou, China, [3] College of Life Sciences, Jiangsu Normal University, Xuzhou, China, [4] Department of Central Laboratory, Xuzhou Central Hospital, Xuzhou, China, [5] Nanjing University of Traditional Chinese Medicine, Nanjing, China

OPEN ACCESS

Edited by:
Bianca Nitzsche, Charité – Universitätsmedizin Berlin, Germany

Reviewed by:
Pasquale Ditonno, University of Bari, Italy
Mariana Chantre Justino, Rio de Janeiro State University, Brazil

***Correspondence:**
Cong-hui Han
hanchdoctor@st.btbu.edu.cn
Lin Hao
haolinxuzhou@163.com

†These authors have contributed equally to this work and share first authorship

Specialty section:
This article was submitted to Genitourinary Oncology, a section of the journal Frontiers in Oncology

Received: *26 March 2021*
Accepted: *07 June 2021*
Published: *23 June 2021*

Citation:
Dong Y, Ma W-m, Shi Z-d, Zhang Z-g, Zhou J-h, Li Y, Zhang S-q, Pang K, Li B-b, Zhang W-d, Fan T, Zhu G-y, Xue L, Li R, Liu Y, Hao L and Han C-h (2021) Role of NRP1 in Bladder Cancer Pathogenesis and Progression. Front. Oncol. 11:685980. doi: 10.3389/fonc.2021.685980

Bladder urothelial carcinoma (BC) is a fatal invasive malignancy and the most common malignancy of the urinary system. In the current study, we investigated the function and mechanisms of Neuropilin-1 (NRP1), the co-receptor for vascular endothelial growth factor, in BC pathogenesis and progression. The expression of NRP1 was evaluated using data extracted from GEO and HPA databases and examined in BC cell lines. The effect on proliferation, apoptosis, angiogenesis, migration, and invasion of BC cells were validated after *NRP1* knockdown. After identifying differentially expressed genes (DEGs) induced by *NRP1* silencing, GO/KEGG and IPA® bioinformatics analyses were performed and specific predicted pathways and targets were confirmed *in vitro.* Additionally, the co-expressed genes and ceRNA network were predicted using data downloaded from CCLE and TCGA databases, respectively. High expression of NRP1 was observed in BC tissues and cells. *NRP1* knockdown promoted apoptosis and suppressed proliferation, angiogenesis, migration, and invasion of BC cells. Additionally, after *NRP1* silencing the activity of MAPK signaling and molecular mechanisms of cancer pathways were predicted by KEGG and IPA® pathway analysis and validated using western blot in BC cells. *NRP1* knockdown also affected various biological functions, including antiviral response, immune response, cell cycle, proliferation and migration of cells, and neovascularisation. Furthermore, the main upstream molecule of the DEGs induced by *NRP1* knockdown may be *NUPR1*, and *NRP1* was also the downstream target of *NUPR1* and essential for regulation of *FOXP3* expression to activate neovascularisation. *DCBLD2* was positively regulated by *NRP1*, and PPAR signaling was significantly associated with low *NRP1* expression. We also found that NRP1 was a predicted target of miR-204, miR-143, miR-145, and miR-195 in BC development. Our data provide evidence for the biological function and molecular aetiology of NRP1 in BC and for the first time demonstrated an association between NRP1 and NUPR1, FOXP3, and DCBLD2. Specifically, downregulation of *NRP1* contributes to BC progression, which is associated with activation of MAPK signaling and molecular mechanisms involved in

cancer pathways. Therefore, NRP1 may serve as a target for new therapeutic strategies to treat BC and other cancers.

Keywords: NRP1, bladder cancer, proliferation, apoptosis, neovascularisation, migration, invasion

INTRODUCTION

Bladder urothelial carcinoma (BC), one of the most prevalent urologic malignancies worldwide, is refractory to many common treatments (1), and its incidence and mortality rate are the highest among genitourinary tumors in China (2). BC generally has a low cure rate and a high relapse rate. Although most cases are initially diagnosed as non-muscle invasive by pathological examination, discontinuation or delayed treatment due to lack of regular re-examination ultimately leads to muscle invasive BC with a great risk of distant metastasis (3). The 5-year survival rate of metastatic BC is approximately 5%, due to limited available therapies (4). Recently, multiple therapeutic approaches for BC have been explored, however, no obvious improvement has been reported in the overall survival rate. Therefore, novel targets and effective strategies for BC therapy are urgently needed.

Neuropilins (NRPs) are transmembrane glycoprotein receptors with a well-described role in interacting with the semaphorins and vascular endothelial growth factor family members (5). NRP1 encodes certain NRPs and participates in axon guidance and angiogenesis. NRP1 mutations result in fatal abnormalities in the cardiovascular system (6). Further, many studies have observed the abnormally high expression of NRP1 in multiple tumor types, including neuroblastomas and bile duct, gastric, pancreas, lung, prostate, breast, and colon cancers (5, 7). Previously, we have demonstrated that NRP1 was upregulated in patients with BC, correlating with poor prognosis (7). However, the molecular mechanisms underlying how NRP1 regulates the progression of BC remain unclear. Therefore, in the current study, we aimed to observe the regulation of *NRP1* silencing on proliferation, apoptosis, migration, and invasion in BC cells, and elucidate the potential signal pathways involved in the inhibition of BC progression after *NRP1* knockdown, as well as the potential mechanisms employed by NRP1 in BC pathogenesis and progression.

Abbreviations: Bax, BCL2-associated X protein; BC, bladder urothelial carcinoma; Bcl2, BCL2 Apoptosis Regulator; BIRC3, baculoviral IAP repeat containing 3; CCNE2, Cyclin E2; CDK, cyclin-dependent kinase; CST, Cell Signaling Technology; DCBLD2, Discoidin CUB And LCCL Domain Containing 2; FOS, AP-1 Transcription Factor Subunit; GAPDH, glyceraldehyde-3-phosphate dehydrogenase; FGF2, Fibroblast Growth Factor 2; FOXP3, Forkhead Box P3; HGF, Hepatocyte Growth Factor; PDGF, Platelet Derived Growth Factor; PGF, Placental Growth Factor; TGF-β1, Transforming Growth Factor β1; HPV, Human Papilloma Virus; HIV, Human Immunodeficiency Virus; HSV, Herpes Simplex Virus; HTLV-1, Human T-cell Lymphotropic Virus Type 1; EBV, Epstein-Barr Virus; NRP1, Neuropilin 1; NUPR1, Nuclear Protein1; GO, Gene Ontology; HUVEC, Human Umbilical Vein Endothelial Cells; JNK, mitogen-activated protein kinase 8; MAPK, Mitogen-Activated Protein Kinase; MMP9, Matrix Metallopeptidase 9; NF-κB, Nuclear Factor Kappa B; NRP, neuropilin; PBS, phosphate-buffered saline; PI, propidium iodide; qRT-PCR, quantitative real-time reverse transcription polymerase chain reaction; SDEG, significantly differentially expressed genes; shRNA, small hairpin RNA; VEGF, vascular endothelial growth factor.

MATERIALS AND METHODS

Cell Lines

The human bladder immortalized epithelium cell line SVHUC1 and BC cell lines including T24, 5637, J82, UMUC3 and RT4 were purchased from the Cell Resource Center of the Shanghai Institutes for Biological Sciences, Chinese Academy of Sciences (Shanghai, China). All cell lines were cultured as described previously (8). We cultured all cell lines in RPMI 1640 medium with 100 U/mL penicillin, 100 ug/mL streptomycin, and 10% foetal bovine serum at 5% CO2 in a 37°C humidified culture environment. Short-tandem repeat profiling was used to authenticate the cell lines less than 6 months before this project was initiated, and the cells were not in culture for more than 2 months.

Data Mining and Collection

We downloaded three gene expression datasets [GSE3167 (9), GSE65635 (10), and GSE120736 (11)] from GEO (http://www.ncbi.nlm.nih.gov/geo) (12). All studies employed tissue samples gathered from human non-muscle invasive BC and muscle invasive BC tissues. The annotation information provided by the platform was referenced to convert the probes into the corresponding gene symbols. The Human Protein Atlas (HPA) database (https://www.proteinatlas.org/), was used to identify the protein expression of NRP1 in BC tissues (13). BC patients in TCGA cohorts were also included in the study. The relevant lncRNA expression and miRNA data and clinical data of BC were downloaded from TCGA Bladder Carcinoma (TCGA-BLCA) study of the official TCGA website (https://cancergenome.nih.gov/), updated on May 07, 2020. RNA expression (RNA-Seq) data of *NRP1* in different urinary tract cancer cell lines (n = 26) were obtained from the Cancer Cell Line Encyclopedia (CCLE) database (https://portals.broadinstitute.org/ccle/about) (14), updated on January 02, 2019.

RNA Isolation and Quantitative Real-Time Reverse Transcription Polymerase Chain Reaction (qRT-PCR)

According to the manufacturer's instructions, total RNA from each cell line was successfully isolated using Trizol reagent (Life Technologies, Carlsbad, CA, USA), and then cDNA was synthesized using M-MLV Reverse Transcriptase (Promega, Beijing, China). After adding the SYBR Premix Ex Taq II (Perfect Real-Time) kit (TaKaRa Bio, Shiga, Japan), qRT-PCR was subsequently carried out with the following settings: 95°C for

30 s and 39 cycles of 95°C for 5 s and 60°C for 30 s. The DNA dissociation analysis (melting curve) was operated at the end of each run to confirm the absence of primer dimers, mixed-amplicon populations, and nonspecific products. The relative expression of genes was presented as comparative threshold cycle ($2^{-\Delta\Delta Ct}$) values from at least three independent experiments. Actin Beta (*β-actin*) was used to standardise the expression of target genes. The primer sequences were as follows: *NRP1*, forward 5′- CTTGGCCTGACATTGCAATT-3′ and reverse 5′- AGGTTCCTGCATCCGCCTTAATGT-3′; *FOXP3*, forward 5′- ACTGACCAAGGCTTCATCTGTG-3′ and reverse 5′- GGAA CTCTGGGAATGTGCTGTT-3′; *FGF2*, forward 5′- GTCTAT CAAAGGAGTGTGTGC-3′ and reverse 5′- TGCCCAGTTCG TTTCAGTG-3′; *NUPR1*, forward 5′- GCGGGCACGAGAG GAAAC-3′ and reverse 5′- CTCAGTCAGCGGGAATAAGTC-3′; *DCBLD2*, forward 5′- ATGTGGACACACTGTACTAGGC-3′ and reverse 5′- CTGTTGGGATAGGTCTGTGG-3′; *β-actin*, forward 5′- AAACGTGCTGCTGACCGAG -3′ and reverse 5′- TAGCACAGCCTGGATAGCAAC′.

Protein Extraction and Western Blot

Total protein was extracted from cell lines using radioimmunoprecipitation assay lysis buffer (Beyotime, Shanghai, China). Next, the lysates were centrifuged at 12,000 rpm for 30 min at 4°C. The protein concentrations of the lysates were measured using the BCA Protein Assay kit (Genechem, Shanghai, China). Equal amounts of protein (60 μg/lane) were separated by 10% sodium dodecyl sulphate-polyacrylamide gel electrophoresis and then transferred onto PVDF membranes with a pore size of 0.45 μm (Millipore, Billerica, MA, USA). After blocking the membranes with 5% skim milk in TBST at 25°C for 60 mins, the membranes were incubated at 4°C overnight with the following primary antibodies at the stated dilutions: NRP1 (1:1000, Cell Signaling Technology (CST) Shanghai Biological Reagents Company Limited, Shanghai, China), baculoviral IAP repeat containing (BIRC) 3 (1:600, CST), cyclin dependent kinase (CDK) 6 (1:800, CST), Cyclin E (CCNE) 2 (1:800, CST), AP-1 transcription factor subunit (FOS) (1:600, CST), CDK2 (1:1000, CST), CDK4 (1:1500, CST), and β-actin (1:800, CST). After washing in TBST, the membranes were further incubated for 2 h with a secondary anti-mouse (1:3000) or anti-rabbit (1:4000) antibody, as appropriate. Finally, the presentation of target protein bands was enhanced using chemiluminescence (Millipore). The expression levels of target proteins were quantified by densitometry (BioRad image analysis programme) and normalised with respect to β-actin levels.

Lentivirus-Mediated RNA Interference

Interfering RNAs were delivered by transfection of T24 and 5637 cells with lentivirus vector (GV118, Genechem, Shanghai, China) packaging plasmids containing short hairpin RNAs (shRNAs).To decrease the levels of endogenous *NRP1* or *NUPR1*, *NRP1* specific shRNAs (shNRP1) or *NUPR1* specific shRNAs (shNUPR1) were cloned into GV118 lentivirus vector, and shNRP1 lentivirus 3.30μl (3E+8 TU/ml), or shNUPR1 lentivirus 3.30μl (7E+8 TU/ml), or negative control shRNAs lentivirus 1.00μl (1E+9 TU/ml) were added into each well (5×10^4 cells per well in 6-well plates) in the presence of 5μg/mL polybrene. Forty-eight hours after infection, cells expressing shRNA were selected using 0.5mg/mL puromycin for 10 days. qRT-PCR was used to test the expression of *NRP1* or *NUPR1* in infected cells. The target sequence of shNRP1-1 was 5′-GCCTTGAATGCACTTATAT-3′, that of shNRP1-2 was 5′-GACCCATACCAGAGAATTA-3′, and that of shNRP1-3 was 5′-AACGATAAATGTGGCGATA-3′. The sequence of the control shRNAs was 5′-TTCTCCGAACGTGTCACGT-3′. The sequence of shNUPR1-1 was 5′-CCAAGCTGCAGAAT TCAGA-3′.

MTT Assay

Cells were seeded in 96-well cell culture plates at an initial density of 0.2×10^4 cells/well in triplicate at a volume of 200 μL/well. According to the experimental requirements, cells were incubated with 100 μL of 0.5 mg/mL sterile 3-(4, 5-dimethyl-2-thiazolyl)-2,5-diphenyl-2H-tetrazolium bromide (MTT; Sigma, USA) at 37°C for different time points. After 4 h, the culture medium was removed and 150 μL of DMSO (Sigma) was added to each well for 10 min to fully dissolve the crystals. Finally, we measured the absorbance values of each well at 490 nm with 570 nm as the reference wavelength to generate the growth curve.

Colony Formation Assay

Cells were cultured in 60-mm plates at a density of 0.5×10^3 cells/plate for 14 days. The culture medium was then removed. The cells were carefully washed with phosphate-buffered saline (PBS) twice and subsequently fixed with 10% formaldehyde for 5 min, which was followed by staining with 1% crystal violet for 30s. The stain was washed away slowly with running water and the plates were dried at room temperature before counting the number of colonies.

Tube Formation Assay

A volume of 200μL precooled Matrigel (BD Biosciences, San Jose, CA, USA) was pipetted into wells of a 24-well plate and polymerised at 37°C for 30 min. Subsequently, human umbilical vein endothelial cells (HUVECs) were added to the wells at a density of 0.2×10^4 cells/well in 200μL conditioned medium and incubated at 5% CO_2 at 37°C for 12 h. Bright-field microscopy at 100× magnification was used to capture the images. The overall length of the complete tubule structures was measured to quantify the capillary tubes.

Flow Cytometric Apoptosis Test

Cells were digested with 0.25% trypsin, washed with PBS, and centrifuged at 1000 rpm for 5 min. The supernatant was aspirated, and, according to the instructions of the Annexin-V-APC apoptosis determination kit (Ebioscience, USA), we added 100 μl of 1× binding buffer cautiously to each tube. Next, 5 μl of propidium iodide (PI) (Sigma) and 5 μl of Annexin-V-APC were added to the tubes. The tubes were then incubated at room temperature for 15 min, protected from light, before placing on ice. Within 1 h, apoptosis was assessed using the BD FACSCalibur flow cytometer (BD Biosciences).

Flow Cytometry Cell Cycle Analysis

Cells were digested with 0.25% trypsin, washed with PBS, and centrifuged at 1000 rpm for 5 min. The cell pellet was washed twice with PBS, and resuspended in 0.5 mL of PBS. The tubes were oscillated on a low-speed oscillator, and 70% ice-cold ethanol was added to fix the cells overnight at 4°C. The fixed cells were subsequently centrifuged at 1000 rpm for 5 min. The supernatant was discarded, and the pellet was washed with PBS and resuspended. Bovine pancreatic RNase (Fermentas, Lithuania) was added at a final concentration of 2 mg/mL and the tubes were incubated in a 37°C water bath for 30 min. PI was added at a final concentration of 65 μg/mL, followed by incubation in an ice bath for 30 min protected from light. Finally, cell cycle detection and data analysis were performed using a BD FACSCalibur flow cytometer filtration and FLOWJO Software (Tree Star, Inc, Ashland, OR, USA).

Transwell Cell Migration Assay

Cells in the logarithmic growth stage were digested, centrifuged and resuspended in serum-free medium. A volume of 750 μL culture medium with serum was added to the bottom of a 24-well plate, and migration chambers were placed in the wells. We added 600 μL of 30% serum-free medium to each chamber and added 100 μL of cell suspension at a density of 1×10^5 cells/mL. After incubation at 37°C for 24 h, the medium was removed from the chambers, and the wells were washed twice with PBS. Migrated cells were fixed by formaldehyde for 30 min before a 15-min staining with Giemsa stain, followed by washing twice with PBS. The non-migrated cells in the bottom of the chamber were scraped off with cotton swabs. Migrated cells were counted in three random fields of view using a light microscope (200×), and images were captured.

Transwell Cell Invasion Assay

Matrigel was diluted using serum-free medium and mixed well by pipet. A volume of 100 μL prepared Matrigel was added to Transwell chambers in a 24-well plate and incubated at 37°C overnight for gelling. Cells in the logarithmic growth stage were digested, centrifuged, and resuspended in serum-free medium. A volume of 500 μL cell suspension at a density of 1×10^5 cells/mL was placed in the chamber. We subsequently added 750 μL culture medium with serum in the bottom of the wells of a 24-well plate and placed the Transwell chambers into the wells. After incubation at 37°C for 12 h, the medium was removed from the chambers, and the wells were washed twice with PBS. The invasive cells were fixed by formaldehyde at room temperature for 30 min, followed by a 15-min staining with Giemsa stain, and then washed twice with PBS. The non-invasive cells on the bottom of the chamber were scraped off with cotton swabs. Invasive cells were counted in three random fields of view using a light microscope (200×), and images were captured.

Affymetrix Gene Expression Profile Chip Detection

We extracted total RNA from normal control cells and *NRP1*-knockdown cells with TRIZOL reagent as described above and quantified RNA using the NanoDrop ND-2000 (Thermo Scientific, USA). RNA integrity was further analysed using the Agilent Bioanalyzer 2100 (Agilent Technologies, USA). cDNA libraries were constructed after confirming RNA purity (A260/A280: 1.7-2.2) and RNA integrity (RNA integrity number ≥7.0). Total RNA was transcribed to double-stranded cDNA and synthesised to cRNA. In this process, 2nd-cycle cDNAs were generated and further hybridised onto the microarray after fragmentation and biotin labelling. Microarrays were washed and stained on the GeneChip Fluidics Station 450, and subsequent scanning was performed using the GeneChip Scanner 3000 (Affymetrix, USA). The genes with fold change ≥2.0 and P<0.05 were considered significantly differentially expressed genes (SDEGs).

GO and KEGG Enrichment Analyses

GO analysis is a commonly-used approach for annotating genes and gene products with their molecular functions and associated biological pathways and cellular components (15). KEGG is a useful resource for the systematic analysis of gene functions and related high-level genome functional information (16). In this paper, the DOSE (17) and clusterProfiler (18) packages of the statistical software R (Version 3.6.3) were used for mining information related to the biological effects of differential expressed genes and implementing pathway enrichment. Subsequently, the ggplot2 and pROC packages were used for high-quality graph generation. GSEA is a computational method that determines whether a previously-defined set of genes shows statistically significant, concordant differences between two biological states (19). GSEA4.0.3 was used for GSEA analysis. The functional gene set file "c2.cp.kegg.v7.0.symbols.gmt" was used to summarise specific and well-defined signaling. The number of substitutions per analysis was set at 1,000, and gene sets with $p < 0.05$ were recognised as significantly enriched.

Analysis of Gene Expression Profiles by Ingenuity® Pathway Analysis (IPA®)

The DEGs were analysed by IPA®, which can predict downstream effects and identify new targets or candidate biomarkers and can obtain data analysis and interpretation to understand the experimental results within the context of biological systems. IPA® data analysis is divided into five modules: canonical pathway analysis, disease and function analysis, upstream analysis, molecular interaction network analysis, and regulator effects analysis.

Construction of the Competing Endogenous RNA (ceRNA) Sankey Diagram

To further analyse the potential regulators of the hub genes, we established a ceRNA network. miRNAs related to NRP1 were predicted in TargetScan. Then, using the edgeR package in the R statistical environment, significant differentially expressed long non-coding RNAs (DElncRNAs) were identified in 411 BC and 19 adjacent non-cancer bladder tissues from TCGA database. | Log2FC | > 2.0 and FDR adjusted to $p < 0.05$ were set as the thresholds. Besides, the significant differentially expression miRNAs (DEmiRNAs) were identified with the thresholds of

|Log2 FC| > 1.0 and adj. *p*-value < 0.05 in 415 BC and 19 adjacent non-cancer bladder tissues from the TCGA database. Using miRcode (http://www.mircode.org/), the DElncRNA related DEmiRNA was predicted, while the DEmiRNA with different regulated trend to both NRP1 and lncRNAs were reserved. Finally, the ceRNA network was sankey diagram, which was visualised using dycharts online platform (https://dycharts.com).

Statistical Analysis

All statistical analyses were conducted using SAS 9.43 statistical software (SAS Institute Inc., Cary, NC, USA). One-way ANOVA was carried out to perform significance tests on the data groups. Significant differences in continuous data (mean ± standard deviation) were evaluated using the Student's *t*-test. A $p < 0.05$ was considered to be statistically significant.

RESULTS

NRP1 Is Upregulated in BC

The expression of NRP1 was previously shown to be significantly higher in BC samples compared to adjacent noncancerous tissues (7) (**Figure 1A**). Analysis of the expression of *NRP1* in published profiles (9–11) from MIBC patients showed a frequent upregulation compared to NMIBC tissues (**Figure 1B**). Furthermore, IHC staining data from the Human Protein Atlas (HPA) database was retrieved to confirm the expression of NRP1 protein. While the NRP1 staining in normal bladder tissues was generally not detected, a high proportion of the BC tissues displayed high (1/12), moderate (4/12) or low (6/12) NRP1 staining, which was typically located in the cytoplasm and membrane of cancer cells (**Figures 1C, D**). The qRT-PCR was employed to assess *NRP1* mRNA expression in BC cell lines, and a significant advancement in T24, 5637, J82 and UMUC3 cells comparing to human SVHUC1 cell was observed (**Figure 1E**).

NRP1 Modulates BC Cells Proliferation and Angiogenesis

Transfection efficiencies of shNRP1s in T24 and 5637 cells were 87.6% and 81.4% (shNRP1-1), 67.6% and 60.9% (shNRP1-2), 68.6.0% and 60.0% (shNRP1-3), respectively (**Figure 2A**), therefore shNRP1-1 was selected to be used in subsequent functional studies. In colony formation assays, *NRP1* knockdown caused a significant reduction in colony number in both T24 and 5637 BC cells ($p < 0.05$ for both; **Figure 2B**). Additionally, MTT assays indicated that *NRP1* knockdown significantly inhibited growth of T24 and 5637 cells, and compared to control cells, the growth rate decreased by nearly 2.0-fold after 5 days (**Figure 2C**). Further, conditioned medium from shNRP1 T24 or 5637 cells was able to significantly suppress tubule formation by HUVECs ($p < 0.05$ for both; **Figure 2D**). These results demonstrate that NRP1 may play a role in promoting proliferation and angiogenesis in BC.

Silencing NRP1 Promotes BC Cell Apoptosis and Cell Cycle Arrest

To explore the possible mechanism of the proliferation-promoting function of NRP1, apoptosis was examined in *NRP1*-knockdown

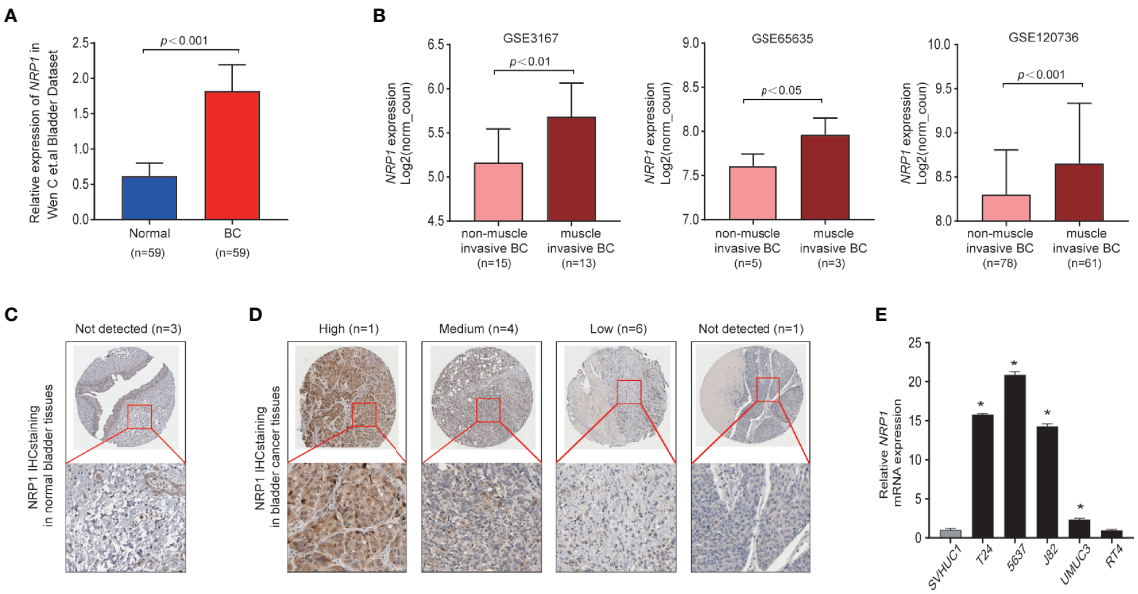

FIGURE 1 | NRP1 is upregulated in BC. **(A)** NRP1 was overexpressed in BC tissues (n = 59) compared with that in normal bladder tissues (n = 59) in the Wen C et al. bladder dataset. **(B)** Expression of *NRP1* was upregulated in muscle invasive BC tissues compared with that in non-muscle invasive BC tissue samples in the GSE3167, GSE65635, and GSE120736 datasets, respectively. **(C)** Representative IHC images of NRP1 in normal bladder tissues and in **(D)** BC tissues. **(E)** The levels of the *NRP1* mRNA in SVHUC1 cell line and five BC cell lines examined using real-time PCR. The average *NRP1* mRNA expression was normalised to the expression of β-actin. Three independent experiments were conducted for each assay and $^*p < 0.01$ *vs*. the SVHUC1 group.

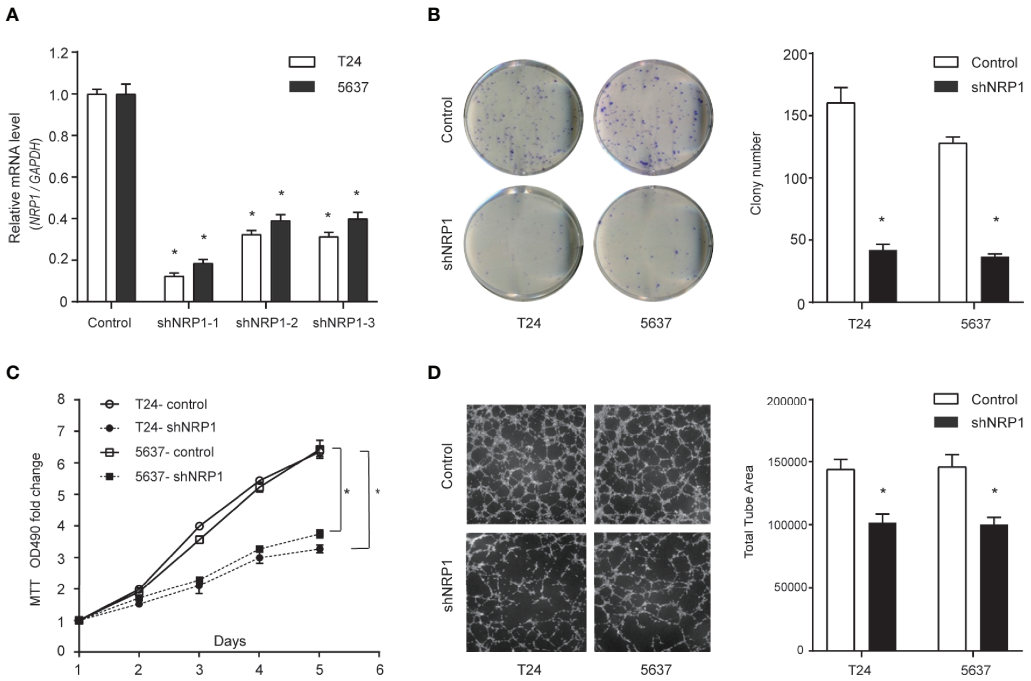

FIGURE 2 | Downregulation of NRP1 reduces BC cells proliferation and angiogenesis. **(A)** T24 and 5637 cells were infected with lentivirus-expressing *NRP1* shRNA-1, shRNA-2, and shRNA-3, or a control shRNA; the *NRP1* mRNA level as measured using qRT-PCR. **(B)** Downregulation of NRP1 reduced the mean colony number in the colony formation assay. **(C)** MTT assays revealed that downregulation of NRP1 significantly reduced the growth rate of BC cells. **(D)** Downregulation of NRP1 reduced tubule formation of vascular endothelial cell. Three independent experiments were conducted for each assay, and data are presented as the mean ± standard error of the mean, $^*p < 0.01$ *vs*. the control group.

cells. Silencing *NRP1* increased the proportion of apoptotic cells compared to control cells (**Figure 3A**). Moreover, cell cycle arrest serves as a primary mechanism for inducing apoptosis and flow cytometry analysis showed that *NRP1* knockdown caused a significant decrease in the percentage of cells in the G0/G1 peak, and an increase in the percentage of cells in the G2/M peak, however statistically significant changes were not observed in the S peak (**Figure 3B**), indicating that NRP1 may promote proliferation in BC cells by reducing apoptosis through mediating the G0/G1 and G2/M phase transitions.

NRP1 Modulates the Migration and Invasion of BC

To evaluate whether NRP1 affects the process of migration and invasion in BC, we performed Transwell assays in T24 and 5637 cells following *NRP1* knockdown. *NRP1* knockdown significantly weakened the migration and invasion abilities in T24 and 5637 cells (**Figures 3C, D**). Migration and invasion in T24 cells decreased by 51% ($p < 0.05$) and 72% ($p < 0.05$) after *NRP1* knockdown, respectively, and by 61% ($p < 0.05$) and 65% ($p < 0.05$), respectively, in 5637 cells. Our results indicate that silencing NRP1 inhibited the migration and invasion ability of BC cells.

DEGs Between NRP1 Knockdown and Control Group

To better understand the potential molecular mechanisms underlying BC malignant progression associated with NRP1, we further conducted Affymetrix Gene Chip hybridisation analysis in T24 cells following stable *NRP1* knockdown. After subsequent bioinformatic and normalization analyses, we distinguished the two groups clearly by hierarchical clustering and principal component analyses. According to the microarray expression profiling data, 599 upregulated and 880 downregulated genes had at least 2-fold expression change ($p < 0.05$ for all) following *NRP1* knockdown (**Figures 4A, B**).

GO Classification and KEGG Pathway Enrichment Analysis of DEGs

GO classification analyses of the upregulated and downregulated DEGs induced by *NRP1* silencing were performed, and a total of 405 and 166 remarkably (adj. p-value ≤ 0.05) enriched GO terms including biological process (BP), cellular component (CC) and molecular function (MF) were obtained, respectively. The upregulated DEGs were primarily involved in epigenetically related biological processes, such as regulation of DNA packaging, chromatin silencing, cell differentiation, nuclear and cell division. The downregulated genes were mainly enriched in the regulation of metabolic process, cell communication and cellular response to multiple factors (**Supplementary Table 2**). **Supplementary Figures 1A, B** represents the prior significantly enriched GO terms of upregulated and downregulated DEGs in each classification in the bubble graphs. The results of KEGG pathway analysis (**Supplementary Table 3**) indicated that the upregulated DEGs were significantly enriched in 14 terms, such as

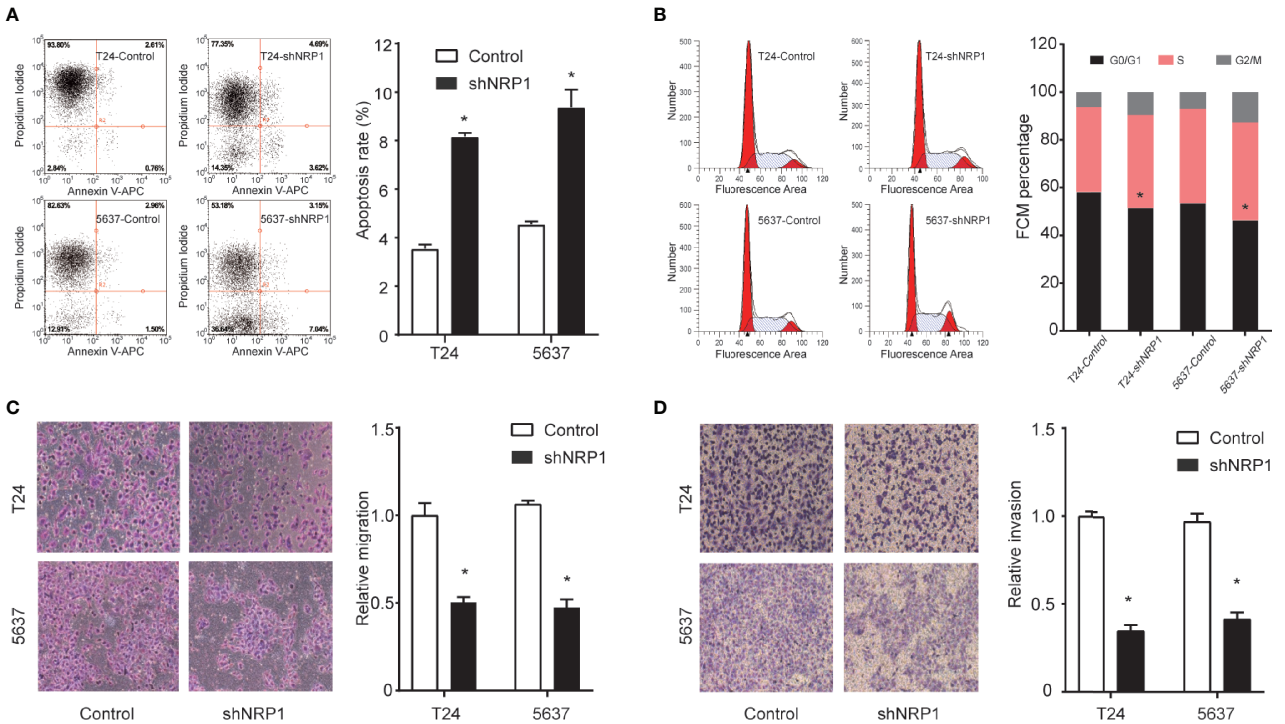

FIGURE 3 | NRP1 modulates BC cells apoptosis, cell cycle, migration, and invasion. **(A)** Apoptosis assay and quantitation of apoptotic cells of T24 and 5637 cells after *NRP1* knockdown or control shRNA expression. **(B)** Flow cytometric analysis of T24 and 5637 cells following *NRP1* knockdown or control shRNA expression. **(C, D)** Images and normalised migration **(C)** or invasion **(D)** of T24 and 5637 cells following *NRP1* knockdown or control shRNA expression. Three independent experiments were conducted for each assay, and data are presented as the mean ± standard error of the mean, $^*p < 0.05$ *vs*. the control group.

mitogen-activated protein kinase (MAPK) signaling, IL-17 signaling, Hippo signaling pathway, Transcriptional misregulation in cancer, and EGFR tyrosine kinase inhibitor resistance (**Figure 4C**); and the downregulated DEGs were remarkably enriched in 19 terms, such as P53 signaling, PI3K-AKT signaling, ECM-receptor interaction, mTOR signaling pathway, etc. (**Figure 4F**). The relationship between the selected pathways and their corresponding genes, and the clustering of the expression profiles were displayed in the chord plot (**Figures 4D, E**) and circular dendrogram (**Figures 4G, H**).

IPA® Bioinformatics Analysis-Canonical Pathway Analysis

The canonical pathway analysis by IPA® shows for enrichment of the DEGs in the canonical signaling pathway. Our analysis revealed highly significant overlap of 398 canonical pathways ($p < 0.05$) related to tumorigenesis and tumor progression (**Supplementary Table 4**). Interferon signaling (-log P = 8.1, z-score = -2.714), JAK/STAT signaling (-log P = 1.39, z-score = -3),ERK/MAPK signaling (-log P = 1.49, z-score=1.606), p53 signaling (-log P = 2.84, z-score = 1.732), Toll-like receptor signaling (-log P = 2.13, z-score = 1.667), NF-κB signaling (-log P = 2.1, z-score = 1.342), cell cycle (-log P = 4.35, z-score = 0.632), and TGF-β signaling (-log P = 3.92, z-score = 0.775) were affected by *NRP1 k*nockdown in BC T24 cells (**Figure 5A**). Z-score > 0 indicates that the pathway is activated and z-score < 0 indicates that it is inhibited. Among these pathways, interferon signaling was the top enriched signaling pathway ranked in the |z-score| > 2. The effect of DEGs on signal transfer in the interferon signaling pathway are demonstrated in **Figure 5B**.

NRP1 Is Associated With the Molecular Mechanisms of Cancer Pathways

Among these significantly activated pathways, the molecular mechanisms of cancer pathway was chosen to examine the potential role of NRP1 in BC (**Supplementary Table 5**). A gene interaction network in this pathway was constructed to identify the potential NRP1-regulated genes, and NRP1 was presumed to influence the development of BC by regulating the expression of these genes (**Figure 6A**). Western blot was further performed to confirm the dysregulation of certain known tumor-associated genes in T24 cells with *NRP1* knockdown. Consistent with gene chip analysis results, the protein expression of BIRC3 and CDK6 were significantly upregulated following *NRP1* knockdown, while CDK4, CCNE2, FOS, and CDK2 were significantly downregulated (**Figure 6B**).

NRP1 Is Associated With the MAPK Signaling Pathway

According to the results of KEGG pathway and IPA® canonical pathway analyses of the altered gene sets, we found that the

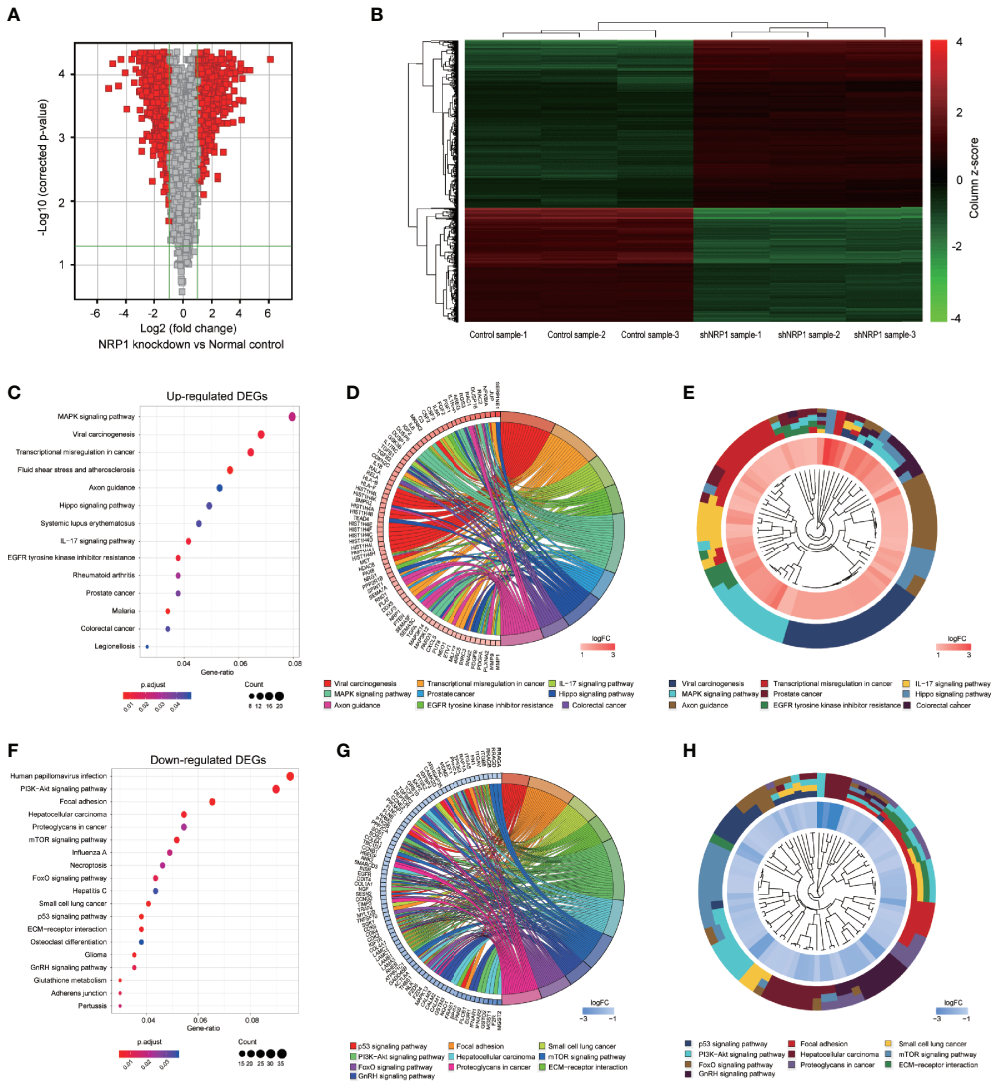

FIGURE 4 | KEGG pathway analysis of DEGs following knockdown of NRP1. **(A)** Gene expression volcano plot of T24 cells transfected with *NRP1* shRNA and a control shRNA vector. The red color on the left side represents 599 upregulated genes, and that on the right side represents 880 downregulated genes ($log_2FC > 2$ and p-value < 0.05). **(B)** Heatmap and hierarchical cluster analysis of T24 cells transfected with *NRP1* shRNA and a control shRNA vector. Column represents sample, and row represents gene, green represents a lower level gene expression, and red represents a relatively higher of gene expression. **(C)** Bubble plot of KEGG pathway analysis of upregulated DEGs. KEGG pathway description was assigned to y-axis and gene ratio was assigned to horizontal axis as the proportion of differential genes in the whole gene set. The dot size represents the gene counts in a certain pathway. **(D)** KEGG Chord plot of the relationship between the enrichment pathways and their corresponding genes in the upregulated DEGs list. A gene was linked to a certain pathway by the colored bands, and blue-to-red coding next to the genes indicates log FC. **(E)** KEGG Cluster of the upregulated DEG grouped by their functional categories. The inner ring shows the color-coded logFC, and the outer ring represents the assigned signaling pathways. **(F)** Bubble plot, **(G)** KEGG Chord plot, and **(H)** KEGG Cluster plot of KEGG pathway analysis of downregulated DEGs.

DEGs following *NRP1* knockdown were significantly associated with activation of MAPK signaling pathway. Western blot analysis confirmed that NRP1 function was closely associated with the ERK/MAPK and MAPK8 (JNK)/MAPK signaling. Moreover, Ras, phospho-Raf (p-Raf), p-ERK1/2, and matrix metallopeptidase 9 (MMP9) were all decreased in *NRP1*-knockdown cells (**Figure 6C**), indicating that ERK/MAPK pathway activation is modulated by NRP1. Further, the expression of JNK/MAPK signaling-related key proteins, such as p-JNK, p-c-jun, and cyclin B1, were significantly lower in *NRP1*-knockdown cells (**Figure 6D**), however, the expressions of BCL2-associated X protein (BAX)/BCL2 apoptosis regulator (BCL2) and caspase 3 were higher, which was consistent with bioinformatics signaling enrichment assays. These results suggest NRP1 as an effect factor of MAPK signaling that contributes to cell cycle modulation and drives tumorigenesis in BC (**Figure 6E**).

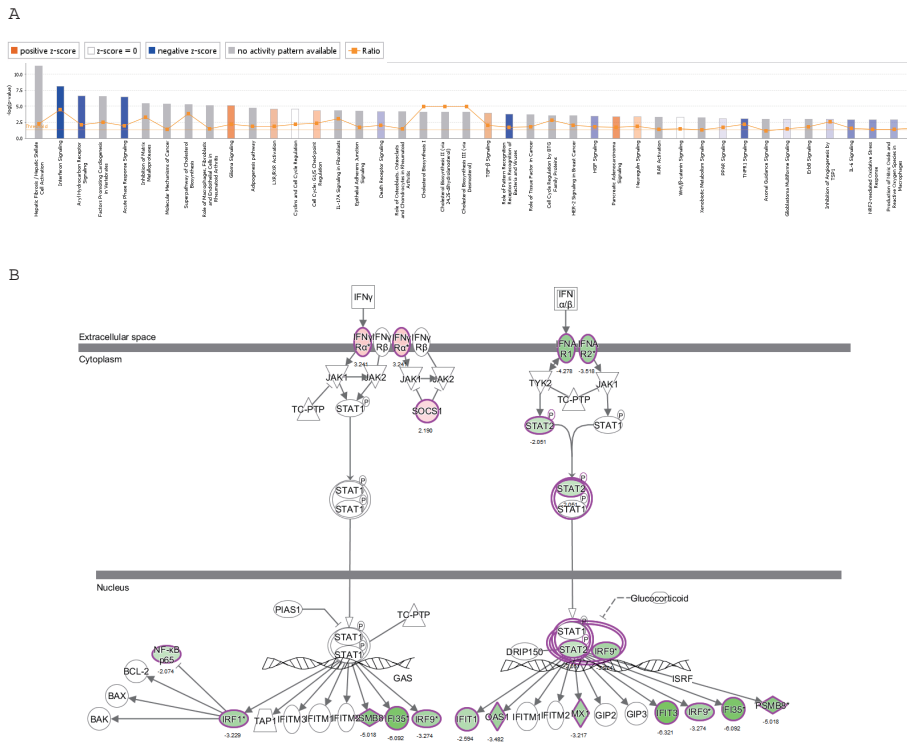

FIGURE 5 | The canonical pathway analysis by IPA®. **(A)** The enrichment of the DEGs in the canonical signaling pathway, sorted by –log(P). **(B)** The effect of experimental data on signal transfer in the interferon signaling pathway.

IPA® Bioinformatics Analysis-Diseases and Functional Analysis

Disease and functional analysis by IPA® evaluated the positive or negative correlation between NRP1 and other diseases or functions (**Figure 7A**). The annotation of diseases or functions with significant activation were cancer (z-score = 2.568), proliferation of tumor cells (z-score = 2.479), migration of endothelial cells (z-score = 2.535), cell movement of endothelial cells (z-score = 2.354), neovascularization (z-score = 2.073), etc. Alternatively, antiviral response (z-score = -3.213), immune response of cells (z-score = -2.974) and G1 phase (z-score = -2.176) were significantly inhibited (**Supplementary Table 6**). NRP1 silencing was related to many cancer-related functions, which is consistent with the results of cell function experiments. The heatmap demonstrates the relationship between DEG expression and activation or inhibition of diseases and function categories (**Figure 7B**). Antiviral response (z-score = -3.213) was the most significantly affected annotation sorted by | z-score| (**Supplementary Figure 2**).

IPA® Bioinformatics Analysis-Upstream Analysis and Validation

Analysis was performed to predict the upstream regulatory factors of DEGs (**Supplementary Table 7**. The predictive interactions were supported by literature based on the Ingenuity Pathway Knowledge Base (IPKB). IPA predicted upstream regulators related to tumorigenesis that were contained in the DEGs list, such as HIF1α (z-score = 2.376, overlap *p*-value = 1.2E-11), TGFβ (z-score = 4.222, overlap *p*-value = 1.181E-44), MAPK1 (z-score = 4.399, overlap *p*-value = 2.73E-29). Moreover, nuclear protein 1 (*NUPR1*) was predicted to be most strongly activated, with 74 consistent activated DEGs, while IFNB1 was predicted to be the most strongly repressed, with 37 consistent repressions. The *NUPR1* regulatory network containing the interacting genes in the DGEs list was presented in **Figure 7C**. The DEGs following *NRP1* silencing are primarily downstream of *NUPR1* in BC cells. Further validation by qRT-PCR found that *NRP1* was significantly downregulated when *NURP1* was knocked down (transfection efficiencies of shNUPN1 were respectively 85.3% and 64.6% inT24 and 5637 cells) (**Figure 7D**), suggesting that *NRP1* was regulated by *NUPR1*.

IPA® Bioinformatics Analysis-Molecular Interaction Network Analysis

IPA® uses a network generation algorithm to segment the molecular interaction network into multiple networks and scores each network. The score is based on the hypergeometric distribution, and the -log(P) value was obtained by Fisher's exact test. The top-ranked molecular interaction network was primarily enriched in diseases and functions related to cancer, organismal injury as well as abnormalities and cell cycle

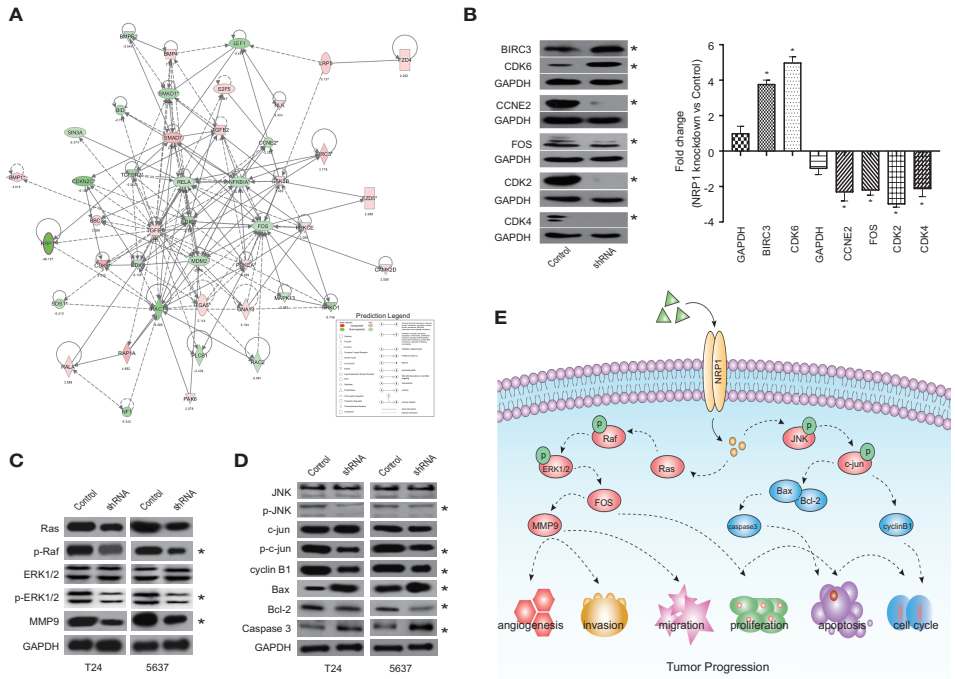

FIGURE 6 | Validation of pathways associated with NRP1 silencing. **(A)** The gene network map of molecular mechanisms of cancer pathway including the potential NRP1-regulated genes. **(B)** The protein expression of some known tumor-associated genes in molecular mechanisms of cancer pathway were confirmed using western blot in T24 cells with *NRP1* knockdown. Western blot was performed in three independent experiments and independently represent each internal control (GAPDH). **(C)** Western blot of ERK/MAPK related protein expression in T24 and 5637 BC cells after *NRP1* knockdown. **(D)** Western blot of JNK/MAPK related protein expression in T24 and 5637 BC cells after *NRP1* knockdown. **(E)** Proposed model for the molecular mechanisms underlying the action of NRP1 in BC progression. *$p < 0.05$ vs. the control group.

(**Supplementary Table 8**). The network including the altered genes following *NRP1* silencing are presented in **Figure 7E**.

IPA® Bioinformatics Analysis-Regulator Effects

The regulatory effect network analysis shows the interaction between genes and regulators and functions in the IPKB (**Supplementary Table 9**). The consistency score is a measure of causal consistency and dense connections between upstream regulatory factors and diseases and functions in IPKB. The higher the consistency score is, the more accurate the results of the regulatory effects prediction. The result of regulator analysis shows that *CX3CL1*, *FOXP3*, and *IFNA2* act as regulators through *FGF2, IL1B, MMP9, NRP1, PLAT, TGFB1, TLR3, TNFAIP3*, and *TNFSF10* to activate neovascularization; while NRP1 was predicted to bind with FOXP3 and FGF2 directly (**Figure 7F**). Further qRT-PCR detection showed that after *NRP1* silencing *FOXP3* was significantly upregulated, but *FGF2* gene was minor downregulated insignificantly (**Figure 7G**).

Analyses of *NRP1* in BC Cells *via* CCLE

The expression of *NRP1* can be detected in a variety of malignant cells (**Figure 8A**) and urinary tract cancer cells (**Figure 8B**) in Cancer Cell Line Encyclopedia (CCLE) database. Using the co-expression tool on expression data extracted from the 26 urinary tract cancer cell samples, we obtained lists of genes that are co-expressed with *NRP1*. Genes that harbor a correlation coefficient > 0.5 or <-0.5, and *p*-value <0.01 were selected. A total of 445 genes were positively and 433 were negatively correlated with *NRP1* expression (**Supplementary Table 10**). The expression data for the top 20 related up-and downregulated groups were depicted in heatmaps (**Figure 8C**). Notably, in the positive correlation list, *DCBLD2* was highly correlated with *NRP1* of 0.775, while the fold change of *DCBLD2* was -4.917 in T24 cells after *NRP1* knockdown by Gene Chip analysis, and *DCBLD2* was also found by qRT-PCR significantly downregulated by 0.751 Log2 fold in 5637 cells with *NRP1* silencing (**Figure 8D**). To identify the differentially activated signaling pathways in BC cells, Gene Set Enrichment Analysis (GSEA) was performed and the most significantly enriched signal transduction pathways were selected (**Figure 8E** and **Supplementary Table 11**). Focal adhesion, melanoma, and GAP junction were differentially enriched in phenotypes with high *NRP1* expression, while Peroxisome proliferator-activated receptor (PPAR) signaling and multiple metabolism-related pathways were significantly enriched in low *NRP1* expression phenotypes.

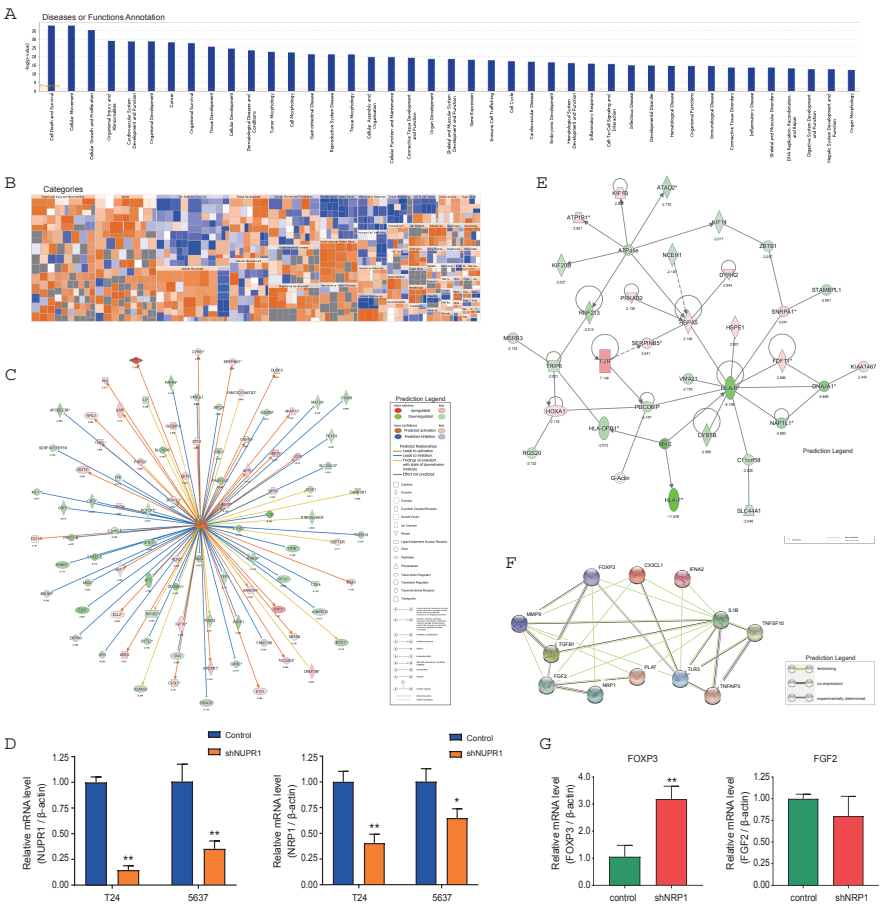

FIGURE 7 | Disease and functional, upstream and network analysis by IPA®. **(A)** Disease and functional analysis using IPA® evaluated the positive or negative correlation between NRP1 and other diseases or functions, which were ranked by log (*p*-value). **(B)** The heatmap demonstrates the relationship between DEGs expression and activation or inhibition of diseases and functions categories. **(C)** Upstream analysis predicted that the NUPR1 regulatory network was activated after *NRP1* was knocked down. **(D)** T24 and 5637 cells were infected with lentivirus-expressing NUPR1 or a control shRNA; the *NUPR1* and *NRP1* mRNA level was measured using qRT-PCR. **(E)** The molecular interaction network analysis predicted interaction among the molecules in the dataset and found that the top-ranked molecular interaction network was primarily enriched in the diseases and function categories of cancer, organismal injury and abnormalities and cell cycle, which including the altered genes after *NRP1* silencing are shown. **(F)** The regulatory effect network analysis revealed that NRP1 may be a regulator in neovascularisation activation. **(G)** the mRNA expression of *FOXP3 and FGF2* gene in 5637 cells with *NRP1* silencing were measured using qRT-PCR. $^{*}p < 0.05$ *vs*. the control group. $^{**}p < 0.01$ *vs*. the control group.

Construction of the ceRNA Sankey Diagram

Significant differential expressed lncRNA (DElncRNA), and differential expressed miRNA (DEmiRNA) between BC and adjacent non-cancer bladder tissues in the The Cancer Genome Atlas (TCGA) database were identified. A total of 1116 DElncRNAs (761 upregulated and 355 downregulated), and 368 DEmiRNAs (307 upregulated and 61 downregulated) were obtained (**Supplementary Figure 3** and **Supplementary Table 12**). Besides, miRNAs related to NRP1 were predicted in TargetScan. After selecting the miRNAs with differently regulated trends for both NRP1 and lncRNAs, a ceRNA Sankey diagram was constructed, including 38 lncRNA squares, four miRNA squares, and one NRP1 square (**Figure 8F**). NRP1 may be regulated by miR-204, miR-143, miR-145 and miR-195.

DISCUSSION

NRPs are a class of approximately 130-kDa multifunctional non-tyrosine kinase receptors. The main functional domain of NRPs consists of five domains: one intracellular, one transmembrane, and three extracellular (a1a2, b1b2, and c) domains (20). The membrane domain directly binds to type III semaphorins and VEGF and can initiate downstream signaling. Knockout of NRP1 and NRP2, the two major NRP subtypes, in mice induces hypoplasia and deficiency in the neural system, emphasising

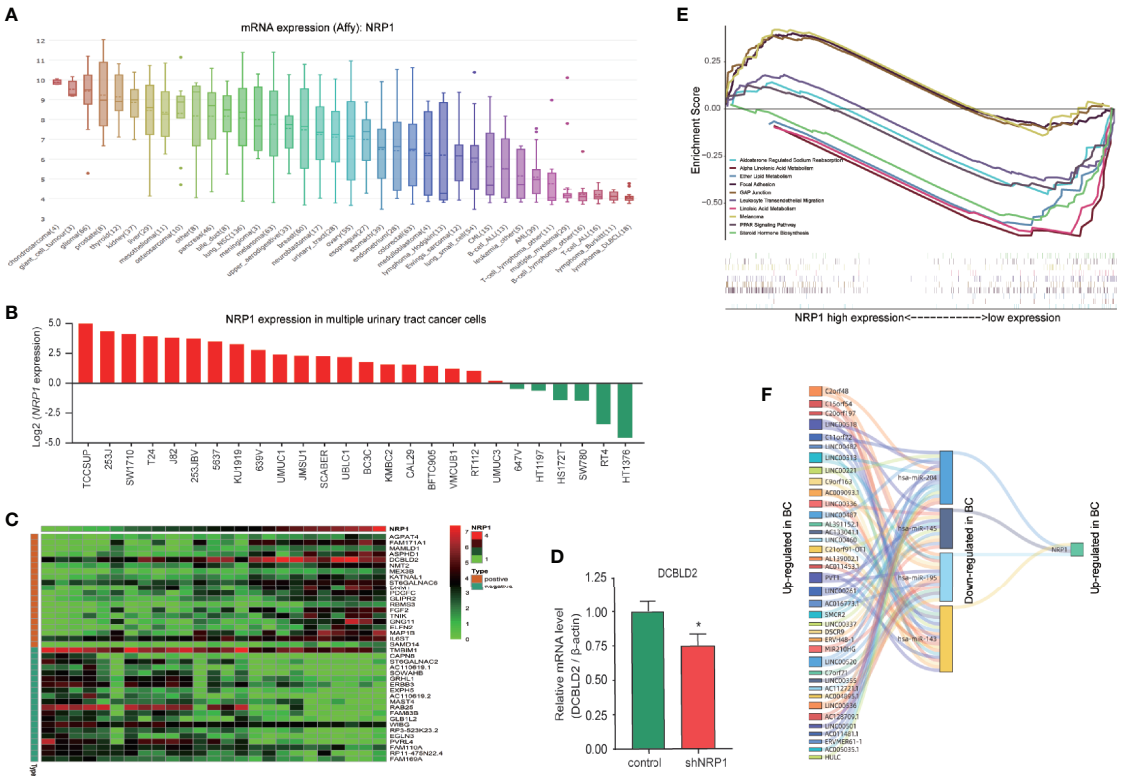

FIGURE 8 | Co-expressed genes analysis and ceRNA network prediction. **(A)** *NRP1* mRNA expression in various cancer cell lines obtained from CCLE database. The abscissa is the tumor type and sample size, and the ordinate is the expression of target genes. **(B)** *NRP1* mRNA expression in 26 urinary tract cancer cells extracted from CCLE database. We took the logarithm *of* the original data for better visualization. **(C)** Heatmap of the top 20 co-expressed genes with *NRP1* in urinary tract cancer cells in both upregulated and downregulated groups. **(D)** the mRNA expression of *DCBLD2* in 5637 cells with *NRP1* silencing were measured using qRT-PCR. $^{*}p < 0.05$ *vs*. the control group. **(E)** The significantly enriched signal transduction pathways of co-expressed genes of *NRP1* in urinary tract cancer cells obtained using GSEA analysis. **(F)** A ceRNA sankey diagram of NRP1 constructed using the data extracted from TCGA database.

their roles in neural development (21). NRP1 is overexpressed in numerous human tumor tissues, including breast, lung, colorectal, and hepatocellular cancer (5, 22). Further, NRP1 expression is positively associated with prostate-specific antigen and Gleason score in prostatic cancer (23), while overexpression may contribute to autocrine-paracrine interactions in pancreatic cancer (24). Herein, high-expressed NRP1 was detected in a variety of BC cell lines by qRT-PCR and human BC tissues by IHC, whose overexpression has been reported to be associated with tumor progression and poor prognosis in patients with BC; however, the underlying molecular mechanisms remain poorly understood (7). Therefore, identifying the mechanisms by which NRP1 modulates the progression of BC may prove significant for exploring and optimising the therapeutic strategy for urological malignancies.

In this study, by comparing the expression of *NRP1* in muscle invasive BC tissues to that in non-muscle invasive BC tissues, we found that increasing *NRP1* was significantly associated with advanced tumor stage. Besides, silencing *NRP1* could promote apoptosis and reduce proliferation, angiogenesis, migration, and invasion in two aggressive BC cell lines. These results clearly identify NRP1 as a tumor promoter in BC and suggest that it has the potential to serve as a target for BC treatment. To better understand how NRP1 drive BC progression, global gene expression profiling using microarray technology and bioinformatics analysis were then performed. According to the enriched KEGG pathway items, the alteration of MAPK signaling contains the largest number of upregulated DEGs. MAPK signaling has been reported to modulate several key biological processes during the development and progression of BC and is regarded as a regulator of cell proliferation, angiogenesis, invasion, and metastasis (25). Ceccarelli et al. reported that NRP1 is responsible for keratinocyte growth factor-dependent ERK/MAPK pathway activation in human adipogenesis (26). Thus, we sought to explore the impact of NRP1 on MAPK pathway activation in BC cells. Key protein markers for MAPK signaling pathway were examined by western blot, and the results indicated that silencing of NRP1 would decrease the activity of phosphorylated ERK and JNK. Additionally, BAX/BCL2 and caspase 3 were upregulated, implying that NRP1 knockdown attenuated anti-apoptotic signals, allowing for the induction of apoptosis. Collectively, these findings suggested that NRP1 could be considered as a vital contributor in BC tumorigenesis and progression through MAPK signaling.

Canonical pathway analysis by IPA® also revealed that all significantly altered genes following *NRP1* knockdown exhibited a significant enrichment in many tumorigenesis- and development-related pathways, which is consistent with the results of KEGG and western blot analysis. Among these pathways, interferon signaling was the top enriched signaling pathway ranked in the |z-score|>2. The expression of interferon-γ receptor was significantly increased after *NRP1* silencing, which is not only used as a therapeutic agent for BC treatment but is activation in bladder tumor cells is required for Bacillus Calmette-Guérin-induced tumor elimination and tumor-specific immune memory (27). Additionally, the molecular mechanisms of cancer pathway were chosen to explore the alteration of tumor-related genes following *NRP1* knockdown in BC. In total, 48 genes were significantly enriched in this pathway. Among these DEGs identified, *CDK6* was the most significantly upregulated gene, and *CDK2* was the most significantly downregulated gene. CDK6 plays an important role in the cell cycle. To drive the progression of the cell cycle, CDK6 binds to, and is activated by, cyclin D to enhance the transition through the G1 phase (28). Wang et al. confirmed that the increased expression of CDK6 was synchronous with the development of BC, indicating that it could be considered a prognostic biomarker for patients with BC (29). Additionally, abnormal CDK6 expression has been detected in breast cancer (30), pancreatic cancer (31), malignant glioma (32), and medulloblastoma (33). Activation of cyclin E/CDK2 and cyclin D1/CDK4 in cell cycle progression could contribute to urothelial proliferation (34), while downregulation of CDK2 in BC was first reported in this study. Collectively, our bioinformatic analysis indicated that NRP1 may influence BC progression through CDK6 and CDK2, as well as BIRC3, CDK4, CCNE2 and FOS, although this requires further validation.

According to the disease and function analysis, we found that *NRP1* knockdown is associated with many malignant tumor-related functions. Among them, antiviral response was the most significantly affected annotation sorted by | z-score|. There is a growing appreciation for roles played by NRP1 in the immune response, especially in the function of regulatory T cell response to virus infection (35, 36). In fact, investigations of the possible correlation between infection with different viruses, including human papilloma virus (HPV), human immunodeficiency virus (HIV), polyomavirus (BK) virus, herpes simplex virus, human T cell lymphotropic virus type 1 (HTLV-1), or Epstein-Barr virus (EBV), and the occurrence of BC are underway (37, 38). As reported, the prevalence of HPV varies greatly in BC cases, while a strong positive association between EBV infection and pathogenesis of primary urothelial transitional cell carcinoma has been found (38). Although only a limited number of BC cases have been linked with HIV infection, BC is part of the growing list of cancers that may be encountered in HIV-infected patients (39). Although the association between NRP1 and HPV remains elusive, HIV could lead to upregulation of NRP1 and suppress the expression of semaphorin 3a in the podocyte (40), while inhibiting VEGF from binding to NRP1 in endothelial cells to block angiogenesis and induce apoptosis (41). Besides, the NRP1 contains domains that directly interact with HTLV-1 (36) and EBV (42). Furthermore, NRP1 is identified as an EBV entry factor, its overexpression enhances EBV infection in nasopharyngeal epithelial cells (42), and highly expressed NRP1 could be consider as an undesirable independent prognostic factor in EBV-associated lymphomas (43). Taken together, the antiviral effect of NRP1 may provide new sight into the understanding of BC therapy.

The regulatory effect network analysis speculated that *NRP1, FGF2, IL1B, MMP9, PLAT, TGFB1, TLR3, TNFAIP3*, and *TNFSF10* might activate neovascularization through interacting with *CX3CL1, FOXP3*, and *IFNA2*, and NRP1 was predicted to directly bind with FGF2 and FOXP3. It has been reported that, in addition to VEGF and semaphorins 3a, NRP1 also specifically binds with several growth factors, including fibroblast growth factor 2 (FGF2), hepatocyte growth factor, platelet derived growth factor, placental growth factor, and transforming growth factor β1 (TGF-β1) (44). FGF2 can promote tumor angiogenesis and metastasis (45, 46). There is also evidence showing that FOXP3 suppresses angiogenesis by inhibiting VEGF expression in breast cancer (47), and on T regulatory cells, FOXP3 contributes to immunosuppression in a NRP1-dependent manner (48). In our study, the results of Gene Chip analysis showed that after *NRP1* silencing *FOXP3* gene was upregulated by 2.188 Log^2 fold and *FGF2* was downregulated by 1.026 Log^2 fold. Besides, validation in 5637 cells suggested that when *NRP1* was knocked down *FOXP3* was significantly upregulated, but *FGF2* gene was minor downregulated insignificantly. Our findings are in line with trends found in the literature (45, 47). We therefore speculate that *NRP1* silencing exert anti-angiogenic effects by upregulating *FOXP3* expression. To the best of our knowledge, this is the first time that a negative correlation has been revealed between NRP1 and FOXP3. Certainly, the specific role of NRP1 in FOXP3 as well as FGF2 mediated angiogenesis requires further exploration by biological experiments. On the other hand, cumulating evidence indicates that MAPK signaling activation is associated with VEGF-mediated tumor progression in bladder cancer (49), which was also observed in epidermal cancer stem cells but in a NRP1-dependent manner to enhance angiogenic potential, invasion and migration (50). These findings also coincide with our observations in BC cells that NRP1 silencing lead to the inhibition of angiogenesis and MAPK signaling activity.

The co-expressed genes with *NRP1* in multiple urinary tract cancer cells were obtained, and the corresponding pathways were identified. *DCBLD2*, the co-expressed gene, was also remarkably downregulated by 2.298 Log^2 fold by Gene Chip analysis in T24 cells after *NRP1* knockdown. Besides, PPAR signaling pathways were significantly enriched in low *NRP1* expression phenotypes. Although no study has directly demonstrated the interaction between DCBLD2 or PPAR signaling and NRP1, there is evidence of a potential association. DCBLD2, a neuropilin-related transmembrane protein expressed in endothelial cells (ECs), promotes endothelial VEGF signaling and regulates EC angiogenesis, proliferation and migration, which may serve as a therapeutic target for angiogenesis regulation. DCBLD2 also

associates with VEGFR2 and regulates its complex formation and mediates its trafficking (51). PPAR signaling has a pleiotropic impact on the regulation of cell growth and differentiation, and its role in the angiogenesis suppression is present in a VEGFR2-dependent manner (52).

We also performed upstream analysis to predict upstream regulators of DEGs following *NRP1* silencing, such as HIF1α, TGFβ, and MAPK1, which were all related to tumorigenesis. Notably, NUPR1, which is a transcription factor regulating a complex network of pathways and whose role in various types of cancer including BC has been reported yet remains incompletely understood, was predicted to be most strongly activated (53). NUPR1 participates in the regulation of tumor cell autophagy, apoptosis, growth, migration, and invasion (54); however, no study describing the association with NRP1 has been reported before. Herein, taken together results of Gene Chip analysis that *NUPR1* expression was not detected and *DCBLD2* was significantly downregulated after stable *NRP1* knockdown, it is reasonable to speculate that *NRP1* may be the downstream target of *NUPR1* and essential for regulation of *DCBLD2* expression. Further cell *in vitro* experiments showed a significant decrease of *NRP1* when *NURP1* was knocked down, and a significant decrease of *DCBLD2* after *NRP1* silencing, which demonstrated for the first time that *NRP1* is the downstream target of *NUPR1* and the upstream regulator of *DCBLD2*. Certainly, the specific roles of NUPR1 and DCBLD2 in NRP1 mediated malignant phenotype require further exploration by biological experiments.

Additionally, the ceRNA network analysis results demonstrate that NRP1 may be regulated by miR-204, miR-143, miR-145 and miR-195 in BC. These miRNAs are associated with neovascularisation and all involve VEGF regulation, however, miR-145 has been reported to directly interact with NRP1. miR-145 plays an crucial role in the regulation of interferon-β induction in BC cells (55), and the miR-145-3p/NRP1 axis targeted by the circRNA009723 (circDcbld1) might be a feasible approach to regulate vascular smooth muscle cell migration and alleviate intimal hyperplasia (circDcbld1) (56).

Taken together, these findings provide novel insights into the molecular mechanisms by which NRP1 drives the pathogenesis and progression of cancer. It would be reasonable to believe that targeting NRP1 may be a potential new therapeutic strategy that would be beneficial for more patients with BC or other cancers. Further research into the crucial mechanisms of NRP1 dysregulation in BC development is ongoing to better understand the biological basis of malignancy progression.

In conclusion, we provided evidence for NRP1 expression patterns in BC and found that inhibiting NRP1 expression could promote apoptosis and suppress proliferation, angiogenesis, migration, and invasion of BC cells, implying the potential of NRP1 as an attractive target in BC therapy. We also predicted and confirmed the effect of NRP1 on the activity of MAPK signaling and the dysregulation of genes involved in molecular mechanisms of cancer pathways. *NRP1* silencing also affected various biological functions, including antiviral response, immune response, cell cycle, proliferation and migration of cells, and neovascularisation. In addition, to our knowledge, the association between *NRP1* and *NUPR1, FOXP3*, and *DCBLD2*, for the first time, has been demonstrated. By analysing data extracted from multiple urinary tract cancer cells, PPAR signaling was found significantly associated with low *NRP1* expression. Moreover, NRP1 was predicted to be targeted by miR-204, miR-143, miR-145, and miR-195 in BC development. Further research into the crucial mechanisms of NRP1 dysregulation in BC aggression is also required to improve our understanding of the biological basis of malignancy progression.

DATA AVAILABILITY STATEMENT

The datasets presented in this study can be found in online repositories. The names of the repository/repositories and accession number(s) can be found in the article/**Supplementary Material**.

AUTHOR CONTRIBUTIONS

YD, W-mM, Z-dS, Z-gZ, LH, and C-hH designed this study. YD, W-mM, J-hZ, and LH performed experiments and analysed data. YaL, S-qZ, KP, LX, and B-bL performed bioinformatics analysis. G-yZ, RL, YiL, and C-hH provided technical support. W-dZ and TF performed the statistical analyses. YD, W-mM, and Z-dS drafted the manuscript. Z-gZ, LH, and C-hH provided critical comments, suggestions, and revised the manuscript. Z-dS, LH, and C-hH provided funding support. All authors contributed to the article and approved the submitted version.

FUNDING

This work was supported by the National Natural Science Foundation of China [grant numbers 82004110 and 81774089]; the Medical Innovation Team Project of Jiangsu Province [grant number CXTDA-2017-48]; the Key Research and Development Program of Jiangsu Province [grant numbers BE2020758 and BE2019637]; the High-level health talents "Six One Project" top talents [grant number LGY2019058]; the Key Project of Xuzhou Science and Technology [grant numbers KC19075 and KC18036]; and the Outstanding Medical Talent Project of Xuzhou [grant number 22 (2017)].

ACKNOWLEDGMENTS

We appreciate the public database provider and maintenance staffs.

SUPPLEMENTARY MATERIAL

The Supplementary Material for this article can be found online at: https://www.frontiersin.org/articles/10.3389/fonc.2021.685980/full#supplementary-material

REFERENCES

1. Siegel RL, Miller K D, Jemal A. Cancer Statistics, 2019. *CA Cancer J Clin* (2019) 69(1):7–34. doi: 10.3322/caac.21551
2. Feng RM, Zong YN, Cao S M, Xu RH. Current Cancer Situation in China: Good or Bad News From the 2018 Global Cancer Statistics? *Cancer Commun (Lond)* (2019) 39(1):22. doi: 10.1186/s40880-019-0368-6
3. Smaldone MC, Jacobs BL, Smaldone A M, Hrebinko RLJr. Long-Term Results of Selective Partial Cystectomy for Invasive Urothelial Bladder Carcinoma. *Urology* (2008) 72(3):613–6. doi: 10.1016/j.urology.2008.04.052
4. Vashistha V, Quinn DI, Dorff T B, Daneshmand S. Current and Recent Clinical Trials for Perioperative Systemic Therapy for Muscle Invasive Bladder Cancer: A Systematic Review. *BMC Cancer* (2014) 14:966–80. doi: 10.1186/1471-2407-14-966
5. Jubb AM, Strickland LA, Liu SD, Mak J, Schmidt M, Koeppen H. Neuropilin-1 Expression in Cancer and Development. *J Pathol* (2012) 226(1):50–60. doi: 10.1002/path.2989
6. Kawasaki T, Kitsukawa T, Bekku Y, Matsuda Y, Sanbo M, Yagi T, et al. A Requirement for Neuropilin-1 in Embryonic Vessel Formation. *Development* (1999) 126(21):4895–902. doi: 10.1242/dev.126.21.4895
7. Cheng W, Fu D, Wei ZF, Xu F, Xu XF, Liu YH, et al. NRP-1 Expression in Bladder Cancer and its Implications for Tumor Progression. *Tumour Biol* (2014) 35(6):6089–94. doi: 10.1007/s13277-014-1806-3
8. Pang K, Zhang Z, Hao L, Shi Z, Chen B, Zang G, et al. The ERH Gene Regulates Migration and Invasion in 5637 and T24 Bladder Cancer Cells. *BMC Cancer* (2019) 19(1):225. doi: 10.1186/s12885-019-5423-9
9. Dyrskjot L, Kruhoffer M, Thykjaer T, Marcussen N, Jensen JL, Moller K, et al. Gene Expression in the Urinary Bladder: A Common Carcinoma *in Situ* Gene Expression Signature Exists Disregarding Histopathological Classification. *Cancer Res* (2004) 64(11):4040–8. doi: 10.1158/0008-5472.CAN-03-3620
10. Borisov N, Tkachev V, Suntsova M, Kovalchuk O, Zhavoronkov A, Muchnik I, et al. A Method of Gene Expression Data Transfer From Cell Lines to Cancer Patients for Machine-Learning Prediction of Drug Efficiency. *Cell Cycle* (2018) 17(4):486–91. doi: 10.1080/15384101.2017.1417706
11. Song BN, Kim SK, Mun JY, Choi YD, Leem S H, Chu IS. Identification of an Immunotherapy-Responsive Molecular Subtype of Bladder Cancer. *EBioMedicine* (2019) 50:238–45. doi: 10.1016/j.ebiom.2019.10.058
12. Edgar R, Domrachev M, Lash AE. Gene Expression Omnibus: NCBI Gene Expression and Hybridization Array Data Repository. *Nucleic Acids Res* (2002) 30(1):207–10. doi: 10.1093/nar/30.1.207
13. Uhlen M, Fagerberg L, Hallstrom BM, Lindskog C, Oksvold P, Mardinoglu A, et al. Proteomics. Tissue-Based Map of the Human Proteome. *Science* (2015) 347(6220):1260419. doi: 10.1126/science.1260419
14. Barretina J, Caponigro G, Stransky N, Venkatesan K, Margolin AA, Kim S, et al. The Cancer Cell Line Encyclopedia Enables Predictive Modelling of Anticancer Drug Sensitivity. *Nature* (2012) 483(7391):603–7. doi: 10.1038/nature11003
15. The Gene Ontology C. Expansion of the Gene Ontology Knowledgebase and Resources. *Nucleic Acids Res* (2017) 45(D1):D331–D8. doi: 10.1093/nar/gkw1108
16. Kanehisa M, Furumichi M, Tanabe M, Sato Y, Morishima K. KEGG: New Perspectives on Genomes, Pathways, Diseases and Drugs. *Nucleic Acids Res* (2017) 45(D1):D353–D61. doi: 10.1093/nar/gkw1092. Kanehisa M,Goto S. KEGG: kyoto encyclopedia of genes and genomes. Nucleic Acids Res (2000) 28(1):27-30. doi: 10.1093/nar/28.1.27.
17. Yu G, Wang LG, Yan G R, He QY. DOSE: An R/Bioconductor Package for Disease Ontology Semantic and Enrichment Analysis. *Bioinformatics* (2015) 31(4):608–9. doi: 10.1093/bioinformatics/btu684
18. Yu G, Wang LG, Han Y, He QY. Clusterprofiler: An R Package for Comparing Biological Themes Among Gene Clusters. *OMICS* (2012) 16(5):284–7. doi: 10.1089/omi.2011.0118
19. Subramanian A, Tamayo P, Mootha VK, Mukherjee S, Ebert BL, Gillette MA, et al. Gene Set Enrichment Analysis: A Knowledge-Based Approach for Interpreting Genome-Wide Expression Profiles. *Proc Natl Acad Sci U S A* (2005) 102(43):15545–50. doi: 10.1073/pnas.0506580102
20. Appleton BA, Wu P, Maloney J, Yin J, Liang WC, Stawicki S, et al. Structural Studies of Neuropilin/Antibody Complexes Provide Insights Into Semaphorin and VEGF Binding. *EMBO J* (2007) 26(23):4902–12. doi: 10.1038/sj.emboj.7601906
21. Chen H, Bagri A, Zupicich JA, Zou Y, Stoeckli E, Pleasure SJ, et al. Neuropilin-2 Regulates the Development of Selective Cranial and Sensory Nerves and Hippocampal Mossy Fiber Projections. *Neuron* (2000) 25(1):43–56. doi: 10.1016/S0896-6273(00)80870-3
22. Lin J, Zhang Y, Wu J, Li L, Chen N, Ni P, et al. Neuropilin 1 (NRP1) Is a Novel Tumor Marker in Hepatocellular Carcinoma. *Clin Chim Acta* (2018) 485:158–65. doi: 10.1016/j.cca.2018.06.046
23. Yacoub M, Coulon A, Celhay O, Irani J, Cussenot O, Fromont G. Differential Expression of the Semaphorin 3A Pathway in Prostatic Cancer. *Histopathology* (2009) 55(4):392–8. doi: 10.1111/j.1365-2559.2009.03406.x
24. Fukahi K, Fukasawa M, Neufeld G, Itakura J, Korc M. Aberrant Expression of Neuropilin-1 and -2 in Human Pancreatic Cancer Cells. *Clin Cancer Res* (2004) 10(2):581–90. doi: 10.1158/1078-0432.CCR-0930-03
25. Dangle PP, Zaharieva B, Jia H, Pohar KS. Ras-MAPK Pathway as a Therapeutic Target in Cancer–Emphasis on Bladder Cancer. *Recent Pat Anticancer Drug Discov* (2009) 4(2):125–36. doi: 10.2174/157489209788452812
26. Ceccarelli S, Nodale C, Vescarelli E, Pontecorvi P, Manganelli V, Casella G, et al. Neuropilin 1 Mediates Keratinocyte Growth Factor Signaling in Adipose-Derived Stem Cells: Potential Involvement in Adipogenesis. *Stem Cells Int* (2018) 2018:1075156. doi: 10.1155/2018/1075156
27. Antonelli AC, Binyamin A, Hohl TM, Glickman M S, Redelman-Sidi G. Bacterial Immunotherapy for Cancer Induces CD4-Dependent Tumor-Specific Immunity Through Tumor-Intrinsic Interferon-Gamma Signaling. *Proc Natl Acad Sci U S A* (2020) 117(31):18627–37. doi: 10.1073/pnas.2004421117
28. Meyerson M, Harlow E. Identification of G1 Kinase Activity for Cdk6, a Novel Cyclin D Partner. *Mol Cell Biol* (1994) 14(3):2077–86. doi: 10.1128/mcb.14.3.2077
29. Wang G, Zheng L, Yu Z, Liao G, Lu L, Xu R, et al. Increased Cyclin-Dependent Kinase 6 Expression in Bladder Cancer. *Oncol Lett* (2012) 4(1):43–6. doi: 10.3892/ol.2012.695
30. Fogli S, Del Re M, Curigliano G, van Schaik RH, Lancellotti P, Danesi R. Drug-Drug Interactions in Breast Cancer Patients Treated With CDK4/6 Inhibitors. *Cancer Treat Rev* (2019) 74:21–8. doi: 10.1016/j.ctrv.2019.01.006
31. Sacaan AI, Thibault S, Hong M, Kondegowda NG, Nichols T, Li R, et al. CDK4/6 Inhibition on Glucose and Pancreatic Beta Cell Homeostasis in Young and Aged Rats. *Mol Cancer Res* (2017) 15(11):1531–41. doi: 10.1158/1541-7786.MCR-17-0172
32. Li B, He H, Tao BB, Zhao ZY, Hu GH, Luo C, et al. Knockdown of CDK6 Enhances Glioma Sensitivity to Chemotherapy. *Oncol Rep* (2012) 28(3):909–14. doi: 10.3892/or.2012.1884
33. Raleigh DR, Choksi PK, Krup AL, Mayer W, Santos N, Reiter JF. Hedgehog Signaling Drives Medulloblastoma Growth *via* CDK6. *J Clin Invest* (2018) 128(1):120–4. doi: 10.1172/JCI92710
34. Chang HR, Lian JD, Lo CW, Chang YC, Yang M Y, Wang CJ. Induction of Urothelial Proliferation in Rats by Aristolochic Acid Through Cell Cycle Progression *Via* Activation of Cyclin D1/Cdk4 and Cyclin E/Cdk2. *Food Chem Toxicol* (2006) 44(1):28–35. doi: 10.1016/j.fct.2005.06.002
35. Hwang JY, Sun Y, Carroll C R, Usherwood EJ. Neuropilin-1 Regulates the Secondary CD8 T Cell Response to Virus Infection. *mSphere* (2019) 4(3):e00221–19. doi: 10.1128/mSphere.00221-19
36. Kusunoki H, Tanaka T, Kohno T, Matsuhashi K, Hosoda K, Wakamatsu K, et al. A Novel Neuropilin-1-Binding Sequence in the Human T-Cell Lymphotropic Virus Type 1 Envelope Glycoprotein. *Biochim Biophys Acta Proteins Proteom* (2018) 1866(4):541–8. doi: 10.1016/j.bbapap.2018.02.003
37. Abol-Enein H. Infection: Is it a Cause of Bladder Cancer? *Scand J Urol Nephrol Suppl* (2008) 218):79–84. doi: 10.1016/s1473-3099(19)30402-5
38. Chuang C K, Liao SK. Epstein-Barr Virus Infection in Urothelial Transitional Cell Carcinoma Tissues. *BJU Int* (2004) 93(4):495–8. doi: 10.1111/j.1464-410x.2003.04687.x
39. Gaughan EM, Dezube BJ, Bower M, Aboulafia DM, Bohac G, Cooley TP, et al. HIV-Associated Bladder Cancer: A Case Series Evaluating Difficulties in Diagnosis and Management. *BMC Urol* (2009) 9:10. doi: 10.1186/1471-2490-9-10
40. Korgaonkar SN, Feng X, Ross MD, Lu TC, D'Agati V, Iyengar R, et al. HIV-1 Upregulates VEGF in Podocytes. *J Am Soc Nephrol* (2008) 19(5):877–83. doi: 10.1681/ASN.2007050629
41. Jia H, Lohr M, Jezequel S, Davis D, Shaikh S, Selwood D, et al. Cysteine-Rich and Basic Domain HIV-1 Tat Peptides Inhibit Angiogenesis and Induce

Endothelial Cell Apoptosis. *Biochem Biophys Res Commun* (2001) 283 (2):469–79. doi: 10.1006/bbrc.2001.4790
42. Wang HB, Zhang H, Zhang JP, Li Y, Zhao B, Feng GK, et al. Neuropilin 1 is an Entry Factor That Promotes EBV Infection of Nasopharyngeal Epithelial Cells. *Nat Commun* (2015) 6:6240. doi: 10.1038/ncomms7240
43. Gu YY, Luo B, Li CY, Huang LS, Chen G, Feng ZB, et al. Expression and Clinical Significance of Neuropilin-1 in Epstein-Barr Virus-Associated Lymphomas. *Cancer Biomark* (2019) 25(3):259–73. doi: 10.3233/CBM-192437
44. West DC, Rees CG, Duchesne L, Patey SJ, Terry CJ, Turnbull JE, et al. Interactions of Multiple Heparin Binding Growth Factors With Neuropilin-1 and Potentiation of the Activity of Fibroblast Growth Factor-2. *J Biol Chem* (2005) 280(14):13457–64. doi: 10.1074/jbc.M410924200
45. Sun HJ, Cai WW, Gong LL, Wang X, Zhu XX, Wan MY, et al. FGF-2-Mediated FGFR1 Signaling in Human Microvascular Endothelial Cells is Activated by Vaccarin to Promote Angiogenesis. *BioMed Pharmacother* (2017) 95:144–52. doi: 10.1016/j.biopha.2017.08.059
46. Teng Y, Guo B, Mu X, Liu S. KIF26B Promotes Cell Proliferation and Migration Through the FGF2/ERK Signaling Pathway in Breast Cancer. *BioMed Pharmacother* (2018) 108:766–73. doi: 10.1016/j.biopha.2018.09.036
47. Li X, Gao Y, Li J, Zhang K, Han J, Li W, et al. FOXP3 Inhibits Angiogenesis by Downregulating VEGF in Breast Cancer. *Cell Death Dis* (2018) 9(7):744. doi: 10.1038/s41419-018-0790-8
48. Campos-Mora M, Contreras-Kallens P, Galvez-Jiron F, Rojas M, Rojas C, Refisch A, et al. CD4+Foxp3+T Regulatory Cells Promote Transplantation Tolerance by Modulating Effector CD4+ T Cells in a Neuropilin-1-Dependent Manner. *Front Immunol* (2019) 10:882. doi: 10.3389/fimmu.2019.00882
49. Takeuchi A, Eto M, Shiota M, Tatsugami K, Yokomizo A, Kuroiwa K, et al. Sunitinib Enhances Antitumor Effects Against Chemotherapy-Resistant Bladder Cancer Through Suppression of ERK1/2 Phosphorylation. *Int J Oncol* (2012) 40(5):1691–6. doi: 10.1159/000331881
50. Grun D, Adhikary G, Eckert RL. NRP-1 Interacts With GIPC1 and SYX to Activate P38 MAPK Signaling and Cancer Stem Cell Survival. *Mol Carcinog* (2019) 58(4):488–99. doi: 10.1002/mc.22943
51. Nie L, Guo X, Esmailzadeh L, Zhang J, Asadi A, Collinge M, et al. Transmembrane Protein ESDN Promotes Endothelial VEGF Signaling and Regulates Angiogenesis. *J Clin Invest* (2013) 123(12):5082–97. doi: 10.1172/JCI67752
52. Meissner M, Hrgovic I, Doll M, Kaufmann R. Ppardelta Agonists Suppress Angiogenesis in a VEGFR2-Dependent Manner. *Arch Dermatol Res* (2011) 303(1):41–7. doi: 10.1007/s00403-010-1091-y
53. Mansour SMA, Ali SA, Nofal S, Soror SH. Targeting NUPR1 for Cancer Treatment: A Risky Endeavor. *Curr Cancer Drug Targets* (2020) 20(10):768–78. doi: 10.2174/1568009620666200703152523
54. Li A, Li X, Chen X, Zeng C, Wang Z, Li Z, et al. NUPR1 Silencing Induces Autophagy-Mediated Apoptosis in Multiple Myeloma Cells Through the PI3K/AKT/Mtor Pathway. *DNA Cell Biol* (2020) 39(3):368–78. doi: 10.1038/cddis.2016.175
55. Noguchi S, Yamada N, Kumazaki M, Yasui Y, Iwasaki J, Naito S, et al. Socs7, a Target Gene of Microrna-145, Regulates Interferon-Beta Induction Through STAT3 Nuclear Translocation in Bladder Cancer Cells. *Cell Death Dis* (2013) 4:e482. doi: 10.1038/cddis.2013.11
56. Rong ZH, Chang NB, Yao QP, Li T, Zhu XL, Cao Y, et al. Suppression of Circdcbld1 Alleviates Intimal Hyperplasia in Rat Carotid Artery by Targeting Mir-145-3p/Neuropilin-1. *Mol Ther Nucleic Acids* (2019) 18:999–1008. doi: 10.1016/j.omtn.2019.10.023

Conflict of Interest: The authors declare that the research was conducted in the absence of any commercial or financial relationships that could be construed as a potential conflict of interest.

frontiers in Oncology

ORIGINAL RESEARCH
published: 15 September 2021
doi: 10.3389/fonc.2021.714267

M6A Classification Combined With Tumor Microenvironment Immune Characteristics Analysis of Bladder Cancer

Huili Zhu, Xiaocan Jia, Yuping Wang, Zhijuan Song, Nana Wang, Yongli Yang and Xuezhong Shi**

Department of Epidemiology and Biostatistics, College of Public Health, Zhengzhou University, Zhengzhou, China

OPEN ACCESS

Edited by:
Bianca Nitzsche, Charité – Universitätsmedizin Berlin, Germany

Reviewed by:
Vito Mancini, University of Foggia, Italy
Riccardo Tellini, Careggi University Hospital, Italy

***Correspondence:**
Yongli Yang
ylyang377@zzu.edu.cn
Xuezhong Shi
xzshi@zzu.edu.cn

Specialty section:
This article was submitted to Genitourinary Oncology, a section of the journal Frontiers in Oncology

Received: *25 May 2021*
Accepted: *25 August 2021*
Published: *15 September 2021*

Citation:
Zhu H, Jia X, Wang Y, Song Z, Wang N, Yang Y and Shi X (2021) M6A Classification Combined With Tumor Microenvironment Immune Characteristics Analysis of Bladder Cancer. Front. Oncol. 11:714267. doi: 10.3389/fonc.2021.714267

Background: Studies have shown that N6-methyl adenosine (m6A) plays an important role in cancer progression; however, the underlying mechanism of m6A modification in tumor microenvironment (TME) cell infiltration of bladder cancer remains unclear. This study aimed to investigate the role of m6A modification in TME cell infiltration of bladder cancer.

Methods: The RNA expression profile and clinical data of bladder cancer were obtained from The Cancer Genome Atlas and Gene Expression Omnibus. We assessed the m6A modification patterns of 664 bladder cancer samples based on 20 m6A regulators through unsupervised clustering analysis and systematically linked m6A modification patterns to TME cell infiltration characteristics. Gene ontology and gene set variation analyses were conducted to analyze the underlying mechanism based on the assessment of m6A methylation regulators. Principal component analysis was used to construct the m6A score to quantify m6A modification patterns of bladder cancer.

Results: The genetic and expression alterations in m6A regulators were highly heterogeneous between normal and bladder tissues. Three m6A modification patterns were identified. The cell infiltration characteristics were highly consistent with the three immune phenotypes, including immune rejection, immune inflammation, and immune desert. The biological functions of three m6A modification patterns were different. Cox regression analyses revealed that the m6A score was an independent signature with patient prognosis (HR = 1.198, 95% CI: 1.031–1.390). Patients with a low-m6A score were characterized by increased tumor mutation burden, PD-L1 expression, and poorer survival. Patients in the low-m6A score group also showed significant immune responses and clinical benefits in the CTLA-4 immunotherapy cohort (p =0.0069).

Conclusions: The m6A methylation modification was related to the formation of TME heterogeneity and complexity. Assessing the m6A modification pattern of individual bladder cancer will improve the understanding of TME infiltration characteristics.

Keywords: m6A, bladder cancer, mutation burden, tumor microenvironment, immunotherapy

INTRODUCTION

Post-transcriptional modification is an important regulatory step in many physiological and disease progressions. More than 100 different types of post-transcriptional RNA chemical modifications have been identified in organisms (1). N6-methyl adenosine (m6A), one of the most abundant modifications in eukaryotic cells, has been identified as a post-transcriptional regulatory factor in various types of RNA, including messenger RNA, microRNA, and long non-coding RNA. It is also considered to be the most common RNA molecule with abundant modifications and plays an important role in the development of tumors (2). Like DNA and protein modification, m6A modification is a reversible process regulated by writers, readers, and erasers (3). Although the m6A methylation immunoprecipitation high-throughput sequencing technology has broken the understanding of m6A methylation site modification, the RNA fragments targeted by the technology are limited to around 100 nt long; thus, the methylation sites altered by single nucleotides cannot be detected (4). While the photo cross-linking assists m6A sequencing technology and m6A single-base resolution, purple foreign precipitation technology made the RNA m6A methylation site detection more accurate (5). In addition, the m6A regulatory factor is closely related to the activity of the urinary system tumor-related signaling pathways (6); therefore, exploring the relationship between m6A regulatory molecules and target gene RNA modification will help in understanding the mechanism behind the occurrence and development of bladder cancer.

The tumor microenvironment (TME) can promote tumor cell proliferation, invasion, and metastasis by regulating different signaling pathways (7). In the TME, certain types of lymphocytes can infiltrate into the tumor interior, which are called tumor-infiltrating lymphocytes, including T lymphocytes, B lymphocytes, and antigen-presenting dendritic cells (8, 9). Tumor-infiltrating lymphocytes mediate immunosuppression of the TME, which can help tumor cells achieve immune escape and then promote malignant development of tumors (10); therefore, different tumor immunophenotypes may be identified by analyzing the complexity and heterogeneity of the TME. The accurate prediction of the clinical efficacy of different immunotherapeutic approaches would also be improved (11, 12).

Recent studies have shown that different m6A modifications play an important role in different biological processes, such as inflammation, innate immunity, and TME (13–16). It has been shown that methylation of mRNA m6A accelerated the activation and function of dendritic cells (17). Li et al. (18) found that m6A-modified methylation controlled the steady-state differentiation of T cells by controlling the IL-7/STAT5/SOCS signaling pathway. Due to technical limitations, these studies were necessarily limited to one or two m6A regulators and cell types, but the antitumor effect was characterized by multiple tumor suppressor factors interacting through a high degree of synergy. The potential role of m6A modification in the tumor TME cell infiltration of bladder cancer has not been reported; hence, this study aimed to elucidate the role of m6A methylation modification combined with the TME of bladder cancer.

MATERIAL AND METHODS

Bladder Cancer Data Sources and Study Design

TCGA-BLCA (a dataset that included RNA sequencing data, genome mutation data, and clinical data) was downloaded from The Cancer Genome Atlas (TCGA) (https://tcga-data.nci.nih.gov/tcga/, accessed on January 12, 2020) (19). GSE13507 (a dataset that included RNA sequencing data and clinical data) was downloaded from the Gene-Expression Omnibus (GEO) (https://www.ncbi.nlm.nih.gov/geo/, accessed on January 12, 2020) (20). The transcripts per kilobase million (TPM) value was closer to the data of the GEO chip. We used the fpkm function of the "limma" package in R to convert the FPKM value of the RNA data to the TPM value (21). Compliant data sets were subjected to copy number variation (CNV) analysis. The plot of m6A regulator copy number changes in the chromosome was drawn using the "Rcircos" package.

NMF Consensus Molecular Clustering of 20 m6A Modulators

We used 20 m6A regulators to determine different m6A methylation modifications in bladder cancer, including 12 readers (YTHDC1, HNRNPA2B1, YTHDC2, FMR1, YTHDF1, YTHDF2, YTHDF3, IGF2BP1, IGF2BP2, IGF2BP3, LRPPRC, RBMX), 7 writers (METTL3, ZC3H13, METL16, RBM15, RBM15B, WTAP, VIRMA) and 1 eraser (ALKBH5). According to the expression of 20 m6A regulators, unsupervised cluster analysis in the "ConsensuClusterPlus" package was used to identify different m6A modification patterns.

Gene Set Variation Analysis and Gene Enrichment Function Annotation

We downloaded the gene sets of the "c2.cp.kegg.v6.2 symbol" from the Molecular Signatures Database (MSigDB) (22). Then, the "GSVA" package for enrichment analysis was used to study the difference in the activities of m6A modification patterns in biological processes (23). The gene ontology (GO) function annotations of m6A-modified phenotype-related genes were analyzed using the "clusterProfiler" package and FDR <0.01.

Immune Cell Difference Analysis

The TME-infiltrating immune cell gene set was obtained from the research of Pornpimol Charoentong. The gene set had a variety of human immune cell subtypes, including activated CD8 T cells, activated dendritic cells, giant natural killer T cells, and regulatory T cells. The single sample gene set enrichment analysis (ssGSEA) algorithm quantified the immune cell infiltration in bladder cancer TME. The difference analysis of immune cells was used to observe the difference between the m6A patterns of immune cells.

Screening of Differentially Expressed Genes Among Different Phenotypes of m6A

Different m6A modification patterns were typed by the consensus clustering algorithm. The R package "limma"

screened the m6A differentially expressed genes (DEG) between different m6A phenotypes. The gene with adjusted $p < 0.001$ was deemed as significant DEG. The relationship between m6A gene characteristics and related biological pathways was further explored through the correlation analysis.

Construction of m6A Gene Signature

Differential genes determined in different m6A clusters were normalized in bladder cancer samples to extract crossover genes. The unsupervised clustering method was used to analyze the degree of overlap, with the patients divided into several groups for further analysis. The consensus clustering algorithm was used to determine the number of gene clusters and their stability. Then, univariate Cox regression analysis was used to analyze the prognosis of each gene. Taking into account the correlation between genes, the traditional Cox regression model was not used directly; therefore, the differential genes related to prognosis obtained by univariate Cox regression were further analyzed with principal component analysis (PCA). Finally, PCA analysis was applied to construct the m6A-related gene signature and evaluate the m6A gene signature of each bladder cancer patient, which was called m6A score. Patients were divided into the high-score group and low-score group based on the maximally selected rank statistics.

Statistical Analysis

Correlation coefficients between the TME-infiltrating immune cells and the expression of m6A regulators were calculated by Spearman and differential expression analyses. One-way analysis of variance and the Kruskal–Wallis test were utilized to perform comparisons among three groups. Based on the correlation between m6A score and patient survival, the R package of "survminer" was used to determine the cutoff point for each dataset subgroup. Patients were then divided into the high-m6A score group or low-m6A score group based on the maximally selected rank statistics. The survival curves for the prognostic analysis were generated using the Kaplan–Meier method and log-rank test to identify the significance of differences. Univariate and multivariate Cox regression analyses were used to confirm the prognostic value of m6A score and various clinical characteristics. All statistical analyses were performed with R version 3.6.3.

RESULTS

The Genetic Variation Landscape of m6A Regulatory Factors in Bladder Cancer

This study identified 20 m6A regulators in bladder cancer, including 12 readers, 7 writers, and 1 eraser. **Figure 1A** shows the incidence of copy number variation and somatic mutations of the m6A regulatory factors in bladder cancer. **Figure 1B** shows the mutation frequency of each gene obtained by statistical analysis of the copy number of m6A. **Figure 1C** shows the m6A copy number circle diagram, which shows the position of the CNV mutation of the m6A regulatory factor on the chromosome. **Figure 1D** represents a further analysis of the m6A difference. The m6A-related gene difference analysis between normal samples and tumor samples indicated that CNV mutations may be significantly related to m6A modulator expression disorder. Compared with normal tissues, the expression of CNV-increased m6A modulators of bladder cancer tissues (such as METL3 and YTHDF1) was significantly increased. Conversely, the expression of CNV-deficient m6A modulators of bladder cancer tissues (such as ZC3H13 and WTAP) was reduced.

Identification of m6A Methylation Modification Patterns Mediated by Regulators

The GSE13507 (N = 165) of the GEO database and TCGA-BLCA (N = 403) datasets with complete survival data and corresponding clinical information were included to match the RNA samples. The m6A prognosis network diagram showed that most of the expression of m6A-related genes were positively correlated, with only negative correlations between IGFBP3 and ALKBH5, IGFBP3, and WTAP (**Figure 2A**). Based on the expression of m6A regulators, three modification patterns were eventually identified (**Figure S1**). The survival analysis of the m6A modification pattern showed that patients with modification patterns B and C had better survival rates than pattern A patients (**Figure 2B**).

Characteristics of TME Cell Infiltration Under Different m6A Modification Patterns

We used GSVA analysis to investigate the differences in biological function of different m6A modification patterns. As shown in **Figure 2C**, we observed the difference in functional pathways between different patterns. M6Acluster-A were mainly concentrated in stromal and carcinogenic activation pathways; m6Acluster-B were associated with immune activation, including the activation of the chemokine signaling pathway, T cell receptor signaling pathway, cytokine–cytokine receptor interaction, and Jak stat signaling pathways; and m6Acluster-C was significantly associated with immune desert biological processes (**Figure 2D**). Subsequent analysis of TME cell infiltration showed that m6Acluster-B was significantly enriched for innate immune infiltration of cells, including macrophages, mast cells, eosinophils, MDSC cells, and plasmacytoid dendritic cells. Three m6A modification patterns showed significantly different infiltration characteristics of TME cells (**Figure 3A**). The results of the PCA analysis showed significant differences between the transcriptome profiles of the three m6A modification patterns (**Figure 3B**). The heat map shows that m6A-related genes were highly expressed in m6Acluster-A, while most genes were negligibly expressed in m6Acluster-B and m6Acluster-C (**Figure 3C**). GO enrichment analysis showed that the differential genes were mainly enriched in the biological process (BP), embryonic skeletal system development, sodium ion homeostasis, and monovalent inorganic cation homeostasis (**Figure 3D**).

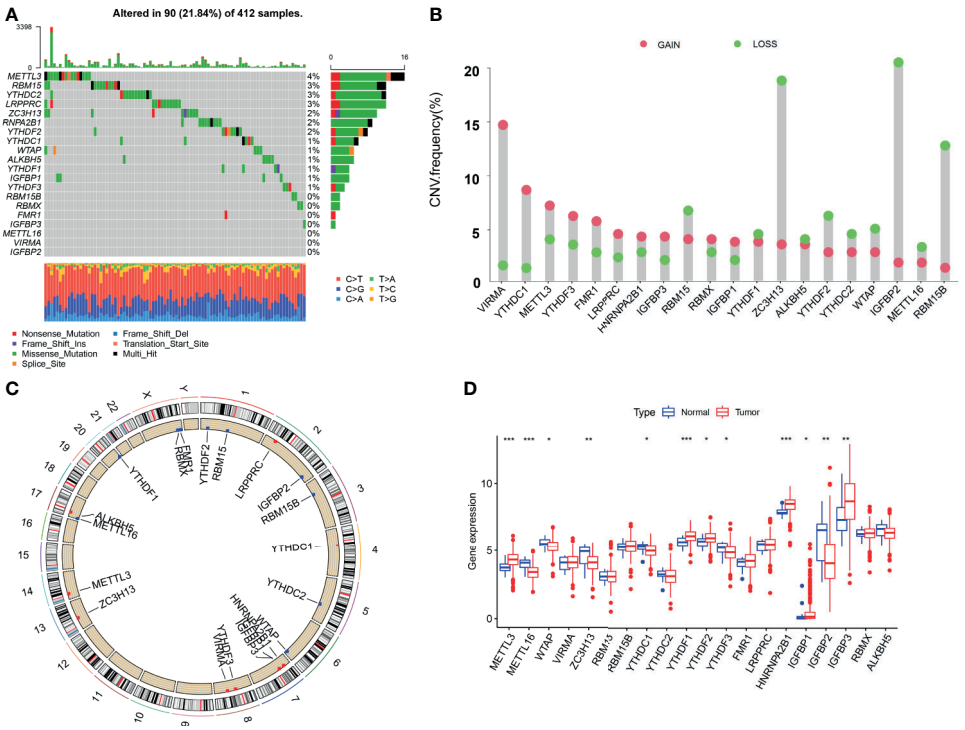

FIGURE 1 | Genetic landscape and expression changes of the m6A regulator in bladder cancer. **(A)** Mutation frequency of the m6A regulators of bladder cancer patients in the TCGA-BLCA cohort. **(B)** A histogram plotting the mutation frequency of each gene obtained by statistical analysis of the copy number of m6A. The abscissa was the m6A-related gene, and the ordinate was the mutation frequency. Red represents an increase in copy number, and green represents loss of copy number. **(C)** The m6A copy number circle graph. Red represents the sample with missing gene copy number than the sample with increasing copy number. Green represents the sample with missing gene copy number than the sample with increasing copy number. **(D)** The box plot of m6A differential expression analysis. Red represents the tumor sample, and green represents the normal sample. The *** represents p < 0.0001, ** represents p < 0.01, * represents p < 0.05.

Construction of m6A Gene Signature and Functional Annotation

In addition, we identified 44 m6A phenotype-associated DEGs. **Table 1** shows that univariate Cox regression analysis identified differential genes related to the prognosis of bladder cancer. Consistent with the m6A modification pattern, the unsupervised clustering algorithm also revealed three m6A modification genomic phenotypes (gene-Cluster A, gene-Cluster B, and gene-Cluster C) (**Figure S2**). The heat map of genetic modification patterns included clinical information. Most genes were low-expressed in gene-Cluster B and high-expressed in gene-Cluster C (**Figure 4A**).

Further survival analysis revealed significant differences among the three m6A modification genomic phenotypes in bladder cancer ($p < 0.001$). The survival curve showed that patients with gene-Cluster C had the worst prognosis (**Figure 4B**). M6A regulators were the source of prominent differences in the three m6A modification genomic phenotypes (**Figure 4C**). We developed an m6 score based on the m6A-related signature to quantify the m6A modification patterns in individual bladder cancer patients. Patients were divided into the high-m6A score group and the low-m6A score group according to the optimal cutoff value (1.3530). The alluvial diagram showed the flow of m6A score fraction construction (**Figure 4D**). Immune correlation analysis showed that the m6A score was significantly positively correlated with CD4 T immune cells, CD8 T immune cells, and dendritic immune cells (**Figure 4E**). The m6A score differed not only in the m6Acluster but also in the gene-Cluster. Differential expression analysis of m6A score in m6Acluster showed the highest score was in m6Acluster-B compared to the other clusters (**Figure 4F**). The highest score was in gene-Cluster B (**Figure 4G**).

Modification Characteristics of Molecular Subtype m6A and Tumor Somatic Mutations

Survival analysis showed that the prognosis of patients in the low-m6A score group was poorer than that in the high-m6A score group ($p < 0.001$) (**Figure 5A**). Bladder cancer samples were divided into a high mutation load group and a low mutation load group according to the expression of tumor mutation burden (TMB) (4.6578). Survival analysis of tumor mutation burden revealed that the prognosis of the group with a high tumor mutation burden was better than that of patients with a low tumor mutation burden ($p < 0.001$) (**Figure 5B**). More importantly, the survival curve of TMB combined with the m6A

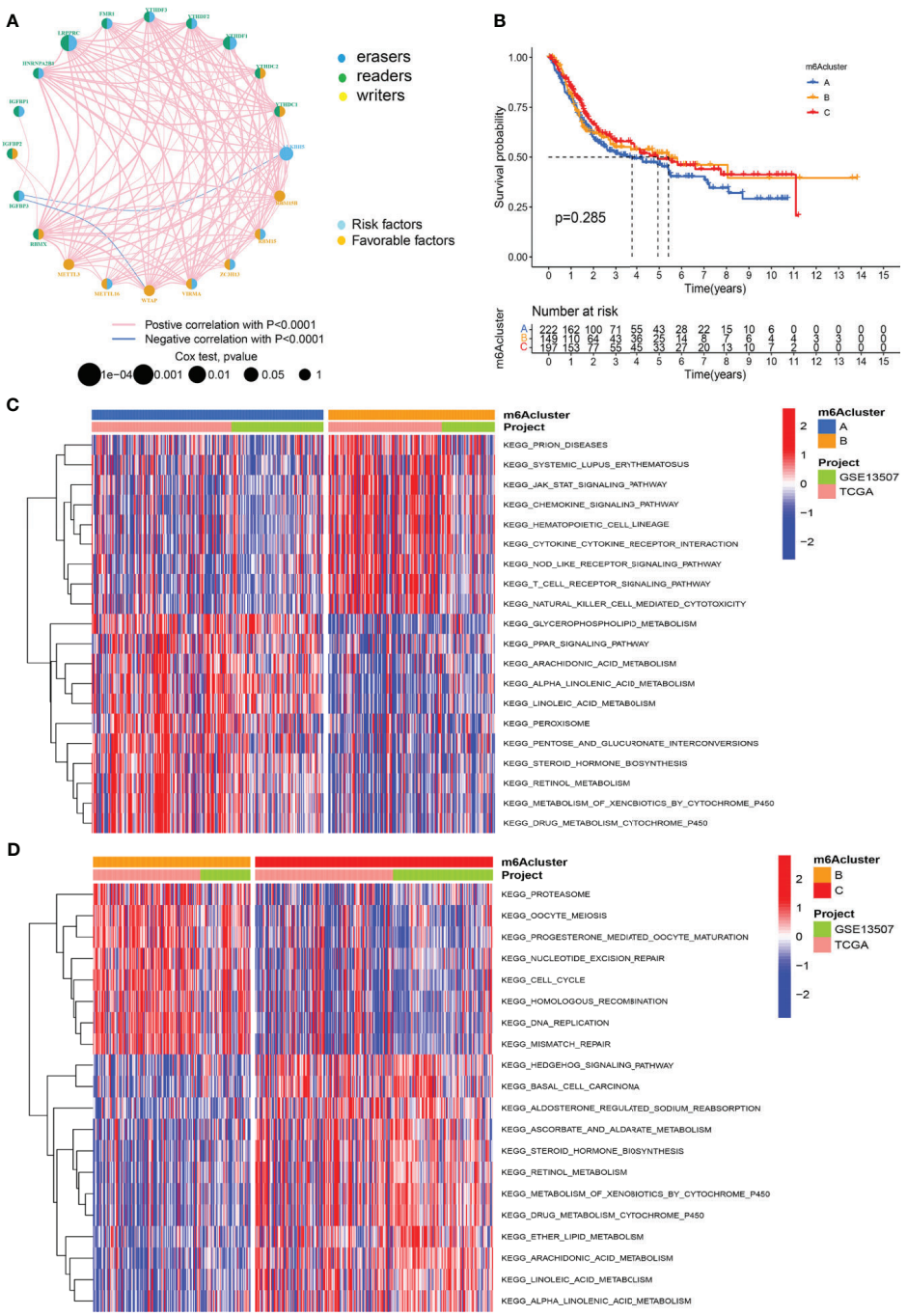

FIGURE 2 | M6A methylation modification patterns and the biological characteristics of each pattern. **(A)** M6A regulates the prognosis network diagram. **(B)** Survival analysis for m6A modification patterns. **(C)** GSVA analyzed the differences between functional pathways in m6A modification patterns. Blue represents the m6A modification pattern A, and orange represents the m6A modification pattern B. **(D)** GSVA analyzed the differences between functional pathways in m6A modification patterns. Orange represents the m6A modification pattern B, and red represents the m6A modification pattern C.

score showed that the patients in both the low tumor mutation group and the low-m6A score group had the worst prognosis (**Figure 5C**). The frequency (96.83%) was higher than the total gene mutation frequency of the high-m6A score group (87.39%) (**Figures 5D, E**).

M6A Clinical Correlation Analysis

According to the results of univariate and multivariate Cox regression analyses, the m6 score was identified as an independent prognostic variable of bladder cancer (**Figures 6A, B**). Through the survival analysis, we found that bladder cancer patients died mainly

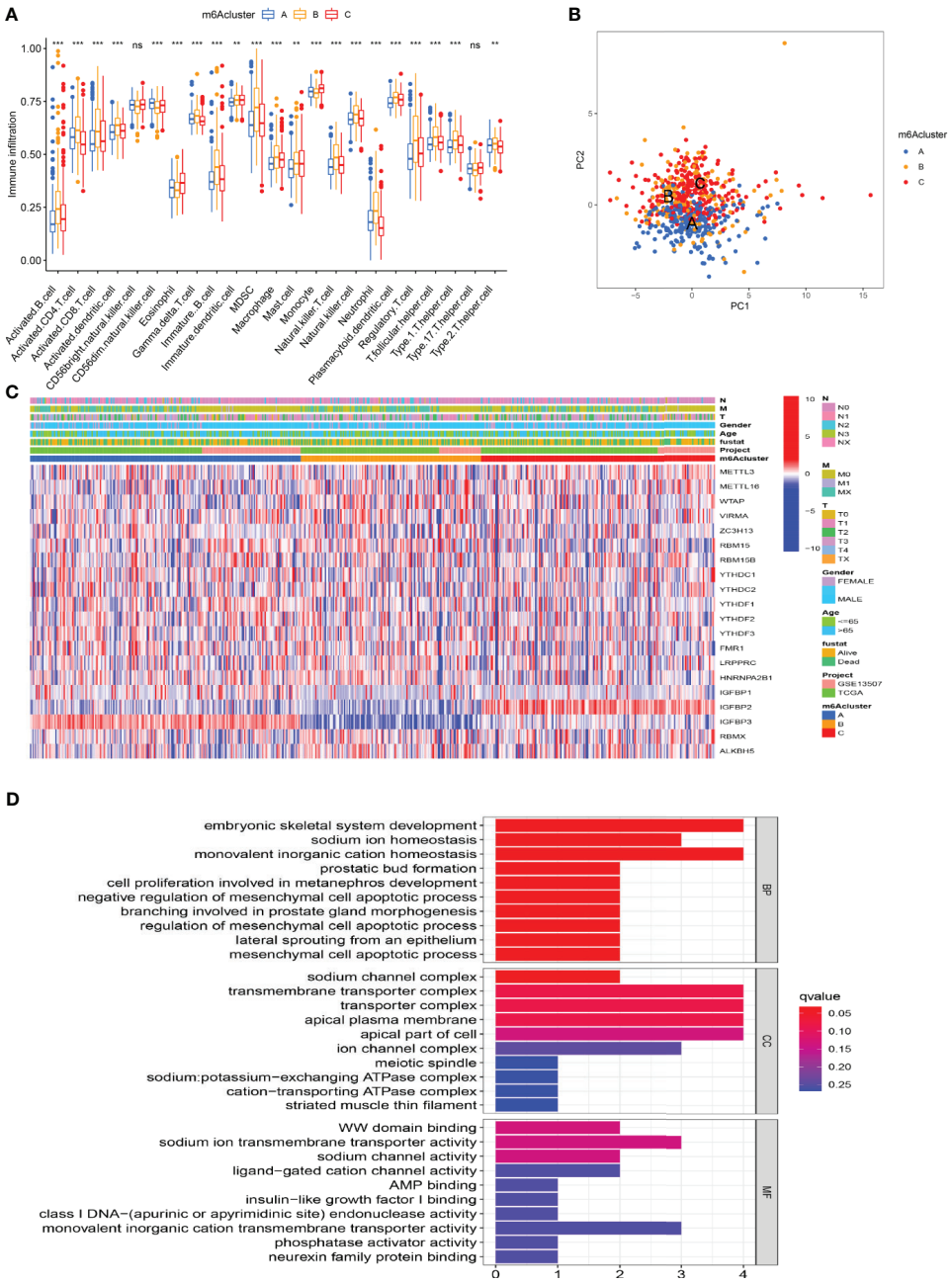

FIGURE 3 | Characterization of TME cell infiltration and transcriptome features in three m6A modification patterns. **(A)** The differential expression analysis of 23 immune cells among three m6A modification patterns. The *** represents p < 0.0001, ** represents p < 0.01 and ns represents no significance. **(B)** The scatter plot of PCA analysis. **(C)** Unsupervised clustering of 20 m6A regulators of bladder cancer. **(D)** GO enrichment analysis of m6A-related genes.

in the low-m6A score group (**Figure 6C**). The log-rank test showed that the survival time was significant between the high-m6A score group and the low-m6A score group (**Figure 6D**). Stratified analysis showed that patients in the high-m6A score group had a better prognosis than patients in the low-m6A score group of the male, N0, N1, M0, M1, T0–2, and T3–4 (**Figures 6E–I**). Based on the risk stratification analysis of tumor mutation burden, **Figure 6J** shows that m6A was suitable for the high- and low-score groups of tumor mutation burden (p = 1.6e-06). PD-L1 played an important role in bladder cancer. **Figure 6K** shows that PD-L1 made a difference between the high-m6A score group and the low-m6A score group (p = 2.1e-13).

Immunotherapy Analysis

Analysis of immunotherapy scores in the high-m6A score and low-m6A score groups showed that ICI therapy represented by

TABLE 1 | Univariate Cox regression analysis of differential genes in bladder cancer.

Gene	HR	95% *CI*	*p* value
TNFRSF21	0.9046	0.8186–0.9995	0.0490
SCNN1G	0.9328	0.8773–0.9919	0.0263
KRT7	0.9496	0.9041–0.9974	0.0389
STX2	1.2006	1.0597–1.3602	0.0041
DNAJB5	1.1432	1.0032–1.3026	0.0446
TNFAIP8L3	1.2044	1.0868–1.3348	0.0004
CRTAC1	0.9089	0.8614–0.9589	0.0005
ALDH1L1	0.9112	0.8494–0.9775	0.0094
ATOH8	0.8672	0.7941–0.9471	0.0015
KLHL3	0.7762	0.6638–0.9077	0.0010
ATP1A4	0.8503	0.7612–0.9498	0.0041
SHH	0.8887	0.8166–0.9671	0.0062
RBL1	1.3445	1.1126–1.6248	0.0022
MPPED2	0.8573	0.7570–0.9709	0.0153
KIFC1	1.2270	1.0540–1.4285	0.0083
CDKN3	1.2234	1.0844–1.3802	0.0010
RRM2	1.1268	1.0063–1.2616	0.0385
SBSN	1.0876	1.0370–1.1407	0.0006
NEIL3	1.1924	1.0313–1.3785	0.0175
TPM3	1.2968	1.0539–1.5957	0.0141

HR, hazard rate; CI, confidence interval.

the CTLA-4/PD-1 inhibitor played an important role in antitumor therapy. **Figure 7A** shows CTLA4 negative and PD-L1 negative therapy was different between the high-m6A score group and low-m6A score group (p = 0.00025). PD-1 immunotherapy showed no difference between the high-m6A score group and low-m6A score group (**Figure 7B**). **Figure 7C** shows CTLA-4 immunotherapy was different between the high-m6A score group and the low-m6A score group (p = 0.0069). CTLA-4/PD-1 immunotherapy showed no difference between the high-m6A score group and low-m6A score group (**Figure 7D**).

DISCUSSION

Determining the role of m6A RNA methylation modification in tumor mutation burden cell infiltration will help understand the mechanism of TME antitumor immune response. In this study, we confirmed three m6A methylation modification patterns based on 20 m6A regulators characterized by different immune phenotypes. The combination of TME cell infiltration characteristics in different m6A modification patterns will improve the knowledge of TME antitumor immune response of bladder cancer.

In this study, we found that three m6A methylation modification patterns had a significant correlation with immune activation and other pathways. M6Acluster-A was characterized by the activation of immunity and lymphocyte infiltration. M6Acluster-B featured the presence of immune cells, as well as the activation of EMT and Wnt signaling pathways, which was consistent with the immune rejection phenotype. M6Acluster-C was consistent with the immune desert phenotype. The immune rejection phenotype showed the presence of a large number of immune cells and the forming of immune cells inside the cancer (8). The immune desert phenotype was related to immune tolerance and lack of activated and initiated T cells (24). The above studies were in line with our findings. This confirmed that m6A modification patterns had a very important significance in shaping a different TME landscape. Many recent studies have found that the biological functions of immune cells play an important role in the TME and cancer immunotherapy (25, 26). The relevant immune cells in the TME mainly included antitumor immune cells and tumor-promoting immune cells. It is worth noting that these two types of cells play different roles in different stages of tumor progression. Antitumor immune cells mainly include effector T cells (CD8+ cytotoxic T cells and effector CD4+ T cells) and dendritic cells (27). The mechanism of CD4+ T cells was to use the cross to provide tumor antigens and costimulatory molecules to CD8+ T cells, allowing dendritic cells to activate CD8+ T cells (28, 29); hence, a comprehensive analysis of the m6Acluster will help us understand the infiltration characteristics of TME cells.

Further, reflecting the results for m6A modification patterns, m6A-related signature genes' differences were related to the immune-related pathway. This demonstrated the importance of m6A modification patterns in shaping variant TME landscapes. Due to the heterogeneity and specificity of m6A-modified individuals, we constructed a score model to assess the m6A modification pattern of individual patients with bladder cancer. The m6A modification pattern of the immune rejection phenotype had a higher m6A score, while the m6A modification pattern of the immunoinflammatory phenotype had a lower m6A score. The m6A score was positively correlated with CD4 T immune cells, CD8 T immune cells, and dendritic immune cells. This indicated that the m6A score was a dependable and stable tool for the comprehensive assessment of the modification pattern of individual tumor m6A. In addition, while univariate and multivariate Cox regression analysis indicated that the m6A score may be an independent prognostic factor, a study has suggested distinguishing between invasive and non-invasive micropapillary carcinoma of the bladder, as the latter may not predict a poor prognosis (30). Variant histology may be related to survival outcomes (31). Further studies on the relationship between variant histology and m6A are still needed. Even so, we observed that the m6A score was strongly related to the tumor immunophenotype. The frequency of gene mutations in the low-m6A score group was higher than the total gene mutation frequency in the high-m6A score group. The immunotherapy scores of the high-m6A score and low-m6A score group were different. There are different treatment methods for CTLA-4 immunotherapy between the high and low groups. The high-m6A score group of bladder cancer patients had obvious clinical advantages. This indicated that m6A modification may influence the curative effect of immunotherapy.

Previous studies had shown that m6A-related genes, including METTL3, were negatively correlated with the recurrence of bladder cancer patients (32, 33). The expression of the catalytic subunit METTL3 of MTC was significantly upregulated in bladder cancer tissues and was related to the development and progression of bladder cancer patients (25). Studies also found that YTHDF1/YTHDF3 can preferentially identify the m6A-modified region in

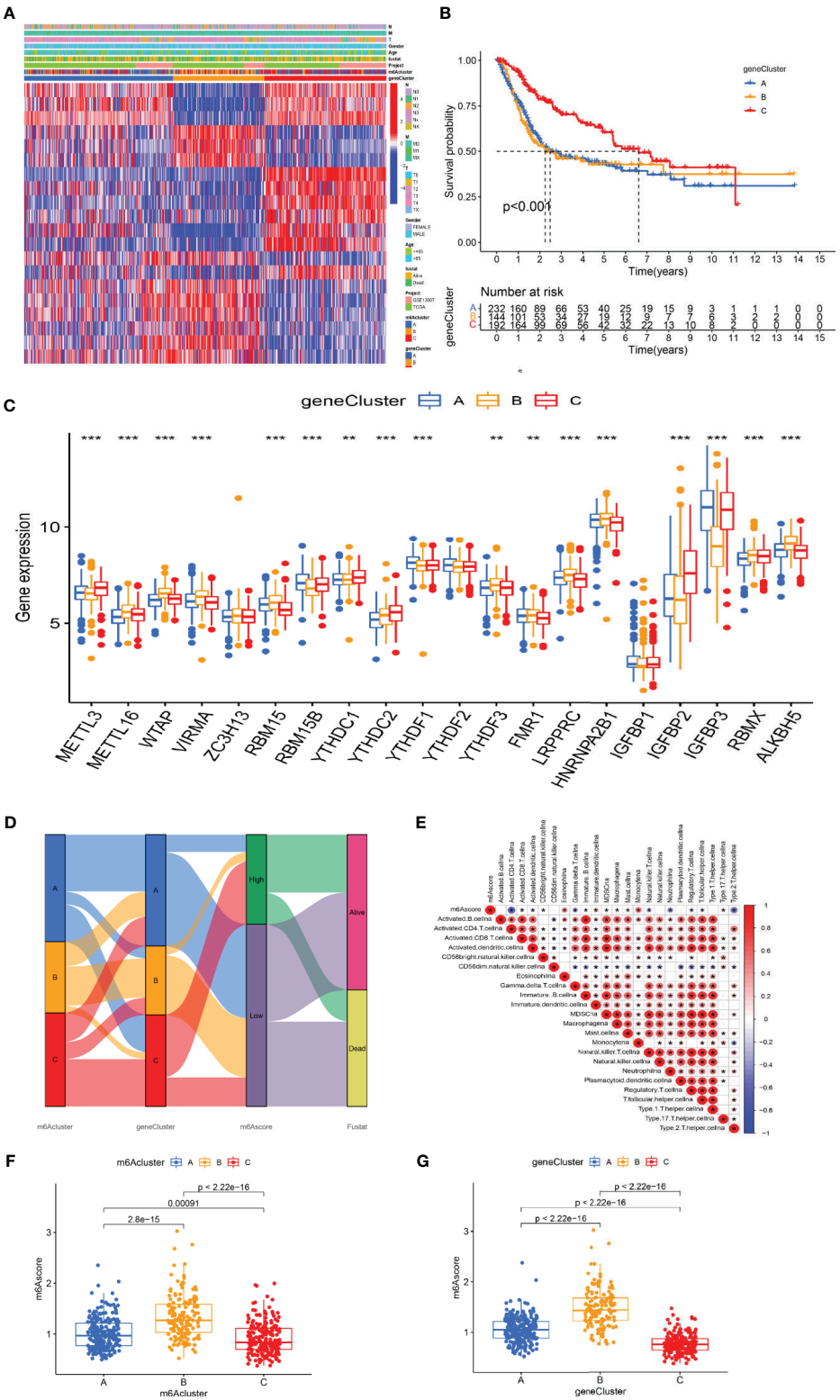

FIGURE 4 | The development of m6A signature. **(A)** The heat map of genetic modification patterns. **(B)** Survival curves of different gene-Clusters. **(C)** Box plot of the differential expression analysis of m6A-related genes among different gene-Clusters. The *** represents p < 0.0001, ** represents p < 0.01. **(D)** Sankey diagrams of different genotypes. **(E)** The correlation analysis between the m6A score and immune cells, with red indicating positive correlation and blue indicating negative correlation. **(F)** Differential expression analysis of the m6A score in the m6A cluster. **(G)** Difference analysis of the m6A score in the gene-Cluster.

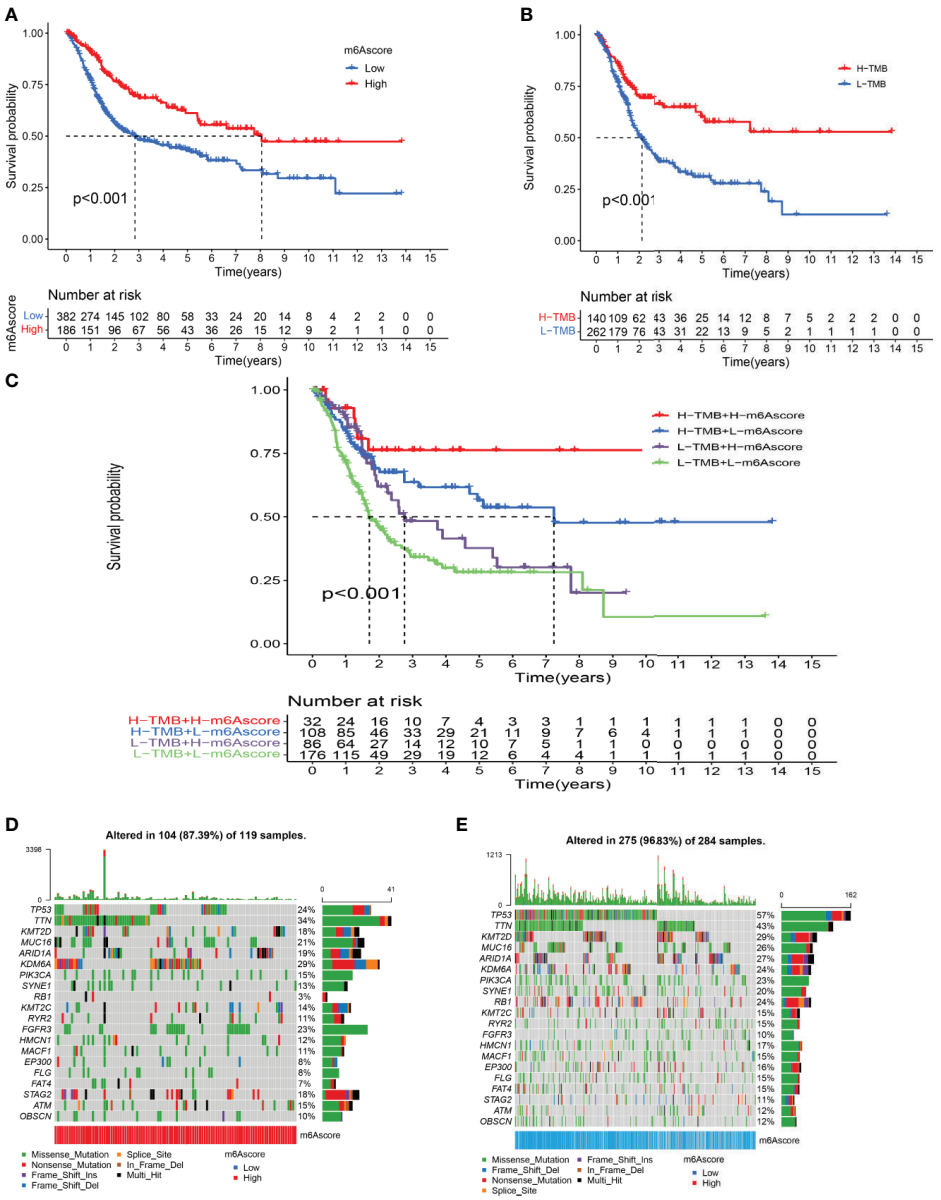

FIGURE 5 | Characterization of m6A modifications in tumor somatic mutation. **(A)** Survival analysis of the high-m6A score group and low-m6A score group. **(B)** Survival analysis of tumor mutation burden. **(C)** Survival analysis of TMB combined with m6A score. **(D)** Waterfall chart of the high-m6A score group. **(E)** Waterfall chart of the low-m6A score group.

the 3 untranslated regions of ITGA6, promoting ITGA6 translation and enhancing the growth and metastasis of bladder cancer cells (33, 34). ALKBH5 can demethylate CDCP1 and regulate CDCP1 protein expression negatively (35). The expression level of METTL14 of bladder cancer and tumor-initiating cells showed a decrease, and it was significantly related to the clinical severity and prognosis of bladder cancer (36). The molecular mechanism and cellular effect of m6A RNA methylation modification of other molecules, especially methylation recognition proteins, were not fully understood in bladder cancer, with different or the same methyltransferases or demethylases working in different ways. The evaluation of mutational driver genes based on tumor was the key basis for cancer diagnosis and treatment. The results showed that, compared with the high-m6A score group, the mutation rate of TP53 in the low-m6A score group was significantly higher, while the TTN mutation rate in the high group was increased. Previous studies had shown that different TP53 mutations found in separate clusters of tumor may also cause TP53 mutations at a later stage. Detection of TP53 mutations can help identify early-stage lesions

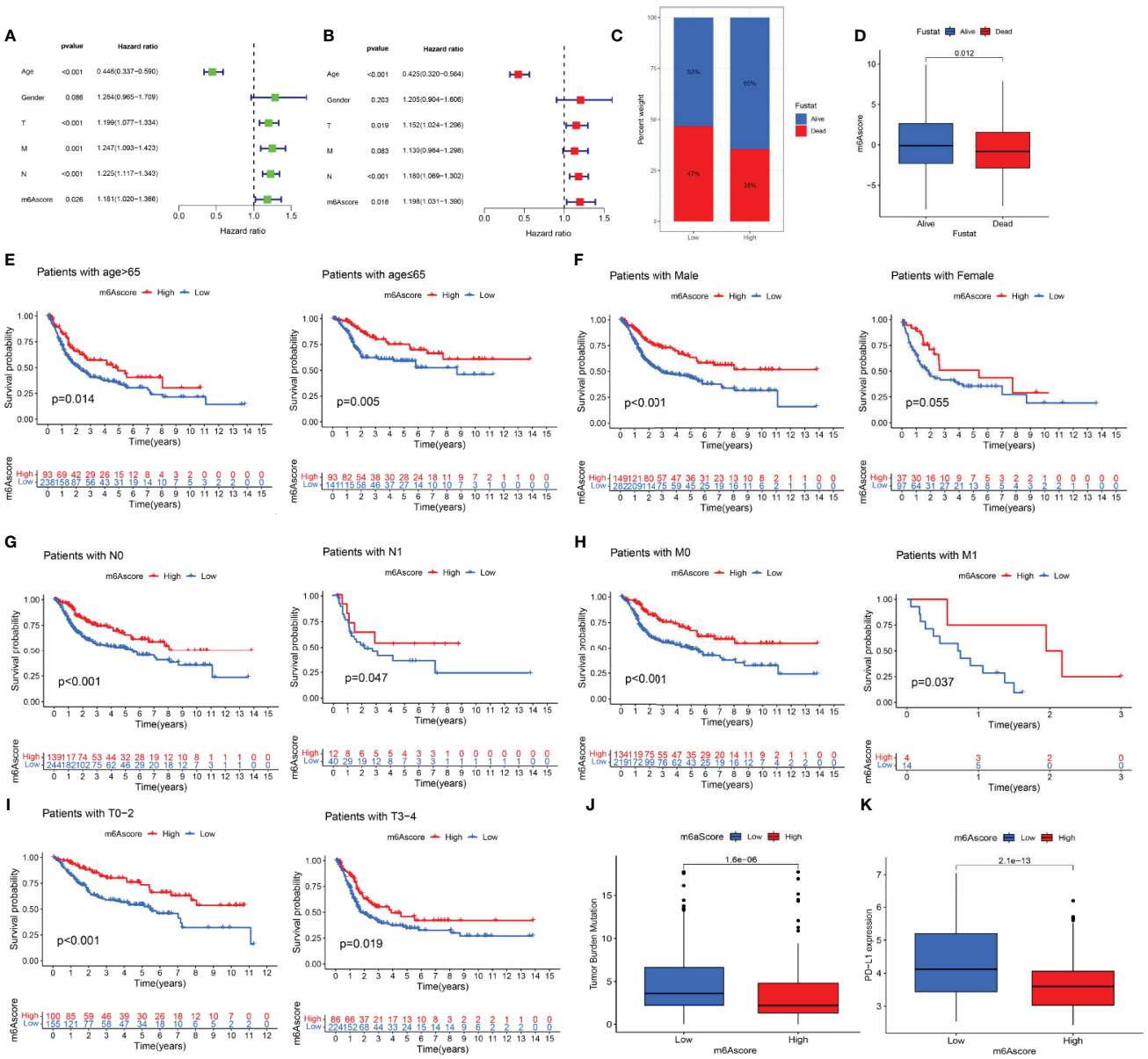

FIGURE 6 | The prognostic value of the m6A score and the correlation between the clinicopathological features and m6A score. **(A)** Univariate Cox regression analysis of the m6 score for bladder cancer was shown by forest plot. **(B)** Multivariate Cox regression analysis of m6 score for bladder cancer was shown by forest plot. **(C)** Stratified analysis of the m6A score for bladder cancer patients by status. **(D)** Stratified analysis of the m6A score for bladder cancer patients by status. **(E)** Stratified analysis of the m6A score for bladder cancer patients by age. **(F)** Stratified analysis of the m6A score for bladder cancer patients by gender. **(G)** Stratified analysis of the m6A score for bladder cancer patients by N. **(H)** Stratified analysis of the m6A score for bladder cancer patients by M. **(I)** Stratified analysis of the m6A score for bladder cancer patients by T. **(J)** Stratified analysis of the m6A score for bladder cancer patients by tumor mutation burden. **(K)** Stratified analysis of the m6A score for bladder cancer patients by PD-L1.

that are at high risk of development (37). TTN mutations in tumors will increase, while its immunostimulatory characteristics will also appear higher. At the same time, it has been found that the TTN mutation load represents a high TMB state (38). This indicates intricate interactions between different modifications of m6A and immune genes in the TME. The abnormal expression mechanism of m6A RNA methylation modification regulatory molecules in bladder cancer is still unclear, so we need to develop a new treatment method based on m6A RNA methylation modification to regulate the TME.

In its clinical and practical applications, our study has its advantages. First, the m6A score may be used to assess m6A methylation patterns and corresponding TME cell infiltration characteristics in individual bladder cancer patients to further

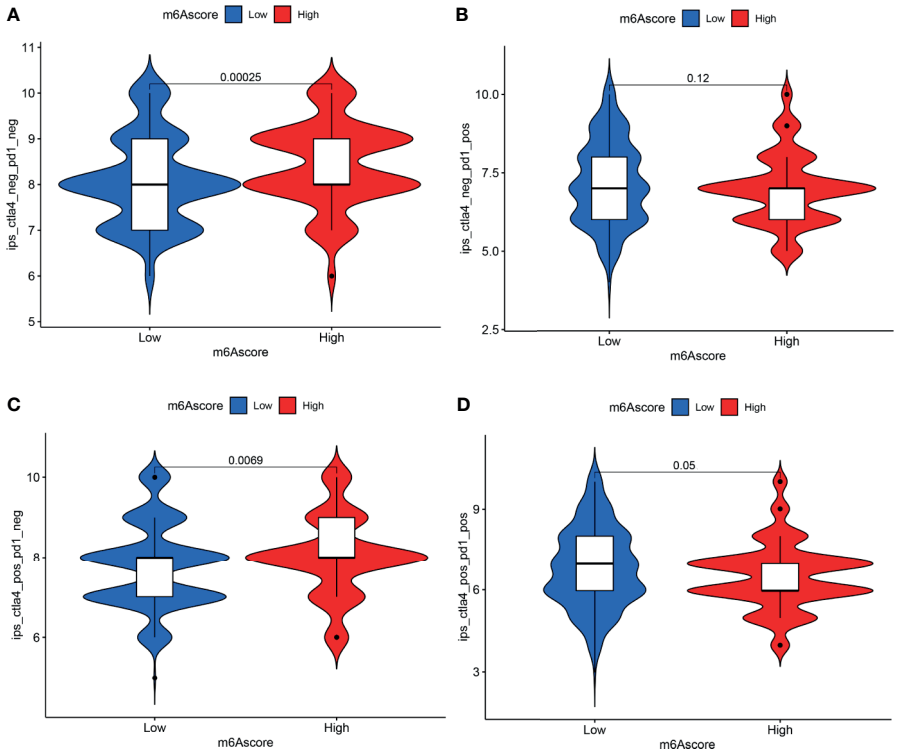

FIGURE 7 | Analysis of m6A modification patterns in anti-PD-L1 and CTLA-4 immunotherapy. **(A)** Differential analysis for low-m6A score group and high-m6A score group in CTLA-4 negative and PD-L1 negative therapy. **(B)** Differential analysis for low-m6A score group and high-m6A score group in anti-PD-L1 immunotherapy. **(C)** Differential analysis for low-m6A score group and high-m6A score group in anti-CTLA-4 immunotherapy. **(D)** Differential analysis for low-m6A score group and high-m6A score group in anti-PD-L1 combined with CTLA-4 immunotherapy.

define the immune phenotype of tumor. Second, after investigating the association between m6A score and clinicopathological features, we suggest that the m6A score may be used as an independent prognostic biomarker for patients with bladder cancer. Finally, the m6A score may predict the efficacy of CTLA-4 immunotherapy in patients with bladder cancer, providing new insights that may guide individualized treatment of patients with bladder cancer. The current study has a few limitations that need to be acknowledged. On the one hand, we only explored the molecular mechanism of m6A modification through 20 RNA methylation regulatory factors that had been identified, while no other regulatory factors were incorporated into the m6A modification mode. On the other hand, we did not explore the relationship between m6A modification and the variant histology of bladder cancer. We therefore need to introduce new regulatory factors and clinicopathological features to improve the accuracy of the model in future studies.

CONCLUSIONS

In this study, we comprehensively assessed the m6A modification patterns based on 20 m6A regulators. The difference in m6A modification patterns may be an important factor in the diversity and complexity of individual TME. The assessment of m6A modification patterns in individual bladder cancer will enhance our knowledge of TME infiltration characteristics and provide the basis for guiding immunotherapy strategies.

DATA AVAILABILITY STATEMENT

The datasets presented in this study can be found in online repositories. The names of the repository/repositories and accession number(s) can be found in the article/**Supplementary Material**.

AUTHOR CONTRIBUTIONS

HZ designed this study. HZ, XS, YY, XJ and ZS downloaded and analyzed the data. HZ wrote this manuscript. HZ, YY, NW and YW explained the data. YY reviewed and revised the manuscript. All authors contributed to the article and approved the submitted version.

FUNDING

This research was funded by the National Natural Science Foundation of China (No. 82073670).

ACKNOWLEDGMENTS

This data for this work was obtained from the TCGA and GEO databases. We are grateful for the access to these meaningful resources and to the staff who work to expand and improve the databases.

SUPPLEMENTARY MATERIAL

The Supplementary Material for this article can be found online at: https://www.frontiersin.org/articles/10.3389/fonc.2021.714267/full#supplementary-material

REFERENCES

1. Boccaletto P, Machnicka MA, Purta E, Piatkowski P, Baginski B, Wirecki TK, et al. MODOMICS: A Database of RNA Modification Pathways. 2017 Update. *Nucleic Acids Res* (2018) 46(D1):D303–7. doi: 10.1093/nar/gkx1030
2. Ma S, Chen C, Ji X, Liu J, Zhou Q, Wang G, et al. The Interplay Between M6a RNA Methylation and Noncoding RNA in Cancer. *J Hematol Oncol* (2019) 12 (1):121. doi: 10.1186/s13045-019-0805-7
3. Yang Y, Hsu PJ, Chen YS, Yang YG. Dynamic Transcriptomic M(6)A Decoration: Writers, Erasers, Readers and Functions in RNA Metabolism. *Cell Res* (2018) 28(6):616–24. doi: 10.1038/s41422-018-0040-8
4. Zhang C, Chen Y, Sun B, Wang L, Yang Y, Ma D, et al. M(6)A Modulates Haematopoietic Stem and Progenitor Cell Specification. *Nature* (2017) 549 (7671):273–6. doi: 10.1038/nature23883
5. Koh CWQ, Goh YT, Goh WSS. Atlas of Quantitative Single-Base-Resolution N(6)-Methyl-Adenine Methylomes. *Nat Commun* (2019) 10(1):5636. doi: 10.1038/s41467-019-13561-z
6. Lobo J, Barros-Silva D, Henrique R, Jerónimo C. The Emerging Role of Epitranscriptomics in Cancer: Focus on Urological Tumors. *Genes* (2018) 9 (11):552. doi: 10.3390/genes9110552
7. Vander Heiden MG, DeBerardinis RJ. Understanding the Intersections Between Metabolism and Cancer Biology. *Cell* (2017) 168(4):657–69. doi: 10.1016/j.cell.2016.12.039
8. Joyce JA, Fearon DT. T Cell Exclusion, Immune Privilege, and the Tumor Microenvironment. *Science (New York NY)* (2015) 348(6230):74–80. doi: 10.1126/science.aaa6204
9. Lei X, Lei Y, Li JK, Du WX, Li RG, Yang J, et al. Immune Cells Within the Tumor Microenvironment: Biological Functions and Roles in Cancer Immunotherapy. *Cancer Lett* (2020) 470:126–33. doi: 10.1016/j.canlet.2019.11.009
10. Ge Z, Ding S. The Crosstalk Between Tumor-Associated Macrophages (TAMs) and Tumor Cells and the Corresponding Targeted Therapy. *Front Oncol* (2020) 10:590941. doi: 10.3389/fonc.2020.590941
11. Lambrechts D, Wauters E, Boeckx B, Aibar S, Nittner D, Burton O, et al. Phenotype Molding of Stromal Cells in the Lung Tumor Microenvironment. *Nat Med* (2018) 24(8):1277–89. doi: 10.1038/s41591-018-0096-5
12. Lee HW, Chung W, Lee HO, Jeong DE, Jo A, Lim JE, et al. Single-Cell RNA Sequencing Reveals the Tumor Microenvironment and Facilitates Strategic Choices to Circumvent Treatment Failure in a Chemorefractory Bladder Cancer Patient. *Genome Med* (2020) 12(1):47. doi: 10.1186/s13073-020-00741-6
13. Sun T, Wu R, Ming L. The Role of M6a RNA Methylation in Cancer. *Biomed Pharmacother = Biomed Pharmacother* (2019) 112:108613. doi: 10.1016/j.biopha.2019.108613
14. Zheng Q, Hou J, Zhou Y, Li Z, Cao X. The RNA Helicase DDX46 Inhibits Innate Immunity by Entrapping M(6)A-Demethylated Antiviral Transcripts in the Nucleus. *Nat Immunol* (2017) 18(10):1094–103. doi: 10.1038/ni.3830
15. Li M, Zha X, Wang S. The Role of N6-Methyladenosine mRNA in the Tumor Microenvironment. *Biochim Biophys Acta Rev Cancer* (2021) 1875(2):188522. doi: 10.1016/j.bbcan.2021.188522
16. Zhu J, Xiao J, Wang M, Hu D. Pan-Cancer Molecular Characterization of M(6)A Regulators and Immunogenomic Perspective on the Tumor Microenvironment. *Front Oncol* (2020) 10:618374. doi: 10.3389/fonc.2020.618374
17. Wang H, Hu X, Huang M, Liu J, Gu Y, Ma L, et al. Mettl3-Mediated mRNA M (6)A Methylation Promotes Dendritic Cell Activation. *Nat Commun* (2019) 10(1):1898. doi: 10.1038/s41467-019-09903-6
18. Li HB, Tong J, Zhu S, Batista PJ, Duffy EE, Zhao J, et al. M(6)A mRNA Methylation Controls T Cell Homeostasis by Targeting the IL-7/STAT5/SOCS Pathways. *Nature* (2017) 548(7667):338–42. doi: 10.1038/nature23450
19. The Cancer Genome Atlas Program. Available at: https://www.cancer.gov/about-nci/organization/ccg/research/structural-genomics/tcga.
20. Barrett T, Wilhite SE, Ledoux P, Evangelista C, Kim IF, Tomashevsky M, et al. NCBI GEO: Archive for Functional Genomics Data Sets–Update. *Nucleic Acids Res* (2013) 41(Database issue):D991–5. doi: 10.1093/nar/gks1193
21. Zhao S, Ye Z, Stanton R. Misuse of RPKM or TPM Normalization When Comparing Across Samples and Sequencing Protocols. *RNA (New York NY)* (2020) 26(8):903–9. doi: 10.1261/rna.074922.120
22. Liberzon A, Birger C, Thorvaldsdóttir H, Ghandi M, Mesirov JP, Tamayo P. The Molecular Signatures Database (MSigDB) Hallmark Gene Set Collection. *Cell Syst* (2015) 1(6):417–25. doi: 10.1016/j.cels.2015.12.004
23. Foroutan M, Bhuva DD, Lyu R, Horan K, Cursons J, Davis MJ. Single Sample Scoring of Molecular Phenotypes. *BMC Bioinf* (2018) 19(1):404. doi: 10.1186/s12859-018-2435-4
24. Kim JM, Chen DS. Immune Escape to PD-L1/PD-1 Blockade: Seven Steps to Success (or Failure). *Ann Oncol* (2016) 27(8):1492–504. doi: 10.1093/annonc/mdw217
25. Yang F, Jin H, Que B, Chao Y, Zhang H, Ying X, et al. Dynamic M(6)A mRNA Methylation Reveals the Role of METTL3-M(6)A-CDCP1 Signaling Axis in Chemical Carcinogenesis. *Oncogene* (2019) 38(24):4755–72. doi: 10.1038/s41388-019-0755-0
26. Marzagalli M, Ebelt ND, Manuel ER. Unraveling the Crosstalk Between Melanoma and Immune Cells in the Tumor Microenvironment. *Semin Cancer Biol* (2019) 59:236–50. doi: 10.1016/j.semcancer.2019.08.002
27. Takeuchi A, Saito T. CD4 CTL, A Cytotoxic Subset of CD4(+) T Cells, Their Differentiation and Function. *Front Immunol* (2017) 8:194. doi: 10.3389/fimmu.2017.00194
28. Racioppi L, Nelson ER, Huang W, Mukherjee D, Lawrence SA, Lento W, et al. CaMKK2 in Myeloid Cells Is a Key Regulator of the Immune-Suppressive Microenvironment in Breast Cancer. *Nat Commun* (2019) 10(1):2450. doi: 10.1038/s41467-019-10424-5
29. Zhang X, Zhao H, Shi X, Jia X, Yang Y. Identification and Validation of an Immune-Related Gene Signature Predictive of Overall Survival in Colon Cancer. *Aging* (2020) 12(24):26095–120. doi: 10.18632/aging.202317
30. Sanguedolce F, Russo D, Mancini V, Selvaggio O, Calo B, Carrieri G, et al. Prognostic and Therapeutic Role of HER2 Expression in Micropapillary Carcinoma of the Bladder. *Mol Clin Oncol* (2019) 10(2):205–13. doi: 10.3892/mco.2018.1786
31. Sanguedolce F, Calò B, Mancini V, Zanelli M, Palicelli A, Zizzo M, et al. Non-Muscle Invasive Bladder Cancer With Variant Histology: Biological Features and Clinical Implications. *Oncology* (2021) 99(6):345–58. doi: 10.1159/000514759
32. Han Y, Zheng Q, Tian Y, Ji Z, Ye H. Identification of a Nine-Gene Panel as a Prognostic Indicator for Recurrence With Muscle-Invasive Bladder Cancer. *J Surg Oncol* (2019) 119(8):1145–54. doi: 10.1002/jso.25446
33. Han J, Wang JZ, Yang X, Yu H, Zhou R, Lu HC, et al. METTL3 Promote Tumor Proliferation of Bladder Cancer by Accelerating Pri-Mir221/222 Maturation in M6a-Dependent Manner. *Mol Cancer* (2019) 18(1):110. doi: 10.1186/s12943-019-1036-9
34. Jin H, Ying X, Que B, Wang X, Chao Y, Zhang H, et al. N(6)-Methyladenosine Modification of ITGA6 mRNA Promotes the Development and Progression of Bladder Cancer. *EBioMedicine* (2019) 47:195–207. doi: 10.1016/j.ebiom.2019.07.068
35. Yu H, Yang X, Tang J, Si S, Zhou Z, Lu J, et al. ALKBH5 Inhibited Cell Proliferation and Sensitized Bladder Cancer Cells to Cisplatin by M6a-CK2α-Mediated Glycolysis. *Mol Ther Nucleic Acids* (2021) 23:27–41. doi: 10.1016/j.omtn.2020.10.031
36. Gu C, Wang Z, Zhou N, Li G, Kou Y, Luo Y, et al. Mettl14 Inhibits Bladder TIC Self-Renewal and Bladder Tumorigenesis Through N(6)-Methyladenosine of Notch1. *Mol Cancer* (2019) 18(1):168. doi: 10.1186/s12943-019-1084-1
37. Olivier M, Hollstein M, Hainaut P. TP53 Mutations in Human Cancers: Origins, Consequences, and Clinical Use. *Cold Spring Harbor Perspect Biol* (2010) 2(1):a001008. doi: 10.1101/cshperspect.a001008

38. Oh JH, Jang SJ, Kim J, Sohn I, Lee JY, Cho EJ, et al. Spontaneous Mutations in the Single TTN Gene Represent High Tumor Mutation Burden. *NPJ Genom Med* (2020) 5:33. doi: 10.1038/s41525-019-0107-6

Conflict of Interest: The authors declare that the research was conducted in the absence of any commercial or financial relationships that could be construed as a potential conflict of interest.

Publisher's Note: All claims expressed in this article are solely those of the authors and do not necessarily represent those of their affiliated organizations, or those of the publisher, the editors and the reviewers. Any product that may be evaluated in this article, or claim that may be made by its manufacturer, is not guaranteed or endorsed by the publisher.

frontiers in Oncology

REVIEW
published: 05 November 2021
doi: 10.3389/fonc.2021.781414

The Role and Clinical Potentials of Circular RNAs in Prostate Cancer

*Mohammad Taheri[1], Sajad Najafi[2], Abbas Basiri[3], Bashdar Mahmud Hussen[4], Aria Baniahmad[5], Elena Jamali[6] and Soudeh Ghafouri-Fard[7]**

[1] Skull Base Research Center, Loghman Hakim Hospital, Shahid Beheshti University of Medical Sciences, Tehran, Iran, [2] Student Research Committee, Department of Medical Biotechnology, School of Advanced Technologies in Medicine, Shahid Beheshti University of Medical Sciences, Tehran, Iran, [3] Urology and Nephrology Research Center, Shahid Beheshti University of Medical Sciences, Tehran, Iran, [4] Department of Pharmacognosy, College of Pharmacy, Hawler Medical University, Erbil, Iraq, [5] Institute of Human Genetics, Jena University Hospital, Jena, Germany, [6] Department of Pathology, Loghman Hakim Hospital, Shahid Beheshti University of Medical Sciences, Tehran, Iran, [7] Department of Medical Genetics, School of Medicine, Shahid Beheshti University of Medical Sciences, Tehran, Iran

Globally, prostate cancer (PCa) is the second most commonly diagnosed cancer in men globally. Early diagnosis may help in promoting survival in the affected patients. Circular RNAs (circRNAs) are a novel class of non-coding RNAs (ncRNAs) which have been found to show extensive dysregulation in a handful of human diseases including cancers. Progressions in RNA identification techniques have provided a vast number of circRNAs exhibiting either up-regulation or down-regulation in PCa tissues compared to normal adjacent tissues. The mechanism of action is not clear for most of dysregulated circRNAs. Among them, function of a number of newly identified dysregulated circRNAs have been assessed in PCa cells. Increase in cell proliferation, migration, invasion, and metastasis have been reported for up-regulated circRNAs which suggest their role as oncogenes. On the other hand, down-regulated circRNAs have shown tumor suppressing actions in experimental studies. Furthermore, in a majority of studies, circRNAs have been found to sponge microRNAs (miRNAs), negatively regulating expression or activity of the downstream miRNAs. Additionally, they have been identified in interaction with regulatory proteins. This axis consequently regulates a signaling pathway, a tumor suppressor, or an oncogene. Easy, quick, and reliable detection of circRNAs in human body fluids also suggests their potentials as biomarker candidates for diagnosis and prediction of prognosis in PCa patients. In this review, we have discussed the role and potentials of a number of dysregulated circRNAs in PCa.

Keywords: circular RNAs, prostate cancer, diagnosis, prognosis, biomarker

OPEN ACCESS

Edited by:
Bianca Nitzsche, Charité – Universitätsmedizin Berlin, Germany

Reviewed by:
Soichiro Yamamura, University of California, San Francisco, United States
Mariana Chantre Justino, Rio de Janeiro State University, Brazil

***Correspondence:**
Soudeh Ghafouri-Fard
s.ghafourifard@sbmu.ac.ir

Specialty section:
This article was submitted to Genitourinary Oncology, a section of the journal Frontiers in Oncology

Received: *22 September 2021*
Accepted: *20 October 2021*
Published: *05 November 2021*

Citation:
Taheri M, Najafi S, Basiri A, Hussen BM, Baniahmad A, Jamali E and Ghafouri-Fard S (2021) The Role and Clinical Potentials of Circular RNAs in Prostate Cancer. Front. Oncol. 11:781414. doi: 10.3389/fonc.2021.781414

INTRODUCTION

Prostate cancer (PCa) accounts for more than 1 in 5 new cancer cases in men (1). High age is the main risk factor for PCa. Race, environmental and genetic factors are known as other predisposing factors (2). Majority of PCa cases are diagnosed with diseases of low to intermediate risk, and a minority of 30% experience shorter survival in case of distant metastasis of the malignancy (3). Gleason score is the most commonly used grading system for prediction of outcomes in PCa

patients (4). The scores range from 6-10 with high scores corresponding to malignant PCa cells and lower survival in PCa patients. The main biomarker currently used for diagnosis of PCa is prostate-specific antigen (PSA) which harbors good diagnostic values, however cannot distinguish PCa from resembling milder prostate disorders like benign prostate hyperplasia (BPH) and prostatitis (5). Non-coding RNAs (ncRNAs) have been studied in PCa and their role in development, progression, and metastasis of malignancy has been evaluated in a handful of *in vitro* and *in vivo* experiments. Among ncRNAs, microRNAs (miRNAs) and lncRNAs [see more at (6, 7)] have been studied more in PCa compared with circRNAs and their roles and mechanisms in development and progression of PCa have been clarified due to the historical priority of discovery and facility of detection in research studies.

NCRNAS

A large proportion of eukaryotic genome encodes no protein which is termed as non-coding RNAs (ncRNAs). These transcripts have been primarily described as junk DNA and now known to have essential regulatory roles. Circular RNAs (circRNAs) are covalently closed RNA transcripts usually belonging to a novel type of ncRNAs, namely long non-coding category (lncRNAs). CircRNAs have been primarily reported in viroids (8). Hsu and Coca-Prados (9) reported the first circRNAs in eukaryotes in 1979 *via* electron microscopy in HeLa cells. Compared to linear types of regulatory RNAs and even among ncRNAs, less attention has been paid to circRNAs. However, increasing evidence demonstrates their biological functions. CircRNAs are believed to be formed *via* back-splicing from pre-messenger RNA (pre-mRNA) or originated from differentially spliced transcripts (10). The main characteristic of circRNAs as their names suggest is their determinant circular form which develops *via* covalent linkages between the 5′ and 3′ ends and sometimes 5′-2′ phosphodiester bonds. CircRNAs exhibit dissimilarities to conventional linear RNAs such as mRNAs and transfer RNAs (tRNAs) which include lacking capping and polyadenylated (poly A) tail at their 5′ and 3′ ends, respectively. Lack of open ends makes RNA loops resistant to RNA degrading enzyme RNase R which facilitates biochemical characterization of circRNAs (11). Several approaches based on non-polyadenylation characteristic of circRNAs, rRNA-depletion, and RNase R-resistance have been developed for detection of circRNAs (12). The qRT-PCR analysis following RNase R treatment is the most common approach used for validation of circRNAs (13). Also, fast and easy detection of circRNAs can be conducted through rolling-circle amplification (RCA) (14). This technique does not require any advanced equipment or fluorescent probes and is performed just using qRT-PCR machine and gel electrophoresis. First, the circRNAs using first-generation primers is reverse transcribed generating a multimeric cDNA through RCA method compared to a monomeric cDNA for linear RNA template. Then using second-generation primer, the circRNAs-specific ligation site is spanned and subsequently can be seen on gel electrophoresis (15). High-throughput RNA sequencing (RNA-seq) along with bioinformatics tools [e.g., CircMiner (16)] and confirmatory techniques like quantitative real-time polymerase chain reaction (qRT-PCR, where the junction/fusion site is known) and Fluorescence *in situ* hybridization (FISH) have helped substantial progression in identification of differentially expressed circRNAs in cancerous tissues. Although qRT-PCR is the most common approach for experimental detection of circRNAs, however, currently, no easy, quick, and cheap technique is available for diagnostics to detect a specific circRNA, and so it is suggested that we have a long way to bring circRNAs to clinical setting (17).

CircRNAs have been identified in large quantities and have been revealed to be expressed widely in animal cells. Thousands of circRNAs are transcribed in considerable fractions from a large number of human genes (18). The number of identified unique circRNAs are more than twice of the linear counterparts (19). However, they are usually found in lesser quantities compare with their linear counterparts (10). In mammals, circRNAs show conservation in their sequences among different species, are mainly found in cytoplasm, and demonstrate specific tissue, cellular and developmental stage distribution (20, 21), even more specific compared to corresponding mRNA isoforms (22). Precise functions of circRNAs have not been clarified, but regulatory roles have been described for an increasing number of them. The first circRNA, which its function has been characterized, was CDR1as (21). CDR1as was shown to play role in gene expression at posttranscriptional stage *via* binding to and sponging miR-7. This circRNA is involved in brain development (21). Aberrant expression of circRNAs have been associated with pathological conditions such as cardiovascular diseases (23), sudden cardiac death (SCD) (24), neurodegenerative and psychiatric disorders (25, 26), kidney diseases (27), inflammation (28), autoimmune diseases (29) and particularly various types of cancer. Cellular studies have shown a vast number of circRNAs to be dysregulated in cancer tissues compared to normal tissues and this imbalance can enhance tumor development and progression *via* affecting cell cycle. Aberrant expression includes either up- or down-regulation in levels of circRNAs compared to those in normal cells. Up-regulated circRNAs in cancer are known as oncogenes. These oncogenic circRNAs such as circMBOAT2 (30) and circFOXO3 (31) accelerate tumor cell proliferation, migration, invasion, and metastasis, while suppressing apoptosis. On the other hand, down-regulated circRNAs are considered as tumor suppressors. CircRNAs can be detected in high abundance due to their stability in body fluids like serum and urine, and can also be specifically expressed in extracellular vesicles (32, 33). Therefore, their detection provides easy, rapid, reliable, and minimally invasive diagnostic routes for many types of cancers and other pathological conditions. The expression levels of circRNAs in a majority of studies have been significantly correlated with clinicopathological features in cancerous patients, accordingly they can help in prediction of the disease

prognosis. Most importantly, targeting oncogenic circRNAs or reversing intermediates using RNA interference (RNAi) and antisense oligonucleotides (ASO) or enhancing expression of circRNA with tumor suppressing functions has suggested new therapeutical potentials in fighting against malignancies. Thus, circRNAs have been introduced as novel diagnostic and prognostic biomarkers and therapeutical targets particularly in cancer.

In this review, we focus on a number of circRNAs being dysregulated in prostate cancer (PCa), with an overview of the studies assessed the tumorigenic and anti-carcinogenic roles of them in PCa tissues and finally, their potential applications in diagnosis and prediction of prognosis in PCa patients.

CIRCRNAS IN PCA

In various studies, thousands of circRNAs have been found to show aberrant expression in PCa tissues compared to normal adjacent tissue (NAT) or also between several stages of malignancy including primary and metastatic PCa (34, 35). Some of these circRNAs promote PCa cell tumorigenicity enhancing cell proliferation, invasion and metastasis. An increased resistance to chemotherapy agents is another impact of oncogenic circRNAs, which can affect the survival in PCa patients (36). Regulatory effects on expression of androgens or their receptors and resistance to them or reverse interactions which play role in development of PCa have also been reported for several circRNAs [e.g., circRNA-17 (37), circSMARCA5 (38), and circRNA-51217 (39)]. For some other circRNAs such as circ-ITCH (40) and circMBOAT2 (30), a correlation has been recognized between circRNA expression levels and prognosis in PCa patients. Precise mechanism of action for circRNAs has been poorly understood. In bioinformatics-constructed regulatory networks such as Gene Ontology (GO), Kyoto Encyclopedia of Genes and Genomes (KEGG) pathway, and competing endogenous RNA (ceRNA) network analyses to predict the function of circRNAs and also, RNA-pull down assays, an interaction between circRNAs and targeted miRNAs is frequently reported. Along with main miRNAs sponging activity, circRNAs also have been shown to exert their regulatory functions through interactions with proteins particularly RNA-binding proteins, which play role in RNAs maturation and influence various cellular functions (41). RNA-binding proteins can interplay with circRNA junctions and participate in splicing, processing, folding, stabilization, and localization of circRNAs (42). An example of circRNAs interacting with RNA-binding proteins are has_circ_0000020 (interacting with HuR, FMRP and EIF4A3) (43).

Also, interaction of circRNA with other ncRNAs particularly miRNAs, based on their complementary sequences has been reported in a set of experiments. Additionally, circRNAs can regulate RNA-binding proteins, and linear protein-coding mRNAs (44). These studies suggest an axis through which the circRNA affects (mainly reverses) expression or activity [see review in (45)] of a mediator miRNA as a target, which itself impacts a specific target signaling pathway, a tumor suppressor or an oncogene. Thus, it is thought that an oncogenic circRNA exerts its function through a signaling axis eventually activates an oncogene or through a signaling pathway accelerates cell cycle. Based on tissue, cancer or malignancy stage-specific expression of a circRNA in PCa, diagnostic analyses have unveiled reliability of a set of circRNAs as potential biomarkers in distinguishing PCa from any other condition or among cancer stages. Association between expression level of a circRNA and clinicopathological features in PCa patients like tumor stage, grade, lymph node metastasis in addition to prognosis, also has been found in a number of studies. For instance, Greene et al. (35) have reported that circRNAs not only demonstrate differential expression in PCa tissues, but also are expressed aberrantly according to the androgen dependency, which is known to play role in the pathogenesis of the disease. Furthermore, targeting aberrantly expressed circRNAs in PCa has exhibited hopeful results in a number of studies decreasing aggressiveness and tumorigenesis in cell and *in vivo* studies.

UP-REGULATED CIRCRNAS IN PCA

Up-regulated circRNAs, as discussed above, act as oncogenic ncRNAs promoting tumorigenic features of tumor cell lines and also, increase tumor progression *in vivo*. CircRNA knockdown using specific small interfering RNA (siRNA) or overexpression by encoding vectors have been employed in functional analysis. Enhanced tumor cell proliferation, invasion and migration have been reported following over-expression of these circRNAs, in cell viability and colony formation, migration and invasion assays, respectively. Suppressed apoptosis is also reported in functional analysis of up-regulated circRNAs. Furthermore, oncogenic circRNAs could decrease chemosensitivity and radiosensitivity of the cancer cell lines to the current therapeutical approaches of PCa (46, 47). As a result, decreased effectiveness of the cancer therapeutics and eventually adverse consequences such as shortened survival is predicted for the patients.

For instance, Zhang et al. (48) have identified 89 circRNAs which showed aberrant expression in PCa tissues, among them 32 circRNAs showed increased expression and remaining 57 demonstrated to be down-regulated. In further investigations, 5 prominently overexpressed circRNAs in comparison to their corresponding mRNAs in PCa tissues including hsa_circ_0006754, hsa_circ_0005848, hsa_circ_0006410, hsa_circ_0003970, and hsa_circ_AKAP7 were recognized. Interaction networks revealed 215 linkages between 5 selected circRNAs and corresponding miRNAs. Several miRNAs including miR-204-5p, miR-3160-5p, and miR-548 were identified as the most prominent targets of associated circRNAs which play role in suppression or promotion of carcinogenesis or *via* enhancing apoptosis, inhibiting cell proliferation or PI3K/AKT signaling pathway, respectively. MAPK signaling pathway was known as the most important signaling pathway affected by the selected circRNAs, while other pathways like hormone-associated and lipid metabolism-related were also involved in the carcinogenic axes of the highly expressed circRNAs.

Survival rate analysis in PCa patients by the Kaplan-Meier curve unveiled a positive correlation between higher expression of cognate genes corresponding to anti-carcinogenic circRNAs (hsa_circ_0006410, hsa_circ_AKAP7 and hsa_circ_0005848) and better overall survival (OS) in PCa patients. Also, Yu et al. (49) identified 13 circRNAs in association with resistance to enzalutamide as an androgen deprivation therapy (ADP) drug used against PCa. Six miRNAs, 167 mRNAs, and 10 hub genes were identified as targets of the circRNAs. Among them, 8 prognostic-associated mRNAs were shown to be associated with survival rates in PCa patients, also with an AUC of 0.816 confirming the accuracy of miRNAs signature in detection of PCa. Additionally, knockdown experiments revealed that circRNA hsa_circ_0047641 promote PCa cell proliferation, migration, and invasion. CircMBOAT2 is another circRNA participating in the pathogenesis of PCa through increasing cell proliferation, migration, and invasion of malignant cells. This circRNA significantly up-regulates mTOR expression through sequestering miR-1271-5p, leading to the activation of the PI3K/Akt cascade (50).

CircSLC19A1 is another up-regulated circRNA in PCa tissues. CircSLC19A1 knock down has suppressed viability of PCa cells and their proliferation through modulation of miR-326/MAPK1 axis (51). CircABCC4 is an example of up-regulated circRNAs in PCa tissues and cell lines which enhances expression of FOXP4 through sequestering miR-1182. CircABCC4 silencing has inhibited proliferation of PCa as well as their migratory potential and invasiveness. Besides, circABCC4 knock down has attenuated growth of PCa *in vivo*. Cumulatively, circABCC4 accelerates malignant behavior of PCa (52).

Table 1 summarizes the studies on a set of up-regulated circRNAs in PCa.

DOWN-REGULATED CIRCRNAS IN PCA

Decreased expression in high throughput RNA analyses of PCa tissues compared to paired NATs draws attention to a second group of dysregulated circRNAs. Down-regulated circRNAs exhibit anti-oncogenic behaviors in experimental analyses inhibiting proliferation, migration, invasion, and metastasis of PCa cells. Sponge activity is seen for a majority of circRNAs which mainly show reverse regulation on downstream miRNAs. Inhibited miRNAs are mainly oncogenic RNAs which activate their corresponding oncogenes or inactivate related tumor suppressors. Mediator miRNAs, predominantly act *via* a signaling axis which firstly regulate expression a downstream protein, and itself makes changes to a signaling pathway. Affected known signaling pathways in PCa like MEK/ERK and Wnt/β-Catenin have been reported in a handful of studies on down-regulated circRNAs (see **Table 2**).

Circular RNA Itchy E3 ubiquitin protein ligase (circ-ITCH) is an example for down-regulated circRNAs in PCa which has been studied in four distinct experiments (77–79). Wang et al. (92) demonstrated that circ-ITCH down-regulation increases PCa cell proliferation and decreases apoptosis *in vitro*, while its up-regulation decreases cell proliferation and *in vivo* tumor growth. Luciferase assay showed direct interaction of circ-ITCH with microRNA miR-17-5p and reverse relationship between their expression levels, which reveals that circ-ITCH acts as sponge for downstream miR-17-5p. miR-17-5p, itself negatively regulates expression of HOXB13, which is known as a tumor suppressor gene being involved in development and progression of PCa. Yuan et al. (78) showed the same experimental results about consequences of circ-ITCH down-regulation, although miR-197 was identified as target miRNA for circ-ITCH. Also, miR-17 was detected as target of circ-ITCH in a study by Li et al. (79). Furthermore, they demonstrated that down-regulation of circ-ITCH is associated with up-regulation of expression of proteins involved in β-catenin, p-AKT, and p-mTOR signaling pathways indicating that circ-ITCH negatively regulates these pathways which have role in the progression of various tumors like PCa. In another study, Huang et al. (40) assessed the correlation between circ-ITCH expression and clinicopathological features, survival and prognosis in PCa. Direct association between low circ-ITCH levels and more aggressive clinicopathological features, poor survival, and unfavorable prognosis confirmed the experimental studies identifying circ-ITCH as a tumor suppressor circRNA in PCa. circAMOTL1L is another down-regulated circRNA in PCa. Its down-regulation has promoted PCa cell migration and invasion *in vitro*, while its overexpression has decreased tumor growth *in vivo*. circAMOTL1L has been shown to regulate expression of EMT-related genes (81).

Figure 1 illustrates the role of several circRNAs in PCa *via* modulating the PI3K/AKT/mTOR and MAPK/ERK pathways.

PI3K signaling cascade linking RTK signaling results in downstream activation of PI3K/AKT/mTOR, elevating cell proliferation and survival. Besides, the MAPK-ERK signaling cascade also called the Raf/MEK/ERK pathway, is the main signal pathway of the MAPK signal cascade. The main MAPK/ERK kinase kinase (MEKK) components are the Raf family members Raf-1, A-Raf and B-Raf. Activated Raf activates MEK-1/2 by phosphorylating serine residues. Moreover, MEK-1/2 upregulates ERK-1/2 through phosphorylating the threonine and tyrosine residues of ERK-1/2. Activated ERK can regulate the phosphorylation of some nuclear transcription factors that are directly involved in the modulation of cell proliferation and differentiation. A recent study has demonstrated that overexpression of circMBOAT2 significantly upregulates mTOR expression *via* sponging miR-1271-5p, leading to the activation of the PI3K/Akt cascade, eventually elevating the cell proliferation, migration, and invasion of prostate cancer (50). Another research has denoted that circSLC19A1 elevates the expression level of MAPK1 by downregulating the miR-326 expression, thereby promoting prostate cancer cell proliferation, migration and invasion (51). Green arrows indicate upregulation of target genes modulated *via* circRNAs; red arrows depict inhibition by them.

DIAGNOSTIC AND PROGNOSTIC APPLICATIONS OF CIRCRNAS IN PCA

As discussed above, circRNAs are found in extracellular vesicles extracted from plasma, exhibit high resistance to degradation

TABLE 1 | Up-regulated circRNAs in PCa.

circRNA (Other terms)	Clinical Cases	Cell Lines	Target genes/ Regulators/ sponged miRNAs	Affected Signaling Pathway/ Process	Findings on over-expressed or silenced circRNA in PCa cellular experiments	Ref. (s)
hsa_circ_0006754, hsa_circ_0005848, hsa_circ_0006410, hsa_circ_0003970, and hsa_circ_AKAP7 signature	2 PCa patient tissues and matched NATs for RNA-Seq and also, 20 PCa patients and matched NATs for qRT-PCR verification	–	miR-204-5p, miR-3160-5p, and miR-548	PI3K-AKT, MAPK, hormone and lipid-related pathways	–	(29)
CircABCC4	47 PCa tissues and paired NATs	PC3 and DU145 human PCa cell lines	miR-1182/ FOXP4 signaling axis	–	Its silencing suppressed PCa cell proliferation, migration and invasion *in vitro* and tumor propagation *in vivo*	(53)
circMBOAT2 (has_circ_0007334)	Two cohorts (cohort1: 50 PCa patient tissues and paired NATs; cohort 2: 62 PCa patients)	PC-3, DU145, VCaP, LNCaP, and C4-2B PCa cell lines and RWPE-1 healthy prostate epithelial cells	miR-1271-5p/mTOR axis	mTOR	circMBOAT2 depletion using specific siRNA inhibited PCa cell proliferation, migration and invasion *in vitro* and overexpression showed reverse effects and also, tumor progression and metastasis *in vivo*	(30)
circFOXO3	53 PCa tissues and paired NATs	LNCaP, 22Rv1, DU145, PC-3 and WPMY-1	miR-29a-3p/ SLC25A15 cascade		circFOXO3 knockdown suppressed PCa cell proliferation and increased apoptosis though making arrest in cell cycle	(31)
circ_0057558	25 PCa tissues	22RV1, DU145, and PC3 human PCa cell lines and 293T human kidney epithelial cells	miR-206/ USP33/c-Myc axis	–	Circ_0057558 silencing inhibited PCa cell proliferation and colony formation, and caused arrest in cell cycle *in vitro* and tumor growth *in vivo* Overexpression attenuated sensitivity to chemotherapy agent docetaxel	(46)
circ_0088233	46 PCa tissues and paired NATs	22Rv1, Du145, LNCaP, and RWPE-1	miR-185-3p	–	circ_0088233 knockdown inhibited PCa cell proliferation, migration and invasion and induced G1 phase cell cycle arrest and also, apoptosis	(54)
circMYLK	17 PCa tissues and paired NATs	DU145, LNCaP, PC-3, PC-3MIE8 and RWPE-1	miR-29a	–	circMYLK up-regulation promoted PCa cell proliferation, migration and invasion and suppressed apoptosis	(55)
circHIPK3 (hsa_circ_0000284)	26 PCa tissues and paired NATs	LNCaP, PC3, DU145, 22Rv1, and RWPE-1	miR-193a-3p/MCL1 axis	–	circHIPK3 knockdown inhibited PCa cell proliferation and invasion *in vitro* and tumor growth *in vivo*	(56)
	60 PCa tissues and paired NATs	22RV1, PC-3, DU145, LNCaP, and RWPE-1	miR-338-3p/ ADAM17 axis	–	circHIPK3 knockdown inhibited PCa cell proliferation and invasion	(57)
	Serum samples of 35 PCa tissues and 35 heathy volunteers	RWPE-1, 22Rv1, and DU145	miR-212/ BMI-1 axis	–	circHIPK3 knockdown suppressed PCa cell proliferation, migration and invasion and enhanced apoptosis *in vitro* and tumor growth *in vivo*	(58)
circ0005276	90 PCa tissues and paired NATs	PC-3, DU145, VCaP, LNCaP, and RWPE-1 cells	FUS/XIAP axis	–	circ0005276 knockdown inhibited PCa cell proliferation and migration	(59)
circ_0006404	30 PCa tissues and paired NATs	LNCaP-AI and DU145 LNCaP, and WPMY-1	miR-1299/ CFL2 axis	–	circ_0006404 knockdown suppressed PCa cell proliferation, viability and metastasis and increased apoptosis *in vitro* and also, inhibited tumor growth *in vivo*	(60)
circ-ZNF609	30 PCa tissues and paired NATs	22Rv1, LNCaP, DU145, VCaP and RWPE-1	miR-501-3p/ HK2 axis	–	circ-ZNF609 knockdown supressed tumor progression and radioresistance in PCa cell lines *in vitro* and also, increased radiosensitivity *in vivo*	(47)
circ-SMARCA5	21 PCa tissues and paired NATs	22RV1, DU145, PC-3, LNCaP and WPMY-1	–	–	circ-SMARCA5 knockdown inhibited PCa cell proliferation, and induced apoptosis *via* G1 phase cell cycle arrest	(38)
circ-102004	16 PCa tissues and 6 BPH tissues	PC3 and 22RV1 PC3 and 22RV1	–	ERK, JNK, Hedgehog, AKT, and Wnt/β-Catenin	Overexpression increased PCa cell proliferation, migration, and invasion and inhibited apoptosis *in vitro*, also increased tumor progression *in vivo*	(61)

(Continued)

TABLE 1 | Continued

circRNA (Other terms)	Clinical Cases	Cell Lines	Target genes/ Regulators/ sponged miRNAs	Affected Signaling Pathway/ Process	Findings on over-expressed or silenced circRNA in PCa cellular experiments	Ref. (s)
circPDHX (hsa_circ_0003768)	75 PCa tissues and paired NATs	PC3 and 22RV1 PC3 and 22RV1	miR-378a-3p/IGF1R axis	–	circPDHX knockdown inhibited PCa cell proliferation, colony formation and invasion *in vitro* and tumor progression *in vivo*	(62)
circAGO2	24 PCa tissues and paired NATs	PC-3	HuR	–	circAGO2 overexpression increased PC-3 cell proliferation and invasion *in vitro* and tumor growth *in vivo*	(59)
circ-TRPS1	80 PCa tissues and paired NATs	PC3, LnCaP, DU145 and RWPE-1	miR-124-3p/ EZH2 axis	–	circ-TRPS1 knockdown inhibited PCa cell proliferation and invasion *in vitro* and *in vivo*	(63)
circNOLC1	80 PCa tissues and 16 NATs	DU145, PC3, C4-2, LNCaP, 22RV1, and RWPE1	miR-647/ PAQR4 axis	As downstream of NF-kB	circNOLC1 overexpression increased PCa cell proliferation and migration *in vitro* and knockdown reversed the effects, also increased tumor growth *in vivo*	(62)
circ_0057553	37 PCa tissues and paired NATs	22RV1, PC3, DU145, LNCap, and RWPE1	miR-515-5p/ YES1 axis	Glycolysis	circ_0057553 silencing suppressed PCa cell proliferation, migration, and invasion, also increased apoptosis *in vitro.* Furthermore, inhibited tumor progression *in vivo*	(64)
circ-0016068	42 PCa tissues and paired NATs	DU 145, 22RV1, PC-3, VCaP, and RWPE1	miR-330-3p/ BMI-1 axis	–	circ-0016068 knockdown suppressed PCa cell proliferation, migration, invasion, and EMT *in vitro*, also inhibited tumor growth and metastasis *in vivo*	(65)
circ_CCNB2	25 PCa tissues and paired NATs	DU145 and LNCaP	miR-30b-5p/ KIF18A axis	–	circ_CCNB2 knockdown improved PCa cell radiosensitivity by suppressing autophagy *in vitro* and *in vivo*	(66)
circ_0062020	60 PCa tissues and 30 NATs	DU145, LNCaP, and WPMY-1	miR-615-5p/ TRIP13 axis	–	circ_0062020 knockdown induced radiosensitivity in PCa *in vitro* and also, inhibited tumor growth *in vivo*	(16)
circSLC19A1	48 PCa tissues and paired NATs	DU145 cells, PC3 cells, LNCaP cells, 22RV1, and RWPE-1	miR-326/ MAPK1 axis	–	circSLC19A1 knockdown suppressed PCa cell viability, proliferation, migration and invasion	(51)
	–	22Rv1, DU145, LNCaP, PC3, and WPMY-1	miR-497/ SEPT2/ ERK1/2 axis	ERK1/2	circSLC19A1 overexpression promoted PCa cell proliferation and invasion	(33)
hsa_circ_0000735	50 PCa tissues and paired NATs	PC-3, DU145, and RWPE-1	miR-7	–	hsa_circ_0000735 knockdown increased sensitivity to docetaxel in resistant PCa cells, also *in vivo*	(67)
circFMN2	90 PCa tissues and paired NATs	PC-3, DU145, VCaP, LNCaP, and RWPE-1	miR-1238/ LHX2 axis	–	circFMN2 knockdown decreased PCa cell proliferation, colony formation, migration and invasion *in vitro* and also, tumor growth *in vivo*. circFMN2 exerts its hyperproliferative role *via* increasing DNA synthesis and suppressing apoptosis.	(32)
circPVT1	43 PCa tissues and 15 paired NATs	DU145	MYC oncoprotein	–	circPVT1 knockdown inhibits *MYC* expression in PCa cells. circPVT1 stabilizes the MYC protein in high grade of Gleason score (GP4)	(68)
circRNA-51217	–	PC3, LNCaP, C4-2, DU145, and HEK293T	miR-646	TGFβ1/p-Smad2/3	circRNA-51217 promoted PCa cell invasion	(39)
circZMIZ1	Serum samples of 14 PCa patients and paired NATs	DU145, C4-2, LNCaP, 22RV1, and RWPE-1	AR-V7	–	circZMIZ1 knockdown suppressed PCa cell proliferation by making arrest in G1/S phase of cell cycle. circZMIZ1 expression increased in response to androgens.	(69)
circGOLPH3	–	PC-3, and RWPE-1	CBX7	–	circGOLPH3 overexpression promoted PCa cell proliferation and suppressed apoptosis	(70)
circRNA_100146	–	WPMY1, DU145, LNCaP, 22RV1, VCaP, and PC-3	miR-615-5p/ TRIP13 axis		circRNA_100146 knockdown suppressed PCa cell proliferation and metastasis *in vitro* and tumor growth *in vivo*	(71)
circXPO1	48 PCa tissues and 15 paired NATs	WPMY-1, PC-3, DU145, and 22RV	miR-23a	–	circXPO1 overexpression promoted PCa cell proliferation, colony formation, and invasion	(72)

(Continued)

TABLE 1 | Continued

circRNA (Other terms)	Clinical Cases	Cell Lines	Target genes/ Regulators/ sponged miRNAs	Affected Signaling Pathway/ Process	Findings on over-expressed or silenced circRNA in PCa cellular experiments	Ref. (s)
circGNG4	40 PCa tissues and 15 paired NATs	RWPE, PC-3, LNCaP, VCaP, and DUL145	miR-223/ EYA3/c-Myc axis	–	circGNG4 knockdown inhibited tumor cell proliferation, clonal formation, migration, and invasion *in vitro* and tumor growth *in vivo*	(73)
circ-XIAP	52 PCa tissues	RWPE, 22Rv1, VCaP, DU145, and PC3	miR-1182/ TPD52 Axis	–	circ-XIAP knockdown increased sensitivity to Docetaxel in the drug-resistant PCa cells. circ-XIAP knockdown suppressed PCa growth and improved drug sensitivity *in vivo*.	(74)
circDPP4	104 PCa tissues and matched NATs	RWPE, PC3, DU145, LNCaP and 22RV1	miR-195/ cyclin D1 axis	–	circDPP4 knockdown suppressed PCa cell proliferation, migration, and invasion *in vitro* and tumor growth *in vivo*	(75)
hsa_circ_0047641	–	REPW-1, PC3, LNcap, and DU145	–	–	hsa_circ_0047641 knockdown suppressed proliferation, migration, and invasion in enzalutamide-resistant PCa cells	(49)
circ_0001686	30 PCa tissues and matched NATs	REPW-1, CWR22RV1 and LNCaP	miR-411-5p/ SMAD3/ TGFBR2 axis	TGFβ	Overexpression of sponged miR-411-5p suppressed PCa cell proliferation, migration, and invasion *in vitro*, also inhibited tumor growth and metastasis *in vivo*	(76)

and so, are detected in high concentration in easily received liquid biopsies suggesting potential application as biomarkers in diagnosis of various types of cancer (93). Early, quick, and minimal or non-invasive diagnosis based on detection of dysregulated circRNAs in human bio-specimens like blood and urine (94) makes it possible to provide scheduled and real time monitoring of the responses to treatment and prediction of prognosis in PCa patients. Accordingly, early treatment improves patient survival and so, good prognosis could be predicted for the patients. Both classes of dysregulated circRNAs including up- and down-regulated types can be detected in PCa patient samples and used as clinical biomarkers.

Wang et al. (89) have developed the first bioinformatics-based prognosis model for prediction of biochemical recurrence (BCR) in PCa which used a signature comprised of 8 circRNAs. Among them, two circRNAs including circ_17720 and circ_14736 were detected in exosomes extracted from plasma samples of PCa patients. Furthermore, both exhibited down-regulation in PCa tissues compared to NATs. Experimental analyses revealed that they repress PCa cell proliferation. Survival analysis *via* Kaplan-Meier for eight circRNAs showed that up-regulated circRNA correlated with unfavorable BCR-free survival and those with down-regulation changes were associated with less BCR. The area under curve (AUC) in Receiver-operating characteristic (ROC) for the signature was reported to be 0.799.

Greene et al. (95) profiled circRNAs in enzalutamide-chemoresistance in LNCaP PCa cell lines using high-throughput RNA sequencing. In bioinformatics analyses, five aberrantly expressed circRNAs were identified in enzalutamide-resistant LNCaP cells. Among them, hsa_circ_0004870 showed diminished expression in cells with high levels of androgen receptor (AR) compared to low AR-expressing cells and also, in malignant cells related to benign LNCaP cells. The corresponding *BMP39* gene was also showed down-regulation in enzalutamide-resistant cells. Chen et al. (96) showed that a circRNA signature not only can distinguish PCa tissues from healthy prostate tissues, but also help distinguishment of PCa subtypes. Several circRNAs have shown dysregulation in accordance with Gleason score or correlated with advancement of clinicopathological features in PCa patients (see **Table 3**). Mao et al. (98) demonstrated that increased circPDHX expression levels in PCa tissues is correlated with malignant clinicopathological features in PCa patients. Kaplan-Meier analysis to assess the association between circPDHX expression and prognosis revealed that PCa patients with elevated circPDHX levels had poorer survival relative to patients with low levels. Univariate and multivariate regression analyses also showed that circPDHX high expression level along with advanced Gleason score act as independent prognostic factors for PCa patients predicting poorer survival. In diagnostic analyses, acceptable values of AOC in ROC curve, sensitivity, and specificity of 0.64, 80.0%, and 58.7%, respectively, were found for circPDHX showing promising results especially in distinguishment of PCa from healthy people. He et al. (100) evaluated expression of circrNAs in urinary extracellular vesicles. Their study has indicated the accuracy of a urine circRNA classifier (Ccirc) composed of circPLXDC2, circSCAF8, circPDLIM5, circCCNT2, and circSCAMP1 in detection of PCa. Their results demonstrated higher accuracy of Ccirc compared to that for two care risk calculators. Also, the Ccirc showed better value in prediction of high grades of PCa in combination with risk calculators relative to that of standards alone. In another study, Zhong et al. (97) identified 160 autophagy-related circRNAs, then constructed a circRNA signature containing five circRNAs hsa_circ_0001747, hsa_circ_0002100, hsa_circ_0000280, hsa_circ_0000437, and hsa_circ_0001085 with aberrant expression between high risk and low risk groups of PCa patients. Univariate and multivariate Cox regression analyses demonstrated the signature as an independent prognostic indicator in PCa patients. Also, ROC curve showed higher AUC values for the signature compared to conventional indicators like PSA, age, clinicopathological T stage, and Gleason score. Among the signature circRNAs, hsa_circ_0001747 was identified in association with a higher number of autophagy-related genes and

TABLE 2 | Down-regulated circRNAs in PCa.

circRNA (Other terms)	Clinical Cases	Cell Lines	Target genes/ Regulators/ sponged miRNAs	Affected Signaling Pathway/ Process	Findings on over-expressed or silenced circRNA in PCa cellular experiments	Ref. (s)
circ-ITCH	52 PCa tissues and paired NATs	C4-2, LNCaP, DU145, 22Rv1, VCaP, and RWPE-1	miR-17-5p/ HOXB13 axis	–	circ-ITCH overexpression inhibited PCa cell proliferation and increased apoptosis *in vitro*, also repressed tumor growth *in vivo*.	(77)
	–	VCaP, DU 145, PC-3, 22RV1, and RWPE-1	miR-197	–	circ-ITCH overexpression inhibited cell proliferation and increased apoptosis in PC-3 cells.	(78)
	10 PCa tissues and paired NATs	PC3, LNCaP, and RWPE-1	miR-17	Wnt/β-Catenin and PI3K/ AKT/mTOR	circ-ITCH overexpression suppressed PCa cell viability and invasion.	(79)
hsa_circ_0001206	50 PCa tissues and paired NATs	PC-3, DU145, and LNCaP, and RWPE-1	miR-1285-5p	–	hsa_circ_0001206 overexpression suppressed PCa cell proliferation, colony formation, migration, and invasion *in vitro* and also, tumor growth *in vivo*.	(80)
circAMOTL1L (has_circRNA_000350)	3 PCa patient tissues including 35 BPH tissues, 34 low-grade PCa tissues and 28 high-grade PCa tissues	PC3, LNCaP, 1 DU145, and RWPE-1	miR-193a-5p/ protocadherin-α axis	–	circAMOTL1L knockdown promoted PCa cell migration and invasion *in vitro* and conversely, overexpression decreased tumor growth *in vivo*. circAMOTL1L regulates EMT-related genes.	(81)
circUCK2	–	C4-2	miR-767-5p/ TET1 axis	–	circUCK2 overexpression inhibited PCa cell proliferation, and invasion *in vitro* and tumor growth *in vivo*.	(82)
circ_LARP4	55 PCa tissues and paired NATs	LNCaP, DU145, and 22Rv1	–	–	circ_LARP4 up-regulation suppressed PCa cell migration and invasion, also induced expression of tumor suppressor FOXO3.	(83)
circ-MTO1 (has_circ_0076979)	298 PCa tissues and paired NATs	DU-145, VCaP, PC-3, and RWPE-1	miR-630 and miR-17-5p	–	circ-MTO1 overexpression inhibited PCa cell proliferation and invasion.	(84)
circ_KATNAL1 (hsa_circ_0008068)	–	LNCaP, DU145, and PC3, and WPMY-1	miR-145-3p/ *WISP1* axis	–	circ_KATNAL1 overexpression suppressed PCa cell proliferation and invasion, and also, induced apoptosis. circ_KATNAL1 plays its role *via* regulatory effects on expression of caspases and matrix metalloproteases (MMPs).	(85)
circRNA17 (hsa_circ_0001427)	–	CWR22Rv1, C4–2, and 293T	miR-181c-5p/ ARv7 axis	–	circRNA17 reversely regulates expression of androgen receptor variant-7 and accordingly, negatively affects PCa cells invasion and resistance to enzalutamide. circRNA17 overexpression inhibited tumor growth and metastasis *in vivo*.	(37)
circPSMC3	55 PCa tissues and paired NATs	DU145, PC3, LNCap and P69	DGCR8	–	circPSMC3 overexpression repressed PCa cell proliferation through negative regulation of cell cycle.	(86)
circDDX17	20 PCa tissues and paired NATs	22Rv1 and PC-3	miR-346/ LHPP axis	–	circDDX17 overexpression inhibited PCa cell proliferation, migration, and EMT.	(85)
circSLC8A1 (hsa_circ_0000994)	15 PCa tissues and paired NATs	DU145, 22Rv1, LNCaP, PC-3 and WPMY-1	miR-21	MAPK and chemokine pathways	circSLC8A1 knockdown increased PCa cell proliferation and migration.	(87)
circCRKL (hsa_circ_0001206)	45 PCa tissues and paired NATs	DU145, C4-2, 22Rv1, LNCaP, and RWPE-1	miR-141/KLF5 axis	–	circCRKL overexpression inhibited PCa cell migration and invasion *via* suppressing cell cycle and increased apoptosis *in vitro* and also, inhibited tumor growth *in vivo*.	(88)
circ_17720 and circ_14736	144 PCa tissues and paired NATs	PC3, DU145, C4-2, and	–	–		(89)

(Continued)

TABLE 2 | Continued

circRNA (Other terms)	Clinical Cases	Cell Lines	Target genes/ Regulators/ sponged miRNAs	Affected Signaling Pathway/ Process	Findings on over-expressed or silenced circRNA in PCa cellular experiments	Ref. (s)
		LNCaP, and RWPE-1				
hsa_circ_0075542	30 PCa tissues and paired NATs	LNCaP and PC3	miR-1197/ HOXC11 axis	–	hsa_circ_0075542 overexpression inhibited cell proliferation, migration, and invasion and enhanced apoptosis	(90)
circSMARCA5	20 PCa tissues and paired NATs	RWPE-1, DU145, LNCaP, and PC3	miR-181b-5p + miR-17-3p/ TIMP3 axis	–	circSMARCA5 overexpression inhibited PCa cell proliferation, migration, and invasion *in vitro* and suppressed tumor growth and metastasis *in vivo*.	(91)
circSLC8A1 (hsa_circ_0000994)	15 PCa tissues and paired NATs	WPMY-1, PC-3, 22Rv1, DU145, and LNCaP	miR-21	–	circSLC8A1 knockdown promoted PCa cell proliferation and migration	(87)

its knockdown in experimental validation promoted PCa cell proliferation *in vitro* and *in vivo* through autophagy augmentation.

The prognostic value of circRNAs has also assessed in PCa. For instance, expression levels of hsa_circ_0000437, hsa_circ_0000280, and circ_5017 have been correlated with poor survival of patients (97). Moreover, expression of circABCC4 has been associated with advanced clinicopathological features including higher tumor stage, metastasis and poor clinical outcomes (53). Over-expression of circMBOAT2 has also indicated shorted disease-free survival in two independent cohorts of PCa patients (30). Similarly, over-expression of circFOXO3 has been associated with advanced Gleason score and shorter overall survival of PCa patients (31).

Taken together, these results suggest circRNAs as ideal candidates to be used as biomarkers for diagnosis, prediction of prognosis and also provide therapeutical targets in treatment of PCa. Further studies are required to bring the circRNAs to clinical settings as useful tools with diagnostic, prognostic and therapeutical applications. **Table 3** shows the studies which have assessed the diagnostic, prognostic or clinical significance values of circRNAs in PCa.

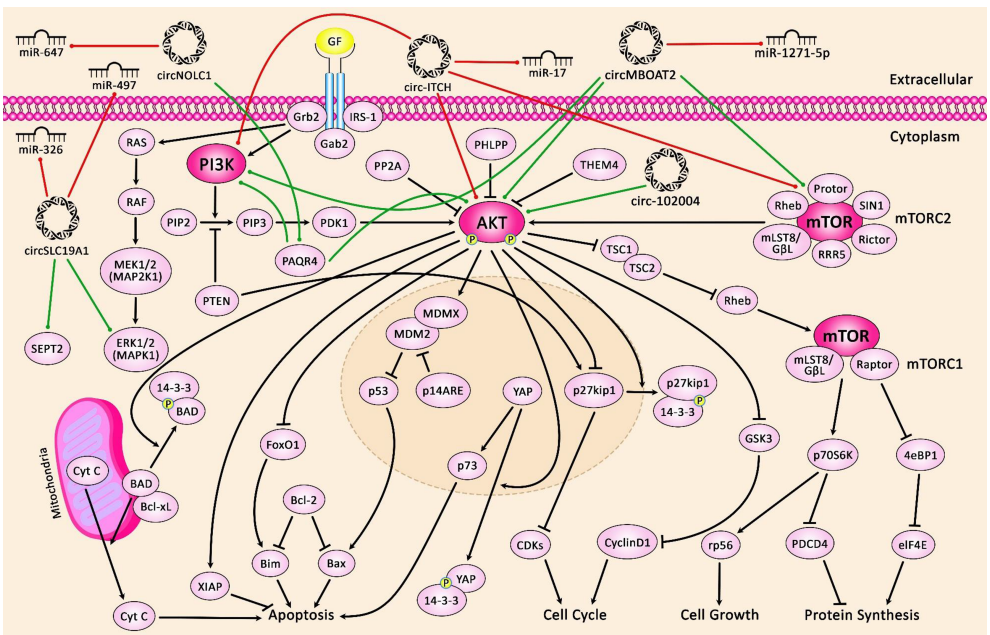

FIGURE 1 | A schematic diagram of the crosstalk between circRNAs and PI3K/AKT/mTOR and MAPK/ERK signaling pathways in prostate cancer. The figure suggests that extracellular circRNAs enter cells.

TABLE 3 | circRNAs with diagnostic or prognostic values in PCa.

Description	Area under Curve (AOC)	Sensitivity	Specificity	Kaplan–Meier analysis	Univariate Cox regression	Multivariate cox regression	Other correlation tests	Ref. (s)
5-circRNA signature	–	–	–	Higher expression of cognate genes for hsa_circ_0006410, hsa_circ_AKAP7 and hsa_circ_0005848 positively correlated with better OS in PCa patients.	–	–	–	(29)
5-circRNA signature	0.827	–	–	PCa patients at the high-risk group with higher expression of hsa_circ_0000437, hsa_circ_0000280, and circ_5017 had lower survival compared to the low-risk group.	Autophagy-related prognostic risk score was correlated with survival in PCa patients.		–	(97)
circABCC4 expression in PCa patients	–	–	–	Higher circABCC4 levels positively correlated with survival in PCa patients	–	–	The Chi-square test showed association between circABCC4 expression and advanced clinicopathological features including higher tumor stage and metastasis	(53)
circMBOAT2 expression in a cohort including 50 PCa patients and matched NATs (high: 31 samples, low: 31 samples)	–	–	–	High circMBOAT2 expression correlated with shorter DFS in two cohorts of PCa patients	Increased expression significantly associated with poorer prognosis in PCa patients.		The χ^2 test demonstrated positive correlation between circMBOAT2 expression and advanced clinicopathological features including higher pathological T stage and Gleason score in PCa patients	(30)
circFOXO3 *via* SLC25A15 axis	–	–	–	High SLC25A15 expression correlated with shorter OS in PCa patients	–	–	- High SLC25A15 circFOXO3 expression was significantly associated with advanced Gleason score in PCa patients - Increased expression of SLC25A15 correlated with poorer prognosis	(31)
circ_0057558	–	–	–	circ_0057558 knockdown in increased OS nude mice	–	–	–	(46)
circHIPK3	–	–	–	–	–	–	High circHIPK3 expression predicted poorer prognosis for PCa patients	(56)
	–	–	–	–	–	–	miR-338-3p high expression levels as target of circHIPK3 correlated with histological grade, lymph node metastasis and distant metastasis.	(57)
circPDHX	0.64	80.0%	58.7%	PCa patients with elevated circPDHX expression levels had poorer survival relative to patients with low levels	circPDHX high expression level along with advanced Gleason score act as independent prognostic factors for PCa patients predicting poorer survival.		High circPDHX expression significantly correlated with high pathological T stage and Gleason score in PCa patients	(98)
circ-TRPS1	–	–	–	–	–	–	The Pearson's correlation test showed an association between increased circ-TRPS1 expression and advanced clinicopathological features including higher T stage, lymph and distant metastasis. High circ-TRPS1 expression correlated with poorer prognosis in PCa patients	(63)
circ-0016068	–	–	–	PCa patients with elevated circ-0016068 expression exhibited	–	–	The Fisher's exact test showed correlation between high circ-0016068 expression and advanced	(65)

(Continued)

TABLE 3 | Continued

Description	Area under Curve (AOC)	Sensitivity	Specificity	Kaplan–Meier analysis	Univariate Cox regression	Multivariate cox regression	Other correlation tests	Ref. (s)
				decreased survival compared to those with lower levels.			clinicopathological features including higher pathological T stage, Gleason score, and lymph node metastasis.	
circ_0062020	–	–	–	–	–	–	The Chi-square test showed correlation between high circ_0062020 expression and advanced clinicopathological features including higher tumor size, TNM stage, Gleason score and lymph node metastasis in PCa patients.	(99)
hsa_circ_0000735	–	–	–	Patients with high hsa_circ_0000735 expression showed shorter OS compared to those with low levels.	–	–	–	(67)
circFMN2	–	–	–	–	–	–	High circFMN2 expression showed association with high pathological T stage, lymph node and distant metastasis. circFMN2 was detected in exosomes extracted from serum of PCa patients.	(32)
circ-ITCH	–	–	–	Low circ-ITCH level significantly correlated with poorer OS in PCa patients.	–	–	Low circ-ITCH expression correlated with advanced clinicopathological characteristics including higher tumor stage, Gleason score and high PSA levels.	(77)
	0.812	88.3%	61.7%	PCa patients with high circ-ITCH expression had better survival including longer DFS and also improved OS.	High circ-ITCH levels were associated with longer DFS in PCa patients.	circ-ITCH level acts as an independent prognostic factor.	Low circ-ITCH levels correlated with unfavorable clinicopathological features including advanced pathological T stage and lymph node metastasis.	(78)
hsa_circ_0001633, hsa_circ_0001206, and hsa_circ_0009061	0.809, 0.774, and 0.711, respectively	–	–	–	–	–	hsa_circ_0001206 and hsa_circ_0009061 expression levels correlated with high Gleason score and tumor stage in PCa patients.	(80)
circ_LARP4	–	–	–	PCa patients with decreased circ_LARP4 expression levels exhibited poorer OS and worse prognosis compared to those with high levels.	–	–	–	(83)
circ-MTO1	–	–	–	PCa patients with high circ-MTO1 levels showed longer OS and DFS.	High circ-MTO1 levels predicted favorable OS and prognosis.	circ-MTO1 expression act as an independent predictive factor predicting better prognosis.	High circ-MTO1 expression levels were significantly associated with better clinicopathological features including lower pathological T stage and N grade in PCa patients.	(84)
circPSMC3	–	–	–	PCa patients with low circPSMC3 expression levels exhibited worse prognosis compared to those with high levels.	–	–	–	(86)
circSLC8A1	–	–	–	–	–	–	Patients with low circSLC8A1 expression exhibited shorter survival compared to those with high levels.	(87)

(Continued)

TABLE 3 | Continued

Description	Area under Curve (AOC)	Sensitivity	Specificity	Kaplan–Meier analysis	Univariate Cox regression	Multivariate cox regression	Other correlation tests	Ref. (s)
circRNA signature	0.799	–	–	Up-regulated circRNAs in the signature were correlated with less survival and down-regulated circRNAs were significantly associated with less recurrence.	–	–	–	(89)

DISCUSSION

CircRNAs are a novel type of ncRNAs for which some regulatory functions are known. Changes in their expression have been found in several disorders especially cancer. High-throughput technologies have helped identification of a vast number of circRNAs which exhibit dysregulation including down- or up-regulation in cancer tissues compared to NATs. Experimental and functional analyses have shown up-regulated circRNAs act as oncogenes, which promote tumorigenicity in cell studies. Conversely, down-regulated circRNAs play role as tumor suppressors and inhibit tumorigenic behaviors of cancer cell lines. In the majority of circRNAs, existence of interactions between them and miRNAs has revealed a mechanism through which circRNAs exert their roles and regulate cellular processes especially cell cycle. Precise understanding of action mechanisms may help finding therapeutic targets for cancer therapy. Clinical assessments, also have unveiled circRNAs as ideal candidates for diagnostic and prognostic applications. Similar to many cancers, a number of circRNAs have been identified to be dysregulated in PCa. In this review, we assessed the preeminent studies on the role of circRNAs in PCa in two categories of down- (**Table 1**) and up-regulated (**Table 2**) circRNAs focusing on functional experiments. Oncogenic circRNAs promote tumorigenicity *via* increasing cell proliferation, migration, and invasion *in vitro* and tumor growth and metastasis *in vivo*. Sponged miRNAs have been recognized in the majority of studies, through them circRNAs exert their roles *via* an axis which finally affects expression or activity of oncogenes or tumor suppressors, or directly influence the cell cycle.

miR-204-5p, miR-3160-5p, miR-548, miR-1182, miR-1271-5p, miR-29a-3p, miR-206, miR-185-3p, miR-29a, miR-193a-3p, miR-338-3p, miR-1299, miR-501-3p, miR-378a-3p, miR-124-3p, miR-152-3p, miR-647, miR-515-5p, miR-330-3p, miR-30b-5p, miR-615-5p, miR-326, miR-497, miR-7, miR-1238 and miR-646 are among the most important cancer-related miRNAs being sponged by circRNAs. The sponging effects of circRNAs on these miRNAs have a crucial role in the regulation of activity of cancer-related pathways. CircFOXO3/miR-29a-3p, circ_0057558/miR-206, circ_0088233/miR-185-3p, circMYLK/miR-29a, circHIPK3/miR-193a-3p, circHIPK3/miR-338-3p, circHIPK3/miR-212, circ_0006404/miR-1299, circ-ZNF609/miR-501-3p, circPDHX/miR-378a-3p, circ-TRPS1/miR-124-3p, circNOLC1/miR-647 are examples of circRNAs/miRNAs axes with crucial roles in the pathogenesis of PCa.

Furthermore, diagnostic and prognostic values of circRNAs have been reviewed. Acceptable values have been reported for a set of circRNAs in PCa which suggest diagnostic and prognostic potentials of circRNAs. Some studies have proposed the role of circRNAs for easy, quick and less invasive diagnosis and prediction of prognosis of PCa patients based on their expression levels in liquid biopsies. However, based on the heterogeneous pattern of expression of circRNAs among patients, multi-gene panels are more promising than individual circRNAs. In addition, they may have therapeutic potentials, however further studies are required to utilize the potentials of circRNAs in clinical settings. It is also necessary to appraise expression of circRNAs in different settings to find possible factors that affect their expression in various cellular contexts.

AUTHOR CONTRIBUTIONS

SN, ArB, and SG-F wrote the draft and revised it. MT designed and supervised the study. AbB, BMH, and EJ collected the data and designed the figures and tables. All authors contributed to the article and approved the submitted version.

REFERENCES

1. Sung H, Ferlay J, Siegel RL, Laversanne M, Soerjomataram I, Jemal A, et al. Global Cancer Statistics 2020: GLOBOCAN Estimates of Incidence and Mortality Worldwide for 36 Cancers in 185 Countries. *CA: Cancer J Clin* (2021) 71(3):209–49. doi: 10.3322/caac.21660
2. Rawla P. Epidemiology of Prostate Cancer. *World J Oncol* (2019) 10(2):63–89. doi: 10.14740/wjon1191
3. Schymura MJ, Sun L, Percy-Laurry A. Prostate Cancer Collaborative Stage Data Items–Their Definitions, Quality, Usage, and Clinical Implications: A Review of SEER Data for 2004-2010. *Cancer* (2014) 120 Suppl 23:3758–70. doi: 10.1002/cncr.29052
4. Gleason DF. Histologic Grading of Prostate Cancer: A Perspective. *Hum Pathol* (1992) 23(3):273–9. doi: 10.1016/0046-8177(92)90108-F
5. Carter HB. Prostate-Specific Antigen (PSA) Screening for Prostate Cancer: Revisiting the Evidence. *JAMA* (2018) 319(18):1866–8. doi: 10.1001/jama.2018.4914

6. Malik B, Feng FY. Long Noncoding RNAs in Prostate Cancer: Overview and Clinical Implications. *Asian J Androl* (2016) 18(4):568–74. doi: 10.4103/1008-682X.177123
7. Hasegawa T, Lewis H, Esquela-Kerscher A. Chapter 12 - The Role of Noncoding RNAs in Prostate Cancer. In: J Laurence, editor. *Translating MicroRNAs to the Clinic*. Boston: Academic Press (2017). p. 329–69.
8. Sanger HL, Klotz G, Riesner D, Gross HJ, Kleinschmidt AK. Viroids are Single-Stranded Covalently Closed Circular RNA Molecules Existing as Highly Base-Paired Rod-Like Structures. *Proc Natl Acad Sci USA* (1976) 73(11):3852–6. doi: 10.1073/pnas.73.11.3852
9. Hsu M-T, Coca-Prados M. Electron Microscopic Evidence for the Circular Form of RNA in the Cytoplasm of Eukaryotic Cells. *Nature* (1979) 280 (5720):339–40. doi: 10.1038/280339a0
10. Chen L-L. The Biogenesis and Emerging Roles of Circular RNAs. *Nat Rev Mol Cell Biol* (2016) 17(4):205–11. doi: 10.1038/nrm.2015.32
11. Suzuki H, Zuo Y, Wang J, Zhang MQ, Malhotra A, Mayeda A. Characterization of RNase R-Digested Cellular RNA Source That Consists of Lariat and Circular RNAs From pre-mRNA Splicing. *Nucleic Acids Res* (2006) 34(8):e63–e. doi: 10.1093/nar/gkl151
12. López-Jiménez E, Rojas AM, Andrés-León E. J Xiao, editor. *Circular RNAs: Biogenesis and Functions*. Singapore: Springer Singapore (2018). p. 17–33.
13. Szabo L, Salzman J. Detecting Circular RNAs: Bioinformatic and Experimental Challenges. *Nat Rev Genet* (2016) 17(11):679–92. doi: 10.1038/nrg.2016.114
14. Boss M, Arenz C. A Fast and Easy Method for Specific Detection of Circular RNA by Rolling-Circle Amplification. *Chembiochem Eur J Chem Biol* (2020) 21(6):793–6. doi: 10.1002/cbic.201900514
15. Zeng X, Lin W, Guo M, Zou Q. A Comprehensive Overview and Evaluation of Circular RNA Detection Tools. *PLoS Comput Biol* (2017) 13(6):e1005420. doi: 10.1371/journal.pcbi.1005420
16. Asghari H, Lin YY, Xu Y, Haghshenas E, Collins CC, Hach F. CircMiner: Accurate and Rapid Detection of Circular RNA Through Splice-Aware Pseudo-Alignment Scheme. *Bioinf (Oxford England)* (2020) 36(12):3703–11. doi: 10.1093/bioinformatics/btaa232
17. Jiang F, Hong F, Shah MW, Shen X. Circular RNAs as Diagnostic Biomarkers in Gastric Cancer: A Meta-Analysis Review. *Pathol Res Pract* (2019) 215 (6):152419. doi: 10.1016/j.prp.2019.04.011
18. Salzman J, Gawad C, Wang PL, Lacayo N, Brown PO. Circular RNAs are the Predominant Transcript Isoform From Hundreds of Human Genes in Diverse Cell Types. *PLoS One* (2012) 7(2):e30733. doi: 10.1371/journal.pone.0030733
19. Hua JT, Chen S, He HH. Landscape of Noncoding RNA in Prostate Cancer. *Trends Genet* (2019) 35(11):840–51. doi: 10.1016/j.tig.2019.08.004
20. Salzman J, Chen RE, Olsen MN, Wang PL, Brown PO. Cell-Type Specific Features of Circular RNA Expression. *PLoS Genet* (2013) 9(9):e1003777. doi: 10.1371/journal.pgen.1003777
21. Memczak S, Jens M, Elefsinioti A, Torti F, Krueger J, Rybak A, et al. Circular RNAs are a Large Class of Animal RNAs With Regulatory Potency. *Nature* (2013) 495(7441):333–8. doi: 10.1038/nature11928
22. Guo JU, Agarwal V, Guo H, Bartel DP. Expanded Identification and Characterization of Mammalian Circular RNAs. *Genome Biol* (2014) 15 (7):409. doi: 10.1186/s13059-014-0409-z
23. Ding Y, Lu C, Zhang W, Wang Y, Li Y, Zhu Y, et al. The Emerging Role of Circular RNAs in Cardiovascular Diseases. *J Physiol Biochem* (2021) 77:343–53. doi: 10.1007/s13105-021-00807-y
24. Tian M, Cao Z, Pang H. Circular RNAs in Sudden Cardiac Death Related Diseases: Novel Biomarker for Clinical and Forensic Diagnosis. *Mol (Basel Switzerland)* (2021) 26(4). doi: 10.3390/molecules26041155
25. Chen D, Hao S, Xu J. Revisiting the Relationship Between Alzheimer's Disease and Cancer With a circRNA Perspective. *Front Cell Dev Biol* (2021) 9:647197. doi: 10.3389/fcell.2021.647197
26. Mahmoudi E, Green MJ, Cairns MJ. Dysregulation of circRNA Expression in the Peripheral Blood of Individuals With Schizophrenia and Bipolar Disorder. *J Mol Med (Berlin Germany)* (2021) 99:981–91. doi: 10.21203/rs.3.rs-231116/v1
27. Chen XT, Li ZW, Zhao X, Li ML, Hou PF, Chu SF, et al. Role of Circular RNA in Kidney-Related Diseases. *Front Pharmacol* (2021) 12:615882. doi: 10.3389/fphar.2021.615882
28. Shi L, Zhang H, Sun J, Gao X, Liu C. CircSEC24A Promotes IL-1β-Induced Apoptosis and Inflammation in Chondrocytes by Regulating miR-142-5p/SOX5 Axis. *Biotechnol Appl Biochem* (2021). doi: 10.1002/bab.2145
29. Zhai X, Zhang Y, Xin S, Cao P, Lu J. Insights Into the Involvement of Circular RNAs in Autoimmune Diseases. *Front Immunol* (2021) 12:622316. doi: 10.3389/fimmu.2021.622316
30. Shi J, Liu C, Chen C, Guo K, Tang Z, Luo Y, et al. Circular RNA Circmboat2 Promotes Prostate Cancer Progression *via* a miR-1271-5p/mTOR Axis. *Aging (Albany NY)* (2020) 12(13):13255–80. doi: 10.18632/aging.103432
31. Kong Z, Wan X, Lu Y, Zhang Y, Huang Y, Xu Y, et al. Circular RNA Circfoxo3 Promotes Prostate Cancer Progression Through Sponging miR-29a-3p. *J Cell Mol Med* (2020) 24(1):799–813. doi: 10.1111/jcmm.14791
32. Shan G, Shao B, Liu Q, Zeng Y, Fu C, Chen A, et al. Circfmn2 Sponges miR-1238 to Promote the Expression of LIM-Homeobox Gene 2 in Prostate Cancer Cells. *Mol Ther Nucleic Acids* (2020), 21:133–46. doi: 10.1016/j.omtn.2020.05.008
33. Zheng Y, Li JX, Chen CJ, Lin ZY, Liu JX, Lin FJ. Extracellular Vesicle-Derived Circ_SLC19A1 Promotes Prostate Cancer Cell Growth and Invasion Through the miR-497/Septin 2 Pathway. *Cell Biol Int* (2020) 44(4):1037–45. doi: 10.1002/cbin.11303
34. Xia Q, Ding T, Zhang G, Li Z, Zeng L, Zhu Y, et al. Circular RNA Expression Profiling Identifies Prostate Cancer- Specific circRNAs in Prostate Cancer. *Cell Physiol Biochem* (2018) 50(5):1903–15. doi: 10.1159/000494870
35. Greene J, Baird A-M, Lim M, Flynn J, McNevin C, Brady L, et al. Differential CircRNA Expression Signatures May Serve as Potential Novel Biomarkers in Prostate Cancer. *Front Cell Dev Biol* (2021) 9:605686–. doi: 10.3389/fcell.2021.605686
36. Chen Q, Shen H, Zhu X, Liu Y, Yang H, Chen H, et al. A Nuclear lncRNA Linc00839 as a Myc Target to Promote Breast Cancer Chemoresistance *via* PI3K/AKT Signaling Pathway. *Cancer Sci* (2020) 111(9):3279. doi: 10.1111/cas.14555
37. Wu G, Sun Y, Xiang Z, Wang K, Liu B, Xiao G, et al. Preclinical Study Using Circular RNA 17 and Micro RNA 181c-5p to Suppress the Enzalutamide-Resistant Prostate Cancer Progression. *Cell Death Dis* (2019) 10(2):37–. doi: 10.1038/s41419-018-1048-1
38. Kong Z, Wan X, Zhang Y, Zhang P, Zhang Y, Zhang X, et al. Androgen-Responsive Circular RNA Circsmarca5 is Up-Regulated and Promotes Cell Proliferation in Prostate Cancer. *Biochem Biophys Res Commun* (2017) 493 (3):1217–23. doi: 10.1016/j.bbrc.2017.07.162
39. Xu H, Sun Y, You B, Huang C-P, Ye D, Chang C. Androgen Receptor Reverses the Oncometabolite R-2-Hydroxyglutarate-Induced Prostate Cancer Cell Invasion *via* Suppressing the circRNA-51217/miRNA-646/Tgfβ1/P-Smad2/3 Signaling. *Cancer Lett* (2020) 472:151–64. doi: 10.1016/j.canlet.2019.12.014
40. Huang E, Chen X, Yuan Y. Downregulated Circular RNA Itchy E3 Ubiquitin Protein Ligase Correlates With Advanced Pathologic T Stage, High Lymph Node Metastasis Risk and Poor Survivals in Prostate Cancer Patients. *Cancer Biomarkers Section A Dis Markers* (2019) 26(1):41–50. doi: 10.3233/CBM-182111
41. Huang A, Zheng H, Wu Z, Chen M, Huang Y. Circular RNA-Protein Interactions: Functions, Mechanisms, and Identification. *Theranostics* (2020) 10(8):3503–17. doi: 10.7150/thno.42174
42. Janas T, Janas MM, Sapoń K, Janas T. Mechanisms of RNA Loading Into Exosomes. *FEBS Lett* (2015) 589(13):1391–8. doi: 10.1016/j.febslet.2015.04.036
43. Dudekula DB, Panda AC, Grammatikakis I, De S, Abdelmohsen K, Gorospe M. CircInteractome: A Web Tool for Exploring Circular RNAs and Their Interacting Proteins and microRNAs. *RNA Biol* (2016) 13(1):34–42. doi: 10.1080/15476286.2015.1128065
44. López-Jiménez E, Rojas AM, Andrés-León E. RNA Sequencing and Prediction Tools for Circular RNAs Analysis. *Adv Exp Med Biol* (2018) 1087:17–33. doi: 10.1007/978-981-13-1426-1_2
45. Panda AC. Circular RNAs Act as miRNA Sponges. *Adv Exp Med Biol* (2018) 1087:67–79. doi: 10.1007/978-981-13-1426-1_6
46. Ding T, Zhu Y, Jin H, Zhang P, Guo J, Zheng J. Circular RNA Circ_0057558 Controls Prostate Cancer Cell Proliferation Through Regulating miR-206/USP33/c-Myc Axis. *Front Cell Dev Biol* (2021) 9:644397–. doi: 10.3389/fcell.2021.644397
47. Du S, Zhang P, Ren W, Yang F, Du C. Circ-ZNF609 Accelerates the Radioresistance of Prostate Cancer Cells by Promoting the Glycolytic

Metabolism Through miR-501-3p/HK2 Axis. *Cancer Manag Res* (2020) 12:7487–99. doi: 10.2147/CMAR.S257441
48. Zhang L, Zhang W, Li H, Tang X, Xu S, Wu M, et al. Five Circular RNAs in Metabolism Pathways Related to Prostate Cancer. *Front Genet* (2021) 12:636419–. doi: 10.3389/fgene.2021.636419
49. Yu J, Sun S, Mao W, Xu B, Chen M. Identification of Enzalutamide Resistance-Related circRNA-miRNA-mRNA Regulatory Networks in Patients With Prostate Cancer. *Onco Targets Ther* (2021) 14:3833–48. doi: 10.2147/OTT.S309917
50. Shi J, Liu C, Chen C, Guo K, Tang Z, Luo Y, et al. Circular RNA Circmboat2 Promotes Prostate Cancer Progression *via* a miR-1271-5p/mTOR Axis. *Aging (Albany NY)* (2020) 12(13):13255. doi: 10.18632/aging.103432
51. Huang B, Zhou D, Huang X, Xu X, Xu Z. Silencing Circslc19a1 Inhibits Prostate Cancer Cell Proliferation, Migration and Invasion Through Regulating miR-326/MAPK1 Axis. *Cancer Manag Res* (2020) 12:11883–95. doi: 10.2147/CMAR.S267927
52. Huang C, Deng H, Wang Y, Jiang H, Xu R, Zhu X, et al. Circular RNA Circabcc4 as the ceRNA of miR-1182 Facilitates Prostate Cancer Progression by Promoting FOXP4 Expression. *J Cell Mol Med* (2019) 23(9):6112–9. doi: 10.1111/jcmm.14477
53. Huang C, Deng H, Wang Y, Jiang H, Xu R, Zhu X, et al. Circular RNA Circabcc4 as the ceRNA of miR-1182 Facilitates Prostate Cancer Progression by Promoting FOXP4 Expression. *J Cell Mol Med* (2019) 23(9):6112–9. doi: 10.1111/jcmm.14477
54. Deng ZH, Yu GS, Deng KL, Feng ZH, Huang Q, Pan B, et al. Hsa_circ_0088233 Alleviates Proliferation, Migration, and Invasion of Prostate Cancer by Targeting hsa-miR-185-3p. *Front Cell Dev Biol* (2020) 8:528155. doi: 10.3389/fcell.2020.528155
55. Dai Y, Li D, Chen X, Tan X, Gu J, Chen M, et al. Circular RNA Myosin Light Chain Kinase (MYLK) Promotes Prostate Cancer Progression Through Modulating Mir-29a Expression. *Med Sci Monitor Int Med J Exp Clin Res* (2018) 24:3462–71. doi: 10.12659/MSM.908009
56. Li C, Zheng H, Hou W, Bao H, Xiong J, Che W, et al. Long non-Coding RNA Linc00645 Promotes TGF-β-Induced Epithelial–Mesenchymal Transition by Regulating miR-205-3p-ZEB1 Axis in Glioma. *Cell Death Dis* (2019) 10 (10):717. doi: 10.1038/s41419-019-1948-8
57. Cai C, Zhi Y, Wang K, Zhang P, Ji Z, Xie C, et al. CircHIPK3 Overexpression Accelerates the Proliferation and Invasion of Prostate Cancer Cells Through Regulating miRNA-338-3p. *Onco Targets Ther* (2019) 12:3363–72. doi: 10.2147/OTT.S196931
58. Tang Y, Liu J, Li X, Wang W. Exosomal circRNA HIPK3 Knockdown Inhibited Cell Proliferation and Metastasis in Prostate Cancer by Regulating miR-212/BMI-1 Pathway. *J Biosci* (2021) 46.
59. Chen Y, Yang F, Fang E, Xiao W, Mei H, Li H, et al. Circular RNA Circago2 Drives Cancer Progression Through Facilitating HuR-Repressed Functions of AGO2-miRNA Complexes. *Cell Death Differ* (2019) 26(7):1346–64. doi: 10.1038/s41418-018-0220-6
60. Li P, Wang Z, Li S, Wang L. Circ_0006404 Accelerates Prostate Cancer Progression Through Regulating miR-1299/CFL2 Signaling. *Onco Targets Ther* (2021) 14:83–95. doi: 10.2147/OTT.S277831
61. Si-Tu J, Cai Y, Feng T, Yang D, Yuan S, Yang X, et al. Upregulated Circular RNA Circ-102004 That Promotes Cell Proliferation in Prostate Cancer. *Int J Biol Macromol.* (2019) 122:1235–43. doi: 10.1016/j.ijbiomac.2018.09.076
62. Chen W, Cen S, Zhou X, Yang T, Wu K, Zou L, et al. Circular RNA CircNOLC1, Upregulated by NF-KappaB, Promotes the Progression of Prostate Cancer *via* miR-647/PAQR4 Axis. *Front Cell Dev Biol* (2021) 8:624764–. doi: 10.3389/fcell.2020.624764
63. Sha J, Xia L, Han Q, Chi C, Zhu Y, Pan J, et al. Downregulation of Circ-TRPS1 Suppressed Prostatic Cancer Prognoses by Regulating miR-124-3p/EZH2 Axis-Mediated Stemness. *Am J Cancer Res* (2020) 10(12):4372–85. doi: 10.21203/rs.3.rs-48783/v1
64. Zhang Y, Shi Z, Li Z, Wang X, Zheng P, Li H. Circ_0057553/miR-515-5p Regulates Prostate Cancer Cell Proliferation, Apoptosis, Migration, Invasion and Aerobic Glycolysis by Targeting Yes1. *OncoTargets Ther* (2020) 13:11289–99. doi: 10.2147/OTT.S272294
65. Li Q, Wang W, Zhang M, Sun W, Shi W, Li F. Circular RNA Circ-0016068 Promotes the Growth, Migration, and Invasion of Prostate Cancer Cells by Regulating the miR-330-3p/BMI-1 Axis as a Competing Endogenous RNA. *Front Cell Dev Biol* (2020) 8:827–. doi: 10.3389/fcell.2020.00827
66. Cai F, Li J, Zhang J, Huang S. Knockdown of Circ_CCNB2 Sensitizes Prostate Cancer to Radiation Through Repressing Autophagy by the miR-30b-5p/KIF18A Axis. *Cancer Biother Radiopharmaceut* (2020). doi: 10.1089/cbr.2019.3538
67. Gao Y, Liu J, Huan J, Che F. Downregulation of Circular RNA Hsa_Circ_0000735 Boosts Prostate Cancer Sensitivity to Docetaxel *via* Sponging miR-7. *Cancer Cell Int* (2020) 20:334–. doi: 10.1186/s12935-020-01421-6
68. Umemori M, Kurata M, Yamamoto A, Yamamoto K, Ishibashi S, Ikeda M, et al. The Expression of MYC is Strongly Dependent on the Circular PVT1 Expression in Pure Gleason Pattern 4 of Prostatic Cancer. *Med Mol Morphol* (2020) 53(3):156–67. doi: 10.1007/s00795-020-00243-9
69. Jiang H, Lv DJ, Song XL, Wang C, Yu YZ, Zhao SC. Upregulated Circzmiz1 Promotes the Proliferation of Prostate Cancer Cells and is a Valuable Marker in Plasma. *Neoplasma* (2020) 67(1):68–77. doi: 10.4149/neo_2019_190213N116
70. Gong L, Tang Y, Jiang L, Tang W, Luo S. Regulation of Circgolph3 and its Binding Protein CBX7 on the Proliferation and Apoptosis of Prostate Cancer Cells. *Biosci Rep* (2020) 40(12):BSR20200936. doi: 10.1042/BSR20200936
71. Zeng L, Liu Y-M, Yang N, Zhang T, Xie H. Hsa_circRNA_100146 Promotes Prostate Cancer Progression by Upregulating TRIP13 *via* Sponging miR-615-5p. *Front Mol Biosci* (2021) 8:693477–. doi: 10.3389/fmolb.2021.693477
72. Chen H, Zhang P, Yu B, Liu J. The Circular RNA Circxpo1 Promotes Tumor Growth *via* Sponging MicroRNA-23a in Prostate Carcinoma. *Front Oncol* (2021) 11(2925). doi: 10.3389/fonc.2021.712145
73. Xu S, Lian Z, Zhang S, Xu Y, Zhang H. CircGNG4 Promotes the Progression of Prostate Cancer by Sponging miR-223 to Enhance EYA3/c-Myc Expression. *Front Cell Dev Biol* (2021) 9:684125. doi: 10.3389/fcell.2021.684125
74. Zhang H, Li M, Zhang J, Shen Y, Gui Q. Exosomal Circ-XIAP Promotes Docetaxel Resistance in Prostate Cancer by Regulating miR-1182/TPD52 Axis. *Drug Des Devel Ther* (2021) 15:1835–49. doi: 10.2147/DDDT.S300376
75. Yang D, Yang B, Zhu Y, Xia Q, Zhang Y, Zhu X, et al. Circular RNA-DPP4 Serves an Oncogenic Role in Prostate Cancer Progression Through Regulating miR-195/Cyclin D1 Axis. *Cancer Cell Int* (2021) 21(1):379. doi: 10.1186/s12935-021-02062-z
76. Pan J, Liu Z, Yang Z, Liang E, Fang C, Zhang D, et al. Circ_0001686 Promotes Prostate Cancer Progression by Up-Regulating SMAD3/TGFBR2 *via* miR-411-5p. *World J Mens Health* (2021) 0:39. doi: 10.5534/wjmh.200204
77. Zhu Q, Li Y, Guo Y, Hu L, Xiao Z, Liu X, et al. Long non-Coding RNA SNHG16 Promotes Proliferation and Inhibits Apoptosis of Diffuse Large B-Cell Lymphoma Cells by Targeting miR-497-5p/PIM1 Axis. *J Cell Mol Med* (2019) 23(11):7395–405. doi: 10.1111/jcmm.14601
78. Yuan Y, Chen X, Huang E. Upregulation of Circular RNA Itchy E3 Ubiquitin Protein Ligase Inhibits Cell Proliferation and Promotes Cell Apoptosis Through Targeting MiR-197 in Prostate Cancer. *Technol Cancer Res Treat* (2019) 18:1533033819886867. doi: 10.1177/1533033819886867
79. Li S, Yu C, Zhang Y, Liu J, Jia Y, Sun F, et al. Circular RNA Cir-ITCH Is a Potential Therapeutic Target for the Treatment of Castration-Resistant Prostate Cancer. *BioMed Res Int* (2020) 2020:7586521. doi: 10.1155/2020/7586521
80. Liu X, Sun N, Mo N, Lu S, Song E, Ren C, et al. Quercetin Inhibits Kidney Fibrosis and the Epithelial to Mesenchymal Transition of the Renal Tubular System Involving Suppression of the Sonic Hedgehog Signaling Pathway. *Food Funct* (2019) 10(6):3782–97. doi: 10.1039/C9FO00373H
81. Yang Z, Qu C-B, Zhang Y, Zhang W-F, Wang D-D, Gao C-C, et al. Dysregulation of P53-RBM25-Mediated Circamotl1l Biogenesis Contributes to Prostate Cancer Progression Through the Circamotl1l-miR-193a-5p-Pcdha Pathway. *Oncogene* (2019) 38(14):2516–32. doi: 10.1038/s41388-018-0602-8
82. Xiang Z, Xu C, Wu G, Liu B, Wu D. CircRNA-UCK2 Increased TET1 Inhibits Proliferation and Invasion of Prostate Cancer Cells *Via* Sponge MiRNA-767-5p. *Open Med (Wars)* (2019) 14:833–42. doi: 10.1515/med-2019-0097
83. Weng XD, Yan T, Liu CL. Circular RNA_LARP4 Inhibits Cell Migration and Invasion of Prostate Cancer by Targeting FOXO3A. *Eur Rev Med Pharmacol Sci* (2020) 24(10):5303–9. doi: 10.18632/aging.103432

84. Hu Y, Guo B. Circ-MTO1 Correlates With Favorable Prognosis and Inhibits Cell Proliferation, Invasion as Well as miR-17-5p Expression in Prostate Cancer. *J Clin Lab Anal* (2020) 34(3):e23086. doi: 10.1002/jcla.23086
85. Zheng Y, Chen CJ, Lin ZY, Li JX, Liu J, Lin FJ, et al. Circ_KATNAL1 Regulates Prostate Cancer Cell Growth and Invasiveness Through the miR-145-3p/WISP1 Pathway. *Biochem Cell Biol Biochim Biol Cellulaire* (2020) 98(3):396–404. doi: 10.1139/bcb-2019-0211
86. Dong JS, Wu B, Chen XH. Circ PSMC3 Inhibits Prostate Cancer Cell Proliferation by Downregulating DGCR8. *Eur Rev Med Pharmacol Sci* (2020) 24(5):2264–70. doi: 10.26355/eurrev_202003_20492
87. Wang D, Yan S, Wang L, Li Y, Qiao B. Circslc8a1 Acts as a Tumor Suppressor in Prostate Cancer *via* Sponging miR-21. *BioMed Res Int* (2021) 2021:6614591.
88. Nan C, Wang Y, Yang S, Chen Y. circCRKL Suppresses the Progression of Prostate Cancer Cells by Regulating the miR-141/KLF5 Axis. *Pathol Res Practice* (2020) 216(11):153182. doi: 10.1016/j.prp.2020.153182
89. Wang S, Su W, Zhong C, Yang T, Chen W, Chen G, et al. An Eight-CircRNA Assessment Model for Predicting Biochemical Recurrence in Prostate Cancer. *Front Cell Dev Biol* (2020) 8:599494. doi: 10.3389/fcell.2020.599494
90. Han Y, Wen X, Li X, Chen D, Peng L, Lai B, et al. Circular RNA Hsa_Circ_0075542 Acts as a Sponge for microRNA-1197 to Suppress Malignant Characteristics and Promote Apoptosis in Prostate Cancer Cells. *Bioengineered* (2021) 12(1):5620–31. doi: 10.1080/21655979.2021.1967064
91. Xie X, Sun F-K, Huang X, Wang C-H, Dai J, Zhao J-P, et al. Circsmarca5, Inhibits Prostate Cancer Proliferative, Migrative, and Invasive Capabilities *via* the miR-181b-5p/miR-17-3p-TIMP3 Axis. *Aging (Albany NY)* (2021) 13 (15):19908–19. doi: 10.18632/aging.203408
92. Wang X, Wang R, Wu Z, Bai P. Circular RNA ITCH Suppressed Prostate Cancer Progression by Increasing HOXB13 Expression *via* Spongy miR-17-5p. *Cancer Cell Int* (2019) 19(1):328. doi: 10.1186/s12935-019-0994-8
93. Wang S, Zhang K, Tan S, Xin J, Yuan Q, Xu H, et al. Circular RNAs in Body Fluids as Cancer Biomarkers: The New Frontier of Liquid Biopsies. *Mol Cancer* (2021) 20(1):1–10. doi: 10.1186/s12943-020-01298-z
94. Bahn JH, Zhang Q, Li F, Chan TM, Lin X, Kim Y, et al. The Landscape of microRNA, Piwi-Interacting RNA, and Circular RNA in Human Saliva. *Clin Chem* (2015) 61(1):221–30. doi: 10.1373/clinchem.2014.230433
95. Greene J, Baird A-M, Casey O, Brady L, Blackshields G, Lim M, et al. Circular RNAs are Differentially Expressed in Prostate Cancer and are Potentially Associated With Resistance to Enzalutamide. *Sci Rep* (2019) 9(1):10739–. doi: 10.1038/s41598-019-47189-2
96. Chen S, Huang V, Xu X, Livingstone J, Soares F, Jeon J, et al. Widespread and Functional RNA Circularization in Localized Prostate Cancer. *Cell* (2019) 176 (4):831–43.e22. doi: 10.1016/j.cell.2019.01.025
97. Zhong C, Wu K, Wang S, Long Z, Yang T, Zhong W, et al. Autophagy-Related circRNA Evaluation Reveals Hsa_Circ_0001747 as a Potential Favorable Prognostic Factor for Biochemical Recurrence in Patients With Prostate Cancer. *Cell Death Dis* (2021) 12(8):726. doi: 10.1038/s41419-021-04015-w
98. Mao Y, Li W, Hua B, Gu X, Pan W, Chen Q, et al. Circular RNA_PDHX Promotes the Proliferation and Invasion of Prostate Cancer by Sponging MiR-378a-3p. *Front Cell Dev Biol* (2021) 8:602707–. doi: 10.3389/fcell.2020.602707
99. Li H, Zhi Y, Ma C, Shen Q, Sun F, Cai C. Circ_0062020 Knockdown Strengthens the Radiosensitivity of Prostate Cancer Cells. *Cancer Manag Res* (2020) 12:11701–12. doi: 10.2147/CMAR.S273826
100. He Y-D, Tao W, He T, Wang B-Y, Tang X-M, Zhang L-M, et al. A Urine Extracellular Vesicle circRNA Classifier for Detection of High-Grade Prostate Cancer in Patients With Prostate-Specific Antigen 2–10 Ng/mL at Initial Biopsy. *Mol Cancer* (2021) 20(1):96. doi: 10.1186/s12943-021-01388-6

Conflict of Interest: The authors declare that the research was conducted in the absence of any commercial or financial relationships that could be construed as a potential conflict of interest.

Publisher's Note: All claims expressed in this article are solely those of the authors and do not necessarily represent those of their affiliated organizations, or those of the publisher, the editors and the reviewers. Any product that may be evaluated in this article, or claim that may be made by its manufacturer, is not guaranteed or endorsed by the publisher.

frontiers in Oncology

ORIGINAL RESEARCH
published: 09 February 2022
doi: 10.3389/fonc.2022.841054

Decrease of Intracellular Glutamine by STF-62247 Results in the Accumulation of Lipid Droplets in von Hippel-Lindau Deficient Cells

Mathieu Johnson[1,2], *Sarah Nowlan*[1,2], *Gülsüm Sahin*[1,2], *David A. Barnett*[2], *Andrew P. Joy*[2], *Mohamed Touaibia*[1], *Miroslava Cuperlovic-Culf*[3], *Daina Zofija Avizonis*[4] *and Sandra Turcotte*[1,2*]

[1] Department of Chemistry and Biochemistry, Université de Moncton, Moncton, NB, Canada, [2] Atlantic Cancer Research Institute, Moncton, NB, Canada, [3] National Research Council of Canada, Digital Technologies Research Center, Ottawa, ON, Canada, [4] Goodman Cancer Research Centre, McGill University, Montréal, QC, Canada

OPEN ACCESS

Edited by:
Michael Höpfner, Charité Universitätsmedizin Berlin, Germany

Reviewed by:
Chunzhang Yang, National Cancer Institute, United States
Francesco Tabaro, European Molecular Biology Laboratory (EMBL), Italy

***Correspondence:**
Sandra Turcotte
Sandra.turcotte@umoncton.ca

Specialty section:
This article was submitted to Genitourinary Oncology, a section of the journal Frontiers in Oncology

Received: *21 December 2021*
Accepted: *13 January 2022*
Published: *09 February 2022*

Citation:
Johnson M, Nowlan S, Sahin G, Barnett DA, Joy AP, Touaibia M, Cuperlovic-Culf M, Zofija Avizonis D and Turcotte S (2022) Decrease of Intracellular Glutamine by STF-62247 Results in the Accumulation of Lipid Droplets in von Hippel-Lindau Deficient Cells. Front. Oncol. 12:841054. doi: 10.3389/fonc.2022.841054

Kidney cancer is one of the top ten cancer diagnosed worldwide and its incidence has increased the last 20 years. Clear Cell Renal Cell Carcinoma (ccRCC) are characterized by mutations that inactivate the von Hippel-Lindau (VHL) tumor suppressor gene and evidence indicated alterations in metabolic pathways, particularly in glutamine metabolism. We previously identified a small molecule, STF-62247, which target VHL-deficient renal tumors by affecting late-stages of autophagy and lysosomal signaling. In this study, we investigated ccRCC metabolism in VHL-deficient and proficient cells exposed to the small molecule. Metabolomics profiling using 1H NMR demonstrated that STF-62247 increases levels of glucose, pyruvate, glycerol 3-phosphate while glutamate, asparagine, and glutathione significantly decreased. Diminution of glutamate and glutamine was further investigated using mass spectrometry, western blot analyses, enzymatic activities, and viability assays. We found that expression of SLC1A5 increases in VHL-deficient cells treated with STF-62247, possibly to stimulate glutamine uptake intracellularly to counteract the diminution of this amino acid. However, exogenous addition of glutamine was not able to rescue cell viability induced by the small molecule. Instead, our results showed that VHL-deficient cells utilize glutamine to produce fatty acid in response to STF-62247. Surprisingly, this occurs through oxidative phosphorylation in STF-treated cells while control cells use reductive carboxylation to sustain lipogenesis. We also demonstrated that STF-62247 stimulated expression of stearoyl-CoA desaturase (SCD1) and peripilin2 (PLIN2) to generate accumulation of lipid droplets in VHL-deficient cells. Moreover, the carnitine palmitoyltransferase 1A (CPT1A), which control the entry of fatty acid into mitochondria for β-oxidation, also increased in response to STF-62247. CPT1A overexpression in ccRCC is known to limit tumor growth. Together, our results demonstrated that STF-62247 modulates cellular metabolism of glutamine, an amino acid involved in the

autophagy-lysosome process, to support lipogenesis, which could be implicated in the signaling driving to cell death.

Keywords: metabolomics, glutamine (Gln), CCRCC kidney cancer, von Hippel – Lindau, fatty acid, cancer, lipid droplet (LD)

INTRODUCTION

Kidney cancer affects about 431,000 people worldwide and represents 3% of all malignancies (1). Clear cell Renal Cell Carcinoma (ccRCC) originates from renal tubular epithelial cells and accounts for 75% of RCC diagnosis (2). The remaining 25% consist of papillary RCC (15%), chromophobe RCC (5%), and oncocytomas (5%) (3). Unfortunately, these tumors are asymptomatic leaving one-third of patients with metastases at diagnosis. Moreover, 30-40% of patients with localized tumors relapse following surgery (4). Despite the availability of targeted therapies and the approval of immune checkpoint inhibitors, metastatic RCC 5-year survival rate remains low due to intrinsic or acquired resistance (4, 5). ccRCC are characterized by an early loss of chromosome 3p followed by inactivating mutations affecting the von Hippel-Lindau (VHL) tumor suppressor gene that occurs in up to 85% of cases (6–9). The tumor suppressor function of VHL has been demonstrated in nude mice where restoration of its function inhibits tumor formation (10). In addition, VHL loss served as a building block for additional branch mutations observed on the chromatin-remodeling genes PBRM1 (30-40%), SETD2 (8-12%), BAP1(6-8%) (11–14). In the context of VHL loss, or under hypoxic conditions, the hypoxia-inducible factor alpha (HIFα) is stabilized which activates the transcription of genes that regulate oncogenic transformation, angiogenesis, and metabolism (15, 16). The VHL-HIF axis is the foundation of targeted therapies for metastatic RCCs with drugs (e.g., sunitinib, pazopanib, axitinib) that target VEGFR (17).

Metabolic reprogramming has been recognized as a hallmark of cancer (18). Hypoxic conditions observed in tumor microenvironment increased glycolysis supporting cell proliferation (19–21). In addition to HIF-1α and HIF-2α activation, cancer-causing mutations can also directly alter metabolism to promote glutamine utilization. For example, the oncogene c-Myc activates glutaminolysis by repressing miR23a/b while K-Ras mutations stimulate aspartate formation derived from glutamine (22, 23). For a long time, ccRCCs have been known as a metabolic disease. In fact, it has been shown that VHL mutations induce a metabolic switch promoting glutamine reductive carboxylation instead of supporting oxidative phosphorylation to support lipogenesis (24, 25). Glutamine is a non-essential amino acid (NEAA) synthesized *de novo* and metabolized by all cells to support the biosynthesis of nucleotides, glutathione and other NEAA. Glutamine and derivatives have been implicated in epigenetic regulation, such as histone post-translational modifications and DNA methylation levels and can also contribute to resistance to targeted therapy (26, 27). Glutamine is incorporated into the cells through the Solute Carrier (SLC) membrane transporter SLC1A5 as well as others from the SLC6, SLC7 and SLC38 transporter families (28). High expression of SLC1A5 has been reported in several cancers including ccRCC (29–31). Inside mitochondria, glutamine is converted into glutamate by the glutaminase (GLS1), which can then enter Krebs cycle. Inhibitors of GLS1 have been shown to repress cancer growth in tumors addicted to glutamine (24, 25, 32, 33). Finally, glutamine goes through reductive carboxylation to form citrate and support fatty acid production, particularly in VHL-deficient RCC when HIF-2α is overexpressed (24). Changes in fatty acid (FA) metabolism have been documented in ccRCC and accumulation of lipid droplets in the cytosol is a phenotypic characteristic of these tumors (34). For example, it has been shown that HIF-α represses the expression of carnitine palmitoyltransferase 1A (CPT1A) responsible for β-oxidation in the mitochondria (35). In addition, peripilin 2 (PLIN2) and stearoyl-CoA desaturase (SCD1) are highly expressed in HIF-2α dependent ccRCC, both favoring lipid storage (36, 37).

We previously performed metabolomic profiling to identify intracellular and extracellular deregulated metabolites in VHL-inactivated cells compared to cells with the functional gene and we used shRNA against HIF-1α and HIF-2α to further describe those regulated by HIF-α (38). Here, we evaluated the effect of STF-62247 on ccRCC metabolism. STF-62247 is a small molecule, cytotoxic to VHL-inactivated ccRCC compared to cells stably expressing VHL, that we previously identified from a screen (39). We showed that this small molecule affects the autophagic flux by targeting lysosome vulnerabilities observed in tissue from patients with ccRCC (40, 41). Here, we showed that STF-62247 decreased significantly intracellular levels of glutamine and glutamate in VHL-deficient cells without any change in GLS1 activity. However, addition of extracellular glutamine into the media is not sufficient to rescue STF-62247 treated cells. Surprisingly, metabolic flux analysis of glutamine indicated that VHL-deficient cells exposed to the small molecule favor the oxidative tricarboxylic acid (TCA) cycle to produce citrate and increase FA production in contrary to control cells that use reductive carboxylation to support lipogenesis. Finally, we observed that SCD1 and PLIN2 expression, which stimulate the formation of lipid droplets into VHL-deficient RCC, increased in response to STF-62247.

MATERIALS AND METHODS

Cell Culture

The human ccRCC cell lines (RCC4, RCC10 and 786.0) and their isogenic counterparts stably expressing VHL (RCC4/VHL, RCC10/VHL and 786.0/VHL) were kindly provided by Amato J. Giaccia (Stanford University, CA, USA). All cell lines were

tested for mycoplasma and authentication was performed by short tandem repeat (STR) DNA profile at Genetica DNA Laboratories (Burlington, NC, USA). Cells were maintained in DMEM/high glucose medium (GE Healthcare Life Science, UT, USA), supplemented with 10% Fetal bovine serum (FBS) (Wisent Bio Science, QC, Canada), 2 mM L-glutamine and 1mM sodium pyruvate (GE Health Life Sciences, ON, Canada) and cultured at 37˚C in a humidified incubator with 5% CO_2.

Cell Treatment and Metabolite Extraction

Cells were treated with STF-62247 (Cayman Chemical) at 1.25 μM STF-62247 for 24 hr in RCC4 and RCC4/VHL cells and 2.5 μM for 48 hr in 786.0, 786.0/VHL, RCC10 and RCC10/VHL cells. Cells were harvested with the media by scraping and centrifuged at 1,500 x g for 1 min at 4°C. The pellet was washed with cold PBS and then resuspended in 1 mL ice-cold acetonitrile:water solution (1:1). Samples were incubated on ice for 10 min and centrifuged at 16,000 x g for 10 min at 4°C and the supernatants were placed at -80°C.

NMR Experimentation, Data Analysis and Metabolite Quantification

The extract supernatants were dried under a stream of N_2 and dissolved in 0.7 mL deuterium oxide (Aldrich, 99.96% atome ^2H). All ^1H NMR analysis were performed on a Bruker Avance III 400 MHz at 298K and the spectra were obtained using a gradient water presaturation method with 512 scans as previously described (38). Spectra were processed using the Mnova software with exponential apodization, global phase correction, Berstein-polynomial baseline correction and Savitzky-Golay line smoothing and normalization using total spectra area and regions from 0.5 to 4.5 ppm and 5 to 9 ppm were included in the normalization and analysis. Principal component analysis was performed through Matlab vR2010b platform and hierarchical clustering was done with TMeV software with the significance analysis for microarray (SAM) method. Peak assignment was processed through several methods developed in our group and elsewhere based on NMR databases (www.hmdb.ca and www.bmrb.wisc.edu). An automated method for quantification based on multivariable linear regression of spectra with aligned standard metabolite data from databases was developed and used previously.

Glutamine, Glutamate and Leucine Quantification Using LC-MS Analysis

The extract supernatants were filtered through 300 kDa molecular weight cut-off filters (Pall, Ann Arbour, Michigan) at 14,000 x g for 20 min at 4°C to remove any particulates. The flow-through from all samples was then diluted 20-50 fold in acetonitrile:water (9:1) before injection on the LC-MS platform. All samples were spiked with 1 μM of internal standard. The liquid chromatograph was an Agilent 1100 (Agilent, Palo Alto, CA). A Sequant® ZIC-cHILIC chromatographic column (EMD MilliporeCorp. Billerica, MA) was used (150 mm long and 2.1 mm in diameter). The column was packed with 3μm diameter particles with a pore size of 100 Å. The addition of 20 mM ammonium acetate to solvent B (water) was found to be critical for analyte retention and separation. The column flow rate was 100 μL/min, the column back pressure was approximately 180 bar and the sample injection volume was 5 μL. Solvent A was acetonitrile and solvent B was 20 mM aqueous ammonium acetate. The solvent gradient was ramped from 10 - 30% B in 1 min, then to 41% B over 15 min and finally back to 10% B for 24 min to re-equilibrate the column. The observed retention times were as follows: Gln/d5-Gln (22.68 minutes), Glu/d5-Glu (22.25 minutes), Leu/d10-Leu (16.85 minutes) and Ile (17.41 minutes). Note that leucine and isoleucine are nearly baseline resolved. Chromatographic peak widths were roughly 12-15 sec. HR/AM mass spectrometric detection was accomplished with a hybrid quadrupole/Orbitrap mass analyzer (Q-Exactive, Thermo-Fisher Scientific, San Jose, CA) operated in negative ion mode at a resolution of 140,000. The mass-to-charge scan range was 100-500. Measured molecular weights for endogenous glutamine, glutamate and leucine as well as their deuterated analogs were all within 5 ppm of their calculated weights. The observed mass-to-charge values were as follows: Gln (145.0603), Glu (146.0444), d5-Gln (150.0919), d5-Glu (151.0759), Leu (130.0858) and d10-Leu (140.1486). Calibration curves for the LC-MS system were established for a concentration range of 1 nM to 25 μM using the isotopically labeled compounds as internal standards at a level of 1 μM throughout. Interface conditions on the Q-Exactive were as follows: Sheath, auxiliary and sweep gas flow rates (7, 1 and 1 arbitrary units); ionspray voltage (3.5 kV), heated capillary voltage (320°C) and S-lens voltage (50 V). Data was processed using the Quan Browser node of the Xcalibur 3.0.63 software. Calibration curves of analyte peak area relative to that of the appropriate internal standard were plotted as a function of analyte concentration.

Western Blot Analysis

Total proteins were extracted using M-PER lysis buffer (50mM Tris (HCl) pH 7.5, 200 mM NaCl, 0.25% Triton X-100, 10% Glycerol) containing 1X protease and phosphatase inhibitor cocktails. Cell lysates were centrifuged at 12,000 x g for 10 min at 4°C and quantified by BCA protein assay kit (Thermo Fisher scientific) using the SpectraMax Plus 384 microplate reader. Proteins (30μg) were separated on 10-15% SDS-PAGE gel and transferred onto a 0.45-micron PVDF transfer membrane (Immobilon-P, Millipore, IE). Membranes were blocked using 5% skim milk diluted in a solution of 0.075% PBS-Tween (PBS-T) and incubated overnight in 3% BSA with specific primary antibodies against VHL, HIF-1α and HIF-2α (Cell signaling #68547, 14179, 59973), SLC1A5 and β-actin (Santa Cruz Biotechnologies sc-99002 and sc-47778), SLC7A5 (Medical & Biological Laboratories #BMP011), SLC3A2 (Aviva Systems Biology #OAAB00158), ASNS (Signalway #32909), SCD1 (Applied Biological Materials #ABM-G076), PLIN2 (Proteintech #15294-1-AP) and CPT1A (Abcam #ab220789). Immunoblots were washed and incubated with HRP-conjugated secondary antibodies diluted in 5% skim milk PBS-T (Jackson Immunoresearch Laboratories, PA, USA) and visualized using the ClarityTM ECL substrate, (Bio-Rad, ON, Canada) on a Chemidoc MP Imager (Bio-Rad).

Glutaminase and Glutamine Synthetase Activity

For glutaminase activity, 10 µg of protein was mixed with 10 µL of buffer A (50 mM Tris-acetate pH 8.6, 20 mM glutamine, 100 mM K_2HPO_4, 0.2 mM EDTA) and incubated at 37°C for 10 min. Reaction was stopped with 2 µL of HCL 2M. Then, 200 µL of Buffer B (80 mM Tris-acetate pH 9.4, 200 mM hydrazine, 0.25 mM ADP, 2mM NAD and 2.5 U Glutamate deshydrogenase) was added to the sample and absorbance was read at 340 nm on a SpectraMax i3 (Molecular Devices) each 1 min for 5 min and then at 5 min interval for 30 min. GLS activity was calculated according to the Beer's Law $(dAbs/\varepsilon^*d)(10^6)(V_t/V_s)$ where ε = molar extinction coefficient of NADH, d = path length of light through the sample, Vt/Vs= total volume/sample volume. To measure activity of the glutamine synthetase, 40 µg of proteins in 50 µL of lysis buffer (50 mM imidazole-HCl pH6.8) were mixed with 50 µL of reaction buffer (50 mM imidazole pH 6.8, 50 mM glutamine, 25 mM hydroxylamine, 25 mM sodium arsenite, 2 mM $MnCl_2$, 0.16 mM ADP) and incubated for 4 hr at 37°C. Then, 100 µL of stop solution (2.42% $FeCl_3$, 1.45% TCA, 1.82 N HCl) was added and products were centrifuged at 16,000 x g at 4° C for 10 min. Supernatants were transferred into a microplate and absorbance was read at 560 nm. A standard curve of γ-glutamylhydroxamate was generated and used to calculate GS activity and reported in nmol/min/g protein.

Mitochondrial Oxygen Consumption Experiments

Cell respiration was performed on a Oxygraph-2K (Oroboros instrument) in a glass chamber. Cells were trypsinized and 5 x 10^5 cells/mL were added to the chamber and the respiration was measured at the basal level to represent the endogenous respiration state of the cells. The non-coupled resting respiration was measured after adding 2.5 µM of oligomycin followed by the gradual addition of FCCP (up to 2 µM) to evaluate the maximal uncoupled capacity of the electron transport system (ETS). Finally, 2.5 µM antimycin A and 0.5 µM rotenone were added to measure the residual oxygen that occurs independently of oxidative phosphorylation. Respiratory control ratio (RCR) was calculated from the ratio between the uncoupled and non-coupled respiration.

Cell Proliferation, Clonogenic and XTT Assays

Growth curves were performed in 12 well plates with 30,000 cells in duplicate. STF-62247 (1.25 µM), glutamine (10 mM), asparagine (2 mM) or lysophosphatidylcholine 18:1 (25 µM) (Avanti Polar Lipids, Inc.) was added 12 hr after plating. Cells were trypsinized and counted with trypan blue at different time points. For clonogenic assays, 300 cells were seeded in triplicate into 60 mm plates overnight and STF-62247 (0-5 µM) was added to the cells. Plates were incubated at 37°C for 8 days. Colonies were fixed and stained with a solution of crystal violet and quantified. For XTT assays, 5,000 cells were seeded in duplicate in 96 well plates. Cells were treated with STF-62247, BCH (Tocris Bioscience) and L-Glutamic acid γ-(p-nitroanilide) hydrochloride (Sigma-Aldrich) 12 hr after seeding and plates were incubated for 4 days at 37°C. Then, XTT solution (0.3 mg/mL of XTT powder (Sigma-Aldrich), DMEM high glucose without phenol red (Wisent Bio), 20% FBS and 2.65 µg/mL phenazine methosulfate (PMS) (Sigma-Aldrich)) was added to the cells and incubated at 37°C for 1 hr. Absorbance was read at 450 nm on a Spectramax Plus spectrophotometer (Molecular Devices, Sunnyvale, CA). All these assays were performed in biological triplicate.

RNA Isolation and Quantitative Real Time-Polymerase Chain Reaction

Total RNA was isolated from cell lines using TRIzol reagent (Thermo Fisher Scientific) according to the manufacturer's protocol. The RNA was quantified using the Nanodrop ND-1000 (Thermo Fisher Scientific) and its purity was assessed by the ratio absorbance 260/280. RNAs (5µg) were subjected to reverse transcription using SuperScript III reverse transcriptase (Thermo Fisher Scientific). The resulting cDNA was used for real-time qPCR (Realplex^2, Eppendorf) for quantification by SYBR green (Quanta Biosciences). cDNA was first denaturated at 95°C for 3 min followed by hybridization and elongation at 60°C and 72°C, respectively for 40 cycles. RNA expression was normalized to RPLPO expression. All primers sequences were provided by primerbank (https://pga.mgh.harvard.edu/primerbank/) as follow: SLC1A5 forward 5'-TCATGTGGTACGCCCCTGT-3' and reverse 5'-GCGGGCAAAGAGTAAACCCA-3'; SLC3A2 forward 5'-TGAATGAGTTAGAGCCCGAGA-3' and reverse 5'-GTCTTCCGCCACCTTGATCTT-3'; SLC7A5 forward 5'-GTG GACTTCGGGAACTATCACC-3' and reverse 5'-GAACA GGGACCCATTGACGG-3; RPLPO forward 5'-GCAATG TTGCCAGTGTGT-3' and reverse 5'-GCCTTGACCT TTTCAGCAA-3'. mRNA relative expression was calculated with the ΔΔCt method.

Metabolic Flux Studies, $^{13}C_5$-Glutamine Labeling and GC-MS Analysis

Cells were plated in DMEM supplemented with 10% dialyzed FBS (Wisent Bio), 1 mM glutamine and 1 mM sodium pyruvate and 1.25 µM STF-62247 was added for 24 hr. For glutamine metabolic tracing, media was replaced with DMEM without glutamine supplemented with $^{13}C_5$-L-glutamine (Cambridge Isotopes Laboratories, Tewksbury, MA), 10% dialyzed FBS with or without STF-62247 for up to 2 hr. In addition, dishes were kept in unlabeled media as control. Metabolite extraction was performed at different time points as previously described and samples were sent to McGill Metabolomics Core Facility for GC-MS analysis. Briefly, supernatants were dried by spin vacuum, dissolved in a solution of 10 mg/mL methoxyamine: HCl in pyridine, and derivatized with MTBSTFA for 1 hr at 70° C. One microliter of derivatized samples was analyzed through an Agilent 5975C Series GC/MSD with the Triple-Axis HED/EM Detector coupled to a 7890A gas chromatograph equipped with a 7693 autosampler (Agilent, Santa Clara, CA). Data are collected and analyzed by Chemstation software or Mass Hunter. Spectra are identified using Fiehn, Bains (Steadman Metabolism

laboratory, Duke University) or NIST17 databases and authentic samples.

^{14}C-glutamine labeling and Lipid Synthesis

50,000 cells were seeded in 12-well plates in duplicate, and treated with 1.25 μM STF-62247 for 24 hr. The last hour, media was replaced with DMEM supplemented with 0.2 μCi/mL (L-[^{14}C(U)]-Glutamine (American Radiolabeled Chemicals, St-Louis, MO). Lipids were extracted according to a modified version of Bligh and Dyer method (42). Briefly, after trypsinization, a solution of cells (400 μL trypsin and 400 μL PBS for a total of 800 μL) was added to 3 mL methanol and chloroform solution (2:1) followed by the addition of 25 μL of 10% acetic acid. Samples were vortexed and incubated at room temperature for 15 min. Another 2 mL chloroform and 1 mL water were added, in order, before carefully mixing. Samples were centrifuged at 1,000 RPM for 5 min at room temperature. The chloroform phase (on top) was transferred to a new tube and put on the side. Another 2 mL chloroform was added to the samples, mixed and centrifuged like precedently. The chloroform phase was pooled with the first one before being air-dried with nitrogen and resuspended in scintillation liquid. Total extractable counts were obtained using LS 6500 multipurpose scintillation counter (Beckman Coulter™) and normalized with cell number.

Lipid Droplets Quantification

Cells were seeded in 8 well chamber slides and treated for 48 hr with 1.25 μM STF-62247. On the last day, cells were fixed with 3.7% formaldehyde, lipid droplets were stained with HSC LipidTOX™ green neutral lipid stain (ThermoFisher) according to the manufacturer protocol and nuclei were stained with DAPI. Cells were incubated in LipidTOX (1:3000 dilution) for at least 30 min before images were taken using a 60X objective lens on an Olympus Fluoview FV1000 confocal microscope (Olympus). Images were analyzed, and puncta were counted using Fiji (ImageJ) using three pictures for each experimental condition in three biological replicates.

Statistical Analysis

Statistical analyses were performed using RStudio (RStudio Team (2020). RStudio: Integrated Development Environment for R. RStudio, PBC, Boston, MA URL http://www.rstudio.com/) and GraphPad Prism version 6.01 for Windows, GraphPad Software (La Jolla, CA) www.graphpad.com. Data for glutamine and glutamate quantification by LC-MS, enzymatic activities, RCR, radiolabeled glutamine-derived fatty acid synthesis and lipid droplets counts were analyzed using a two-way ANOVA for the comparisons of the two independent variables: VHL status (RCC4 VHL- and VHL+) and treatment conditions (CTL and STF-62247). For cell proliferation and viability, the variables were the treatments (CTL, STF-62247 and/or Gln, Asn or LPC 18:1) and the time points (day 1, 3 and 5). Shapiro-Wilk's and Levene's tests were then used to verify the normality and homogeneity of variance. When two-way ANOVA results showed interaction between the variables, Tukey's multiple comparison *post-hoc* test was used to determine significant differences between means. Metabolites fractions from metabolic flux analysis were also analyzed with a two-way ANOVA with the two factors being conditions (CTL and STF-62247) and time points (20, 60 and 120 min). Sidak's multiple comparisons test was used to compare the significant differences between conditions at each time points (results at 120 min are shown in **Figure 5C**). SLC mRNA levels were analyzed with Student t-test to compare each transporter individually to their respective control (either CTL vs. STF, or RCC4 VHL- vs. RCC4 VHL+). Each experiment has been performed at least three times. When it is applicable, results are presented as the mean and the SEM.

RESULTS

Effect of STF-62247 on RCC Metabolism

To evaluate the effect of STF-62247 on cell metabolism, we used three different RCC cell lines such as RCC4, 786.0 and RCC10 parental cell lines which harbors different mutations on the VHL gene. The RCC4 cells are characterized by a VHL missense mutation at residue 65 (S65W), while 786.0 cells present a frameshift mutation (G104fs*55) leading to a nonfunctional VHL protein (pVHL) and analysis of VHL sequence in RCC10 cells DNA indicated a deletion mutation of the amino acid 159 lysine introducing a stop codon (43). The wild-type VHL gene has been stably reintroduced into the parental cell lines to generate RCC4/VHL, 786.0/VHL and RCC10/VHL. Indeed, pVHL expression is absent in parental cell lines (VHL-) compared to the VHL reintroduced cells (VHL+) (**Figure 1A**). As expected, VHL mutations in the parental cells lead to stabilization and expression of HIF-2α and HIF-1α, except for 786.0 cells that do not express HIF-1α (**Figure 1A**). A phenotypic characteristic of VHL- cells treated with STF-62247, a small molecule identified to target the loss of VHL, is the presence of intracytoplasmic vacuoles, which we demonstrated to be related to enlargement of endolysosomes (39–41, 44). This phenotype is observed mostly in VHL- RCC4 and RCC10 cells compared to their counterpart VHL+ (**Figure 1B**). In addition, these three cell lines (VHL-) are sensitive to STF-62247 compared to the VHL+ cells, particularly RCC4 cells with a IC50 at 1.25 μM. Although 786.0 cells are less sensitive to STF-62247 and present smaller and lower intracytoplasmic vacuoles, they still show selectivity for the loss of VHL (**Figure 1C**). Thus, a metabolic profiling was generated using ^{1}H NMR in the three VHL- cell lines compared to the same cells with the functional VHL gene in response to STF-62247 (**Figure 1D**). Hydrophilic metabolites were extracted from five biological replicates. As previously reported, principal component analysis (PCA) showed altered metabolite patterns in absence or presence of VHL (38). In addition, PCA spectra showed a clear separation in STF-treated cells (STF) compared to control (CTL) in the VHL- RCC4 cell line. A slight alteration in metabolites extracts was observed in STF-treated 786.0 and RCC10 treated cells compared to control. PCA was similar in response to STF-62247 in three VHL+ cell lines (RCC4, 786.0, RCC10). Since RCC4 was the model more sensitive to the small

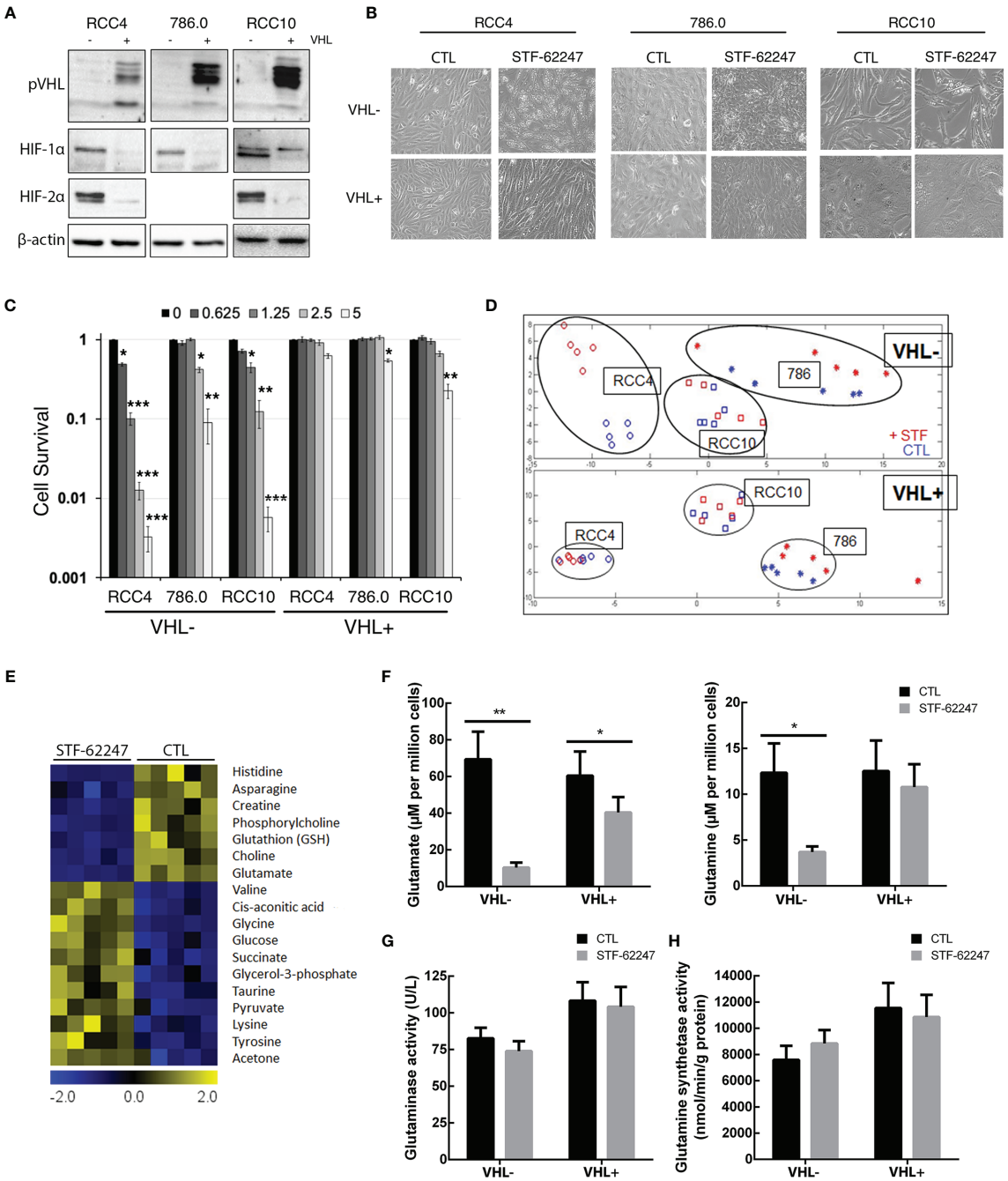

FIGURE 1 | Metabolic profiling in renal cell carcinoma cell lines treated to STF-62247. **(A)** Immunoblot analysis of VHL- RCC cells (RCC4, 786.0 and RCC10) and their counterparts where VHL was reintroduced (indicated by the notation VHL+). Validation of our models was done by detecting pVHL and hypoxia-inducible factors (HIF-1α and HIF-2α). **(B)** Inverted-light microscopy images of vacuolization in VHL- and VHL+ cell lines treated to STF-62247. **(C)** Cell survival was measured by clonogenic assay in VHL- and VHL+ cells. Cells were treated with doses of STF-62247 ranging from 0 to 5 μM. Results are normalized with their respective control (dose 0). Student's *t*-tests were used to evaluate significant differences for each STF-62247 dose (N=3). **(D)** Principal component analysis (PCA) of ^{1}H NMR metabolic data from renal cell carcinoma cell lines. RCC4 cells were treated with STF-62247 at 1.25 μM for 24 hr and 786.0 and RCC10 cells at 2.5 μM for 48 hr (N=5). **(E)** Significance analysis of microarray (SAM) of differentially concentrated intracellular metabolites in RCC4 VHL- cells when treated to 1.25 μM STF-62247 (N=5). **(F)** Intracellular glutamine and glutamate measured by LC-MS in RCC4 VHL- and VHL+ treated with 1.25 μM STF-62247 for 24 hr (N=5). **(G, H)** Enzymatic activity of glutaminase **(G)** and glutamine synthetase **(H)** in RCC4 VHL- and VHL+ cells treated with 1.25 μM STF-62247 for 24 hr (N=3 and N=4 respectively). Results are presented as means and SEM of at least three independent experiments. Two-Way ANOVA followed by Tukey's test was performed to assess significant differences in the results **(F–H)**. (*$p < 0.05$, **$p < 0.01$, ***$p < 0.001$).

molecule and showing the greatest difference on metabolic profiling, we move forward with this cell line to investigate these changes. Significance microarray analysis (SAM) was used to quantify metabolite significant changes in VHL- cells exposed to STF-62247 (**Figure 1E**). The results demonstrated that glycolysis components such as glucose, glycerol-3-phosphate and pyruvate were significantly increased in treated cells. In the opposite way, glutamate, glutathione (GSH), and asparagine displayed important decreases in response to STF-62247. Because of its implication in ccRCC, the fate of glutamine was the focus of our investigation. To validate ^{1}H NMR results, quantification of intracellular glutamine and glutamate levels using LC-MS showed a diminution of these two amino acids of 70% and 85% respectively, in VHL- cells in response to STF-62247 supporting our previous findings (**Figure 1F**). No change in glutamine level was observed in VHL+ cells treated with STF-62247 while glutamate decrease by 33%. VHL inactivation did not significantly influence basal intracellular levels of these two amino acids. Next, we measured the activity of glutaminase, the enzyme responsible for the conversion of glutamine into glutamate, which is highly expressed in the kidney. However, no significant difference was observed on glutaminase activity between VHL- and VHL+ cells or in response to STF-62247 (**Figure 1G**). Finally, we quantified the glutamine synthetase activity, which produces glutamine from glutamate. Here, the results showed higher activity in VHL+ cells compared to VHL- cells and a slight increase in response to STF-62247 (**Figure 1H**). These results demonstrated that STF-62247 decreased glutamine and glutamate levels in VHL- cells without affecting GLS activity suggesting that import of glutamine can be altered, or that cytoplasmic glutamine is highly consumed.

Are Glutamine Transporters Responsible for the Glutamine Drop?

Glutamine can be incorporated into the cytoplasm *via* SLC1A5, which can be coupled with SLC7A5 and its chaperone SLC3A2 to exchange glutamine with another amino acid such as leucine (45). First, we quantified mRNA levels of these transporters and showed that SLC1A5 and SLC7A5 are significantly higher in VHL- cells compared to VHL+ and support previous work demonstrating that SLC1A5 and SLC7A5 expression are mediated by HIF-2α (46, 47) (**Figure 2A**). Moreover, our results indicated that mRNA levels of these transporters and the chaperone SLC3A2 significantly decrease in response to STF-62247 in VHL- cells. An opposite effect was seen in VHL+ cells where SLC7A5 and SLC3A2 mRNA levels increased in response to the small molecule although it was not statistically significant, and no effect was observed on SLC1A5 (**Figure 2B**). At the protein level, expression of SLC1A5 and SLC3A2 is also higher in VHL- cells compared to VHL+ cells while SLC7A5 protein expression is similar in both cells. (**Figure 2C**). Curiously, SLC1A5 and SLC3A2 proteins expression was quite contrasting with mRNA levels since both are highly increased, particularly in VHL- cells in response to STF-62247. The presence of several bands for SLC1A5 has been associated to N-glycosylation of the protein, which does not affect its transport activity suggesting that glutamine import is stimulated in VHL- cells (48). Distinctively, glutamine levels are slightly disturbed by STF-62247 in VHL+ cells, which do not depend on glutamine to survive, and the studied SLC are less affected. On the other hand, protein expression of SLC7A5 was only slightly affected in both STF-treated cells. Instead, a slight but uncharacterized lower band appears only in cells exposed to STF-62247 regardless of VHL genetic background. Because of the role of the SLC7A5/SLC3A2 exchanger to export glutamine and import leucine to activate mTOR, this amino acid was further quantified using LC-MS. Our results showed 50% diminution of leucine levels in VHL- cells treated with the small molecule while it remains stable in VHL+ cells which support the mRNA levels data (**Figure 2D**). Moreover, leucine quantities are similar between both VHL- and VHL+ cells. Finally, the sensitivity of ccRCC to SLC1A5 and SLC7A5 inhibition was tested using pharmacological molecules (**Figure 2E**). GPNA, a widely used SLC1A5 inhibitor, was tested alone or in combination with STF-62247. Results showed that GPNA alone, at 1 mM, significantly decreased cell viability by about 25% in VHL- cells. When GPNA was combined with STF-62247, viability further decreased in VHL- cells supporting the importance of glutamine for these cells. Inhibition of SLC7A5 by BCH did not affect cell viability in both cell lines alone or in combination with STF-62247. Additionally, the results indicated a slight increase of viability in VHL+ cells in response to STF-62247. This effect could be attributed to the use of XTT assay that measures the activity of the mitochondrial dehydrogenase enzymes present in metabolically active cells. In comparison, this effect was not observed using clonogenic assay (**Figure 1C**) or cell counts (**Figures 3C**, **4**) and suggest that NADH, which is produced in the mitochondria to support the complex I of the electron transporter chain is higher in VHL+ treated cells and could contribute to viability of these cells. Overall, the results presented here showed an increase in protein expression of glutamine import transporter SLC1A5 that could reflect an activation by the VHL- cells to compensate for the drop of 70% of glutamine, which reduced its mRNA synthesis and, therefore, indicates that the decrease of glutamine in response to STF-62247 is not likely to be related to SLC1A5 or SLC7A5/SLC3A2.

Glutamine Uptake Does Not Rescue Cell Viability

We previously demonstrated that ROS production and ATP levels were not affected in response to STF-62247 although a slight increase in ATP was observed in VHL- cells after 48 hr (41, 49). Furthermore, we showed that STF-62247 has no significant effect on mitophagy (41). Nevertheless, we evaluated the rate of mitochondrial oxygen consumption to study another aspect of mitochondrial oxidative pathway (**Figure 3A**). As expected, VHL- RCC4 cells with constitutively active HIF-1α have a lower respiratory control ratio (RCR) compared to VHL+ cells. However, no significant difference on RCR was observed in response to STF-62247 in both cell lines although a slight increase can be observed in VHL-. Thus, to understand the consequence of glutamine diminution on cell survival, an excess

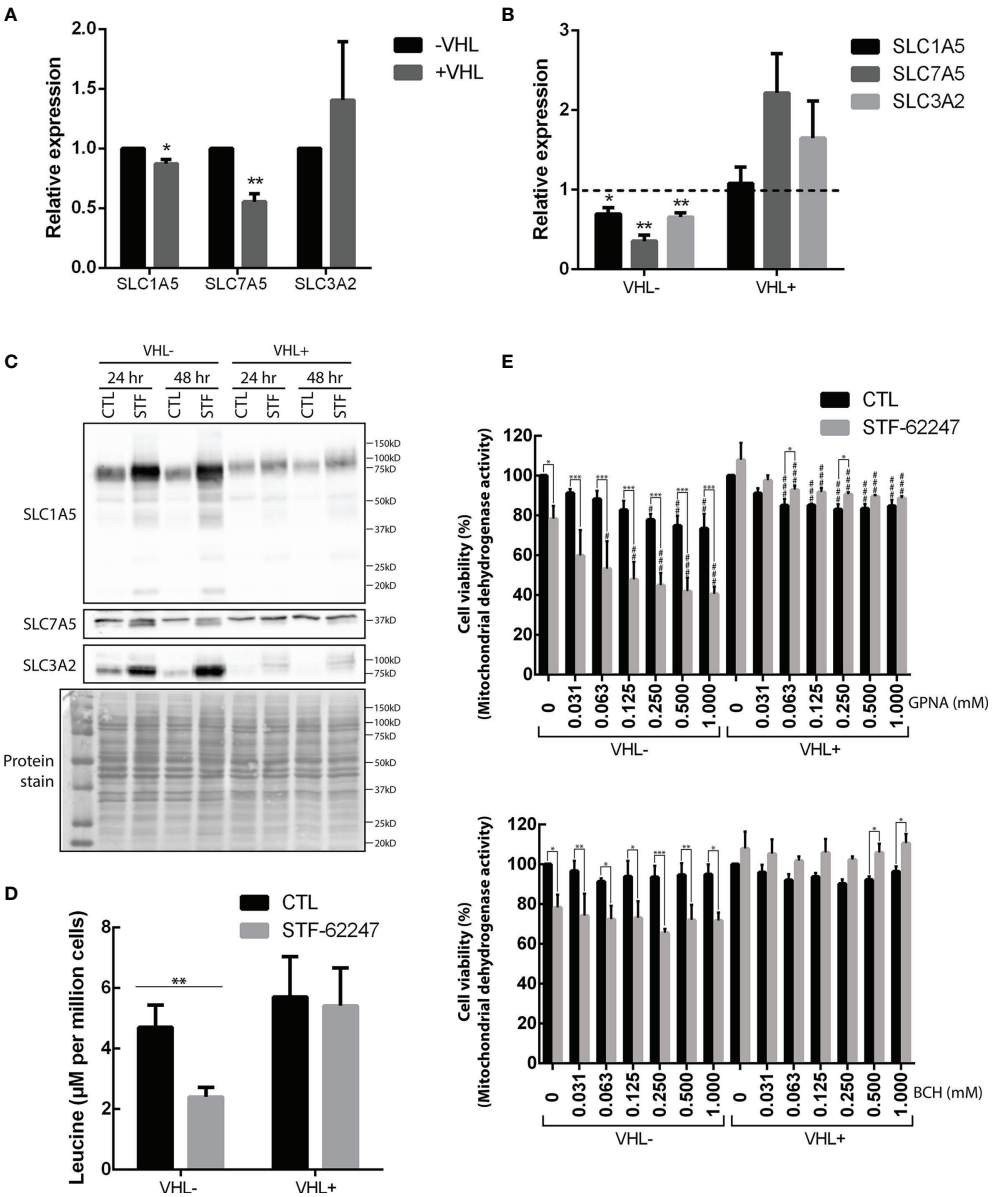

FIGURE 2 | Effects of STF-62247 on glutamine transporters. **(A, B)** mRNA relative expression, measured by RT-qPCR, of glutamine transporters SLC1A5, SLC7A5 and SLC3A2 influenced by **(A)** VHL status and **(B)** STF-62247. RCC4 VHL- and VHL+ were treated with 1.25 µM STF-62447 for 24 hr. Results for treated cells are compared to control cells (represented by the dotted line at 1). Results are presented as means and SEM of three independent experiments. **(C)** Glutamine transporters, SLC1A5, SL7A5 and SLC3A2, protein levels in RCC4 VHL- and VHL+ treated to STF-62247 for 24 and 48 hr. **(D)** Intracellular leucine was measured by LC-MS in RCC4 VHL- and VHL+ treated with 1.25 µM STF-62247 for 24 hr (N=6). Student's *t*-tests were performed to compare results between VHL- and VHL+ cells **(A)** or between controls and treated cells **(B, D)** (*$p < 0.05$, **$p < 0.01$, ***$p < 0.001$). **(E)** Cell viability was evaluated by XTT assay in RCC4 VHL- and VHL+ cells. SLC1A5 and SLC7A5 inhibitors, GPNA and BCH respectively, were tested alone (concentrations from 0 to 1 mM) or combined with 1.25 µM STF-62247 (N=3). Two-Way ANOVA followed by Tukey's test was performed to assess statistically significant results. Comparison between CTL and STF-62247 conditions for each concentration of inhibitor (GPNA or BCH) are denoted with the following statistical marks *$p < 0.05$, **$p < 0.01$ or ***$p < 0.001$. Comparison of each inhibitor concentrations (x-axis) are made with their respective control (0 mM columns, with or without STF-62247) and statistical significances are denoted by $^{\#}p < 0.05$, $^{\#\#}p < 0.01$ or $^{\#\#\#}p < 0.001$.

of this amino acid was added to the cells exposed to STF-62247. Proliferation and viability curves indicated that VHL- cells and VHL+ control cells were not affected by 10 mM glutamine (**Figures 3B, C**). As anticipated, STF-62247 decrease proliferation in VHL- RCC4 cells, but no change was observed when glutamine concentration was increased. Instead, the results showed that the percentage of viable VHL- cells exposed to STF-62247 trend to further decrease in the presence of 10 mM glutamine while the viability of functional VHL cells was not affected by STF-62247 or by the excess of glutamine. To confirm

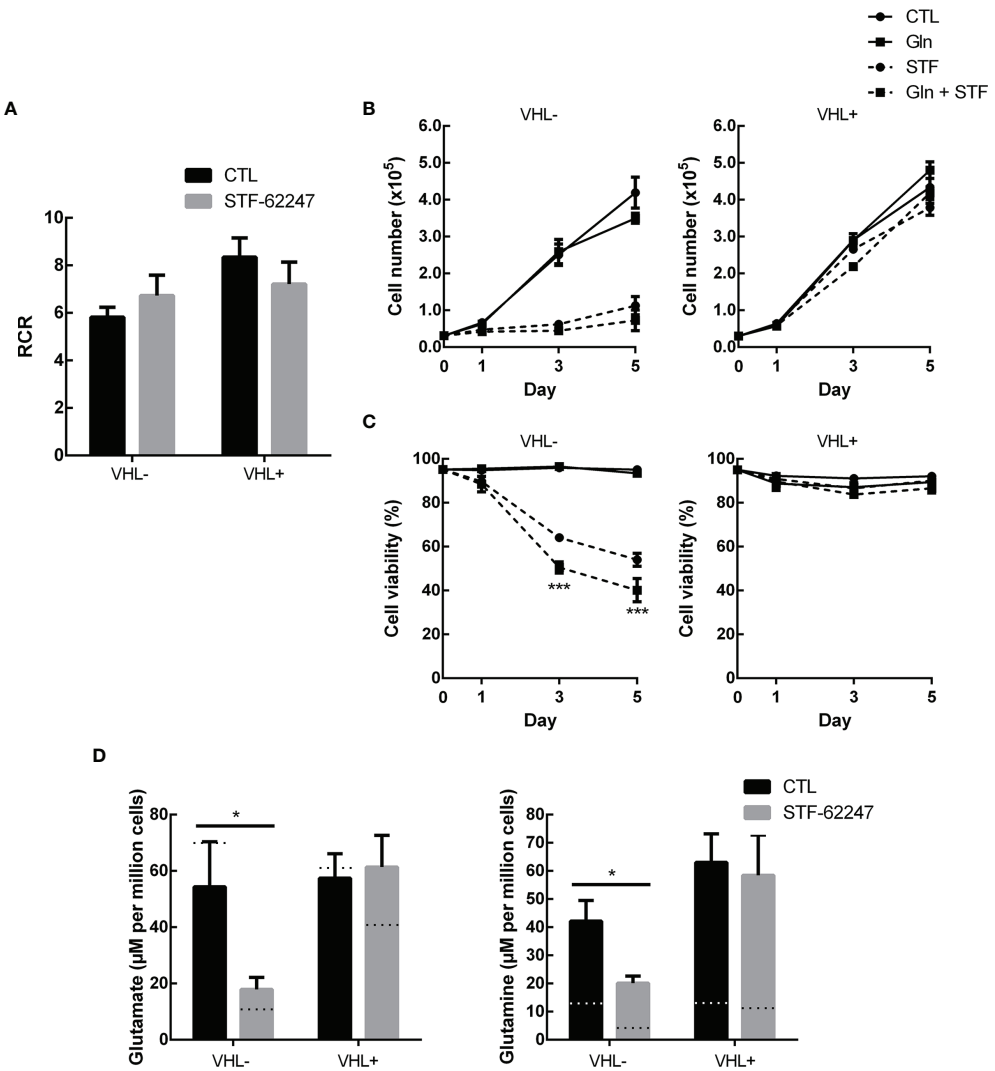

FIGURE 3 | Glutamine excess is not sufficient to overcome stress from STF-62247 **(A)** Respiratory control ratio (RCR) measured with an Oxygraph-2K (Oroboros) in RCC4 VHL- and VHL+ treated with 1.25 μM STF-62247 for 24 hr (N=3). **(B)** Proliferation and **(C)** Viability of RCC4 VHL- and VHL+ treated with 1.25 μM STF-62247 and/or an excess of 10 mM glutamine. Cells were counted on days 0, 1, 3 and 5 with trypan blue to evaluate cells viability (N=3). Statistical marks shown in cell proliferation and viability curves are either between CTL and Gln, or between STF and STF + Gln conditions. **(D)** Intracellular glutamate and glutamine measured by LC-MS in RCC4 VHL- and VHL+. Cells were seeded in media containing 10 mM glutamine and treated with 1.25 μM STF-62247 for 24 hr (N=6). Dotted lines represent values from data obtained from cells incubated in normal media containing 2 mM glutamine (Data from **Figure 1C**). Results are presented as means and SEM of at least three independent experiments. Statistical analyses (Two-Way ANOVA followed by Tukey's test) were performed to assess significant differences in the results **(A–D)**. (*$p < 0.05$).

the internalization of the excess glutamine into the cells, quantification of glutamine and glutamate was performed by LC-MS (**Figure 3D**). Results indicated 3.5 times more intracellular glutamine in VHL- cells when 10 mM glutamine was present in the media. This augmentation was higher in VHL + cells. However, intracellular levels of glutamate were slightly influenced by the increase of glutamine. When cells were treated with STF-62247, intracellular glutamine and glutamate levels decrease by 42% and 67% in VHL- cells, respectively. The level of these two amino acids was unchanged in cells with the functional VHL gene. Altogether, these results indicate that mitochondrial functions are relatively unaffected by STF-62247. In addition, supplementation of glutamine was not sufficient to rescue cell viability suggesting that glutamine is consumed to support other metabolic functions in response to STF-62247.

Metabolic Flux of Glutamine in Response to STF-62247

To better understand the fate of glutamine in STF-treated cells, we used U-$^{13}C_5$-glutamine to further study intracellular metabolic flux in VHL- cells exposed to the small molecule (**Figure 5A**). Normally, cells using the oxidative TCA cycle are

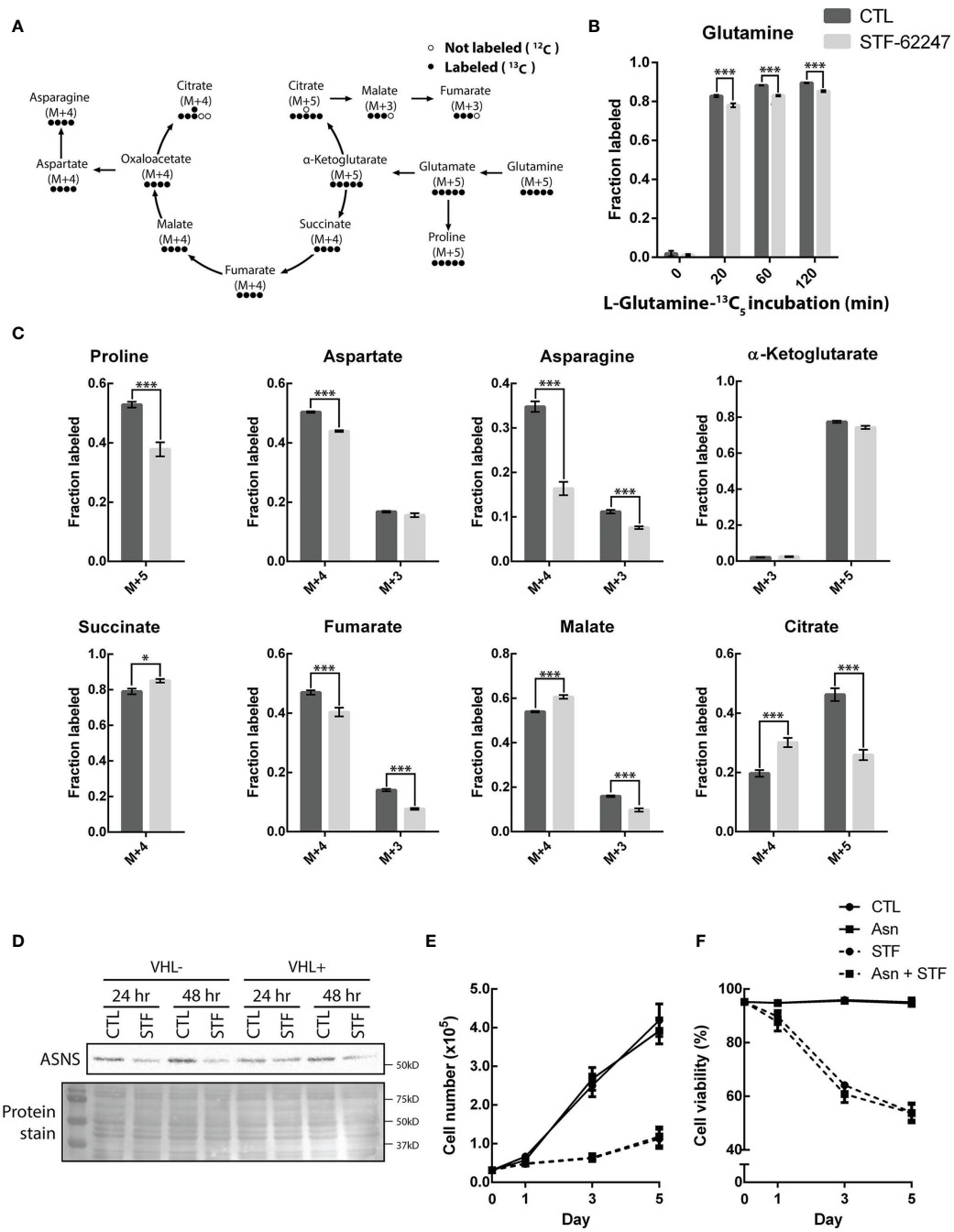

FIGURE 4 | STF-62247 causes a shift in glutamine metabolic flux and increases the use of the oxidative TCA cycle. **(A)** Simplified schematic representation of the carbon exchange in glutamine metabolism. Arrows do not always represent direct metabolic reactions. **(B)** L-Glutamine-13C5 incorporation, assessed by GC-MS, in RCC4 VHL- untreated and treated with 1.25 μM STF-62247 for 24 hr (N=3). **(C)** Metabolites fractions labeled from L-Glutamine-13C5 (120 min incubation) in RCC4 VHL- untreated or treated with STF-62247 for 24 hr (N=3). Metabolites derived from oxidative TCA: Succinate M+4, Fumarate M+4, Malate M+4, Aspartate M+4, Asparagine M+4, Citrate M+4, α-Ketoglutarate M+3. Metabolites derived from reductive TCA: Citrate M+5, Malate M+3, Fumarate M+3, Aspartate M+3 and Asparagine M+3. **(D)** Immunoblot analysis of asparagine synthetase (ASNS) in RCC4 VHL- and VHL+ after 24 hr and 48 hr of STF-62247 treatment. **(E)** Proliferation **(F)** and viability of RCC4 VHL- treated with 1.25 μM STF-62247 and/or 2 mM Asparagine (Asn). Cells were counted on days 0, 1, 3 and 5 with trypan blue to evaluate cells viability (N=3). Statistical marks shown in cell proliferation and viability curves are either between CTL and Asn, or between STF and STF + Asn conditions. Results are presented as means and SEM of three independent experiments. Statistical analyses (Two-Way ANOVA followed by Sidak's **(B, C)** or Tukey's test **(E, F)**) were performed to assess significant differences in the results. (*$p < 0.05$, ***$p < 0.001$).

enriched in succinate, fumarate, malate and citrate M+4. However, when cells go into the reductive carboxylation pathway, citrate M+5, malate M+3 and fumarate M+3 are generated. Cells were treated with STF-62247 for 24 hr and then, the media was changed for labeled media. Metabolites were extracted after 0, 20, 60 and 120 min. Labeled glutamine was already well incorporated after 20 min and had reached about 90% of all intracellular glutamine after 120 min (**Figure 5B**). Glutamine levels were also lower in STF-treated cells. Interestingly, levels of succinate M+4, malate M+4 and citrate M+4 were significantly higher in response to STF-62247 (**Figure 5C**). Oppositely, levels of citrate M+5, malate M+3 and fumarate M+3 decreased when cells were treated with STF-62247. Adding to that, the very low levels of α-ketoglutarate M+3, coming from oxidative TCA, show that glutamine is metabolized to form citrate, but that citrate does not continue in the Krebs cycle to generate more α-ketoglutarate. Therefore, independently of the glutamine direction into the Krebs cycle, cells are using glutamine to form citrate. Outside of the Krebs cycle, proline M+5, aspartate M+4, and asparagine, both M+4 and M+3 decreased in response to STF-62247 (**Figure 5C**). Moreover, exogenous asparagine becomes an essential amino acid for cancer cells when glutamine levels decline. We observed a decrease in ASNS protein expression in cells exposed to STF-62247 for 24 hr and 48 hr (**Figure 5D**). Then, proliferation and viability assays were performed using media supplemented with asparagine, but no significant changes were observed in control cells or cells exposed to STF-62247 (**Figure 5E**). These results suggest that while control cells favor reductive carboxylation to produce fatty acid, VHL- cells treated with STF-62247 are using the oxidative TCA cycle to produce citrate.

Glutamine-Derived Fatty Acid Synthesis and Lipogenesis Are Increased With STF-62247

To determine whether the drop of glutamine can impact FA production, cells were radiolabeled with ^{14}C-glutamine and FA synthesis was measured in both cells with functional and non-functional VHL treated with STF-62247. To our surprise, results indicated that FA generated by glutamine was significantly increased in cells exposed to STF-62247 in VHL- cells while no change was observed in VHL+ cells with the functional gene (**Figure 5A**). Then, cells were exposed to an exogenous source of lysophospholipid in the form of lysophosphatidylcholine 18:1 (LPC 18:1), alone or in combination with STF-62247. Increased uptake of LPC is observed in hypoxic cells to sustain proliferation and survival (50). When we observed cell phenotype after 72 hr of treatment, cells were unaffected by treatment with LPC alone. However, when LPC was combined with STF-62247, the size and number of intracytoplasmic vacuoles increased both in VHL- and VHL+ cells (**Figure 5B**). Thus, we evaluated whether the addition of this lipid would affect cell proliferation and viability when treated in combination with STF-62247. However, proliferation and cell viability were not affected by LPC alone or combined with STF-62247 regardless of VHL genetic status (**Figures 5C, D**).

Thus, to study *de novo* lipogenesis and understand the increase of glutamine-derived FA, we evaluated the expression of SCD1, which assures the conversion of saturated FAs into monounsaturated FAs coming from palmitic acid or stearic acid generated from citrate species. Western blot analyses indicated that SCD1 protein is expressed at higher level in RCC4 VHL- cells and increased in response to STF-62247 independently of VHL status (**Figure 5E**). Moreover, FAs and generated products can be stored in lipid droplets (LD) or used for β-oxidation through CPT1A. To further investigate this pathway, PLIN2 expression, a protein associated with LDs, and CPT1A were evaluated. CPT1A is known to be repressed by HIF-α and is highly expressed in VHL+ cells, particularly at 24 hr when confluency is lower (**Figure 5E**). Furthermore, we observed that CPT1A increased, more prominently, in VHL- cells treated with STF-62247. On the other hand, PLIN2 expression is also higher in VHL- cells exposed to STF-62247 while staining of LDs with LipidTOX confirmed these findings (**Figures 5E, F**). Quantification of LDs demonstrated at least two-fold increase in LDs in VHL- cells treated with the small molecule (**Figure 5G**). As expected, PLIN2 and LDs are almost absent from VHL+ cells. Altogether, findings from these studies suggested that intracellular glutamine levels decreased in VHL-mutated cells to sustain lipid demands or storage under this metabolic stress.

DISCUSSION

Metabolomics studies informed about cancer cell activities by analyzing intracellular metabolites. Major platforms such as 1H NMR, LC-MS/MS and GC-MS have been used to dress a metabolite profiling of RCC mostly in plasma and urine from patient samples (51–53). Using *ex vivo* 1H NMR, a study revealed higher levels of lactate, glutamate, pyruvate, and creatine in RCC tumors compared to normal adjacent tissues and a decrease in acetate, malate, valine, and aspartate (54). In addition, labeling of ccRCC identified reprogrammed metabolic pathways like glycolysis, fatty acid oxidation, and metabolism of amino acids such as tryptophan, arginine and glutamine (24, 51, 55, 56). Besides, metabolomics in cultured RCC cells allows the opportunity to identify changes in metabolites in response to drug treatment or in drug-resistant cells (57). In the present study, we evaluated the effect of a small molecule targeting the loss of VHL on cell metabolism by performing metabolomic profiling using 1H NMR. We observed significant changes in metabolites affected in ccRCC such as valine, creatine, pyruvate, glutathione and glutamate. The drop of glutamate and glutamine observed in VHL- ccRCC cells in response to STF-62247 was particularly interesting since these tumors rely on glutamine for growth and proliferation. In fact, glutaminase inhibitors showed anti-proliferative activity *in vitro* and *in vivo* in mice in a wide range of cancer models including RCC (33, 58, 59). However, clinical trials using GLS inhibitor Telaglenastat (CB-839) combined with the mTOR inhibitor everolimus showed a modest improvement of progression-free survival (PFS) from 1.9 months to 3.8 months while it fails to increase PFS in

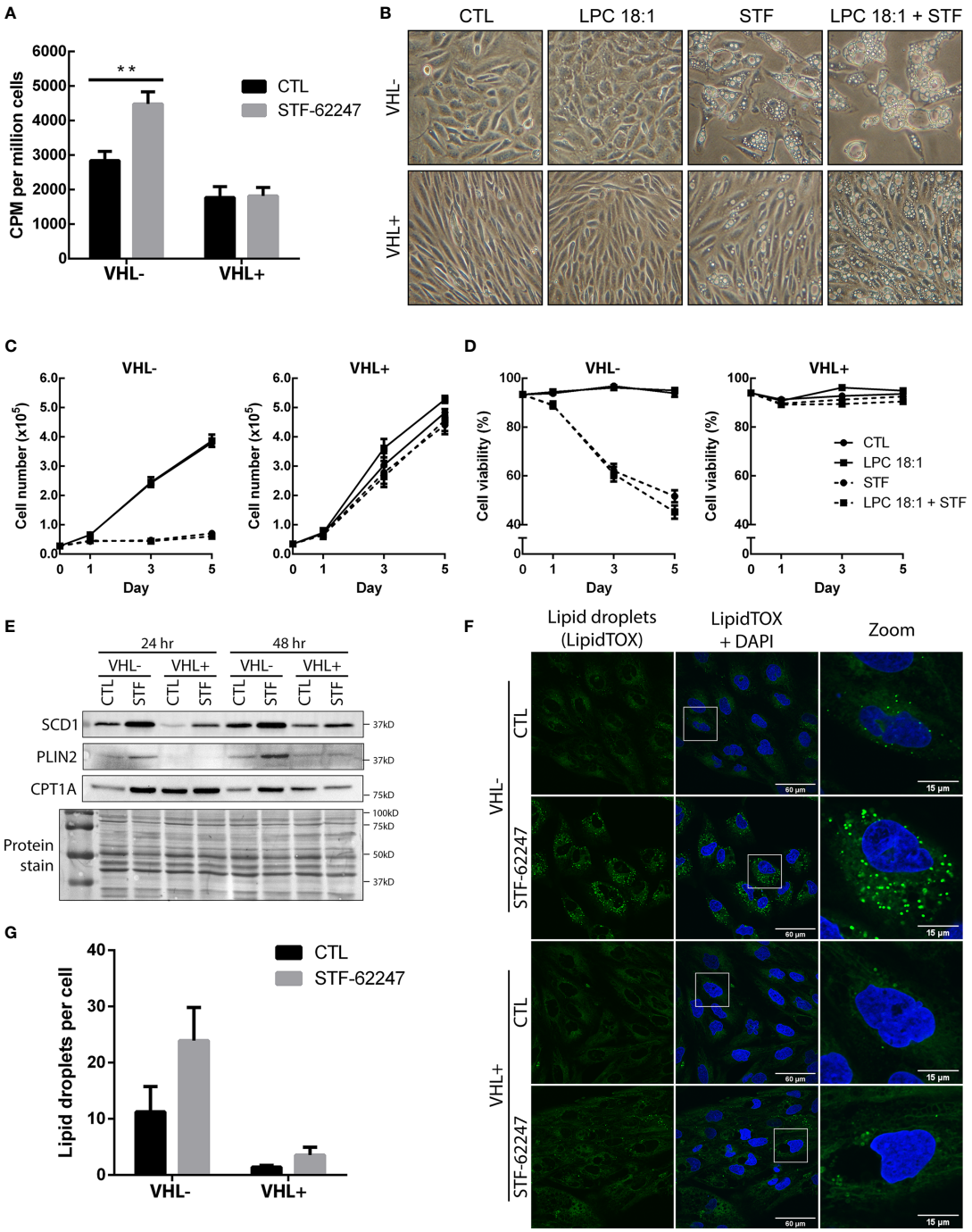

FIGURE 5 | Increase usage of glutamine to produce fatty acids result in the accumulation of lipid droplets in VHL deficient cells. **(A)** Incorporation of radiolabeled carbon (C14) from glutamine into fatty acids in RCC4 VHL- and VHL+ cells after 24 hr of STF-62247 treatment. Culture media was changed for the last hour of treatment with media containing 0,2 µCi/mL (L-[14C(U)]-Glutamine. Radioactivity (counts per minute (CPM)) was measured in lipid extracts from RCC4 VHL- and VHL+ and normalized with the number of cells (N=4). **(B)** Inverted-light microscopy images of vacuolization in RCC4 VHL- and VHL+ cells treated with 1.25 µM STF-62247 and/or 25 µM LPC 18:1 after 3 days. **(C)** Proliferation **(D)** and viability of RCC4 VHL- and VHL+ cells treated with 1.25 µM STF-62247 and/or 25 µM LPC 18:1. Cells were counted on days 0, 1, 3 and 5 with trypan blue to evaluate cells viability (N=3). Statistical marks shown in cell proliferation and viability curves are either between CTL and LPC 18:1, or between STF and STF + LPC 18:1 condition. **(E)** Immunoblot analysis of proteins implicated in fatty acids and lipid droplets metabolism. Cells were treated for 24 hr and 48 hr with 1.25 µM STF-62247. **(F)** Immunofluorescence of fixed RCC4 VHL- and VHL+ cells stained with LipidTOX (green) and DAPI (blue) after being treated for 48 hr with 1.25 µM STF-62247 (N=3). **(G)** Lipid droplets (LipidTOX) puncta **(F)** were analyzed and counted with Fiji (ImageJ). Results are presented as means and SEM of at least three independent experiments. Statistical analyses (Two-Way ANOVA followed by Tukey's test) were performed to assess significant differences in the results **(A, C, D, G)**. (**$p < 0.01$).

advanced ccRCC in combination with cabozantinib (33). Our study demonstrated that STF-62247 significantly decreased intracellular levels of glutamine and glutamate without affecting GLS activity, ATP levels, mitochondrial oxygen consumption or mitochondrial membrane potential (data not shown) in VHL- cells. STF-62247 did not significantly change ROS levels and no mitophagy or apoptosis was observed (39, 41, 49). Nevertheless, we were surprised that addition of extracellular glutamine did not rescue, even partly, the viability of VHL- cells in response to STF-62247 due to the importance of this amino acid in RCC metabolic reprogramming. Our results indicated that mitochondria are barely influenced by STF-62247.

Glutamine is taken up in cells mostly through SLC transporters such as SLC1A5. Studies reported high expression of SLC1A5 under hypoxic conditions, which is mediated through HIF-2α, as well as in tumors sample including ccRCC (29, 30, 47). In agreement with these reports, VHL- cells show higher mRNA levels and protein expression of SLC1A5. Glycosylation sites at N163 and N212 are responsible for the localization of SLC1A5 at the plasma membrane and post-translational modifications regulate its stability, trafficking and transport activity (60). Also, a recent paper identified a SLC1A5 variant with a mitochondrial targeting sequence that contribute to ATP production and GSH synthesis (47). Our work did not investigate the effect of STF-62247 on this specific isoform since our findings suggest that mitochondria and related cellular mechanisms are not disturbed by the glutamine drop Instead, we show that STF-62247 increases SLC1A5 protein expression at a very high level compared to VHL+ cells suggesting that this augmentation is to fulfill the glutamine demand. Furthermore, our results by LC-MS/MS with glutamine supplementation suggest that import of glutamine is effective although it was not sufficient to rescue cell viability. We also investigated the expression of SLC7A5 and the chaperone SLC3A2 which work in tandem with SLC1A5 to export glutamine and drive leucine uptake necessary for proliferation and mTORC1 regulation although this mechanism seems to be cell type-dependent (61). SLC7A5 has also been shown to be regulated through HIF-2α (46, 62). Our results showed decrease of the three SLC at the mRNA level in response to STF in VHL- cells while their levels are either unchanged or stimulated in VHL +. This could be explained by the fact that glutamine levels are not affected by the small molecule in VHL+ cells and the SLC are less solicited. On protein expression, we observed an increase of SLC3A2 in cells exposed to STF-62247 but SLC7A5 was mostly unaffected except for the presence of a small band in treated cells. It is surprising that components of this heterodimer are differently expressed although the activity of this transporter can be independent of protein expression. Also, it is known that the chaperone SLC3A2 can also heterodimerize with SLC7A11, but it has not been analyzed in our study. An interesting study demonstrated that SLC7A5 can be internalized by endocytosis, ubiquitinated by the Nedd4-2 ubiquitin-ligase and targeted to the lysosome for degradation (63). The importance of this mechanism remains unknown. Another study showed the localization of SLC7A5/SLC3A2 to the lysosomes, which depend on the protein LAPTM4b to promote the uptake of leucine and mTORC1 activation (45). Our results show significant decrease of leucine in STF-treated VHL- cells, which can be related to mTORC1 inhibition previously reported in VHL-deficient cells (39, 49). It could be interesting to evaluate the localization of these transporters since we showed that STF-62247 accumulates in lysosomes and blocks late-stages of autophagy. We cannot exclude that the drop in leucine might be independent of the coupling system SLC1A5 and SLC7A5/SLC3A2.

Metabolomic flux analysis in presence of labeled glutamine indicated that VHL- cells use the oxidative TCA cycle to produce citrate and maintain energy in response to STF-62247. This metabolic reprogramming could be reflected in the slight increase of mitochondrial oxygen consumption observed in VHL- cells. Since we observed an increase in glucose and pyruvate by NMR in response to STF, it would have been interesting to evaluate the fate of both glutamine and glucose in labeled cells, a limitation of our study. Our metabolomic flux analysis also confirmed the diminution of asparagine and aspartate observed in NMR profiling. Cells can utilize glutamine not only as a source of carbon through the Krebs cycle, but also as a source of nitrogen to produce asparagine *via* the asparagine synthetase (ASNS). This asparagine is generally not used by the cells to fuel the TCA cycle but becomes essential to maintain protein synthesis in tumor cells in deprivation of glutamine (64). Interestingly, in glutamine-deprived cells, asparagine was shown to increase the protein levels of GS, which is important for nucleotide biosynthesis (65). Another study showed that asparagine supplementation alone was sufficient to prevent apoptotic cell death induced by glutamine deprivation (66). Moreover, it has been reported that inhibition of glutaminolysis and depletion of asparagine when autophagy is inhibited causes death in colon cancer cells (67). Our observations indicated that exogenous addition of asparagine or glutamine was not sufficient to prevent VHL-deficient cells from death, although we do see an increase in GS activity. Glutamine and asparagine levels are important to maintain mTOR activities, and deprivation of these amino acids can inhibit mTOR, supporting our previous reports (41, 49, 68).

Alterations in lipid metabolism are often reported in cancer cells such as ccRCC that are characterized by accumulation of lipid droplets. Extracellular uptake of FA is mainly observed in normal cells, but cancer cells prefer to synthesize their own. FA metabolism comprises both catabolism and anabolism of FA. The first one contributes to generating energy through fatty acid oxidation (β-oxidation) and TCA cycle, and the second serves to produce FA from acetyl-CoA and other enzymes such as ATP citrate lyase (ACLY), acetyl-coA carboxylase (ACC) and fatty acid synthase (FASN). Then, FA generated *de novo* are converted into monounsaturated fatty acid by SCD1 and later on in triglycerides and other lipids used for membrane synthesis. Excess lipid can be stored into lipid droplets. Our results demonstrated that VHL- cells utilize glutamine to produce FA as measured using (14)C-glutamine. Thus, we decided to move forward into *de novo* lipogenesis pathway and showed that SCD1 expression is higher

in VHL- compared to VHL+ cells. Indeed, a recent report investigated SCD1 protein expression in renal cancer patients using The Cancer Genome Atlas (TCGA) (69). Interestingly, they showed that higher expression of SCD1 was associated with better overall survival and may antagonize the development of more aggressive tumors, which is quite different from other cancer types although another report on chronic myeloid leukemia has similar observations (70). In fact, we showed that STF-62247 increased SCD1 expression in VHL- cells exposed to STF-62247, and not expectingly, in VHL+ cells. Furthermore, we observed an increase of lipid droplets and PLIN2 protein expression in response to STF-62247, both already highly expressed in ccRCC with a loss of VHL. RCC patients with high expression of PLIN2 exhibited better disease-free survival than patients with low levels of PLIN2 (71). In addition, this group also demonstrated that PLIN2 decreases cell proliferation, migration, and invasion, which supports our results on cell survival where VHL- cells exposed to STF-62247 have higher protein expression of PLIN2. The higher level of lipid droplets observed in VHL- compared to VHL+ cells support published paper by Welford group (35). They showed that CPT1A is repressed by HIF-α, which is highly expressed in VHL- cells and causes lipid droplets accumulation in these cells. Interestingly, while we observed increase of lipid droplets, we also showed an increase of CPT1A, which controls FA entry in the mitochondria for β-oxidation, in response to STF-62247 in VHL- cells. Moreover, CPT1A remains stable in VHL+ cells treated to STF-62247. In the same study, they revealed that glucose is necessary for lipid droplets formation in renal cancer cell lines, and not glutamine. This finding was surprising since cells with a loss of VHL are known to depend on glutamine to generate citrate, acetyl-CoA and FA. It would be interesting to elucidate if the rise of glucose observed by NMR in response to STF-62247 is associated with the accumulation of lipid droplets observed in VHL- cells and if, when cells are treated to STF-62247, glutamine can also be used for the formation of the lipid droplets we observed. Overexpression of CPT1A has been reported in other cancer types and normal cells to promote tumor growth and cell proliferation. The increased expression of CPT1A specifically in VHL- cells treated to STF-62247 is quite intriguing since high expression of CPT1A limits tumor progression in VHL-mutated tumors (35). It remains unclear whether increased expression of CPT1A is associated with cell death induced in STF-62247 but this small molecule alters cellular metabolism, particularly glutamine, shown to be involved in the autophagy-lysosome processes. While the identification of STF-62247 intracellular target is still under investigation and points us toward endolysosomal processes, the fate of glutamine in response to STF-62247 helps us to better understand the mechanism of action of this small molecule. Increased levels of key enzymes related to specific lipids could cause perturbations in membrane integrity that can lead to aberrant stress for the cells. We exploit vulnerabilities in ccRCC such as VHL mutations to improve our knowledge of these tumors and develop new types of targeted therapy for patients suffering from this disease.

DATA AVAILABILITY STATEMENT

The raw data supporting the conclusions of this article will be made available by the authors, without undue reservation.

AUTHOR CONTRIBUTIONS

ST conceived and designed the research. MJ performed the experiments presented in **Figures 2C, E**, **3–5**. SN performed the experiments presented in **Figures 1D–F**, **Figures 2A, B, D** and **3D**. G.S accomplished **Figures 1G, H**. MT and MC-C realized 1H-NMR analyses. AJ and DB performed LC-MS/MS analyses. DZ performed GC-MS analyses presented in **Figure 5**. MJ prepared the figures. ST and MJ wrote and edited the manuscript. All authors contributed to the article and approved the submitted version.

FUNDING

This work was funded by the Canadian Institutes for Health Research (CIHR grant 326436). ST is supported by a research chair from the Canadian Cancer Society (706199). MJ was supported by New Brunswick Innovation Research Assistantship program (RAI 2018-054). SN is supported by a trainee award from the Beatrice Hunter Cancer Research Institute with funds provided by the Cancer Research Training Program and New Brunswick Health Research Foundation.

ACKNOWLEDGMENTS

We want to thank the Atlantic Cancer Research Institute (Moncton, Canada) for providing access to installations and cell culture reagents. We also want to thank Prof. Marc Surette and his team for their help with radiolabeled lipid experiments.

REFERENCES

1. Bray F, Ferlay J, Soerjomataram I, Siegel RL, Torre LA, Jemal A, et al. Global Cancer Statistics 2018: GLOBOCAN Estimates of Incidence and Mortality Worldwide for 36 Cancers in 185 Countries. *CA Cancer J Clin* (2018) 68:394–424. doi: 10.3322/caac.21492
2. Hsieh JJ, Purdue MP, Signoretti S, Swanton C, Albiges L, Schmidinger M, et al. Renal Cell Carcinoma. *Nat Rev Dis Primers* (2017) 3:17009. doi: 10.1038/nrdp.2017.9
3. Moch H, Cubilla AL, Humphrey PA, Reuter VE, Ulbright TM. The 2016 WHO Classification of Tumours of the Urinary System and Male Genital Organs-Part A: Renal, Penile, and Testicular Tumours. *Eur Urol* (2016) 70:93–105. doi: 10.1016/j.eururo.2016.02.029
4. Rini BI, Campbell SC, Escudier B. Renal Cell Carcinoma. *Lancet* (2009) 373:1119–32. doi: 10.1016/S0140-6736(09)60229-4
5. Linehan WM. Genetic Basis of Kidney Cancer: Role of Genomics for the Development of Disease-Based Therapeutics. *Genome Res* (2012) 22:2089–100. doi: 10.1101/gr.131110.111
6. Gerlinger M, Horswell S, Larkin J, Rowan AJ, Salm MP, Varela I, et al. Genomic Architecture and Evolution of Clear Cell Renal Cell Carcinomas Defined by Multiregion Sequencing. *Nat Genet* (2014) 46:225–33. doi: 10.1038/ng.2891

7. Nickerson ML, Jaeger E, Shi Y, Durocher JA, Mahurkar S, Zaridze D, et al. Improved Identification of Von Hippel-Lindau Gene Alterations in Clear Cell Renal Tumors. *Clin Cancer Res* (2008) 14:4726–34. doi: 10.1158/1078-0432.CCR-07-4921
8. Young AC, Craven RA, Cohen D, Taylor C, Booth C, Harnden P, et al. Analysis of VHL Gene Alterations and Their Relationship to Clinical Parameters in Sporadic Conventional Renal Cell Carcinoma. *Clin Cancer Research: An Off J Am Assoc Cancer Res* (2009) 15:7582–92. doi: 10.1158/1078-0432.CCR-09-2131
9. Mitchell TJ, Turajlic S, Rowan A, Nicol D, Farmery JHR, O'Brien T, et al. Timing the Landmark Events in the Evolution of Clear Cell Renal Cell Cancer: TRACERx Renal. *Cell* (2018) 173:611–23.e617. doi: 10.1016/j.cell.2018.02.020
10. Iliopoulos O, Kibel A, Gray S, Kaelin WGJr. Tumour Suppression by the Human Von Hippel-Lindau Gene Product. *Nat Med* (1995) 1:822–6. doi: 10.1038/nm0895-822
11. Cancer Genome Atlas Research, Network. Comprehensive Molecular Characterization of Papillary Renal-Cell Carcinoma. *N Engl J Med* (2016) 374:135–45. doi: 10.1056/NEJMoa1505917
12. Dalgliesh GL, Furge K, Greenman C, Chen L, Bignell G, Butler A, et al. Systematic Sequencing of Renal Carcinoma Reveals Inactivation of Histone Modifying Genes. *Nature* (2010) 463:360–3. doi: 10.1038/nature08672
13. Turajlic S, Xu H, Litchfield K, Rowan A, Chambers T, Lopez JI, et al. Tracking Cancer Evolution Reveals Constrained Routes to Metastases: TRACERx Renal. *Cell* (2018) 173:581–94.e512. doi: 10.1016/j.cell.2018.03.057
14. Turajlic S, Xu H, Litchfield K, Rowan A, Horswell S, Chambers T, et al. Deterministic Evolutionary Trajectories Influence Primary Tumor Growth: TRACERx Renal. *Cell* (2018) 173:595–610.e511. doi: 10.1016/j.cell.2018.03.043
15. Ivan M, Kondo K, Yang H, Kim W, Valiando J, Ohh M, et al. HIFalpha Targeted for VHL-Mediated Destruction by Proline Hydroxylation: Implications for O2 Sensing. *Science* (2001) 292:464–8. doi: 10.1126/science.1059817
16. Jaakkola P, Mole DR, Tian YM, Wilson MI, Gielbert J, Gaskell SJ, et al. Targeting of HIF-Alpha to the Von Hippel-Lindau Ubiquitylation Complex by O2-Regulated Prolyl Hydroxylation. *Science* (2001) 292:468–72. doi: 10.1126/science.1059796
17. Ellis LM, Hicklin DJ. VEGF-Targeted Therapy: Mechanisms of Anti-Tumour Activity. *Nat Rev Cancer* (2008) 8:579–91. doi: 10.1038/nrc2403
18. Hanahan D, Weinberg RA. Hallmarks of Cancer: The Next Generation. *Cell* (2011) 144:646–74. doi: 10.1016/j.cell.2011.02.013
19. Kim JW, Tchernyshyov I, Semenza GL, Dang CV. HIF-1-Mediated Expression of Pyruvate Dehydrogenase Kinase: A Metabolic Switch Required for Cellular Adaptation to Hypoxia. *Cell Metab* (2006) 3:177–85. doi: 10.1016/j.cmet.2006.02.002
20. Masson N, Ratcliffe PJ. Hypoxia Signaling Pathways in Cancer Metabolism: The Importance of Co-Selecting Interconnected Physiological Pathways. *Cancer Metab* (2014) 2:3. doi: 10.1186/2049-3002-2-3
21. Papandreou I, Cairns RA, Fontana L, Lim AL, Denko NC. HIF-1 Mediates Adaptation to Hypoxia by Actively Downregulating Mitochondrial Oxygen Consumption. *Cell Metab* (2006) 3:187–97. doi: 10.1016/j.cmet.2006.01.012
22. Gao P, Tchernyshyov I, Chang TC, Lee YS, Kita K, Ochi T, et al. C-Myc Suppression of miR-23a/B Enhances Mitochondrial Glutaminase Expression and Glutamine Metabolism. *Nature* (2009) 458:762–5. doi: 10.1038/nature07823
23. Son J, Lyssiotis CA, Ying H, Wang X, Hua S, Ligorio M, et al. Glutamine Supports Pancreatic Cancer Growth Through a KRAS-Regulated Metabolic Pathway. *Nature* (2013) 496:101–5. doi: 10.1038/nature12040
24. Gameiro PA, Yang J, Metelo AM, Perez-Carro R, Baker R, Wang Z, et al. *In Vivo* HIF-Mediated Reductive Carboxylation is Regulated by Citrate Levels and Sensitizes VHL-Deficient Cells to Glutamine Deprivation. *Cell Metab* (2013) 17:372–85. doi: 10.1016/j.cmet.2013.02.002
25. Okazaki A, Gameiro PA, Christodoulou D, Laviollette L, Schneider M, Chaves F, et al. Glutaminase and Poly(ADP-Ribose) Polymerase Inhibitors Suppress Pyrimidine Synthesis and VHL-Deficient Renal Cancers. *J Clin Invest* (2017) 127:1631–45. doi: 10.1172/JCI87800
26. Reid MA, Dai Z, Locasale JW. The Impact of Cellular Metabolism on Chromatin Dynamics and Epigenetics. *Nat Cell Biol* (2017) 19:1298–306. doi: 10.1038/ncb3629
27. Wise DR, Thompson CB. Glutamine Addiction: A New Therapeutic Target in Cancer. *Trends Biochem Sci* (2010) 35:427–33. doi: 10.1016/j.tibs.2010.05.003
28. Scalise M, Pochini L, Galluccio M, Console L, Indiveri C. Glutamine Transport and Mitochondrial Metabolism in Cancer Cell Growth. *Front Oncol* (2017) 7:306. doi: 10.3389/fonc.2017.00306
29. Huang F, Zhao Y, Zhao J, Wu S, Jiang Y, Ma H, et al. Upregulated SLC1A5 Promotes Cell Growth and Survival in Colorectal Cancer. *Int J Clin Exp Pathol* (2014) 7:6006–14.
30. Liu Y, Yang L, An H, Chang Y, Zhang W, Zhu Y, et al. High Expression of Solute Carrier Family 1, Member 5 (SLC1A5) is Associated With Poor Prognosis in Clear-Cell Renal Cell Carcinoma. *Sci Rep* (2015) 5:16954. doi: 10.1038/srep16954
31. Ren P, Yue M, Xiao D, Xiu R, Gan L, Liu H, et al. ATF4 and N-Myc Coordinate Glutamine Metabolism in MYCN-Amplified Neuroblastoma Cells Through ASCT2 Activation. *J Pathol* (2015) 235:90–100. doi: 10.1002/path.4429
32. Abu Aboud O, Habib SL, Trott J, Stewart B, Liang S, Chaudhari AJ, et al. Glutamine Addiction in Kidney Cancer Suppresses Oxidative Stress and Can Be Exploited for Real-Time Imaging. *Cancer Res* (2017) 77:6746–58. doi: 10.1158/0008-5472.CAN-17-0930
33. Emberley E, Pan A, Chen J, Dang R, Gross M, Huang T, et al. The Glutaminase Inhibitor Telaglenastat Enhances the Antitumor Activity of Signal Transduction Inhibitors Everolimus and Cabozantinib in Models of Renal Cell Carcinoma. *PloS One* (2021) 16:e0259241. doi: 10.1371/journal.pone.0259241
34. Heravi G, Yazdanpanah O, Podgorski I, Matherly LH, Liu W. Lipid Metabolism Reprogramming in Renal Cell Carcinoma. *Cancer Metastasis Rev* (2021). doi: 10.1007/s10555-021-09996-w
35. Du W, Zhang L, Brett-Morris A, Aguila B, Kerner J, Hoppel CL, et al. HIF Drives Lipid Deposition and Cancer in ccRCC *via* Repression of Fatty Acid Metabolism. *Nat Commun* (2017) 8:1769. doi: 10.1038/s41467-017-01965-8
36. Qiu B, Ackerman D, Sanchez DJ, Li B, Ochocki JD, Grazioli A, et al. HIF2alpha-Dependent Lipid Storage Promotes Endoplasmic Reticulum Homeostasis in Clear-Cell Renal Cell Carcinoma. *Cancer Discovery* (2015) 5:652–67. doi: 10.1158/2159-8290.CD-14-1507
37. von Roemeling CA, Marlow LA, Wei JJ, Cooper SJ, Caulfield TR, Wu K, et al. Stearoyl-CoA Desaturase 1 is a Novel Molecular Therapeutic Target for Clear Cell Renal Cell Carcinoma. *Clin Cancer Res* (2013) 19:2368–80. doi: 10.1158/1078-0432.CCR-12-3249
38. Cuperlovic-Culf M, Cormier K, Touaibia M, Reyjal J, Robichaud S, Belbraouet M, et al. (1)H NMR Metabolomics Analysis of Renal Cell Carcinoma Cells: Effect of VHL Inactivation on Metabolism. *Int J Cancer* (2016) 138:2439–49. doi: 10.1002/ijc.29947
39. Turcotte S, Chan DA, Sutphin PD, Hay MP, Denny WA, Giaccia AJ. A Molecule Targeting VHL-Deficient Renal Cell Carcinoma That Induces Autophagy. *Cancer Cell* (2008) 14:90–102. doi: 10.1016/j.ccr.2008.06.004
40. Bouhamdani N, Comeau D, Coholan A, Cormier K, Turcotte S. Targeting Lysosome Function Causes Selective Cytotoxicity in VHL-Inactivated Renal Cell Carcinomas. *Carcinogenesis* (2020) 41:828–40. doi: 10.1093/carcin/bgz161
41. Bouhamdani N, Comeau D, Cormier K, Turcotte S. STF-62247 Accumulates in Lysosomes and Blocks Late Stages of Autophagy to Selectively Target Von Hippel-Lindau-Inactivated Cells. *Am J Physiol Cell Physiol* (2019) 316:C605–20. doi: 10.1152/ajpcell.00483.2018
42. Bligh EG, Dyer WJ. A Rapid Method of Total Lipid Extraction and Purification. *Can J Biochem Physiol* (1959) 37:911–7. doi: 10.1139/y59-099
43. Krieg M, Haas R, Brauch H, Acker T, Flamme I, Plate KH. Up-Regulation of Hypoxia-Inducible Factors HIF-1alpha and HIF-2alpha Under Normoxic Conditions in Renal Carcinoma Cells by Von Hippel-Lindau Tumor Suppressor Gene Loss of Function. *Oncogene* (2000) 19:5435–43. doi: 10.1038/sj.onc.1203938
44. Hay MP, Turcotte S, Flanagan JU, Bonnet M, Chan DA, Sutphin PD, et al. 4-Pyridylanilinothiazoles That Selectively Target Von Hippel-Lindau Deficient Renal Cell Carcinoma Cells by Inducing Autophagic Cell Death. *J Med Chem* (2010) 53:787–97. doi: 10.1021/jm901457w
45. Milkereit R, Persaud A, Vanoaica L, Guetg A, Verrey F, Rotin D. LAPTM4b Recruits the LAT1-4f2hc Leu Transporter to Lysosomes and Promotes Mtorc1 Activation. *Nat Commun* (2015) 6:7250. doi: 10.1038/ncomms8250

46. Elorza A, Soro-Arnaiz I, Melendez-Rodriguez F, Rodriguez-Vaello V, Marsboom G, de Carcer G, et al. HIF2alpha Acts as an Mtorc1 Activator Through the Amino Acid Carrier SLC7A5. *Mol Cell* (2012) 48:681–91. doi: 10.1016/j.molcel.2012.09.017
47. Yoo HC, Park SJ, Nam M, Kang J, Kim K, Yeo JH, et al. A Variant of SLC1A5 Is a Mitochondrial Glutamine Transporter for Metabolic Reprogramming in Cancer Cells. *Cell Metab* (2020) 31:267–83.e212. doi: 10.1016/j.cmet.2019.11.020
48. Scalise M, Pochini L, Console L, Losso MA, Indiveri C. The Human SLC1A5 (ASCT2) Amino Acid Transporter: From Function to Structure and Role in Cell Biology. *Front Cell Dev Biol* (2018) 6:96. doi: 10.3389/fcell.2018.00096
49. Bouhamdani N, Joy A, Barnett D, Cormier K, Leger D, Chute IC, et al. Quantitative Proteomics to Study a Small Molecule Targeting the Loss of Von Hippel-Lindau in Renal Cell Carcinomas. *Int J Cancer* (2017) 141:778–90. doi: 10.1002/ijc.30774
50. Sun RC, Denko NC. Hypoxic Regulation of Glutamine Metabolism Through HIF1 and SIAH2 Supports Lipid Synthesis That is Necessary for Tumor Growth. *Cell Metab* (2014) 19:285–92. doi: 10.1016/j.cmet.2013.11.022
51. Wettersten HI, Hakimi AA, Morin D, Bianchi C, Johnstone ME, Donohoe DR, et al. Grade-Dependent Metabolic Reprogramming in Kidney Cancer Revealed by Combined Proteomics and Metabolomics Analysis. *Cancer Res* (2015) 75:2541–52. doi: 10.1158/0008-5472.CAN-14-1703
52. Chinello C, Cazzaniga M, De Sio G, Smith AJ, Gianazza E, Grasso A, et al. Urinary Signatures of Renal Cell Carcinoma Investigated by Peptidomic Approaches. *PloS One* (2014) 9:e106684. doi: 10.1371/journal.pone.0106684
53. Ganti S, Weiss RH. Urine Metabolomics for Kidney Cancer Detection and Biomarker Discovery. *Urologic Oncol* (2011) 29:551–7. doi: 10.1016/j.urolonc.2011.05.013
54. Gao H, Dong B, Jia J, Zhu H, Diao C, Yan Z, et al. Application of *Ex Vivo* (1) H NMR Metabonomics to the Characterization and Possible Detection of Renal Cell Carcinoma Metastases. *J Cancer Res Clin Oncol* (2012) 138:753–61. doi: 10.1007/s00432-011-1134-6
55. Metallo CM, Gameiro PA, Bell EL, Mattaini KR, Yang J, Hiller K, et al. Reductive Glutamine Metabolism by IDH1 Mediates Lipogenesis Under Hypoxia. *Nature* (2011) 481:380–4. doi: 10.1038/nature10602
56. Weiss RH. Metabolomics and Metabolic Reprogramming in Kidney Cancer. *Semin Nephrol* (2018) 38:175–82. doi: 10.1016/j.semnephrol.2018.01.006
57. Sato T, Kawasaki Y, Maekawa M, Takasaki S, Morozumi K, Sato M, et al. Metabolomic Analysis to Elucidate Mechanisms of Sunitinib Resistance in Renal Cell Carcinoma. *Metabolites* (2020) 11:1–16. doi: 10.3390/metabo11010001
58. Harding JJ, Telli M, Munster P, Voss MH, Infante JR, DeMichele A, et al. A Phase I Dose-Escalation and Expansion Study of Telaglenastat in Patients With Advanced or Metastatic Solid Tumors. *Clin Cancer Res* (2021) 27:4994–5003. doi: 10.1158/1078-0432.CCR-21-1204
59. Wicker CA, Hunt BG, Krishnan S, Aziz K, Parajuli S, Palackdharry S, et al. Glutaminase Inhibition With Telaglenastat (CB-839) Improves Treatment Response in Combination With Ionizing Radiation in Head and Neck Squamous Cell Carcinoma Models. *Cancer Lett* (2021) 502:180–8. doi: 10.1016/j.canlet.2020.12.038
60. Console L, Scalise M, Tarmakova Z, Coe IR, Indiveri C. N-Linked Glycosylation of Human SLC1A5 (ASCT2) Transporter is Critical for Trafficking to Membrane. *Biochim Biophys Acta* (2015) 1853:1636–45. doi: 10.1016/j.bbamcr.2015.03.017
61. Cormerais Y, Massard PA, Vucetic M, Giuliano S, Tambutte E, Durivault J, et al. The Glutamine Transporter ASCT2 (SLC1A5) Promotes Tumor Growth Independently of the Amino Acid Transporter LAT1 (Slc7a5). *J Biol Chem* (2018) 293:2877–87. doi: 10.1074/jbc.RA117.001342
62. Bouthelier A, Melendez-Rodriguez F, Urrutia AA, Aragones J. Differential Contribution of N- and C-Terminal Regions of HIF1alpha and HIF2alpha to Their Target Gene Selectivity. *Int J Mol Sci* (2020) 21:1–16. doi: 10.3390/ijms21249401
63. Barthelemy C, Andre B. Ubiquitylation and Endocytosis of the Human LAT1/SLC7A5 Amino Acid Transporter. *Sci Rep* (2019) 9:16760. doi: 10.1038/s41598-019-53065-w
64. Pavlova NN, Hui S, Ghergurovich JM, Fan J, Intlekofer AM, White RM, et al. As Extracellular Glutamine Levels Decline, Asparagine Becomes an Essential Amino Acid. *Cell Metab* (2018) 27:428–38.e425. doi: 10.1016/j.cmet.2017.12.006
65. Tardito S, Oudin A, Ahmed SU, Fack F, Keunen O, Zheng L, et al. Glutamine Synthetase Activity Fuels Nucleotide Biosynthesis and Supports Growth of Glutamine-Restricted Glioblastoma. *Nat Cell Biol* (2015) 17:1556–68. doi: 10.1038/ncb3272
66. Zhang J, Fan J, Venneti S, Cross JR, Takagi T, Bhinder B , et al. Asparagine Plays a Critical Role in Regulating Cellular Adaptation to Glutamine Depletion. *Mol Cell* (2014) 56:205–18. doi: 10.1016/j.molcel.2014.08.018
67. Li J, Song P, Zhu L, Aziz N, Zhou Q, Zhang Y, et al. Synthetic Lethality of Glutaminolysis Inhibition, Autophagy Inactivation and Asparagine Depletion in Colon Cancer. *Oncotarget* (2017) 8:42664–72. doi: 10.18632/oncotarget.16844
68. Krall AS, Xu S, Graeber TG, Braas D, Christofk HR. Asparagine Promotes Cancer Cell Proliferation Through Use as an Amino Acid Exchange Factor. *Nat Commun* (2016) 7:11457. doi: 10.1038/ncomms11457
69. Jeffords E, Freeman S, Cole B, Root K, Chekouo T, Melvin RG, et al. Y-Box Binding Protein 1 Acts as a Negative Regulator of Stearoyl CoA Desaturase 1 in Clear Cell Renal Cell Carcinoma. *Oncol Lett* (2020) 20:165. doi: 10.3892/ol.2020.12026
70. Zhang H, Li H, Ho N, Li D, Li S. Scd1 Plays a Tumor-Suppressive Role in Survival of Leukemia Stem Cells and the Development of Chronic Myeloid Leukemia. *Mol Cell Biol* (2012) 32:1776–87. doi: 10.1128/MCB.05672-11
71. Cao Q, Ruan H, Wang K, Song Z, Bao L, Xu T, et al. Overexpression of PLIN2 is a Prognostic Marker and Attenuates Tumor Progression in Clear Cell Renal Cell Carcinoma. *Int J Oncol* (2018) 53:137–47. doi: 10.3892/ijo.2018.4384

Conflict of Interest: The authors declare that the research was conducted in the absence of any commercial or financial relationships that could be construed as a potential conflict of interest.

frontiers in Oncology

REVIEW
published: 28 February 2022
doi: 10.3389/fonc.2022.801842

The Role of Circular RNAs in the Carcinogenesis of Bladder Cancer

Soudeh Ghafouri-Fard[1], *Sajad Najafi*[2], *Bashdar Mahmud Hussen*[3], *Abbas Basiri*[4], *Hazha Jamal Hidayat*[5], *Mohammad Taheri*[6*] and *Fariborz Rashnoo*[7*]

[1] Department of Medical Genetics, School of Medicine, Shahid Beheshti University of Medical Sciences, Tehran, Iran, [2] Student Research Committee, Department of Medical Biotechnology, School of Advanced Technologies in Medicine, Shahid Beheshti University of Medical Sciences, Tehran, Iran, [3] Department of Pharmacognosy, College of Pharmacy, Hawler Medical University, Erbil, Iraq, [4] Urology and Nephrology Research Center, Shahid Beheshti University of Medical Sciences, Tehran, Iran, [5] Department of Biology, College of Education, Salahaddin University-Erbil, Erbil, Iraq, [6] Institute of Human Genetics, Jena University Hospital, Jena, Germany, [7] Skull Base Research Center, Loghman Hakim Hospital, Shahid Beheshti University of Medical Sciences, Tehran, Iran

OPEN ACCESS

Edited by:
Bianca Nitzsche,
Charité Universitätsmedizin Berlin, Germany

Reviewed by:
Ning Li,
Fourth Affiliated Hospital of China Medical University, China
Michael Höpfner,
Charité Universitätsmedizin Berlin, Germany

***Correspondence:**
Mohammad Taheri
Mohammad_823@yahoo.com
Fariborz Rashnoo
fariborz.rashnoo@yahoo.com

Specialty section:
This article was submitted to Genitourinary Oncology, a section of the journal Frontiers in Oncology

Received: 25 October 2021
Accepted: 28 January 2022
Published: 28 February 2022

Citation:
Ghafouri-Fard S, Najafi S, Hussen BM, Basiri A, Hidayat HJ, Taheri M and Rashnoo F (2022) The Role of Circular RNAs in the Carcinogenesis of Bladder Cancer. Front. Oncol. 12:801842. doi: 10.3389/fonc.2022.801842

Circular RNAs (circRNAs) are a group of transcripts with enclosed configurations which can regulate gene expression. These transcripts have important roles in normal development and in the pathogenesis of disorders. Recent evidence has supported involvement of circRNAs in the development of bladder cancer. Several circRNAs such as circ_0058063, hsa-circRNA-403658, circPDSS1, circCASC15, circRNA-MYLK, and circRNA_103809 have been upregulated in bladder cancer samples. On the other hand, hsa_circ_0137606, BCRC-3, circFUT8, hsa_circ_001598, circSLC8A1, hsa_circ_0077837, hsa_circ_0004826, and circACVR2A are among downregulated circRNAs in bladder cancer. Numerous circRNAs have diagnostic or prognostic value in bladder cancer. In this review, we aim to outline the latest findings about the role of circRNAs in bladder cancer and introduce circRNAs for further investigations as therapeutic targets.

Keywords: bladder cancer, ncRNAs, circRNAs, expression, biomarker

INTRODUCTION

Non-coding RNAs (ncRNAs) comprise several groups of RNA transcripts whose no protein is known to be encoded and thus considered as junk; however, they constitute a majority of expressed RNAs compared to protein-coding transcripts (1). Circular RNAs (circRNAs) are a distinct class of ncRNAs in eukaryotic cells which have been identified *via* electron microscopy in 1979 for the first time (2). Unlike coding-RNAs, circRNAs lack the 5′ cap and 3′ polyadenylated tail and do not mainly encode any protein; therefore, no primary function has been described for them (3). However, peptide-coding circRNAs have also been recognized. Some findings have revealed

developmental, pathogenic, and especially regulatory roles for circRNAs. As their name suggests, a close circular loop in circRNAs is formed by covalent linkages between the 5′ and 3′ ends of their transcripts. CircRNAs compared to their linear counterparts show higher stability against degrading agents like RNase R due to closed ends (4) but are found in lower quantities within the animal cells (5), although higher abundance is reported for some circRNAs (6). Their sequence is evolutionarily conserved, indicating selective pressure for them (6). CircRNAs also show specific cell and tissue tendencies (7). Their elevated levels in several diseases demonstrate their potentials as diagnostic biomarkers and also therapeutic potentials especially in cancers (8). Today, due to development of advanced technologies like high-throughput RNA sequencing (RNA seq) and *in situ* experiments, a huge number of circRNAs have been recognized in animal cells (2). Moreover, their regulatory roles in gene expression and pathogenesis of disorders have been recognized. Similar to other regulatory non-coding RNAs, regulatory functions of circRNAs are suggested to be exerted through modulating gene expression at different levels. Based on the gene region, circRNAs can be divided into three types: those originating from exons (exonic circRNAs), introns (intronic circRNAs), or exon–intron junctions (exon–intron circRNAs) (9). Exonic circRNAs have been found in higher concentrations in cytoplasm compared to the nucleus showing capability of sponging microRNAs (miRNAs) and so can positively affect the expression of target genes leading to their overexpression. Unlike the first type, the other types are more concentrated in the cell nucleus and thus regulate gene expression at the primary steps of transcriptional and posttranscriptional levels (10, 11). CircRNAs have been widely detected in different cells, tissues, and organisms and also during various stages of organism development, playing a role in controlling cell growth and stress (12). Through their regulatory mechanisms in the cell cycle, circRNAs have been found to apply surveillance on eukaryotic cell proliferation and homeostasis. Consistent with these findings, dysregulation of circRNAs has been reported in a vast number of proliferative disorders like different tumors. Bladder cancer (BCa) is an example in which the role of aberrantly expressed circRNAs in tumor development and progression has been studied. Similar to other malignancies, response to treatment in BCa requires early diagnosis which also guarantees better prognosis for the patients. CircRNAs not only have acted as potential biomarkers for BCa with promising characteristics in diagnosis and prediction of prognosis in BCa patients but also have been suggested as therapeutical targets in fighting against malignancy. In this review, we aim to outline the latest findings about the role of circRNAs in BCa.

CircRNAs IN BCA

Upregulated CircRNAs in BCa

In expression analyses *via* high-throughput technologies like microarray and sequencing and also in quantitative PCR studies, a number of circRNAs have been found to be upregulated in samples taken from patients with BCa compared to healthy controls. These kinds of circRNAs are suggested as oncogenes with carcinogenic roles. Accordingly, their overexpressed levels have been shown to promote tumor cell proliferation and invasion in cell studies and also *in vivo* experiments, while their downregulation or knockdown reverses these effects.

Microarray analysis provides a possibility to screen a large number of aberrantly expressed circRNA candidates in a single platform. CircRNA_0058063 is an example which was reported recently by Liang et al. (13) as an upregulated circRNA in cancerous tissues of BCa patients compared to adjacent normal tissues. Microarray results revealed 312 aberrantly expressed circRNAs including 195 upregulated and 117 downregulated ones. CircRNA _0058063 showed a significantly increased expression in both BCa cell lines and tissues. A reverse correlation was seen between circRNA _0058063 expression level and overall survival (OS) in patients. Consistent with expectations, circRNA _0058063 knockdown suppressed tumor cell proliferation and metastasis in BCa BIU-87 cell lines. CircRNA_0058063 was found to act as a miRNA sponge to decrease the expression level of miR-486-3p by making interaction *via* a complementary sequence and induction of silencing. miR-486-3p inhibits the expression of the FOXP4 transcription factor which promotes tumorigenicity in various cancers.

Li et al. (14) using high-throughput sequencing found a number of upregulated RNA transcripts including long non-coding RNAs (lncRNAs), protein-coding mRNAs, and 34 circRNAs in 20 BCa tissues compared with a matched number of adjacent normal bladder tissues in addition to another set of transcripts which were downregulated. In GO and KEGG pathway enrichment analyses, dysregulated RNAs were associated with several signaling pathways controlling different critical cellular processes particularly DNA replication and cell cycle which play a role in the pathogenesis of BCa. In addition, 3 circRNAs including circPGM5 and circKIAA1462 were validated by qPCR. CircRNA PGM5 was demonstrated in the competing endogenous RNA (ceRNA) network to possess recognition sites for miRNAs associated with BCa along with lncRNA MIR194-2HG and AATBC.

Also, robust next-generation sequencing (NGS) technique and confirmatory qRT-PCR have been used to screen dysregulated circRNAs in BCa samples (15). A significant differential expression of a single circRNA is assessed in BCa tissues relative to adjacent normal tissues *via* quantitative reverse transcription polymerase chain reaction (qRT-PCR; also known as real-time RT-PCR). An increasing number of circRNAs have been reported in separate studies to be aberrantly expressed in BCa tissues or in serum or urine samples of patients; thus, these circRNAs have been suggested as potential diagnostic and prognostic biomarkers for BCa patients (16). Hsa-circRNA-403658 is a good instance for a series of circRNAs found to be upregulated in BCa tissues *via* the latter method. Wei *et al.* (17) demonstrated a differential expression of a number of circRNAs in BCa SW780, 5637, T24, J82, and RT4 cell lines cultured in

hypoxic conditions in comparison with CCC-HB-2 healthy bladder epithelial cells using circRNA microarray. Hsa-circRNA-403658 was one of these circRNAs which showed the highest level of increased expression in further evaluation by qRT-PCR assay. Clinical samples of patients with BCa in which higher levels of hsa-circRNA-403658 were seen showed poorer prognosis, larger tumor size, increased metastasis, and higher clinicopathological stage (TNM staging) compared to patients with lower hsa-circRNA-403658 expression levels. As expected, hsa-circRNA-403658 knockdown using specific silencing RNA (siRNA) inhibited circRNA tumorigenic effects. Furthermore, *in vitro* and *in vivo* studies showed that hsa-circRNA-403658 controls the anaerobic glycolysis in hypoxic culture *via* enhancing the promotor activity and consequently positive regulation of lactate dehydrogenase A (LDHA) expression.

Computational studies and network analyses using bioinformatics methods have also facilitated the detection of differentially expressed circRNAs and their pathological roles and potential application as novel biomarkers for BCa (18–20), suggesting their application in early diagnosis and prediction of prognosis as well as their therapeutic potentials. **Figure 1** demonstrates the role of circRNAs in modulating bladder cancer development *via* promoting glycolysis.

Table 1 outlines the most important circRNAs with an elevated expression level in the BCa cell line and also in patients' samples.

Downregulated CircRNAs in BCa

These kinds of circRNAs have been found to exhibit lower expression levels in BCa samples compared to normal adjacent tissues. They are suggested to play a role as tumor suppressors with biological functions controlling the critical cellular processes cell proliferation and extracellular matrix stability and so their downregulation in a set of studies has been shown to facilitate tumor cell proliferation, migration, and invasion. *In vivo* experiments have also demonstrated accelerated tumor progression in the presence of decreased expression of these circRNAs. Similar to the former circRNAs, these kinds have been linked with cell cycle regulation through different miRNA–protein axes, among which are some oncogenes or tumor-suppressor genes which are dysregulated. Bioinformatic analyses, RNA pull-down assays, and luciferase reporter assays have shown single or several miRNAs being sponged in close interaction with circRNAs. The expression of these miRNAs is mainly suppressed *via* upstream circRNAs, and they themselves regulate some actions through affecting downstream molecules. Yet, some miRNAs act upstream of circRNAs exerting a regulatory role on them. Downregulated circRNAs are mainly located in the cytoplasm, so it is suggested that they play their regulatory roles at posttranscriptional or translational steps.

For instance, circSLC8A1 is a circRNA which has been reported by Lu *et al.* (66) to be downregulated in BCa tissues compared to healthy adjacent tissues in a study of 70 patients diagnosed with BCa. They detected a number of aberrantly expressed circRNAs through RNA sequencing. qRT-PCR confirmed a decreased expression of circSLC8A1 in 81% (57/70) of total BCa tissues compared to their matched adjacent tissues. Expression assay in 6 BCa cell lines using qRT-PCR also showed a decreased expression of circSLC8A1 compared to SV-HUC-1 normal bladder cells.

In vitro analyses revealed suppression of tumorigenic impacts following circSLC8A1 overexpression in BCa cell lines. By using different prediction tools, it was demonstrated that circSLC8A1 potentially sponges 7 miRNAs, among which were miR-130b and miR-494 whose interactions with circSLC8A1 were confirmed by RNA pull-down assay and biotin labeling. Overexpression of both miRNAs was associated with oncogenesis in BCa cells. Furthermore, luciferase reporter assay and Western blotting analysis demonstrated that miRNAs can bind to the 3′ end of the phosphatase and tensin homolog (PTEN) tumor suppressor and inhibit its expression. Rescue experiments and immunohistochemistry (IHC) analysis showed that circSLC8A1 acts as a tumor suppressor *via* the miR-130b and miR-494/PTEN/PI3k/Akt signaling axis. **Table 2** summarizes the recent findings of tumorigenicity studies on downregulated circRNAs in BCa. **Figure 2** represents the role of several circRNAs in bladder cancer cells *via* regulating some key signaling cascades.

Diagnostic and Prognostic Values of CircRNA in BCa

As explained above, dysregulated circRNAs cause disturbance in the cellular proliferation leading to malignancies, particularly BCa. On the other side, in the majority of the studies, dysregulation in circRNA expression has been statistically correlated with unfavorable clinicopathological features including high tumor size, histological grade, pathological stage, and presence of distant or lymph node metastasis in uni- or multivariate analyses in BCa patients. Therefore, as a consequence, it has been found that a dysregulation in the circRNA level can predict poorer survival (in terms of overall survival (OS), recurrence-free survival (RFS), disease-free survival (DFS), or progression-free survival (PFS)) and worse prognosis in Kaplan–Meier analyses.

As an example, it was formerly stated that hsa_circRNA_403658 is upregulated in BCa tissues compared to adjacent tissues (17). Kaplan–Meier analysis for the evaluation of survival showed that a high level of hsa_circRNA_403658 expression correlates with shorter survival in BCa patients. Implementation of the χ^2 test to assess the association between circRNA expression and clinicopathological features has revealed a positive correlation between high hsa_circRNA_403658 expression and malignant characteristics including higher tumor volume (size ≥3 cm related to <3 cm), metastasis to distant places and advanced TNM stage (III–IV). In the univariate and multivariate Cox regression test for assessment of prognostic factors, it was demonstrated that hsa_circRNA_403658 is an independent factor for prediction of prognosis in BCa patients (17).

In another study (70), downregulated circRNAs hsa_circ_0077837 and hsa_circ_0004826 in BCa were found to be significantly associated with worse OS and RFS in BCa patients in Kaplan–Meier analysis. Univariate and multivariate Cox regression analyses confirmed that both circRNAs can act as independent prognostic factors compared to other factors in BCa

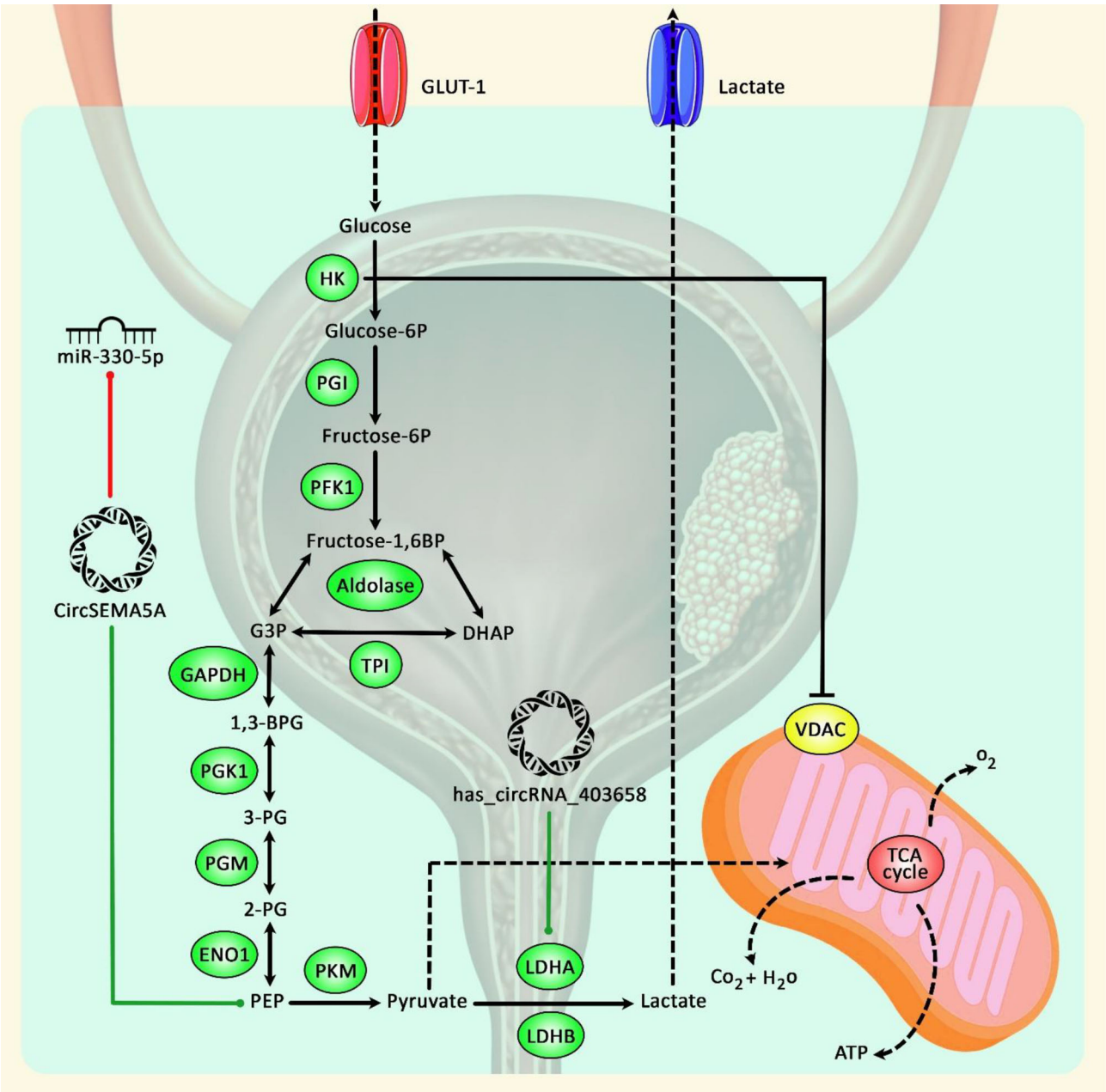

FIGURE 1 | A schematic diagram of the role of circRNAs in promoting bladder cancer progression *via* enhancing glycolysis. Accumulating findings have suggested that upregulation of key glycolysis proteins could play a crucial role in cancer development. As an illustration, a previous study has authenticated that has_circRNA_403658 through upregulation of LDHA-mediated aerobic glycolysis could have a significant part in enhancing bladder cancer cell growth (17). In addition, another research has detected that circSEMA5A *via* sponging miR-330-5p could upregulate the expression level of ENO1, thereby elevating proliferation, invasion, angiogenesis, and glycolysis of bladder cancer cells by facilitating the activation of Akt and β-catenin signaling cascades (21). Green arrows indicate the upregulation of target genes by circRNAs, and red arrows depict inhibitory effects.

patients. The area under the curve (AUC) for assessment of prognostic power of circRNAs revealed 0.775 and 0.790 values for hsa_circ_0077837 and hsa_circ_0004826, respectively, showing acceptable measures and suggesting their potentials as reliable biomarkers for prediction of worse prognosis in BCa patients.

Among other circRNAs, circASXL1 has been reported to have sensitivity and specificity of 0.686 and 0.769, respectively, which suggests its reliable diagnostic power in distinguishing the BCa patients from healthy people (38). A number of circRNAs whose prognostic or diagnostic values have been studied in BCa are shown in **Table 3**.

TABLE 1 | Upregulated circRNAs in BCa.

CircRNA (other terms)	Clinical cases	Cell lines	Target genes/ regulators/ sponged miRNAs	Affected signaling pathway/ process	Findings on overexpressed or silenced circRNA in BCa cellular experiments	Ref. (s)
Circ_0058063	94 BCa and matched NATs	HEK293 and BIU-87, 5637, and RT-112	miR-486-3p/FOXP4 axis miR-145-5p/CDK6 axis	–	Enhanced metastasis, correlation with higher disease stage	(13, 22)
Has_circRNA_403658	123 BCa patient tissues and matched NATs	CCC-HB-2 normal bladder epithelial cells and BCa SW780, 5637, T24, J82, and RT4	LDHA	Glycolysis	Poorer prognosis, larger tumor size, increased metastasis, and higher clinicopathological stage	(17)
CircPDSS1	72 patient tissues and their NATs	HT-1197 and UMUC3	miR-16	–	Increased tumor cell proliferation, migration, and invasion	(23)
CircCASC15 (hsa_circ_0075828)	67 patient tissues and control para-carcinoma tissues	5637, J82, UM-UC-3, T24, and SW780 human BC cell lines and SV-HUC-1 human uroepithelial cell line	miR-1224-5p and CREB1	–	Accelerated cell proliferation	(24)
CircRNA-MYLK	32 patient tissues and control para-carcinoma tissues	EJ, T24, 5673, and BIU-87 BCa cell lines and 293T human embryonic kidney cells	miR-29a, VEGFA	Ras/ERK	Promoted cell proliferation, migration, and epithelial–mesenchymal transition (EMT) *in vitro* and enhanced angiogenesis and metastasis in xenografts	(25)
Hsa_circ_0001361	69 patient tissues and healthy bladder epithelial tissues as matched controls	EJ, UMUC3, RT4, 5637 human BCa cell lines, and SV-HUC-1 uroepithelial cell line	miR-491-5p, MMP9	–	Facilitated *in vitro* and *in vivo* invasion and metastasis	(26)
Circ-VANGL1	87 BCa patient tissues and 37 NATs	T24, 253J, UMUC-3, J82, 5637, and EJ BCa cell lines and	miR-605-3p/VANGL1 axis	–	Promoted *in vitro* cell proliferation, migration, and invasion and *in vivo* BCa propagation	(27)
CircTCF25	4 pairs of BCa tissues and matched NATs in microarray analysis and 40 pairs for qRT-PCR validation	T24 and EJ BCa cell lines	miR-103a-3p/miR-107/CDK6 axis	–	Promoted *in vitro* and *vivo* proliferation and migration	(28)
Hsa_circ_0137439	Urine samples of 10 BCa patients and 10 healthy controls in microarray analysis and 116 BCa samples plus 30 healthy controls in qRT-PCR validation	T24 and 5637 human BCa cell lines	miR-142-5p/MTDH axis	–	Promoted BCa cell proliferation and metastasis	(29)
CircPTK2 (has-circ-0003221)	40 BCa tissues and matched para-carcinoma NATs	T24 and 5637 BCa cell lines	–	–	Promoted BCa cell proliferation and migration	(30)
CircCEP128	40 BCa tissues and matched NATs	293T, J82 and T24 BCa cell lines and SV-HUC-1	miR-145-5p/ *MYD88* axis	MAPK	CircCEP128 silencing inhibited cell viability and mobility and stimulated apoptosis	(31)
Circ0001429	20 BCa tissues and matched NATs	T24 and 5637 SV-HUC-1 and BIU-87	miR-205-5p/VEGFA axis	–	Enhanced propagation, migration, and invasion, and inhibited apoptosis	(32)
CircRGNEF	90 BCa patient tissues and matched NATs	J82, EJ, T24, TCC, UM-UC-3, and RT-4 BCa cell lines and SV-HUC	miR-548/ KIF2C axis	–	Promoted BCa cell proliferation, migration, and invasion	(33)
CircGPRC5a (hsa_circ_02838)	20 early BCa, 40 advanced BCa samples, and 60 NATs	Bladder CSCs	circGprc5a-peptide/ Gprc5a axis	–	Promoted self-renewal and invasion of bladder CSCs	(34)
Hsa_circ_0000144	69 BCa patient tissues and 21 matched NATs	T24, EJ, UMUC3, RT4, and 253J BCa cell lines and SV-HUC-1 cell line	miR-217/ RUNX2 axis	–	Promoted *in vitro* and *in vivo* BCa cell proliferation and invasion	(35)
CircINTS4	40 BCa samples and 40 NATs	RT4, SW780, J82, 5637, T24, UMUC3 BCa cell lines, and SV-HUC	miR-146b/ CARMA3 axis	NF-kB ↑ P38 MAPK ↓	Increased *in vitro* and *in vivo* BCa tumorigenicity	(36)

(Continued)

TABLE 1 | Continued

CircRNA (other terms)	Clinical cases	Cell lines	Target genes/ regulators/ sponged miRNAs	Affected signaling pathway/ process	Findings on overexpressed or silenced circRNA in BCa cellular experiments	Ref. (s)
CircZFR	104 BCa samples and 40 NATs	UMUC3, T24, J82, 5637, SW780, EJ and BIU87 BCa cell lines, and CCC-HB-2 cells	miR-377/ ZEB2 axis	–	Silencing showed inhibition of cell proliferation, migration, and invasion	(37)
CircASXl1 (hsa_circ_0001136)	61 BCa samples and 40 NATs	–	–	–	Correlated with worse clinicopathological features in BCa patients and lower OS	(38)
Hsa_circ_0068871	32 BCa samples and 40 NATs	T24, UMUC3, EJ and J82 BCa cell lines and SV-HUC-1	miR-181a-5p/FGFR3 axis	–	Promoted tumor cell growth	(39)
Circ_102336	64 BCa samples and 40 NATs	T24 and 5637 BCa cell lines and SV-HUC-1 and HEK-293 T cells	miR-515-5p	–	Promoted cell growth Enhanced drug sensitivity in circ_102336 knockdown	(40)
Hsa_circ_0068307	30 BCa samples and 40 NATs	EJ, T24, RT-4 and UM-UC-3 BCa cell lines	miR-147/c-Myc axis	–	Hsa_circ_0068307 knockdown inhibited BCa *in vitro* cell proliferation and migration and *in vivo* xenografts	(41)
Circ_0006332	32 BCa samples and 40 NATs	5637, T24, J82, UM-UC-3, TSCCUP, and SV-HUC-1 BCa cell lines	miR-143/ MYBL2 axis	–	Promoted *in vivo* cancer growth Circ_0006332 knockdown suppressed BCa cell proliferation and invasion	(42)
CircRNA-0071196	80 BCa tissues and 30 para-carcinoma tissues	5637 BCa cell line	miR-19b-3p/CIT axis	–	CircRNA-0071196 silencing decreased BCa cell proliferation and migration	(43)
circZNF139	–	UC3 and 5637 cells BCa cell lines	–	PI3K/AKT	ZNF139/circZNF139 promoted BCa cell proliferation, migration, and invasion	(44)
CircDOCK1	32 BCa samples and 32 NATs	BIU-87, EJ-m3, T24 and 5673 BCa cell lines and SV-HUC-1 cells	hsa-miR-132-3p/ Sox5 axis	–	CircDOCK1 silencing suppressed BCa cell progression *in vitro* and xenograft growth *in vivo*	(45)
CircKIF4A (hsa_circ_0007255)	50 BCa samples and 32 NATs	5637, RT-112, and BIU-87 BCa cell lines and HEK293T cells	miR-375/ 1231/ NOTCH2 axis	–	Promoted BCa *in vitro* cell proliferation and metastasis	(46)
Hsa_circ_0001944	90 BCa samples and 32 NATs	5637, UM-UC-3, T24, and RT-4 BCa cell lines and SV-HUC-1 cells	miR-548/ PROK2 axis	–	Silencing suppressed BCa cell proliferation and invasion *in vitro* and *in vivo*	(47)
CircPRMT5	119 BCa samples and 32 NATs	T24, TCC-SUP, 5637, and UM-UC-3 BCa cell lines, and SV-HUC-1 cells	miR-30c/ SNAIL1/E-cadherin axis	–	Silencing decreased BCa cell migration, invasion *in vitro*, and metastasis *in vivo* Overexpression enhanced BCa cells EMT	(48)
CircGLIS3 (hsa_circ_0002874)	48 BCa samples and 32 NATs	T24, UM-UC-3 BCa cell lines and SV-HUC-1 cells	miR-1273f/ SKP1/cyclin D1 axis		Silencing inhibited BCa cell proliferation, invasion, and migration *in vitro* and cell growth *in vivo* Upregulation promoted G0/G1 phase of cell cycle through miR-1273f/SKP1/ Cyclin D1 axis	(49)
Hsa_circ_0041103	50 BCa samples and 32 NATs	T24, UM-UC-3, RT4, 5637 BCa cell lines, and SV-HUC-1 cells	miR-107/ FOXK1 axis	–	Silencing inhibited BCa cell proliferation and metastasis	(50)
CircEHBP1	186 BCa samples and 32 NATs	UM-UC-3, T24, and 5637 BCa cell lines, and SV-HUC-1 cells	miR-130a-3p/ TGFβR1/ VEGF-D axis	TGF-β/SMAD	Promoted BCa lymph node metastasis *in vivo*	(51)
Circ_0000735	50 BCa samples and 32 NATs	5637, RT-112 and BIU-87 BCa cell lines, and SV-HUC-1 cells	miR-502-5p	–	Knockdown suppressed BCa cell proliferation and invasion *in vitro* and tumorigenesis *in vivo*	(52)
Circ_100984	20 BCa samples and 32 NATs	HT-1376, HTB9, 253J, BT-B, Biu-87 and 5637 BCa cell lines and SV-HUC-1 cells	miR-432-3p/c-Jun/ YBX-1/β-catenin axis	Wnt	Knockdown inhibited BCa cell growth, invasion, metastasis, and EMT *in vivo* and *in vivo*	(53)

(Continued)

TABLE 1 | Continued

CircRNA (other terms)	Clinical cases	Cell lines	Target genes/ regulators/ sponged miRNAs	Affected signaling pathway/ process	Findings on overexpressed or silenced circRNA in BCa cellular experiments	Ref. (s)
circRIMS1 (hsa_circ_0132246)	20 BCa samples and 32 NATs	J82, 5637, T24, EJ, and TCCSUP BCa cell lines and SV-HUC-1 and HEK-293 cells	miR-433-3p/CCAR1/ c-Myc axis	–	Knockdown repressed BCa cell proliferation, invasion, and metastasis *in vivo* and tumor growth *in vivo*	(54)
CircSEMA5A	40 BCa samples and 32 NATs	T24, UM-UC-3, 5637, J82 BCa cell lines, and SV-HUC-1 cells	miR-330-5p/ENO1 axis	Glycolysis ↑	Promoted BCa cell proliferation, invasion, migration capabilities, and angiogenesis *in vivo*	(21)
CircRNA_100146 (hsa_circRNA_100146)	68 BCa samples and 32 NATs	J82, 5637, SW780, and T24 BCa cell lines, and HCV-29 cells	miR-149-5p/RNF2 axis	–	Promoted BCa cell proliferation, invasion, and migration and inhibited apoptosis	(55)
CircBC048201	30 BCa samples and 32 NATs	UM-UC-3 BCa cell lines and SV-HUC-1 cells	miR-1184/ ITGA3 axis	–	Interference inhibited BCa cell proliferation, migration, and invasion	(56)
CircRNA_0071196	80 BCa samples and 30 matched para-carcinoma tissues	The 5637 human BCa cell line	miR-19b-3p/CIT axis	–	Knockdown repressed BCa cell proliferation and migration	(43)
Circ_0061140	42 BCa samples and corresponding NATs	T24, 253j, 5637, J82, RT4, UMUC3 BCa cell lines, and SV-HUC-1 cells	miR-1236	–	Circ_0061140 knockdown repressed BCa cell proliferation and invasion	(57)
Circ_001418	–	–	miR-1297/ EphA2 axis	–	Enhanced BCa cell proliferation and invasion, and decreased apoptosis	(58)
Circ_0067934	54 BCa tissues and corresponding NATs	T24, RT4 and UMUC3 BCa cell lines, and SV-HUC-1 cells	miR-1304-Myc axis	–	Circ_0067934 silencing inhibited BCa cell proliferation, invasion, and migration *in vivo*	(59)
Hsa_circ_0017247	50 BCa tissues and corresponding NATs	UM-UC3, SW780, BIU, and J82 BCa cell lines	–	Wnt/β-catenin	Knockdown inhibited BCa cell growth and promoted apoptosis *in vitro* and repressed tumor growth *in vivo*	(60)
CircFNTA	41 BCa tissues and corresponding NATs	T24, J82, 5637, and UMUC3 BCa cell lines, and SV-HUC cells	miR-370-3p/FNTA axis	KRAS	Enhanced cell invasion and chemo-resistance to cisplatin in BCa cell lines CircFNTA knockdown repressed its tumorigenic effects	(61)
CircRIP2	58 BCa tissues and corresponding NATs	5637 and UM-UC-3 BCa cell lines	miR-1305	Tgf-β2/smad3	Increased BCa cell progression through stimulation of EMT	(62)
CircUVRAG	Experiment was conducted on 20 BALB/c nude mice	T24, EJ, J82, UM-UC-3, TCC, and RT-4 BCa cell lines, and SV-HUC cells	miR-223/ FGFR2 axis	–	Knockdown repressed BCa cell proliferation and metastasis *in vitro* and *in vivo*	(63)
Circ-BPTF	72 BCa tissues and corresponding NATs	UM-UC-3 and T24 BCa cell lines	miR-31-5p/ RAB27A axis	–	Increased *in vitro* and *in vivo* progression of BCa cells	(64)
Circ_0023642	–	J82 and UMUC3 BCa cell lines	miR-490-5p	ERα/ circ_0023642/ miR-490-5p/ EGFR	ERα suppressed BCa cell invasion *in vitro* through downregulation of circ_0023642 *via* expressional modulation of UVRAG host gene and also repressed metastasis *in vivo*	(65)

↑, *activation or increased level;* ↓, *inhibition or decreased level; NAT, normal adjacent tissue.*
VEGFA, vascular endothelial growth factor A; MMP9, matrix metallopeptidase 9; MTDH, metadherin; CSCs, cancer stem cells; IGFIR, type 1 insulin-like growth factor receptor; ERα, estrogen receptor alpha.

DISCUSSION

Circular RNAs (circRNAs) are covalently closed nucleic acid strands which are classified as non-coding RNAs and mainly do not code any protein. They have been found to play a role in gene regulation in several stages. CircRNAs show cell-, tissue-, or species-specific tropism and are known to be dysregulated in tissues in a number of cancers. They have been found to either act as tumor suppressors or exhibit oncogenic roles on overexpression. The causative mechanisms of circRNAs' role in tumorigenicity are vastly being studied. Their dysregulation has mainly been associated with disturbances in cell cycle regulation through activation of several signaling pathways.

In this review, we summarized a number of studies conducted on dysregulated circRNAs in BCa. Dysregulation includes any increase or decrease in circRNA expression levels in BCa tissues or cell studies compared to normal adjacent tissues. To assess the circRNA dysregulation, some high-throughput technologies like RNA sequencing and

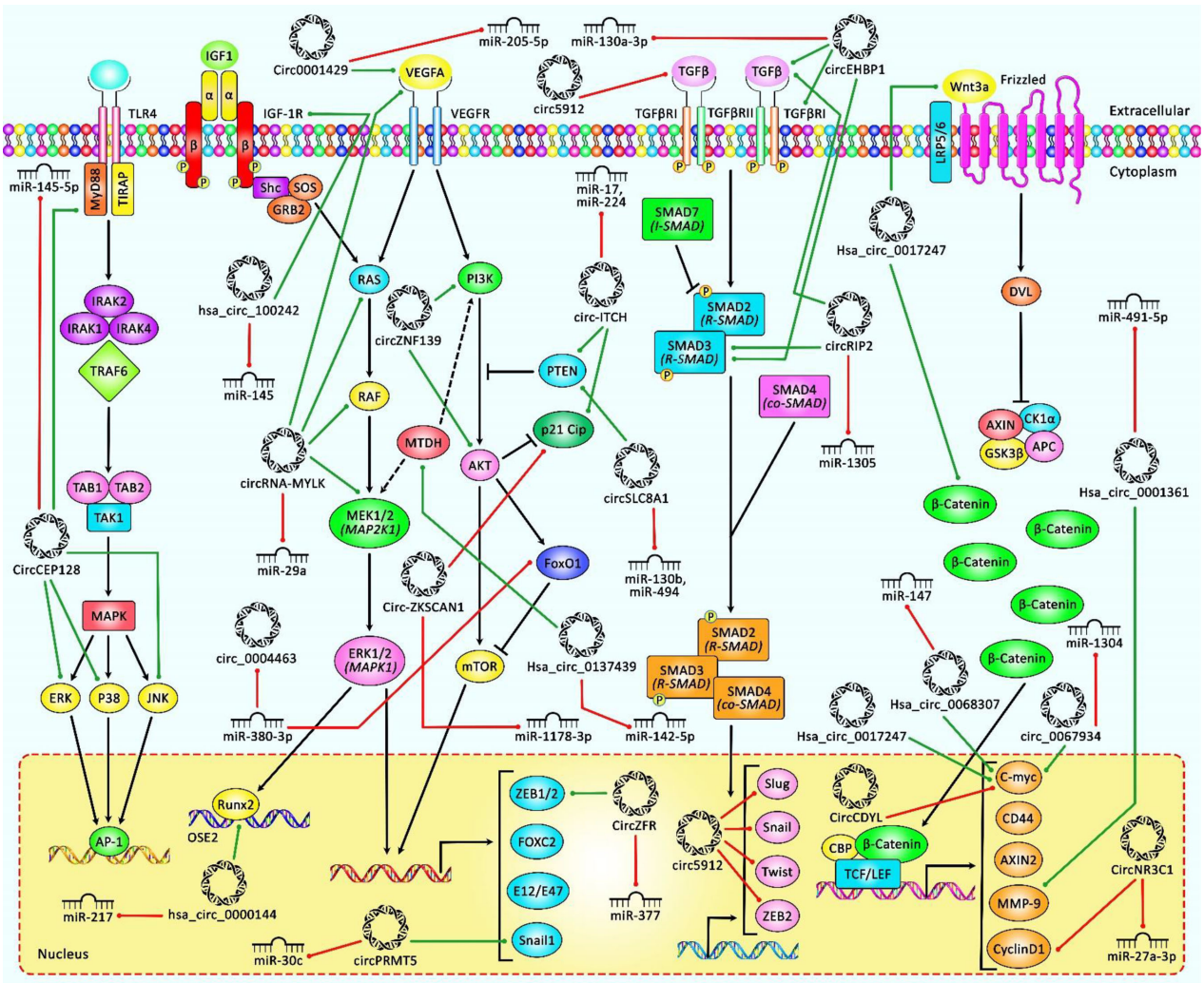

FIGURE 2 | A schematic representation of the role of various circRNAs in human bladder cancer through modulating the PI3K/AKT, MAPK/ERK, TGFβ/SMAD3, and Wnt/β-catenin signaling pathways. According to the diagram, the upregulation or downregulation of several circRNAs could have a considerable role in bladder cancer development through modulation of miRNA levels. Green arrows indicate upregulation of target genes by circRNAs, and red arrows depict inhibition regulated by them. All the information regarding the role of these circRNAs in bladder cancer is shown in **Tables 1**, **2**.

confirmatory qRT-PCR have been employed. Upregulated circRNAs in the first section (**Table 1**) have been found to accelerate tumor cell proliferation and enhance migration and invasion of cancer cell *in vitro*. *In vivo* studies have shown increased tumor progression when these circRNAs are overexpressed. Suppression of upregulated circRNAs *via* specific siRNAs in BCa has confirmed repression of proliferative and migratory potential following their silencing.

Downregulated circRNAs (**Table 2**), on the other hand, have been known to exert their anti-tumorigenic roles *via* suppression of tumor cell proliferation, migration, invasion, and metastasis. Overexpression experiments have confirmed tumor-suppressing roles of the second class of circRNAs *via* diminishing tumor cell malignant behaviors.

Furthermore, correlation studies have shown a significant association between dysregulated circRNA expression levels and worse clinicopathological features including higher tumor size, distant or lymph node metastasis, higher histological grade, pathological stage, and advanced TNM stage in BCa patients (**Table 3**). Statistical analyses have also demonstrated that dysregulation of circRNAs can be used as independent prognostic factors for BCa patients. Acceptable AUC, specificity, or sensitivity values in diagnostic analyses have revealed the diagnostic power of circRNAs in distinguishing BCa from other diseases. Taken together, circRNAs have been suggested as markers with reliable prognostic and diagnostic potential which can be used as biomarkers in either diagnosis or prediction of prognosis in BCa patients. Not only circRNAs but

TABLE 2 | Downregulated circRNAs in BCa.

circRNA (other terms)	Clinical cases	Cell lines	Target genes/ regulators/sponged miRNAs	Affected signaling pathway/ process	Findings on overexpressed or downregulated circRNA in BCa cellular experiments	Ref. (s)
CircBCRC-3	47 BCa patient tissues and matched NATs	BC and EJ BCa cell lines and SV-HUC-1 cells	miR-182-5p/p27 axis	–	Overexpression inhibited BCa cell growth *in vitro* and tumor progression *in vivo*	(67)
CircFUT8	145 BCa patient tissues and 50 matched NATs	T24 and UM-UC-3 BCa cell lines and SV-HUC-1 cells	miR-570-3p/KLF10 axis	–	Overexpression suppressed BCa cell migration and invasion *in vitro* and metastasis *in vivo*	(68)
BCRC4 (hsa_circ_001598)	24 BCa patient tissues and matched NATs	UMUC3 BCa cell lines and SV-HUC-1 cells	miR-101/EZH2 axis	–	Overexpression decreased BCa cell proliferation and also, increased apoptosis	(69)
CircSLC8A1	70 BCa patient tissues and matched NATs	5637, T24, J82, EJ, UMUC, and RT4 BCa cell lines, and SV-HUC-1 cells	miR-130b and miR-494/PTEN/PI3k/Akt signaling axis	PI3k/Akt	Overexpression decreased BCa cell migration and invasion *in vitro* CircSLC8A1 inhibited tumor progression *in vivo*	(66)
Hsa_circ_0077837 and Hsa_circ_0004826	70 BCa patient tissues and matched NATs	EJ, 5637, and T24 BCa cell lines and SV-HUC-1 cells	–	–	Overexpression inhibited BCa cell proliferation, migration, and invasion	(70)
CircACVR2A (hsa_circ_0001073)	140 BCa patient tissues and matched NATs	T24, UM-UC-3, RT4, J82, 5637, HT-1376, TCCSUP BCa cell lines, and SV-HUC-1 cells	miR-626/EYA4 axis	–	Overexpression inhibited BCa cells proliferation, migration, and invasion *in vitro* and tumor progression and metastasis *in vivo*	(71)
Hsa_circ_0002024	20 BCa patient tissues and matched NATs	EJ, 5637, T24, and UMUC-2 and normal human urothelial cells	miR-197-3p	–	Upregulation suppressed BCa cells proliferation, migration, and invasion	(72)
Circ-FOXO3	49 BCa patient tissues and matched NATs	EJ and T24 BCa cell lines	miR-9-5p/TGFBR2 axis	–	Upregulation suppressed BCa cells proliferation, migration, and invasion	(73)
	30 BCa patient tissues and matched NATs	T24, UM-UC-3 and J82 BCa cell lines, and SV-HUC-1 cells	miR-191-5p	–	Overexpression increased apoptosis	(74)
CircNR3C1 (Hsa_circ_0001543)	42 BCa patient tissues and matched NATs	T24, EJ, UMUC3, J82, 5637 BCa cell lines, and SV-HUC-1 cells	-miR-23a-3p -miR-27a-3p/cyclin D1 axis	–	Upregulation suppressed BCa cells proliferation and progression *in vitro* and *in vivo via* arrest in the G0/G1 phase	(75)
CircMTO1	117 BCa patient tissues and matched NATs	UMUC3, SVHUC1, T24, J82, and 5637 and CCC-HB-2 cells	miR-221	–	Overexpression inhibited BCa cell migration and invasion *in vitro* and progression *in vivo*	(76)
Circ-ITCH	72 BCa patient tissues and matched NATs	5637, T24, J82, EJ, UMUC, TCC, 253J, and RT4 BCa cell lines and SV-HUC cells	-miR-224 -miR-17/p21 and PTEN axis	–	Downregulated circ-ITCH inhibited BCa cell proliferation, migration, and invasion *in vitro via* induction of the G1/S phase arrest Tumor progression was suppressed *in vivo*	(77)
CircST6GALNAC6	30 BCa patient tissues and matched NATs	T24, J82, UM-UC-3, 5637, and SW780 and SV-HUC-1 cells	miR-200a-3p/STMN1 signaling axis	–	Overexpression suppressed BCa cell proliferation and migration *in vitro* and metastasis *in vivo*	(78)
Circ_0071662	97 BCa patient tissues and matched NATs	BIU-87, T-24, EJ-28, and J82 BCa cell lines and SV-HUC-1 cells	miR-146-3p	–	Overexpression inhibited BCa cell proliferation and invasion	(79)
Hsa_circ_0018069	41 BCa patient tissues and matched NATs	T24, and Biu-87 BCa cell lines and SV-HUC-1 cells	miR-23c, miR-34a-5p, miR-181b-5p, miR-454-3p, and miR-3666	–	Downregulation correlated with more severe clinicopathological features	(80)
CircPICALM	168 BCa patient tissues and 40 NATs	T24, UM-UC-3, J82, and RT-4 BCa cell lines and SV-HUC-1 cells	miR-1265/STEAP4/ pFAK-Y397 axis	–	Overexpression suppressed BCa cell invasion *in vitro* and metastasis *in vivo*	(81)
Hsa_circ_0091017	40 BCa patient tissues and corresponding NATs	5637, EJ, T24, UMUC-3, RT4 BCa cell lines, and SV-HUC-1 cells	miR-589-5p	–	Overexpression suppressed BCa cell proliferation, migration, and invasion	(82)
Circ-*ZKSCAN1*	68 BCa patient tissues and matched NATs	T24, UM-UC-3, 5637, and EJ BCa cell lines and SV-HUC-1 cells	miR-1178-3p/p21 axis		Overexpression suppressed BCa cell proliferation, migration, and invasion *in vitro* and also tumor progression and invasion *in vivo*	(83)

(Continued)

TABLE 2 | Continued

circRNA (other terms)	Clinical cases	Cell lines	Target genes/ regulators/sponged miRNAs	Affected signaling pathway/ process	Findings on overexpressed or downregulated circRNA in BCa cellular experiments	Ref. (s)
CircHIPK3	44 BCa patient tissues and matched NATs	T24T and UMUC BCa cell lines and SV-HUC-1 and HUVEC normal bladder cells	miR-558/HPSE axis	Angiogenesis	Overexpression repressed BCa cell migration and invasion *in vitro* and also tumor progression, metastasis, and angiogenesis *in vivo*	(84)
CircFAM114A2	31 BCa patient tissues and matched NATs	T24, J82, 5637, and 293T BCa cell lines and SV-HUC-1 cells	miR-762/△NP63 axis	–	Overexpression suppressed BCa cell proliferation, migration, and invasion *in vitro* and tumor growth *in vivo*	(85)
CircPTPRA	104 BCa patient tissues and matched NATs	T24 and UM-UC-3 BCa cell lines and SV-HUC-1 and HEK-293T cells	miR-636/KLF9 axis	–	Overexpression suppressed BCa cell proliferation and knockdown promoted it *in vitro* and tumor growth *in vivo*	(86)
CiRs-6	45 BCa patient tissues and matched NATs	T24 and UM-UC-3 BCa cell lines	miR-653/March1 axis	–	Overexpression inhibited BCa cell proliferation *in vitro* and tumor growth *in vivo*	(87)
CircFNDC3B	82 BCa patient tissues and 56 matched NATs	T24 and UM-UC-3 BCa cell lines and SV-HUC-1 cells	miR-1178-3p/G3BP2 axis	–	Overexpression repressed BCa cell proliferation, migration, and invasion *in vitro* and inhibited tumor growth and metastasis *in vivo*	(88)
CircUBXN7 (hsa_circ_0001380)	30 BCa patient tissues and matched NATs	T24, J82, EJ, RT4, and UM-UC-3 BCa cell lines and SV-HUC-1 cells	miR-1247-3p/ B4GALT3 axis	–	Downregulation correlated with more severe clinicopathological features in BCa patients Overexpression suppressed BCa cell proliferation, migration, and invasion *in vitro* and tumor progression *in vivo*	(89)
CircCDYL	30 BCa patient tissues and matched NATs	EJ and T24T BCa cell lines and SV-HUC-1 cells	c-Myc	–	Overexpression repressed BCa cell proliferation and migration *in vitro*	(90)
Circ5912	45 BCa patient tissues and matched NATs	T24 and SW780 BCa cell lines	–	TGFβ	Knockdown increased BCa cell proliferation and invasion *in vitro* Overexpression decreased EMT through suppression of TGF-β2	(91)
CircRBPMS	90 BCa patient tissues and matched NATs	RT4, UM-UC-3, T24, 5637, and J82 BCa cell lines and SV-HUC-1 cells	miR-330-3p/RAI2/ EMT-ERK axis	KRAS/ERK	Overexpression suppressed BCa cell proliferation and invasion *in vitro* and tumor progression and metastasis *in vivo*	(92)
CircLPAR1 (hsa_circ_0087960)	68 BCa patient tissues and matched NATs	5637 and T24 BCa cell lines and 293 cells	miR-762		Knockdown increased BCa cell invasion	(93)
CircRNA_000285 (hsa_circ_0000285)	146 BCa patient tissues and 98 matched NATs	HTB-9, T24, J82, SW780, and RT4 BCa cell lines and CCC-HB-2 normal bladder cells	–	–	Lower level was seen in chemoresistance to cisplatin	(94)
Cdr1as	32 BCa patient tissues and matched NATs	TCCSUP, 5367, T24, and EJ BCa cell lines	miR-1270/APAF1 axis	–	Cdr1as improved BCa cell's chemosensitivity to cisplatin *in vitro* and *in vivo* Overexpression increased apoptosis in BCa cells	(95)

also other ncRNAs like lncRNAs have shown high stability in biological fluids, making them good biomarkers with easy detection for a number of human diseases particularly diverse types of cancers including BCa, breast cancer, hepatocellular carcinoma, and colorectal cancer (97, 98). Exosomes as extracellular vesicles involved in cellular communications are particularly shown to contain circRNAs in high concentrations and in a stabile form (99). These membranes can be beneficial in the detection of malignancies when derived from cancer cells spreading to blood and detectable in serum. Newly identified circRNAs have been introduced through high-throughput approaches such as next-generation sequencing (NGS), and microarray analysis, which make the huge identification of ncRNAs possible, while qRT-PCR is the main technique with potential in clinical diagnosis and quantification of circRNAs for both prognostic and diagnostic goals, and it is also used as the confirmatory method upon a novel ncRNA as previously reported (100). Vast application of qRT-PCR in quantification of a circRNA, however, is possible when the junction/fusion site is identified (8). Moreover, other technological drawbacks require to be addressed for clinical applications of circRNAs.

In vitro and xenograft studies have confirmed the suitability of circRNAs as therapeutic targets in cancers. However, several issues such as biosafety ones should be solved before application of circRNA-targeting methods in clinical settings.

TABLE 3 | An overview to the diagnostic and prognostic values of dysregulated circRNAs in BCa.

Description	Area under curve	Sensitivity	Specificity	Kaplan–Meier analysis	Univariate Cox regression	Multivariate Cox regression	Other correlation tests	Ref. (s)
Hsa_circRNA_403658 upregulation in BCa patients	–	–	–	hsa_circRNA_403658 high expression correlated with shorter survival in BCa patients.	Increased hsa_circRNA_403658 level was correlated with advanced clinicopathological features such as increased tumor size (≥3 cm), metastasis to distant places, and malignant TNM stage(III–IV). hsa_circRNA_403658 can act as an independent prognostic factor for BCa patients	Increased hsa_circRNA_403658 level was correlated with advanced clinicopathological features including larger tumor size(≥3 cm), lymph node metastasis, distant metastasis, and malignant TNM stage (III-IV).	χ^2 test showed a positive correlation between high hsa_circRNA_403658 expression and malignant clinicopathological features including larger tumor size, advanced tumor TNM stage, and distant metastasis.	(17)
Hsa_circ_0003221 (circPTK2) upregulation in tissue and blood samples of BCa patients	–	–	–	–	–	–	Student's *t* test showed that the expression level is correlated with tumor size, lymph node metastasis, and T stage at BCa patients ($p < 0.05$)	(30)
Hsa_circ_0072995 (circRGNEF) upregulation in BCa patients	–	–	–	–	–	–	High expression level was positively correlated with lymph node metastasis, high T stage, and advanced grades of BCa and also associated with worse prognosis.	(33)
CircGprc5a upregulation in BCa patients	–	—	–	High circGprc5a expression correlated with poorer survival and prognosis in BCa patients.	–	–	–	(34)
CircZFR upregulation in BCa patients	0.8216	–	–	Higher circZFR correlated with poorer prognosis and survival in BCa patients.	circZFR expression correlated with worse PFS and OS.		The chi-square tests showed correlation between circZFR expression and tumor stage, grade, lymph node metastasis, and recurrence in BCa patients.	(37)
CircASXL1 upregulation in BCa patients	0.770	0.686	0.769	BCa patients with higher levels of circASXL1 levels had poorer OS.	High circASXL1 expression correlated with more severe clinicopathological features including higher tumor grade, pathological T stage, distant, and lymph node metastasis.	High circASXL1 expression correlated with malignant clinicopathological features including advanced pathological T stage, distant and lymph node metastasis.	–	(38)
Hsa_circ_0001944 upregulation in BCa patients	–	–	–	High Hsa_circ_0001944 expression correlated with worse prognosis in BCa patients.	–	–	The Pearson's correlation test showed correlation between hsa_circ_0001944 higher expression and larger tumor size, advanced T stage, higher grade, and lymph node metastasis in BCa patientsAlso, poorer prognosis was predicted for patients with higher hsa_circ_0001944 levels.	(47)
CircPRMT5 upregulation in BCa patients	–	–	–	BCa patients with high circPRMT5 or miR-30c expression exhibited poorer survival rate.	–	–	The x^2 test showed that circPRMT5 serum and urine levels in BCa patients are associated with metastasis.	(48)

(Continued)

TABLE 3 | Continued

Description	Area under curve	Sensitivity	Specificity	Kaplan–Meier analysis	Univariate Cox regression	Multivariate Cox regression	Other correlation tests	Ref. (s)
				Correlated with worse prognosis.				
Hsa_circ_0041103 upregulation in BCa patients	–	–	–	Hsa_circ_0041103 expression correlated with unfavorable OS in BCa patients.	–	–	The two-paired independent *t*-test demonstrated positive correlation between high levels of hsa_circ_0041103 and advanced clinicopathological features including larger tumor size, higher pathological T stage, and lymph node metastasis in BCa patients.	(50)
cTFRC upregulation in BCa patients	–	–	–	Patients with higher cTFRC expression level had poorer OS.	–	–	cTFRC expression was positively correlated with advanced tumor T stage, higher grade and lymphatic invasion at BCa patientscTFRC was associated with poor prognosis.	(96)
Circ_0061140 upregulation in BCa patients	–	–	–	BCa patients with high circ_0061140 expression exhibited worse prognosis compared to those with lower levels.	–	–	The χ^2 test showed correlation between high circ_0061140 levels and lymph node or distant metastasis.	(57)
Circ_0067934 upregulation in BCa patients	–	–	–	BCa patients with high circ_0067934 level had shorter 5-year OS and disease-free survival.	–	–	The χ^2 test showed a positive correlation between high circ_0067934 levels and advanced clinicopathological features including tumor size, higher pathological stage, and lymph node metastasis.	(59)
Circ-BPTF upregulation in BCa patients	–	–	–	Patients with higher circ-BPTF expression level had worse OS.	–	–	High cTFRC expression was positively correlated with advanced tumor stage and recurrence in BCa patients.	(64)
CircFUT8 downregulation in BCa patients	–	–	–	Lower circFUT8 levels in BCa patients correlated with worse OS and poor prognosis.	–	–	The chi-square test demonstrated an association between low circFUT8 expression and worse clinicopathological features including lymph node metastasis and high histological grade.	(68)
Hsa_circ_0077837 and Hsa_circ_0004826 downregulation in BCa patients (low: 35 for both and high: 35 for both)	0.775 and 0.790 for hsa_circ_0077837 and hsa_circ_0004826, respectively	–	–	Downregulated hsa_circ_0077837 and hsa_circ_0004826 were associated with lower OS and RFS in BCa patients.	Correlation between high expression of both circRNAs, tumor stage, grade, and lymph node metastasis with shorter OS and RFS in BCa patients. Both circRNAs can act as independent factors for prediction of prognosis in BCa patients.	Correlation between high expression of both circRNAs and lymph node metastasis with shorter OS, and also high expression of hsa_circ_0077837 and lymph node metastasis with shorter RFS in BCa patients.	–	(70)
CircACVR2A downregulation in BCa patients	–	–	–	Low circ-BPTF expression level was associated with worse OS and prognosis in BCa patients.	–	–	Chi-square test showed correlation between low circACVR2A expression and advanced tumor stage, grade, and lymph node metastasis in BCa patients.	(71)

(Continued)

TABLE 3 | Continued

Description	Area under curve	Sensitivity	Specificity	Kaplan–Meier analysis	Univariate Cox regression	Multivariate Cox regression	Other correlation tests	Ref. (s)
Circ-ITCH downregulation in BCa patients	–	–	–	Lower circ-ITCH level positively correlated with shorter OS and poorer prognosis in BCa patients.	–	–	Downregulated circ-ITCH was significantly associated with high pathological tumor stage in BCa patients.	(77)
Circ_0071662 downregulation in BCa patients	–	–	–	Circ_0071662 expression was positively correlated with survival rate in BCa patients.	–	–	Low Circ_0071662 expression correlated with lymph node and distal metastasis and poorer prognosis in BCa patients.	(79)
Hsa_circ_018069 downregulation in BCa patients (diminished in 80.5% (33/41) of cases)	0.709	0.976	0.463	–	–	–	The Student's *t*-test showed that hsa_circ_018069 downregulation correlated with more severe clinicopathological features including high tumor grade, pathological T stage, and tumor muscular invasion.	(80)
CircPICALM downregulation in BCa patients	–	–	–	BCa patients with a diminished level of circPICALM exhibited poorer OS related to those with high levels.	circPICALM expression, histological grade, pathological T stage, and lymph node metastasis correlated with survival in BCa patients.	circPICALM expression and lymph node metastasis demonstrated as independent features for prediction of prognosis in BCa patients.	The chi-square test showed that circPICALM downregulation correlated with unfavorable clinicopathological features including high histological grade, pathological T stage, and lymph node metastasis in BCa patients.	(81)
Circ-ZKSCAN1 downregulation in BCa patients	–	–	–	Downregulated circ-ZKSCAN1 correlated with worse OS and disease-free survival and predict poorer prognosis for BCa patients.	–	–	The chi-square test demonstrated an association between low circ-ZKSCAN1 levels and advanced clinicopathological features including high histological grade, pathological T stage, and lymph node metastasis in BCa patients.	(83)
CiRs-6 downregulation in BCa patients	–	–	–	Higher ciRs-6 was positively correlated with good OS in BCa patients.	–	–	One-way ANOVA test showed that higher ciRs-6 expression was associated with lower tumor grade, pathological T stage, and better prognosis in BCa patients.	(87)
Hsa_circ_0018069 downregulation in BCa patients	0.709	0.976	0.463	–	–	–	The Student's *t*-test showed correlation between low hsa_circ_0018069 levels and clinicopathological features including higher tumor grade, advanced T stage, and muscular invasion depth in BCa patients.	(80)
CircUBXN7 downregulation in BCa patients	–	–	–	Patients with decreased circUBXN7 levels showed shorter OS.	–	–	The chi-square analysis showed correlation between low circUBXN7 expression and advanced pathological T stage and more severe grades in BCa patients.	(89)
Circ5912 downregulation in BCa patients	–	–	–	Patients with higher circ5912 expression had longer OS compared to those with lower levels.	–	–	The one-way ANOVA test showed correlation between higher levels of circ5912 and favorable clinicopathological features including lower tumor grade, stage, and metastasis in BCa patients.	(91)

(Continued)

TABLE 3 | Continued

Description	Area under curve	Sensitivity	Specificity	Kaplan–Meier analysis	Univariate Cox regression	Multivariate Cox regression	Other correlation tests	Ref. (s)
CircFNDC3B downregulation in BCa patients	–	–	–	Patients with lower circFNDC3B levels showed decreased survival.	–	–	The chi-square test revealed a positive correlation between lower circFNDC3B levels and highly advanced clinicopathological features such as higher histological grade, T stage, and metastasis to lymph nodes.	(88)
Circ-ITCH downregulation in BCa patients	–	–	–	Low circ-ITCH levels in BCa patients were positively correlated with poorer OS.	–	–	The chi-square test showed a correlation between low circ-ITCH expression level and more advanced tumor grade in BCa patients.	(77)
Hsa_circ_0000285 downregulation in BCa patients				Higher hsa_circ_0000285 expression was associated with longer OS in BCa patients.	hsa_circ_0000285 level correlated with prognosis in BCa patients.	hsa_circ_0000285 level is an independent prognostic factor for BCa patients.	The chi-square demonstrated correlation between hsa_circ_0000285 expression and clinicopathological features.	(94)
CircLPAR1 downregulation in BCa patients	–	–	–	BCa patients with low circLPAR1 levels had decreased survival compared to those with higher levels.	A correlation was seen between low circLPAR1 levels and decreased DSS in BCa patients.		–	(93)

OS, overall survival; RFS, recurrence-free survival; DDS, disease-specific survival.

Taken together, although circRNAs have shown roles in the development and progression of various human cancers, and their quantification have demonstrated excellent potential in distinguishing patients with BCa from healthy individuals, it seems that application of circRNAs as novel biomarkers needs further investigations, more time, and addressing of technological problems to enter in clinical settings.

AUTHOR CONTRIBUTIONS

SGF and SN wrote the draft and revised it. MT designed and supervised the study. BMH, HJH, FR, and AB collected the data and designed the figures and tables. All authors contributed to the article and approved the submitted version.

REFERENCES

1. Najafi S, Tan SC, Raee P, Rahmati Y, Asemani Y, Lee EHC, et al. Gene Regulation by Antisense Transcription: A Focus on Neurological and Cancer Diseases. *Biomed Pharmacother* (2022) 145:112265. doi: 10.1016/j.biopha.2021.112265
2. Hsu M-T, Coca-Prados M. Electron Microscopic Evidence for the Circular Form of RNA in the Cytoplasm of Eukaryotic Cells. *Nature* (1979) 280 (5720):339–40. doi: 10.1038/280339a0
3. Rahmati Y, Asemani Y, Aghamiri S, Ezzatifar F, Najafi S. CiRS-7/CDR1as; An Oncogenic Circular RNA as a Potential Cancer Biomarker. *Pathol - Res Pract* (2021) 227:153639. doi: 10.1016/j.prp.2021.153639
4. Suzuki H, Zuo Y, Wang J, Zhang MQ, Malhotra A, Mayeda A. Characterization of RNase R-Digested Cellular RNA Source That Consists of Lariat and Circular RNAs From pre-mRNA Splicing. *Nucleic Acids Res* (2006) 34(8):e63. doi: 10.1093/nar/gkl151
5. Lasda E, Parker R. Circular RNAs: Diversity of Form and Function. *RNA (New York NY)* (2014) 20(12):1829–42. doi: 10.1261/rna.047126.114
6. Jeck WR, Sorrentino JA, Wang K, Slevin MK, Burd CE, Liu J, et al. Circular RNAs Are Abundant, Conserved, and Associated With ALU Repeats. *RNA* (2013) 19(2):141–57. doi: 10.1261/rna.035667.112
7. Jeck WR, Sharpless NE. Detecting and Characterizing Circular RNAs. *Nat Biotechnol* (2014) 32(5):453–61. doi: 10.1038/nbt.2890
8. Taheri M, Najafi S, Basiri A, Hussen BM, Baniahmad A, Jamali E, et al. The Role and Clinical Potentials of Circular RNAs in Prostate Cancer. *Front Oncol* (2021) 11:781414. doi: 10.3389/fonc.2021.781414
9. Liu J, Liu T, Wang X, He A. Circles Reshaping the RNA World: From Waste to Treasure. *Mol Cancer* (2017) 16(1):58. doi: 10.1186/s12943-017-0630-y
10. Memczak S, Jens M, Elefsinioti A, Torti F, Krueger J, Rybak A, et al. Circular RNAs are a Large Class of Animal RNAs With Regulatory Potency. *Nature* (2013) 495(7441):333–8. doi: 10.1038/nature11928
11. Li Z, Huang C, Bao C, Chen L, Lin M, Wang X, et al. Exon-Intron Circular RNAs Regulate Transcription in the Nucleus. *Nat Struct Mol Biol* (2015) 22 (3):256–64. doi: 10.1038/nsmb.2959
12. Fischer JW, Leung AKL. CircRNAs: A Regulator of Cellular Stress. *Crit Rev Biochem Mol Biol* (2017) 52(2):220–33. doi: 10.1080/10409238.2016.1276882
13. Liang H, Huang H, Li Y, Lu Y, Ye T. CircRNA_0058063 Functions as a ceRNA in Bladder Cancer Progression *via* Targeting miR-486-3p/FOXP4 Axis. *Biosci Rep* (2020) 40(3). doi: 10.1042/BSR20193484
14. Li M, Liu Y, Zhang X, Liu J, Wang P. Transcriptomic Analysis of High-Throughput Sequencing About circRNA, lncRNA and mRNA in Bladder Cancer. *Gene* (2018) 677:189–97. doi: 10.1016/j.gene.2018.07.041
15. Yang X, Yuan W, Tao J, Li P, Yang C, Deng X, et al. Identification of Circular RNA Signature in Bladder Cancer. *J Cancer* (2017) 8(17):3456–63. doi: 10.7150/jca.19345
16. Pan J, Xie X, Li H, Li Z, Ren C, Ming L. Detection of Serum Long Non-Coding RNA UCA1 and Circular RNAs for the Diagnosis of Bladder Cancer and Prediction of Recurrence. *Int J Clin Exp Pathol* (2019) 12(8):2951–8.
17. Wei Y, Zhang Y, Meng Q, Cui L, Xu C. Hypoxia-Induced Circular RNA has_circRNA_403658 Promotes Bladder Cancer Cell Growth Through Activation of LDHA. *Am J Transl Res* (2019) 11(11):6838–49.
18. Kouhsar M, Azimzadeh Jamalkandi S, Moeini A, Masoudi-Nejad A. Detection of Novel Biomarkers for Early Detection of Non-Muscle-Invasive Bladder Cancer Using Competing Endogenous RNA Network Analysis. *Sci Rep* (2019) 9(1):8434. doi: 10.1038/s41598-019-44944-3
19. Yang J, Chen J, Wu S, Fei X, Wang X, Wang K. Microarray Expression Profiles and Bioinformatics Analyses Reveal Aberrant Circular RNAs Expression in Bladder Cancer. *Onco Targets Ther* (2020) 13:10889–99. doi: 10.2147/OTT.S270747
20. Cai D, Liu Z, Kong G. Molecular and Bioinformatics Analyses Identify 7 Circular RNAs Involved in Regulation of Oncogenic Transformation and Cell Proliferation in Human Bladder Cancer. *Med Sci Monitor Int Med J Exp Clin Res* (2018) 24:1654–61. doi: 10.12659/MSM.908837
21. Wang L, Li H, Qiao Q, Ge Y, Ma L, Wang Q. Circular RNA Circsema5a Promotes Bladder Cancer Progression by Upregulating ENO1 and SEMA5A Expression. *Aging (Albany NY)* (2020) 12(21):21674–86. doi: 10.18632/aging.103971
22. Sun M, Zhao W, Chen Z, Li M, Li S, Wu B, et al. Circ_0058063 Regulates CDK6 to Promote Bladder Cancer Progression by Sponging miR-145-5p. *J Cell Physiol* (2019) 234(4):4812–24. doi: 10.1002/jcp.27280
23. Yu Q, Liu P, Han G, Xue X, Ma D. CircRNA Circpdss1 Promotes Bladder Cancer by Down-Regulating miR-16. *Biosci Rep* (2020) 40(1):BSR20191961. doi: 10.1042/BSR20191961
24. Zhuang C, Huang X, Yu J, Gui Y. Circular RNA Hsa_Circ_0075828 Promotes Bladder Cancer Cell Proliferation Through Activation of CREB1. *BMB Rep* (2020) 53(2):82–7. doi: 10.5483/BMBRep.2020.53.2.059
25. Zhong Z, Huang M, Lv M, He Y, Duan C, Zhang L, et al. Circular RNA MYLK as a Competing Endogenous RNA Promotes Bladder Cancer Progression Through Modulating VEGFA/VEGFR2 Signaling Pathway. *Cancer Lett* (2017) 403:305–17. doi: 10.1016/j.canlet.2017.06.027
26. Liu F, Zhang H, Xie F, Tao D, Xiao X, Huang C, et al. Hsa_circ_0001361 Promotes Bladder Cancer Invasion and Metastasis Through miR-491-5p/MMP9 Axis. *Oncogene* (2020) 39(8):1696–709. doi: 10.1038/s41388-019-1092-z
27. Zeng Z, Zhou W, Duan L, Zhang J, Lu X, Jin L, et al. Circular RNA Circ-VANGL1 as a Competing Endogenous RNA Contributes to Bladder Cancer Progression by Regulating miR-605-3p/VANGL1 Pathway. *J Cell Physiol* (2019) 234(4):3887–96. doi: 10.1002/jcp.27162
28. Zhong Z, Lv M, Chen J. Screening Differential Circular RNA Expression Profiles Reveals the Regulatory Role of Circtcf25-miR-103a-3p/miR-107-CDK6 Pathway in Bladder Carcinoma. *Sci Rep* (2016) 6(1):30919. doi: 10.1038/srep30919
29. Song Z, Zhang Q, Zhu J, Yin G, Lin L, Liang C. Identification of Urinary Hsa_Circ_0137439 as Potential Biomarker and Tumor Regulator of Bladder Cancer. *Neoplasma* (2020) 67(1):137–46. doi: 10.4149/neo_2018_181214N970
30. Xu Z-Q, Yang M-G, Liu H-J, Su C-Q. Circular RNA Hsa_Circ_0003221 (Circptk2) Promotes the Proliferation and Migration of Bladder Cancer Cells. *J Cell Biochem* (2018) 119(4):3317–25. doi: 10.1002/jcb.26492
31. Sun M, Zhao W, Chen Z, Li M, Li S, Wu B, et al. Circular RNA CEP128 Promotes Bladder Cancer Progression by Regulating Mir-145-5p/Myd88 *via* MAPK Signaling Pathway. *Int J Cancer* (2019) 145(8):2170–81. doi: 10.1002/ijc.32311
32. Cao W, Zhao Y, Wang L, Huang X. Circ0001429 Regulates Progression of Bladder Cancer Through Binding miR-205-5p and Promoting VEGFA Expression. *Cancer Biomarkers* (2019) 25:101–13. doi: 10.3233/CBM-182380
33. Yang C, Li Q, Chen X, Zhang Z, Mou Z, Ye F, et al. Circular RNA circRGNEF Promotes Bladder Cancer Progression *via* miR-548/KIF2C Axis Regulation. *Aging (Albany NY)* (2020) 12(8):6865–79. doi: 10.18632/aging.103047
34. Gu C, Zhou N, Wang Z, Li G, Kou Y, Yu S, et al. Circgprc5a Promoted Bladder Oncogenesis and Metastasis Through Gprc5a-Targeting Peptide. *Mol Ther - Nucleic Acids* (2018) 13:633–41. doi: 10.1016/j.omtn.2018.10.008
35. Huang W, Lu Y, Wang F, Huang X, Yu Z. Downregulation of Circular RNA Hsa_Circ_0000144 Inhibits Bladder Cancer Progression *via* Stimulating miR-217 and Suppressing RUNX2 Expression. *Gene* (2018) 678:337–42. doi: 10.1016/j.gene.2018.08.036

36. Zhang X, Liu X, Jing Z, Bi J, Li Z, Liu X, et al. The Circints4/miR-146b/CARMA3 Axis Promotes Tumorigenesis in Bladder Cancer. *Cancer Gene Ther* (2020) 27(3):189–202. doi: 10.1038/s41417-019-0085-y
37. Zhang W-Y, Liu Q-H, Wang T-J, Zhao J, Cheng X-H, Wang J-S. CircZFR Serves as a Prognostic Marker to Promote Bladder Cancer Progression by Regulating miR-377/ZEB2 Signaling. *Biosci Rep* (2019) 39(12). doi: 10.1042/BSR20192779
38. Tang G, Xie W, Qin C, Zhen Y, Wang Y, Chen F, et al. Expression of Circular RNA Circasxl1 Correlates With TNM Classification and Predicts Overall Survival in Bladder Cancer. *Int J Clin Exp Pathol* (2017) 10(8):8495–502.
39. Mao W, Huang X, Wang L, Zhang Z, Liu M, Li Y, et al. Circular RNA Hsa_Circ_0068871 Regulates FGFR3 Expression and Activates STAT3 by Targeting miR-181a-5p to Promote Bladder Cancer Progression. *J Exp Clin Cancer Res* (2019) 38(1):169. doi: 10.1186/s13046-019-1136-9
40. Gong P, Xu R, Zhuang Q, He X. A Novel Circular RNA (Hsa_circRNA_102336), a Plausible Biomarker, Promotes the Tumorigenesis by Sponging miR-515-5p in Human Bladder Cancer. *Biomed Pharmacother* (2020) 126:110059. doi: 10.1016/j.biopha.2020.110059
41. Chen Q, Yin Q, Mao Y, Zhang Z, Wu S, Cheng Z, et al. Hsa_circ_0068307 Mediates Bladder Cancer Stem Cell-Like Properties *via* miR-147/C-Myc Axis Regulation. *Cancer Cell Int* (2020) 20(1):151. doi: 10.1186/s12935-020-01235-6
42. Li M, Liu Y, Liu J, Li W, Li N, Xue D, et al. Circ_0006332 Promotes Growth and Progression of Bladder Cancer by Modulating MYBL2 Expression *via* miR-143. *Aging (Albany NY)* (2019) 11(22):10626–43. doi: 10.18632/aging.102481
43. Liu Z, Yang Y, Yang Z, Xia S, Lin D, Xiao B, et al. Novel circRNA_0071196/miRNA−19b−3p/CIT Axis Is Associated With Proliferation and Migration of Bladder Cancer. *Int J Oncol* (2020) 57(3):767–79. doi: 10.3892/ijo.2020.5093
44. Yao J, Qian K, Chen C, Liu X, Yu D, Yan X, et al. ZNF139/circZNF139 Promotes Cell Proliferation, Migration and Invasion *via* Activation of PI3K/AKT Pathway in Bladder Cancer. *Aging (Albany NY)* (2020) 12(10):9915–34. doi: 10.18632/aging.103256
45. Liu P, Li X, Guo X, Chen J, Li C, Chen M, et al. Circular RNA DOCK1 Promotes Bladder Carcinoma Progression *via* Modulating Circdock1/hsa-miR-132-3p/Sox5 Signalling Pathway. *Cell Proliferation* (2019) 52(4):e12614. doi: 10.1111/cpr.12614
46. Shi Y-R, Wu Z, Xiong K, Liao Q-J, Ye X, Yang P, et al. Circular RNA Circkif4a Sponges miR-375/1231 to Promote Bladder Cancer Progression by Upregulating NOTCH2 Expression. *Front Pharmacol* (2020) 11:605–. doi: 10.3389/fphar.2020.00605
47. Jin M, Lu S, Wu Y, Yang C, Shi C, Wang Y, et al. Hsa_circ_0001944 Promotes the Growth and Metastasis in Bladder Cancer Cells by Acting as a Competitive Endogenous RNA for miR-548. *J Exp Clin Cancer Res* (2020) 39(1):186. doi: 10.1186/s13046-020-01697-6
48. Fang Y, Chen S, Liu Z, Ai W, He X, Wang L, et al. Endothelial Stem Cells Attenuate Cardiac Apoptosis *via* Downregulating Cardiac microRNA−146a in a Rat Model of Coronary Heart Disease. *Exp Ther Med* (2018) 16(5):4246–52.
49. Wu S, Yang J, Xu H, Wang X, Zhang R, Lu W, et al. Circular RNA Circglis3 Promotes Bladder Cancer Proliferation *via* the miR-1273f/SKP1/Cyclin D1 Axis. *Cell Biol Toxicol* (2022) 38:129–46. doi: 10.1007/s10565-021-09591-3
50. Chen LQ, Yi CL, Liu DC, Wang P, Zhu YF, Yuan LP. Hsa_circ_0041103 Induces Proliferation, Migration and Invasion in Bladder Cancer *via* the miR-107/FOXK1 Axis. *Eur Rev Med Pharmacol Sci* (2021) 25(3):1282–90. doi: 10.26355/eurrev_202102_24832
51. Zhu J, Luo Y, Zhao Y, Kong Y, Zheng H, Li Y, et al. Circehbp1 Promotes Lymphangiogenesis and Lymphatic Metastasis of Bladder Cancer *via* miR-130a-3p/Tgfβr1/VEGF-D Signaling. *Mol Ther J Am Soc Gene Ther* (2021) 29(5):1838–52. doi: 10.1016/j.ymthe.2021.01.031
52. Zheng H, Yang C, Tang J. Cyclic RNA Circ_0000735 Sponges miR-502-5p to Promote Bladder Cancer Cell Proliferation and Invasion and Inhibit Apoptosis. *Int J Clin Exp Pathol* (2020) 13(12):2994–3003.
53. Tong L, Yang H, Xiong W, Tang G, Zu X, Qi L. Circ_100984-miR-432-3p Axis Regulated C-Jun/YBX-1/β-Catenin Feedback Loop Promotes Bladder Cancer Progression. *Cancer Sci* (2020) 112(4):1429–42. doi: 10.1111/cas.14774
54. Wang F, Fan M, Cai Y, Zhou X, Tai S, Yu Y, et al. Circular RNA Circrims1 Acts as a Sponge of miR-433-3p to Promote Bladder Cancer Progression by Regulating CCAR1 Expression. *Mol Ther Nucleic Acids* (2020) 22:815–31. doi: 10.1016/j.omtn.2020.10.003
55. Du L, Xu Z, Wang X, Liu F. Integrated Bioinformatics Analysis Identifies microRNA-376a-3p as a New microRNA Biomarker in Patient With Coronary Artery Disease. *Am J Trans Res* (2020) 12(2):633.
56. Jiang P, Zhu Y, Xu Z, Chen X, Xie L. Interference With Circbc048201 Inhibits the Proliferation, Migration, and Invasion of Bladder Cancer Cells Through the miR-1184/ITGA3 Axis. *Mol Cell Biochem* (2020) 474(1-2):83–94. doi: 10.1007/s11010-020-03835-2
57. Feng F, Chen AP, Wang XL, Wu GL. Circ_0061140 Promotes Metastasis of Bladder Cancer Through Adsorbing microRNA-1236. *Eur Rev Med Pharmacol Sci* (2020) 24(10):5310–9. doi: 10.26355/eurrev_202103_25199
58. Peng G, Meng H, Pan H, Wang W. CircRNA 001418 Promoted Cell Growth and Metastasis of Bladder Carcinoma *via* EphA2 by miR-1297. *Curr Mol Pharmacol* (2021) 14(1):68–78. doi: 10.2174/1874467213666200505093815
59. Liu Q, Zhou Q, Zhong P. Circ_0067934 Increases Bladder Cancer Cell Proliferation, Migration and Invasion Through Suppressing miR-1304 Expression and Increasing Myc Expression Levels. *Exp Ther Med* (2020) 19(6):3751–9. doi: 10.3892/etm.2020.8648
60. Gao W, Cui H, Li Q, Zhong H, Yu J, Li P, et al. Upregulation of microRNA-218 Reduces Cardiac Microvascular Endothelial Cells Injury Induced by Coronary Artery Disease Through the Inhibition of HMGB1. *J Cell Physiol* (2020) 235(3):3079–95. doi: 10.1002/jcp.29214
61. Chen J, Sun Y, Ou Z, Yeh S, Huang CP, You B, et al. Androgen Receptor-Regulated circFNTA Activates KRAS Signaling to Promote Bladder Cancer Invasion. *EMBO Rep* (2020) 21(4):e48467. doi: 10.15252/embr.201948467
62. Su Y, Feng W, Shi J, Chen L, Huang J, Lin T. Circrip2 Accelerates Bladder Cancer Progression *via* miR-1305/Tgf-β2/Smad3 Pathway. *Mol Cancer* (2020) 19(1):23–. doi: 10.1186/s12943-019-1129-5
63. Yang C, Wu S, Wu X, Zhou X, Jin S, Jiang H. Silencing Circular RNA UVRAG Inhibits Bladder Cancer Growth and Metastasis by Targeting the microRNA-223/Fibroblast Growth Factor Receptor 2 Axis. *Cancer Sci* (2019) 110(1):99–106. doi: 10.1111/cas.13857
64. Bi J, Liu H, Cai Z, Dong W, Jiang N, Yang M, et al. Circ-BPTF Promotes Bladder Cancer Progression and Recurrence Through the miR-31-5p/RAB27A Axis. *Aging (Albany NY)* (2018) 10(8):1964–76. doi: 10.18632/aging.101520
65. Wu L, Zhang M, Qi L, Zu X, Li Y, Liu L, et al. Erα-Mediated Alterations in Circ_0023642 and miR-490-5p Signaling Suppress Bladder Cancer Invasion. *Cell Death Dis* (2019) 10(9):635. doi: 10.1038/s41419-019-1827-3
66. Lu Q, Liu T, Feng H, Yang R, Zhao X, Chen W, et al. Circular RNA Circslc8a1 Acts as a Sponge of miR-130b/miR-494 in Suppressing Bladder Cancer Progression *via* Regulating PTEN. *Mol Cancer* (2019) 18(1):111. doi: 10.1186/s12943-019-1040-0
67. Xie F, Li Y, Wang M, Huang C, Tao D, Zheng F, et al. Circular RNA BCRC-3 Suppresses Bladder Cancer Proliferation Through miR-182-5p/P27 Axis. *Mol Cancer* (2018) 17(1):144. doi: 10.1186/s12943-018-0892-z
68. He Q, Yan D, Dong W, Bi J, Huang L, Yang M, et al. circRNA Circfut8 Upregulates Krüpple-Like Factor 10 to Inhibit the Metastasis of Bladder Cancer *via* Sponging miR-570-3p. *Mol Ther - Oncolytics* (2020) 16:172–87. doi: 10.1016/j.omto.2019.12.014
69. Faccini J, Ruidavets J-B, Cordelier P, Martins F, Maoret J-J, Bongard V, et al. Circulating miR-155, miR-145 and Let-7c as Diagnostic Biomarkers of the Coronary Artery Disease. *Sci Rep* (2017) 7:42916. doi: 10.1038/srep42916
70. Shen C, Wu Z, Wang Y, Gao S, Da L, Xie L, et al. Downregulated Hsa_Circ_0077837 and Hsa_Circ_0004826, Facilitate Bladder Cancer Progression and Predict Poor Prognosis for Bladder Cancer Patients. *Cancer Med* (2020) 9(11):3885–903. doi: 10.1002/cam4.3006
71. Dong W, Bi J, Liu H, Yan D, He Q, Zhou Q, et al. Circular RNA ACVR2A Suppresses Bladder Cancer Cells Proliferation and Metastasis Through miR-626/EYA4 Axis. *Mol Cancer* (2019) 18(1):95. doi: 10.1186/s12943-019-1025-z
72. Jiang Y, Wei T, Li W, Zhang R, Chen M. Circular RNA Hsa_Circ_0002024 Suppresses Cell Proliferation, Migration, and Invasion in Bladder Cancer by Sponging miR-197-3p. *Am J Transl Res* (2019) 11(3):1644–52.
73. Li Y, Qiao L, Zang Y, Ni W, Xu Z. Circular RNA FOXO3 Suppresses Bladder Cancer Progression and Metastasis by Regulating MiR-9-5p/TGFBR2. *Cancer Manage Res* (2020) 12:5049–56. doi: 10.2147/CMAR.S253412
74. Wang C, Tao W, Ni S, Chen Q. Circular RNA Circ-Foxo3 Induced Cell Apoptosis in Urothelial Carcinoma *via* Interaction With miR-191-5p. *Onco Targets Ther* (2019) 12:8085–94. doi: 10.2147/OTT.S215823

75. Zheng F, Wang M, Li Y, Huang C, Tao D, Xie F, et al. CircNR3C1 Inhibits Proliferation of Bladder Cancer Cells by Sponging miR-27a-3p and Downregulating Cyclin D1 Expression. *Cancer Lett* (2019) 460:139–51. doi: 10.1016/j.canlet.2019.06.018
76. Li Y, Wan B, Liu L, Zhou L, Zeng Q. Circular RNA Circmto1 Suppresses Bladder Cancer Metastasis by Sponging miR-221 and Inhibiting Epithelial-to-Mesenchymal Transition. *Biochem Biophys Res Commun* (2019) 508(4):991–6. doi: 10.1016/j.bbrc.2018.12.046
77. Yang C, Yuan W, Yang X, Li P, Wang J, Han J, et al. Circular RNA Circ-ITCH Inhibits Bladder Cancer Progression by Sponging miR-17/miR-224 and Regulating P21, PTEN Expression. *Mol Cancer* (2018) 17(1):19. doi: 10.1186/s12943-018-0771-7
78. Tan S, Kang Y, Li H, He H-Q, Zheng L, Wu S-Q, et al. Circst6galnac6 Suppresses Bladder Cancer Metastasis by Sponging miR-200a-3p to Modulate the STMN1/EMT Axis. *Cell Death Dis* (2021) 12(2):168. doi: 10.1038/s41419-021-03459-4
79. Abulizi R, Li B, Zhang CG. Circ_0071662, a Novel Tumor Biomarker, Suppresses Bladder Cancer Cell Proliferation and Invasion by Sponging miR-146b-3p. *Oncol Res* (2019). doi: 10.3727/096504019X15740729375088
80. Li M, Wang Y, Liu Y, Zhang X, Liu J, Wang P. Low Expression of Hsa_Circ_0018069 in Human Bladder Cancer and Its Clinical Significance. *BioMed Res Int* (2019). doi: 10.1155/2019/9681863
81. Yan D, Dong W, He Q, Yang M, Huang L, Kong J, et al. Circular RNA circPICALM Sponges miR-1265 to Inhibit Bladder Cancer Metastasis and Influence FAK Phosphorylation. *EBioMedicine* (2019) 48:316–31. doi: 10.1016/j.ebiom.2019.08.074
82. Zhang L, Xia HB, Zhao CY, Shi L, Ren XL. Cyclic RNA Hsa_Circ_0091017 Inhibits Proliferation, Migration and Invasiveness of Bladder Cancer Cells by Binding to microRNA-589-5p. *Eur Rev Med Pharmacol Sci* (2020) 24(1):86–96. doi: 10.26355/eurrev_202001_19898
83. Bi J, Liu H, Dong W, Xie W, He Q, Cai Z, et al. Circular RNA Circ-ZKSCAN1 Inhibits Bladder Cancer Progression Through miR-1178-3p/P21 Axis and Acts as a Prognostic Factor of Recurrence. *Mol Cancer* (2019) 18(1):133. doi: 10.1186/s12943-019-1060-9
84. Li Y, Zheng F, Xiao X, Xie F, Tao D, Huang C, et al. CircHIPK3 Sponges miR-558 to Suppress Heparanase Expression in Bladder Cancer Cells. *EMBO Rep* (2017) 18(9):1646–59. doi: 10.15252/embr.201643581
85. Liu T, Lu Q, Liu J, Xie S, Feng B, Zhu W, et al. Circular RNA FAM114A2 Suppresses Progression of Bladder Cancer *via* Regulating ΔNP63 by Sponging miR-762. *Cell Death Dis* (2020) 11(1):47. doi: 10.1038/s41419-020-2226-5
86. He Q, Huang L, Yan D, Bi J, Yang M, Huang J, et al. CircPTPRA Acts as a Tumor Suppressor in Bladder Cancer by Sponging miR-636 and Upregulating KLF9. *Aging (Albany NY)* (2019) 11(23):11314–28. doi: 10.18632/aging.102530
87. Su Y, Feng W, Zhong G, Ya Y, Du Z, Shi J, et al. ciRs-6 Upregulates March1 to Suppress Bladder Cancer Growth by Sponging miR-653. *Aging (Albany NY)* (2019) 11(23):11202–23. doi: 10.18632/aging.102525
88. Liu H, Bi J, Dong W, Yang M, Shi J, Jiang N, et al. Invasion-Related Circular RNA Circfndc3b Inhibits Bladder Cancer Progression Through the miR-1178-3p/G3BP2/SRC/FAK Axis. *Mol Cancer* (2018) 17(1):161–. doi: 10.1186/s12943-018-0908-8
89. Liu H, Chen D, Bi J, Han J, Yang M, Dong W, et al. Circular RNA Circubxn7 Represses Cell Growth and Invasion by Sponging miR-1247-3p to Enhance B4GALT3 Expression in Bladder Cancer. *Aging (Albany NY)* (2018) 10 (10):2606–23. doi: 10.18632/aging.101573
90. Sun J, Zhang H, Tao D, Xie F, Liu F, Gu C, et al. CircCDYL Inhibits the Expression of C-MYC to Suppress Cell Growth and Migration in Bladder Cancer. *Artif Cells Nanomed Biotechnol* (2019) 47(1):1349–56. doi: 10.1080/21691401.2019.1596941
91. Su Y, Du Z, Zhong G, Ya Y, Bi J, Shi J, et al. Circ5912 Suppresses Cancer Progression *via* Inducing MET in Bladder Cancer. *Aging (Albany NY)* (2019) 11(23):10826–38. doi: 10.18632/aging.102464
92. Yang C, Mou Z, Zhang Z, Wu S, Zhou Q, Chen Y, et al. Circular RNA RBPMS Inhibits Bladder Cancer Progression *via* miR-330-3p/RAI2 Regulation. *Mol Ther Nucleic Acids* (2021) 23:872–86. doi: 10.1016/j.omtn.2021.01.009
93. Lin G, Sheng H, Xie H, Zheng Q, Shen Y, Shi G, et al. Circlpar1 Is a Novel Biomarker of Prognosis for Muscle-Invasive Bladder Cancer With Invasion and Metastasis by miR-762. *Oncol Lett* (2019) 17(3):3537–47. doi: 10.3892/ol.2019.9970
94. Chi BJ, Zhao DM, Liu L, Yin XZ, Wang FF, Bi S, et al. Downregulation of Hsa_Circ_0000285 Serves as a Prognostic Biomarker for Bladder Cancer and Is Involved in Cisplatin Resistance. *Neoplasma* (2019) 66(2):197–202. doi: 10.4149/neo_2018_180318N185
95. Yuan W, Zhou R, Wang J, Han J, Yang X, Yu H, et al. Circular RNA Cdr1as Sensitizes Bladder Cancer to Cisplatin by Upregulating APAF1 Expression Through miR-1270 Inhibition. *Mol Oncol* (2019) 13(7):1559–76. doi: 10.1002/1878-0261.12523
96. Su H, Tao T, Yang Z, Kang X, Zhang X, Kang D, et al. Circular RNA cTFRC Acts as the Sponge of MicroRNA-107 to Promote Bladder Carcinoma Progression. *Mol Cancer* (2019) 18(1):27. doi: 10.1186/s12943-019-0951-0
97. Najafi S, Ghafouri-Fard S, Hussen BM, Hidayat H, Taheri M, Hallajnejad M. Oncogenic Roles of Small Nucleolar RNA Host Gene 7 (SNHG7) Long Non-Coding RNA in Human Cancers and Potentials. *Front Cell Dev Biol* (2022) 9:809345. doi: 10.3389/fcell.2021.809345.
98. Zhang H-D, Jiang L-H, Sun D-W, Hou J-C, Ji Z-L. CircRNA: A Novel Type of Biomarker for Cancer. *Breast Cancer* (2018) 25(1):1–7. doi: 10.1007/s12282-017-0793-9
99. Li Y, Zheng Q, Bao C, Li S, Guo W, Zhao J, et al. Circular RNA is Enriched and Stable in Exosomes: A Promising Biomarker for Cancer Diagnosis. *Cell Res* (2015) 25(8):981–4. doi: 10.1038/cr.2015.82
100. Sayad A, Najafi S, Kashi AH, Hosseini SJ, Akrami SM, Taheri M, et al. Circular RNAs in Renal Cell Carcinoma: Functions in Tumorigenesis and Diagnostic and Prognostic Potentials. *Pathol-Res Pract* (2022) 229:153720. doi: 10.1016/j.prp.2021.153720

Conflict of Interest: The authors declare that the research was conducted in the absence of any commercial or financial relationships that could be construed as a potential conflict of interest.

frontiers | Frontiers in Oncology

ORIGINAL RESEARCH
published: 19 April 2022
doi: 10.3389/fonc.2022.858865

Head-to-Head Comparison of the Expression Differences of NECTIN-4, TROP-2, and HER2 in Urothelial Carcinoma and Its Histologic Variants

*Yu Fan†, Qinhan Li†, Qi Shen†, Zhifu Liu, Zhenan Zhang, Shuai Hu, Wei Yu, Zhisong He, Qun He and Qian Zhang**

Department of Urology, Peking University First Hospital, Institute of Urology, National Research Center for Genitourinary Oncology, Peking University, Beijing, China

OPEN ACCESS

Edited by:
Bianca Nitzsche, Charité Universitätsmedizin Berlin, Germany

Reviewed by:
Vadim S. Koshkin, University of California San Francisco, United States
Umang Swami, University of Utah, United States

***Correspondence:**
Qian Zhang
zhangqianbjmu@126.com

†These authors have contributed equally to this work

Specialty section:
This article was submitted to Genitourinary Oncology, a section of the journal Frontiers in Oncology

Received: *20 January 2022*
Accepted: *21 March 2022*
Published: *19 April 2022*

Citation:
Fan Y, Li Q, Shen Q, Liu Z, Zhang Z, Hu S, Yu W, He Z, He Q and Zhang Q (2022) Head-to-Head Comparison of the Expression Differences of NECTIN-4, TROP-2, and HER2 in Urothelial Carcinoma and Its Histologic Variants. Front. Oncol. 12:858865. doi: 10.3389/fonc.2022.858865

Background: Antibody–drug conjugates (ADC), such as enfortumab vedotin (EV), sacituzumab govitecan (SG), and RC-48, have shown outstanding response rates to local advanced or metastatic urothelial carcinoma (UC). However, their corresponding target expression characteristics in UC and its histologic variants were unknown.

Methods: We detected the expression of NECTIN-4, TROP-2, and HER2, which are the corresponding targets of ADCs EV, SG, and RC-48 in muscle-invasive UC through immunohistochemistry.

Results: 161 consecutive samples from 2017 to 2021 of muscle-invasive UC and its histologic variants were obtained in Peking University First Hospital. Variant histology types included 72UC, 10 squamous carcinomas, 23 glandular carcinomas, 19 small cell carcinomas, 19 micropapillary variants, and 18 nested variants. NECTIN-4 expression was found to be 57/72 (79.2%), 10/10 (100%), 15/23 (65.2%), 4/19 (21.1%), 15/19 (78.9%), and 16/18 (88.9%) in conventional UC, squamous carcinoma, glandular carcinoma, small cell carcinoma, micropapillary, and nested variant, respectively, compared with 65/72 (90.3%), 8/10 (80.0%), 13/23 (56.5%), 3/19 (15.8%), 16/19 (84.2%), and 15/18 (83.3%) of TROP-2, and 26/72 (36.1%), 0, 5/23 (21.7%), 6/19 (31.6%), 5/19 (26.3%), and 7/18 (38.9%) of HER2.

Keywords: urothelial carcinoma, ADC, nectin-4, Trop-2, HER2, histologic variants

INTRODUCTION

Urothelial carcinoma (UC) is the second most common genitourinary tract cancer, affecting >80,000 new patients and causing >17,000 deaths every year in the United States (1). UC commonly arises from the urinary bladder but also involves the renal pelvis, the ureter, or the urethra. Conventional UC is the most common histologic type and accounts for around 90% of all

UC, and the remaining 10% show different histologic variants such as squamous carcinoma, glandular carcinoma, small cell carcinoma, micropapillary variant, and nested variant (2, 3). Squamous carcinoma is the most common subtype, accounting for 3%–5% of all UC, followed by glandular carcinoma of 1.5% and small cell carcinoma of 0.7% (4). Furthermore, Chinese people are reported to have different clinicopathological characteristics and oncologic outcomes of UC in the United States, with more adverse pathological features (5). However, despite multiple histologic subtypes, UC has been managed similarly. For advanced or metastatic UC, cisplatin-based chemotherapy is the first-line therapy due to its high response rate. For the cisplatin-ineligible patients, carboplatin-based chemotherapy combined with an immune checkpoint inhibitor (ICI) is recommended (6). Recently, antibody–drug conjugates (ADC), the emerging agents that combine a cytotoxic agent with a monoclonal antibody (mAb) as a delivery molecule, have been promising as the new treatment approach for advanced or metastatic UC (7).

The study about ADCs could be dated from the late 1950s, when polyclonal and murine monoclonal antibodies were detected preclinically with conjugates comprising radionuclides, toxin, and drugs (8). However, these first-generation ADCs suffered from immune responses to the xenogeneic antibodies, limiting their clinical application. Recently, second- and third-generation ADCs such as enfortumab vedotin (EV), sacituzumab govitecan (SG), and RC-48, using monoclonal mAbs with better-defined precision targets, combined with more toxic payloads have emerged as a new line of approved ADCs. Enfortumab vedotin (EV), a novel ADC composed of an anti-NECTIN-4 antibody with the microtubule-disrupting cytotoxic agent monomethyl auristatin E (MMAE), binds to cells that express NECTIN-4, a cell adhesion molecule highly expressed in many solid tumors including UC. Then, MMAE is internalized and released into the target cells and impairs the formation of the microtubule network (9, 10). TROP-2 is a transmembrane glycoprotein overexpressed in many solid tumors, including UC, and linked with worse prognosis (11, 12). Sacituzumab govitecan (SG) is an ADC composed of SN-38 conjugated to an anti-Trop-2-humanized mAb, resulting in double-stranded DNA breaks during the mitotic S phase of affected cells (13). HER2 is a growth-promoting tyrosine kinase receptor, whose overexpression, though uncommonly, is highly associated with tumor progression and poor prognosis in UC (14, 15).RC48-ADC is a novel humanized anti-HER2 antibody conjugated with MMAE *via* a cleavable linker, impairing the formation of the microtubule network of target cells (16).

During the immunotherapy era, the PD-L1 expression situation was proven to be an important prognostic factor in both bladder cancer and upper tract urothelial carcinoma undergoing immunotherapy (17–19). Although it is still unknown whether a high expression of the ADC-corresponding targets is linked to a better efficacy, the expression of these proteins is believed to be essential for the response to ADC as it is the port of entry to tumor cells. The expression of NECTIN-4 in the muscle-invasive UC is reported to be 68.2% (20), compared with 8.7% of HER2 (14), and TROP-2 is known to be expressed in normal urothelium and in ≤83% of urothelial carcinoma (21). However, it is unknown whether the protein expression is related to the clinicopathologic features of the patient. The head-to-head comparison regarding the expression differences of these targets in UC and its histologic variants is rare, which could have potential implications in therapeutic strategies. In the present study, we conducted a head-to-head comparison of expression differences of NECTIN-4, TROP-2, and HER2 in muscle-invasive UC and its histologic variants, discussing the possible tendency of ADC choice in different pathologic subtypes of UC.

MATERIALS AND METHODS

161 consecutive samples from 2017 to 2021 of muscle-invasive UC and its histologic divergent types were obtained from the patients who underwent radical cystectomy and radical nephroureterectomy without adjuvant or neoadjuvant therapy before in the Department of Urology, Peking University First Hospital. Variant histology types included 10 squamous carcinomas, 23 glandular carcinomas, 19 small cell carcinomas, 19 micropapillary variants, and 18 nested variants. The histopathology of tumors was graded according to the World Health Organization histologic grading system and staged according to the TNM staging system (22, 23). The slides were reviewed by 3 expert urologic pathologists (QH, QS, and SH), and a representative section was chosen and recut to perform immunohistochemical stains. The study was approved by the ethics committee of Peking University First Hospital.

Moreover, the samples with muscle-invasive bladder cancer (MIBC) of conventional pathological type were grouped into luminal and basal/squamous subtypes based on expressions of GATA3 and KRT5/6 through immunohistochemistry (24, 25). Tissues that were KRT5/6-positive and GATA3-negative were considered of basal-like phenotype, while tissues that were GATA3-positive were deemed of luminal-like phenotype. KRT5/6-positive and GATA3-positive were defined as KRT5/6 2+/3+ and GATA3 2+/3+, respectively.

Immunohistochemistry

The expressions of NECTIN-4, TROP-2, and HER2 were evaluated according to standard immunohistochemistry protocols. Briefly, 4-μm-thick sections from formalin-fixed paraffin-embedded specimens were deparaffinized in xylene, rehydrated in decreasing concentrations of ethanol, and washed in distilled water. Following antigen retrieval with Tris–EDTA buffer, endogenous peroxidase blocking with 3% hydrogen peroxidase was performed. Sections were incubated with 10% normal blocking serum in Tris-buffered saline at room temperature for 20 min. The commercially available primary antibodies used in this study were anti-human NECTIN-4, TROP-2, and HER2 rabbit monoclonal antibodies (1:2000, EPR 15613-68, Abcam, Cambridge, MA, USA; 1:500, EPR20043, Abcam; 1:800, D8F12, CST, Danvers, MA, USA; respectively). After being incubated at 4°C for 16 h, the secondary antibodies were added. Next, the sections were

counterstained with hematoxylin at room temperature for 3 min, dehydrated, and covered with a coverslip. According to the guideline protocol, positive controls were human skin tissue, human placenta tissue, and human urothelial carcinoma tissue for NECTIN-4, TROP-2, and HER2, respectively, and negative controls were UC tissues without primary antibodies.

NECTIN-4 expression was evaluated through the histochemical scoring system (H-score), which is defined as the product of intensity (score, 0–3), and percentage of stained cells (0–100). Then the specimens were classified as negative (0; H-score, 0–14), weak (1+; H-score, 15–99), moderate (2+; H-score, 100–199), and strong (3+; H-score, 200–300) (10). TROP-2 staining results were determined as follows: samples were deemed as positive if >10% tumor cells had membranous staining. Positive expression was scored as weak (+1), moderate (2+), and strong (3+). Tumors were classified as negative if <10% of tumor cells had membranous staining (26). For HER2, the staining scores were assessed according to the HER2 test guideline for breast cancer, and HER2 2+ and 3+ were defined as HER2-positive (16, 27).

Statistics

SPSS software (version 26.0; SPSS, Inc., Chicago, IL, USA) was used for statistical analysis of all data, and $P < 0.05$ was considered as statistical significance. A Venn diagram was made through VENNY 2.1 (28).

RESULTS

The cohort included a total of 161 patients: 141 patients with bladder cancer and 20 patients with upper-tract urothelial carcinoma (ratio: 7.05:1); there were 126 men and 35 women (ratio 3.6: 1). The average age at diagnosis was 67.1 years (range 37 to 91 y) (**Table 1**). The samples were grouped based on the presence of divergent differentiation of pathological components into UC (n = 72); squamous carcinoma (n = 10); glandular (n = 23); small cell carcinoma (n = 19); micropapillary (n = 19); and nested (n = 18). Immunohistochemical results of NECTIN-4, TROP-2, and HER2 in different pathological types of UC are shown in **Figure 1** and **Supplementary 1**. Overall, the expressions of NECTIN-4, TROP-2, and HER2 were associated with histologic subtypes, but not to age, year, gender, tumor diameter, tumor location, and TNM grade (**Supplementary 2**).

Urothelial Carcinoma

Overall, 57/72 (79.2%), 65/72 (90.3%), and 26/72 (36.1%) of UCs were positive for NECTIN-4, TROP-2, and HER2, respectively (**Figure 2**). 18 of 72 tissues (25.0%) were positive for all three targets, and 1 of 72 tissues (1.4%) was negative for the three. 52/72 (72.2%) were positive for both TROP-2 and NECTIN-4, 23/72 (31.9%) for both HER2 and TROP-2, and 20/72 (27.8%) for both HER2 and NECTIN-4 (**Figure 1B**). After being grouped by molecular classification, 53 luminal subtypes and 8 basal/squamous subtypes were obtained. The positive rates of NECTIN-4, TROP-2, and HER2 were 41/53 (77.35%), 47/53 (88.7%), and 23/53 (43.4%) in luminal subtypes, and 7/8 (87.5%), 8/8, and 0/6 in basal/squamous subtypes, respectively (**Figures 1C, D**).

Squamous Carcinoma

There were 10 samples with at least 50% of the tumor displaying squamous differentiation, defined histologically by the presence of intracellular bridges or keratin (29). 10/10 (100%) for NECTIN-4, 8/10 (80%) for TROP-2, and 0/10 (0) for HER2 were positive, respectively (**Figures 1B**, **3**).

TABLE 1 | Clinicopathologic characteristics of patients enrolled.

Clinicopathological features	Conventional UC (N = 72)	Squamous carcinoma (N = 10)	Glandular carcinoma (N = 23)	Small cell carcinoma (N = 19)	Nested variants (N = 18)	Micropapillary variants (N = 19)
Age, years (SD, range)	69.89 (8.14, 52–72)	70.5 (13.68, 40–84)	53.87 (11.93, 37–82)	72.05 (10.75, 52–91)	65.61 (7.48, 54–82)	67.26 (7.98, 53–82)
Gender, n (%)						
M	57 (79.2)	7 (70.0)	17 (73.9)	15 (78.9)	14 (77.8)	16 (84.2)
F	15 (20.8)	3 (30.0)	6 (26.1)	4 (21.1)	4 (22.2)	3 (15.8)
Tumor diameters, cm (SD, range)	3.27 (1.40, 1.0–9.0)	5.32 (3.15, 1.5–12.0)	3.71 (2.70, 1.0–14.0)	4.56 (3.16, 1.2–12.0)	3.76 (1.61, 1.5–7.0)	3.30 (1.54. 1.2–6.0)
Tumor site (%)						
Bladder cancer	61 (84.7)	9 (90.0)	21 (91.3)	17 (89.5)	17 (94.4)	16 (84.2)
Upper-tract urothelial carcinoma	11 (15.3)	1 (10.0)	2 (8.7)	2 (10.5)	1 (5.6)	3 (15.8)
T-stage distribution (%)						
T2	30 (41.7)	2 (20.0)	11 (47.8)	4 (21.1)	9 (50.0)	5 (26.3)
T3	29 (40.3)	5 (50.0)	11 (47.8)	14 (73.7)	8 (44.4)	6 (31.6)
T4	13 (18.1)	3 (30.0)	1 (4.3)	1 (5.3)	1 (5.6)	8 (42.1)
Lymph node metastasis (%)						
N0	61 (84.7)	6 (60.0)	18 (78.3)	14 (73.7)	14 (77.8)	10 (52.6)
N1	4 (5.6)	1 (10.0)	2 (8.7)	2 (10.5)	3 (16.8)	3 (15.8)
N2	7 (9.7)	3 (30.0)	3 (13)	3 (15.8)	1 (5.6)	6 (31.6)

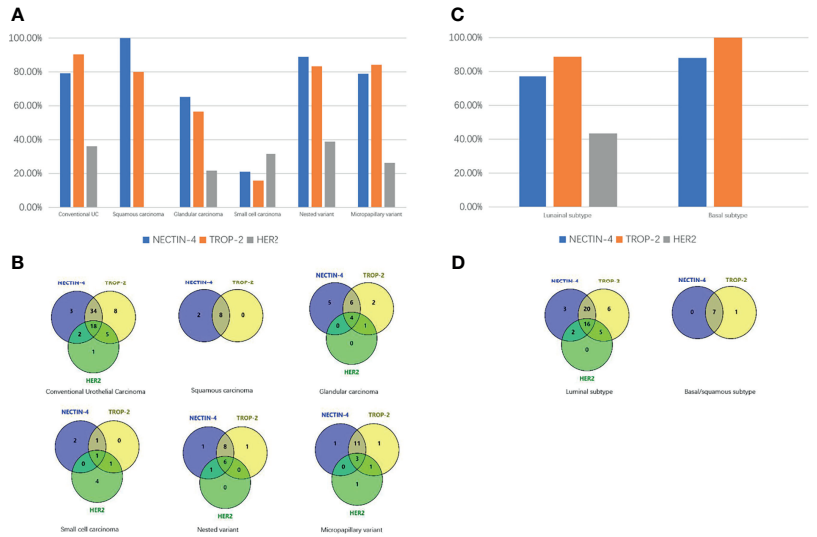

FIGURE 1 | Expression differences of NECTIN-4, TROP-2, and HER2 in different pathologic types of UC. **(A)** Expression differences of HER2, TROP-2, and NECTIN-4 in conventional UC and histologic variants. **(B)** Venn diagram of positive expression distribution of NECTIN-4, TROP-2, and HER2 in conventional UC and histologic variants. **(C)** Expression differences of NECTIN-4, TROP-2, and HER2 in luminal and basal/squamous subtype. **(D)** Venn diagram of positive expression distribution of NECTIN-4, TROP-2, and HER2 in luminal and basal/squamous subtype.

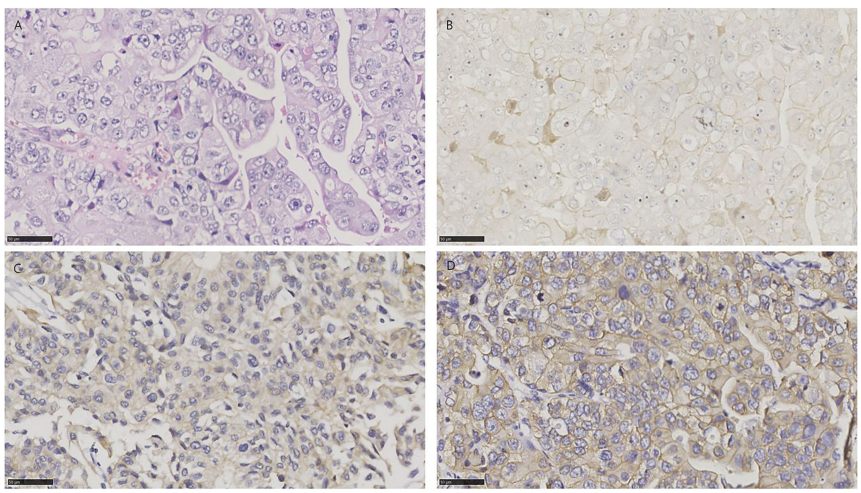

FIGURE 2 | HE and immunohistochemistry for NECTIN-4, TROP-2, and HER2 in conventional urothelial carcinoma. Scale bar: 50 μm. **(A)** HE-stained section of conventional urothelial carcinoma. **(B)** Immunohistochemistry for NECTIN-4 in the same tumor showing moderate staining. **(C)** Immunohistochemistry for TROP-2 in the same tumor showing strong staining. **(D)** Immunohistochemistry for HER2 in the same tumor showing strong staining.

Glandular Carcinoma

Glandular differentiation is histologically characterized by the presence of glandular spaces within the urothelial tumor (30). In all 23 specimens, 13/23 (56.5%) for NECTIN-4, 16/23 (69.5%) for TROP-2, and 5/23 (21.7%) for HER2 were positive, respectively. 4 of 23 tissues (17.4%) were positive for all three targets, and 5 of 23 tissues (21.7%) were negative for the three. 10/23 (43.5%) were positive for both TROP-2 and NECTIN-4, 5/23 (21.7%) for both HER2 and TROP-2, and 4/23 (17.4%) for both HER2 and NECTIN-4 (**Figure 1B**). The clinicopathologic characteristics of samples with three negative ADC targets and samples with at least one positive target are shown in **Supplementary 3**.

Small Cell Carcinoma

There were 19 specimens of small cell carcinoma, characterized by pathological features of spindle cells with scant cytoplasm and

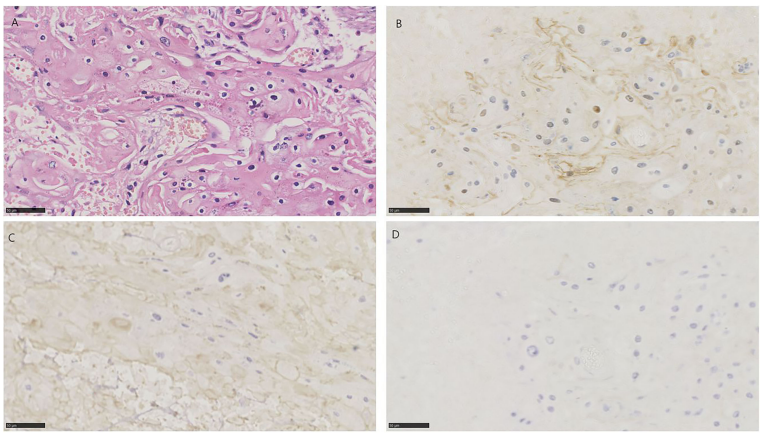

FIGURE 3 | HE and immunohistochemistry for NECTIN-4, TROP-2, and HER2 in urothelial carcinoma with squamous differentiation. Scale bar: 50 μm. **(A)** HE-stained section of urothelial carcinoma with squamous differentiation. **(B)** Immunohistochemistry for NECTIN-4 in the same tumor showing moderate staining. **(C)** Immunohistochemistry for TROP-2 in the same tumor showing moderate staining. **(D)** Immunohistochemistry for HER2 in the same tumor showing negative.

hyperchromatic nuclei with "salt and pepper" chromatin (31). 4/19 (21.1%) for NECTIN-4, 3/19 (15.8%) for TROP-2, and 6/19 (31.6%) for HER2 were positive, respectively (**Figure 4**). Only 1 of 19 tissues (5.3%) was positive for all three targets, and 10 of 19 tissues (52.6%) were negative for the three. 2/19 (10.5%) were positive for both TROP-2 and NECTIN-4, 2/19 (10.5%) for both HER2 and TROP-2, and 1/19 (5.3%) for both HER2 and NECTIN-4 (**Figure 1B**). The clinicopathologic characteristics of samples with three negative ADC targets and samples with at least one positive target are shown in **Supplementary 4**.

Nested Variant

All 18 cases of nested urothelial carcinoma were detected, which are defined as bland nests of urothelial carcinoma [17]. 16/18 (88.9%) for NECTIN-4, 15/18 (83.3%) for TROP-2, and 7/18 (38.9%) for HER2 were positive, respectively (**Figure 5**). 6 of 18 tissues (33.3%) were positive for all three targets, and 1 of 18 tissues (5.6%) was negative for the three. 14/18 (77.8%) were positive for both TROP-2 and NECTIN-4, 6/18 (33.3%) for both HER2 and TROP-2, and 7/18 (38.9%) for both HER2 and NECTIN-4 (**Figure 1B**).

Micropapillary Variant

A micropapillary variant was diagnosed by the presence of multiple nests of tumor within a single lacuna demonstrating small branching papillae or tufts without fibrovascular cores (32). In all 19 specimens, 15/19 (78.9%) for NECTIN-4, 16/19

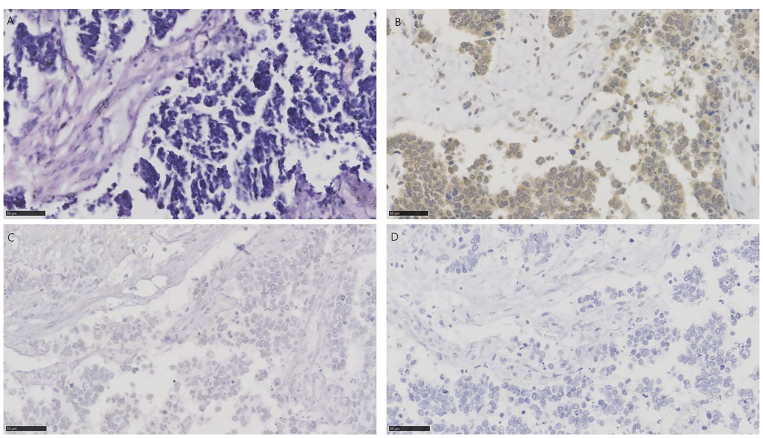

FIGURE 4 | HE and immunohistochemistry for NECTIN-4, TROP-2, and HER2 in urothelial carcinoma with small cell carcinoma. Scale bar: 50 μm. **(A)** HE-stained section of urothelial carcinoma with small cell carcinoma. **(B)** Immunohistochemistry for NECTIN-4 in the same tumor showing moderate staining. **(C)** Immunohistochemistry for TROP-2 in the same tumor showing negative. **(D)** Immunohistochemistry for HER2 in the same tumor showing negative.

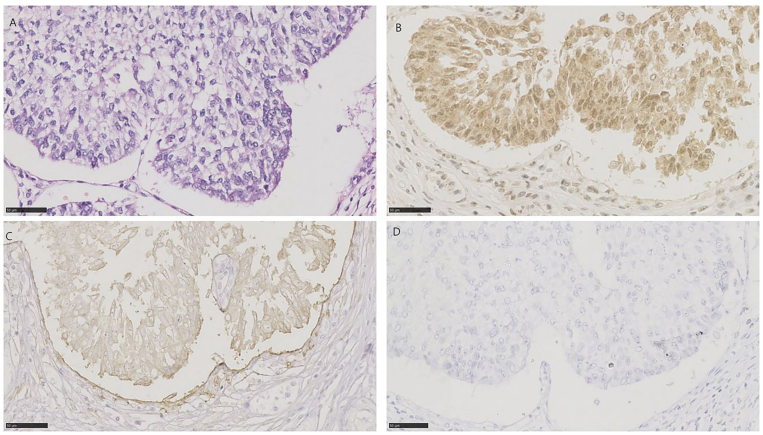

FIGURE 5 | HE and immunohistochemistry for NECTIN-4, TROP-2, and HER2 in nested urothelial carcinoma. Scale bar: 50 μm. **(A)** HE-stained section of nested urothelial carcinoma. **(B)** Immunohistochemistry for NECTIN-4 in the same tumor showing strong staining. **(C)** Immunohistochemistry for TROP-2 in the same tumor showing moderate staining. **(D)** Immunohistochemistry for HER2 in the same tumor showing negative.

(84.2%) for TROP-2, and 5/19 (26.3%) for HER2 were positive, respectively (**Figure 6**). 3 of 19 tissues (15.8%) were positive for all three targets, and 1 of 19 tissues (5.3%) was negative for the three. 14/19 (73.7%) were positive for both TROP-2 and NECTIN-4, 4/19 (21.1%) for both HER2 and TROP-2, and 3/19 (15.8%) for both HER2 and NECTIN-4 (**Figure 1B**).

DISCUSSION

Locally advanced and metastatic urothelial carcinoma often has a poor prognosis, with a median survival chemotherapy of approximately 13 to 15 months (33). The first-line treatment has been cisplatin-based cytotoxic chemotherapy for decades. In cisplatin-ineligible patients, carboplatin is an inferior alternative with a relatively worse objective response rate and median overall survival (34). The appearance of ADC represents a promising therapeutic approach for advanced patients or cisplatin-and carboplatin-ineligible patients. This novel technology targets surface proteins highly enriched in tumor to improve the delivery of cytotoxic molecules to tumor cells and reduce off-tumor toxicity. Three ADCs presented high activity in pretreated local advanced and metastatic UC, namely, EV, SG, and RC-48, targeting at the proteins of NECTIN-4, TROP-2, and HER2, respectively. Cells expressing these transmembrane proteins internalize them through endocytosis, resulting in the delivery and release of

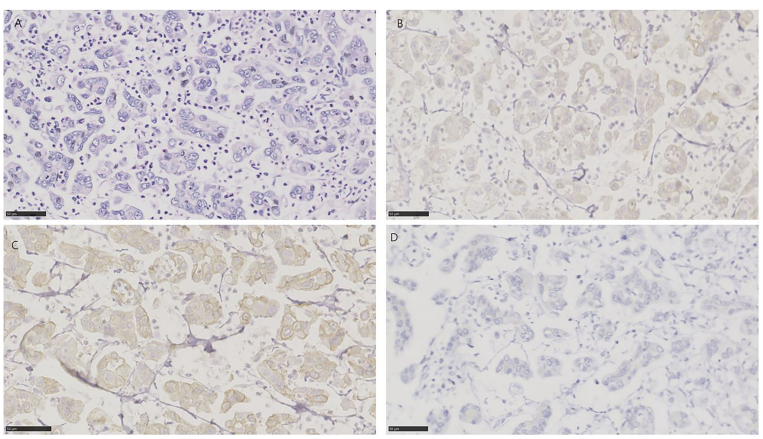

FIGURE 6 | HE and immunohistochemistry for HER2, TROP-2, and NECTIN-4 in micropapillary urothelial carcinoma. Scale bar: 50 μm. **(A)** HE-stained section of micropapillary urothelial carcinoma. **(B)** Immunohistochemistry for NECTIN-4 in the same tumor showing weak staining. **(C)** Immunohistochemistry for TROP-2 in same tumor showing moderate staining. **(D)** Immunohistochemistry for HER2 in the same tumor showing negative.

cytotoxic payload (35). So far, while EV and SG are FDA-approved in locally advanced and metastatic UC, RC-48 is still in clinical trials, although it has shown promising activity.

The expression of corresponding antigens on tumor is essential for appropriate functional delivery of the ADCs as it is the port of entry to tumor cells. However, except for the requirement for HER2-positive in RC-48 treatment, there is no requirement for testing the expressions of NECTIN-4 and TROP-2 in EV and SG treatment (16, 36, 37). In the phase 1 trial of EV, NECTIN-4 expression using an anti NECTIN-4 antibody clone was initially a protocol requirement, which was later removed due to high NECTIN-4 expression in most UC samples. However, these high expression rates are generally based on the UC. After being classified by histologic subtypes, the expression differences of these proteins were unknown.

So far, UC has been treated similarly regardless of its histologic subtypes, which mainly owes to the similar survival outcomes of most histologic variants (38). However, studies have shown that some histologic variants, such as squamous carcinoma and small cell carcinoma, have worse prognosis than UC and have a poorer response to standard chemotherapy (MVAC—methotrexate, vinblastine, doxorubicin, and cisplatin, or GC–gemcitabine and cisplatin) (39, 40), while other variants, such as urachal glandular carcinoma, have superior survival outcome and could be managed more conservatively (41). These suggest that UC should be managed selectively and individually according to its histologic features.

In this study, we confirmed that NECTIN-4 and TROP-2 were highly expressed in UC, while HER2 amplification was relatively low, which is consistent with the former clinical trials. Only 1.4% of conventional UCs were negative for the three targets, indicating that the majority of patients could benefit from the ADC therapy. Chu et al. reported that NECTIN-4 is enriched in luminal subtypes of muscle-invasive bladder cancer than in basal/squamous subtypes (42). In our study, the positive rate of NECTIN-4 in luminal subtypes and basal/squamous subtypes was 41/53 (77.35%) and 7/8 (87.5%), respectively. The difference was not statistically significant ($P = 0.584$). This may be due to the small number of basal/squamous subtypes. For histologic variants, we demonstrated that 0%, 21.7%, 52.6%, 5.6%, and 5.3% of squamous carcinoma, glandular carcinoma, small cell carcinoma, nested variant, and micropapillary variant were negative for the three targets, respectively, suggesting that therapeutic strategies for these subtypes should be made individually. HER2 expression was hardly in both histologic and molecular classifications of the squamous subtype, while TROP-2 and NECTIN-4 were expressed commonly, implying that these patients might benefit more from SG and NE rather than from RC-48. On the contrary, the expression levels of TROP-2 and NECTIN-4 decreased in small cell carcinoma, even being exceeded by that of HER2. Therefore, testing the expression of ADC targets should be considered before treatment and RC-48 may be the better choice for these patients. Furthermore, nested and micropapillary variants, whose survival outcomes and target distributions are similar to UC, are recommended to be managed as UC of the same stage (38).

In addition, these ADCs are unlikely to be cross-resistant as they carry different cytotoxic agents and target different antigens. Therefore, combination or sequence therapy may become the novel approach due to their controllable toxicity. Our study found respectively 72.2%, 90%, 43.5%, 77.8%, and 73.7% of UC, squamous carcinoma, glandular carcinoma, nested variant, and micropapillary variant expressing both TROP-2 and NECTIN-4, while 10.5% of small cell carcinoma, which may have some implications for combination and sequence therapies.

Currently, these ADCs are only recommended in second- or third-line therapy of local advanced and metastatic UC, so the expression situation of their targets could be to some extent ignored as the therapy approaches for the advanced stage are limited. Clinical trials about their application in neoadjuvant therapy of UC are in progress (43, 44). For the early stage, the expression situation of corresponding targets may play an important role in the choice of ACD therapy.

The primary limitation in our study is the lack of relation with therapy outcomes.

Our study only focuses on the head-to head comparison of expression differences of ADC targets, not involved in therapy efficacy. For histologic variants, the therapy efficacy dose depends not only on the expression of corresponding targets but also on the effect of conjugated cytotoxic agents. For example, SN-38, the conjugated cytotoxic payload of SG and the active component of irinotecan, showed efficacy only in colorectal, pancreatic, and lung cancer before (45). Therefore, it is not clear whether SG could achieve desired therapy outcomes in UC even if these histologic subtypes highly express TROP-2. However, the expression of corresponding targets could be seen as the basics of response to ADCs as it is the port of cellular entry for the cytotoxic drug component. Second, we detected target expression only through immunohistochemistry, which was not affirmed by other methods, such as FISH, RNA sequencing, or Western blot. Third, it was a retrospective study with a relatively small sample. These limitations should be addressed in future studies. In addition, samples in our study were from muscle-invasive tumors. Therefore, it is unclear to what extent this applies to metastatic samples.

CONCLUSION

In summary, through a head-to-head comparison of expression differences of NECTIN-4, TROP-2, and HER2 in UC and its histologic variants, we provided evidence for therapeutic strategies for UC in an upcoming ADC ear. We demonstrate that the majority of UC and its histologic variant expressed at least one ADC target, suggesting that ADC is a candidate approach for UC therapy. However, different targets are expressed disparately in different histologic subtypes. Specific intervention strategies should be conducted individually according to the histologic subtypes.

DATA AVAILABILITY STATEMENT

The raw data supporting the conclusions of this article will be made available by the authors, without undue reservation.

AUTHOR CONTRIBUTIONS

QZ and YF contributed to the conception of the study. QL, ZL, QS, SH, and QH performed the experiment. YG, QL, and ZZ contributed significantly to analysis and manuscript preparation. YF and QL performed the data analyses and wrote the manuscript. WY and ZH helped perform the analysis with constructive discussions. All authors contributed to the article and approved the submitted version.

FUNDING

This work was supported by grants from the National Natural Science Foundation of China to Q.Z. (No.82072826) and Special Project of "Group Medical Assistance Project" of Tibet Autonomous Region Health Committee (Grant No. XZ2019ZR-ZY16(Z)).

SUPPLEMENTARY MATERIAL

The Supplementary Material for this article can be found online at: https://www.frontiersin.org/articles/10.3389/fonc.2022.858865/full#supplementary-material

REFERENCES

1. Siegel RL, Miller KD, Jemal A. Cancer Statistics 2020. *CA Cancer J Clin* (2020) 70(1):7–30. doi: 10.3322/caac.21590
2. Amin MB, Smith SC, Reuter VE, Epstein JI, Grignon DJ, Hansel DE, et al. Update for the Practicing Pathologist: The International Consultation On Urologic Disease-European Association of Urology Consultation on Bladder Cancer. *Mod Pathol* (2015) 28(5):612–30. doi: 10.1038/modpathol.2014.158
3. Ploeg M, Aben KK, Hulsbergen-van de Kaa CA, Schoenberg MP, Witjes JA, Kiemeney LA. Clinical Epidemiology of Nonurothelial Bladder Cancer: Analysis of the Netherlands Cancer Registry. *J Urol* (2010) 183(3):915–20. doi: 10.1016/j.juro.2009.11.018
4. Wucherpfennig S, Rose M, Maurer A, Cassataro MA, Seillier L, Morsch R, et al. Evaluation of Therapeutic Targets in Histological Subtypes of Bladder Cancer. *Int J Mol Sci* (2021) 22(21):11547. doi: 10.3390/ijms222111547
5. Singla N, Fang D, Su X, Bao Z, Cao Z, Jafri SM, et al. A Multi-Institutional Comparison of Clinicopathological Characteristics and Oncologic Outcomes of Upper Tract Urothelial Carcinoma in China and the United States. *J Urol* (2017) 197(5):1208–13. doi: 10.1016/j.juro.2016.11.094
6. *NCCN Guidelines Version 6.2020 Bladder Cancer*. Available at: https://www.nccn.org/professionals/physician_gls/pdf/bladder.pdf (Accessed july 16).
7. Sarfaty M, Rosenberg JE. Antibody-Drug Conjugates in Urothelial Carcinomas. *Curr Oncol Rep* (2020) 22(2):13. doi: 10.1007/s11912-020-0879-y
8. Goldenberg DM, Sharkey RM. Sacituzumab Govitecan, a Novel, Third-Generation, Antibody-Drug Conjugate (ADC) for Cancer Therapy. *Expert Opin Biol Ther* (2020) 20(8):871–85. doi: 10.1080/14712598.2020.1757067
9. Samanta D, Almo SC. Nectin Family of Cell-Adhesion Molecules: Structural and Molecular Aspects of Function and Specificity. *Cell Mol Life Sci* (2015) 72 (4):645–58. doi: 10.1007/s00018-014-1763-4
10. Challita-Eid PM, Satpayev D, Yang P, An Z, Morrison K, Shostak Y, et al. Enfortumab Vedotin Antibody-Drug Conjugate Targeting Nectin-4 Is a Highly Potent Therapeutic Agent in Multiple Preclinical Cancer Models. *Cancer Res* (2016) 76(10):3003–13. doi: 10.1158/0008-5472.Can-15-1313
11. Cubas R, Zhang S, Li M, Chen C, Yao Q. Trop2 Expression Contributes to Tumor Pathogenesis by Activating the ERK MAPK Pathway. *Mol Cancer* (2010) 9:253. doi: 10.1186/1476-4598-9-253
12. Avellini C, Licini C, Lazzarini R, Gesuita R, Guerra E, Tossetta G, et al. The Trophoblast Cell Surface Antigen 2 and miR-125b Axis in Urothelial Bladder Cancer. *Oncotarget* (2017) 8(35):58642–53. doi: 10.18632/oncotarget.17407
13. Goldenberg DM, Sharkey RM. Antibody-Drug Conjugates Targeting TROP-2 and Incorporating SN-38: A Case Study of Anti-TROP-2 Sacituzumab Govitecan. *MAbs* (2019) 11(6):987–95. doi: 10.1080/19420862.2019.1632115
14. Fleischmann A, Rotzer D, Seiler R, Studer UE, Thalmann GN. Her2 Amplification Is Significantly More Frequent in Lymph Node Metastases From Urothelial Bladder Cancer Than in the Primary Tumours. *Eur Urol* (2011) 60(2):350–7. doi: 10.1016/j.eururo.2011.05.035
15. Jimenez RE, Hussain M, Bianco FJJr., Vaishampayan U, Tabazcka P, Sakr WA, et al. Her-2/Neu Overexpression in Muscle-Invasive Urothelial Carcinoma of the Bladder: Prognostic Significance and Comparative Analysis in Primary and Metastatic Tumors. *Clin Cancer Res* (2001) 7 (8):2440–7.
16. Sheng X, Yan X, Wang L, Shi Y, Yao X, Luo H, et al. Open-Label, Multicenter, Phase II Study of RC48-ADC, A HER2-Targeting Antibody-Drug Conjugate, in Patients With Locally Advanced or Metastatic Urothelial Carcinoma. *Clin Cancer Res* (2021) 27(1):43–51. doi: 10.1158/1078-0432.Ccr-20-2488
17. Zhang B, Yu W, Feng X, Zhao Z, Fan Y, Meng Y, et al. Prognostic Significance of PD-L1 Expression on Tumor Cells and Tumor-Infiltrating Mononuclear Cells in Upper Tract Urothelial Carcinoma. *Med Oncol* (2017) 34(5):94. doi: 10.1007/s12032-017-0941-2
18. Liu Z, Meng Y, Cao Y, Chen Y, Fan Y, Li S, et al. Expression and Prognostic Value of PD-L1 in Non-Schistosoma-Associated Urinary Bladder Squamous Cell Carcinoma. *Transl Androl Urol* (2020) 9(2):428–36. doi: 10.21037/tau.2020.02.12
19. Ghate K, Amir E, Kuksis M, Hernandez-Barajas D, Rodriguez-Romo L, Booth CM, et al. PD-L1 Expression and Clinical Outcomes in Patients With Advanced Urothelial Carcinoma Treated With Checkpoint Inhibitors: A Meta-Analysis. *Cancer Treat Rev* (2019) 76:51–6. doi: 10.1016/j.ctrv.2019.05.002
20. Hoffman-Censits JH, Lombardo KA, Parimi V, Kamanda S, Choi W, Hahn NM, et al. Expression of Nectin-4 in Bladder Urothelial Carcinoma, in Morphologic Variants, and Nonurothelial Histotypes. *Appl Immunohistochem Mol Morphol* (2021) 29(8):619–25. doi: 10.1097/pai.0000000000000938
21. Faltas B, Goldenberg DM, Ocean AJ, Govindan SV, Wilhelm F, Sharkey RM, et al. Sacituzumab Govitecan, a Novel Antibody–Drug Conjugate, in Patients With Metastatic Platinum-Resistant Urothelial Carcinoma. *Clin Genitourin Cancer* (2016) 14(1):e75–9. doi: 10.1016/j.clgc.2015.10.002
22. Ulbright TM, Amin MB, Balzer B, Berney DM, Epstein JI, Guo C, et al. *WHO Classification of Tumours of the Urinary System and Male Genital Organs*. Lyon, France: International Agency for Research on Cancer (2016).
23. Sobin LH, Gospodarowicz MK, Wittekind C. *TNM Classification of Malignant Tumours, 7th Edition*. Chichester, UK: Wiley-Blackwell (2009).
24. Guo CC, Bondaruk J, Yao H, Wang Z, Zhang L, Lee S, et al. Assessment of Luminal and Basal Phenotypes in Bladder Cancer. *Sci Rep* (2020) 10(1):9743. doi: 10.1038/s41598-020-66747-7
25. Dadhania V, Zhang M, Zhang L, Bondaruk J, Majewski T, Siefker-Radtke A, et al. Meta-Analysis of the Luminal and Basal Subtypes of Bladder Cancer and the Identification of Signature Immunohistochemical Markers for Clinical Use. *EBioMedicine* (2016) 12:105–17. doi: 10.1016/j.ebiom.2016.08.036
26. Bednova O, Leyton JV. Targeted Molecular Therapeutics for Bladder Cancer-A New Option Beyond the Mixed Fortunes of Immune Checkpoint Inhibitors? *Int J Mol Sci* (2020) 21(19):7268. doi: 10.3390/ijms21197268
27. Wolff AC, Hammond ME, Hicks DG, Dowsett M, McShane LM, Allison KH, et al. Recommendations for Human Epidermal Growth Factor Receptor 2 Testing in Breast Cancer: American Society of Clinical Oncology/College of American Pathologists Clinical Practice Guideline Update. *J Clin Oncol* (2013) 31(31):3997–4013. doi: 10.1200/JCO.2013.50.9984

28. Oliveros JC. *Venny. An Interactive Tool for Comparing Lists With Venn's Diagrams* (2007-2015). Available at: https://bioinfogp.cnb.csic.es/tools/venny/index.html.
29. Lopez-Beltran A, Henriques V, Montironi R, Cimadamore A, Raspollini MR, Cheng L. Variants and New Entities of Bladder Cancer. *Histopathology* (2019) 74(1):77–96. doi: 10.1111/his.13752
30. Sfakianos JP, Gul Z, Shariat SF, Matin SF, Daneshmand S, Plimack E, et al. Genetic Differences Between Bladder and Upper Urinary Tract Carcinoma: Implications for Therapy. *Eur Urol Oncol* (2021) 4(2):170–9. doi: 10.1016/j.euo.2020.12.007
31. Fahed E, Hansel DE, Raghavan D, Quinn DI, Dorff TB. Small Cell Bladder Cancer: Biology and Management. *Semin Oncol* (2012) 39(5):615–8. doi: 10.1053/j.seminoncol.2012.08.009
32. Hui Y, Lombardo KA, Quddus MR, Matoso A. Cell Polarity Reversal Distinguishes True Micropapillary Growth From Retraction Artifact in Invasive Urothelial Carcinoma. *Appl Immunohistochem Mol Morphol* (2018) 26(1):e1–6. doi: 10.1097/PAI.0000000000000566
33. Nakagawa T, Taguchi S, Kanatani A, Kawai T, Ikeda M, Urakami S, et al. Oncologic Outcome of Metastasectomy for Urothelial Carcinoma: Who Is the Best Candidate? *Ann Surg Oncol* (2017) 24(9):2794–800. doi: 10.1245/s10434-017-5970-8
34. Freshwater T, Li H, Valiathan C, Li M, Perini R, Bracco OL, et al. Systematic Literature Review and Meta-Analysis of Response to First-Line Therapies for Advanced/Metastatic Urothelial Cancer Patients Who Are Cisplatin Ineligible. *Am J Clin Oncol* (2019) 42(10):802–9. doi: 10.1097/COC.0000000000000585
35. Chau CH, Steeg PS, Figg WD. Antibody-Drug Conjugates for Cancer. *Lancet* (2019) 394(10200):793–804. doi: 10.1016/S0140-6736(19)31774-X
36. Powles T, Rosenberg JE, Sonpavde GP, Loriot Y, DurÃ¡n I, Lee JL, et al. Enfortumab Vedotin in Previously Treated Advanced Urothelial Carcinoma. *N Engl J Med* (2021) 384(12):1125–35. doi: 10.1056/NEJMoa2035807
37. Tagawa ST, Balar AV, Petrylak DP, Kalebasty AR, Loriot Y, FlÃ©chon A, et al. TROPHY-U-01: A Phase II Open-Label Study of Sacituzumab Govitecan in Patients With Metastatic Urothelial Carcinoma Progressing After Platinum-Based Chemotherapy and Checkpoint Inhibitors. *J Clin Oncol* (2021) 39(22):2474–85. doi: 10.1200/jco.20.03489
38. Lobo N, Shariat SF, Guo CC, Fernandez MI, Kassouf W, Choudhury A, et al. What Is the Significance of Variant Histology in Urothelial Carcinoma? *Eur Urol Focus* (2020) 6(4):653–63. doi: 10.1016/j.euf.2019.09.003
39. Minato A, Fujimoto N, Kubo T. Squamous Differentiation Predicts Poor Response to Cisplatin-Based Chemotherapy and Unfavorable Prognosis in Urothelial Carcinoma of the Urinary Bladder. *Clin Genitourin Cancer* (2017) 15(6):e1063–7. doi: 10.1016/j.clgc.2017.07.008
40. Lim JH, Sundar S. Prognosis of Early Stage Small Cell Bladder Cancer Is Not Always Dismal. *ESMO Open* (2019) 4(6):e000559. doi: 10.1136/esmoopen-2019-000559
41. Dutta R, Abdelhalim A, Martin JW, Vernez SL, Faltas B, Lotan Y, et al. Effect of Tumor Location on Survival in Urinary Bladder Adenocarcinoma: A Population-Based Analysis. *Urol Oncol* (2016) 34(12):531.e1–6. doi: 10.1016/j.urolonc.2016.06.009
42. Chu CE, Sjostrom M, Egusa EA, Gibb EA, Badura ML, Zhu J, et al. Heterogeneity in NECTIN4 Expression Across Molecular Subtypes of Urothelial Cancer Mediates Sensitivity to Enfortumab Vedotin. *Clin Cancer Res* (2021) 27(18):5123–30. doi: 10.1158/1078-0432.Ccr-20-4175
43. Fang D, Kitamura H. Cancer Stem Cells and Epithelial-Mesenchymal Transition in Urothelial Carcinoma: Possible Pathways and Potential Therapeutic Approaches. *Int J Urol* (2018) 25(1):7–17. doi: 10.1111/iju.13404
44. *US National Library of Medicine*. ClinicalTrials.gov. Available at: https://clinicaltrials.gov/ct2/show/NCT03924895.
45. de Man FM, Goey AKL, van Schaik RHN, Mathijssen RHJ, Bins S. Individualization of Irinotecan Treatment: A Review of Pharmacokinetics, Pharmacodynamics, and Pharmacogenetics. *Clin Pharmacokinet* (2018) 57(10):1229–54. doi: 10.1007/s40262-018-0644-7

Conflict of Interest: The authors declare that the research was conducted in the absence of any commercial or financial relationships that could be construed as a potential conflict of interest.

Publisher's Note: All claims expressed in this article are solely those of the authors and do not necessarily represent those of their affiliated organizations, or those of the publisher, the editors and the reviewers. Any product that may be evaluated in this article, or claim that may be made by its manufacturer, is not guaranteed or endorsed by the publisher.

frontiers | Frontiers in Oncology

REVIEW
published: 20 May 2022
doi: 10.3389/fonc.2022.879391

Prevention and Treatment of Side Effects of Immunotherapy for Bladder Cancer

Kecheng Lou[1,2†], *Shangzhi Feng*[1,2†], *Guoxi Zhang*[2,3,4], *Junrong Zou*[2,3,4*] *and Xiaofeng Zou*[2,3,4*]

[1] The First Clinical College, Gannan Medical University, Ganzhou, China, [2] Department of Urology, The First Affiliated Hospital of Gannan Medical University, Ganzhou, China, [3] Institute of Urology, The First Affiliated Hospital of Gannan Medical University, Ganzhou, China, [4] Jiangxi Engineering Technology Research Center of Calculi Prevention, Gannan Medical University, Ganzhou, Jiangxi, China

Bladder cancer (BC) is one of the most important tumors of the genitourinary system, associated with high morbidity and mortality rates. Over the years, various antitumor treatments have been developed, and immunotherapy is one of the most effective methods. Immunotherapy aims to activate the body's immune system to kill cancer cells. It has been established that immunotherapy drugs can be classified into "non-targeted" and "targeted" drugs depending on their site of action. Immunotherapy is reportedly effective for BC. Even though it can attack cancer cells, it can also cause the immune system to attack healthy cells, which can occur at any time during treatment and sometimes even after immunotherapy is stopped. Importantly, different types of immunotherapies can cause different side effects. Side effects may manifest themselves as signs or as symptoms. The prevention and treatment of side effects caused by immunotherapy is an important part of cancer patient management.

Keywords: bladder cancer, immunotherapy, immune checkpoints, immune-related adverse events, targeted immunotherapy

OPEN ACCESS

Edited by:
Bianca Nitzsche, Charité Universitätsmedizin Berlin, Germany

Reviewed by:
Aqeel Ahmad, Chinese Academy of Sciences (CAS), China
Ali Akgül, Siirt University, Turkey

***Correspondence:**
Junrong Zou
ydzjr@gmu.edu.cn
Xiaofeng Zou
gyfyurology@yeah.net

[†]*These authors have contributed equally to this work and share first authorship*

Specialty section:
This article was submitted to Genitourinary Oncology, a section of the journal Frontiers in Oncology

Received: *19 February 2022*
Accepted: *19 April 2022*
Published: *20 May 2022*

Citation:
Lou K, Feng S, Zhang G, Zou J and Zou X (2022) Prevention and Treatment of Side Effects of Immunotherapy for Bladder Cancer. Front. Oncol. 12:879391. doi: 10.3389/fonc.2022.879391

INTRODUCTION

BC is among the top ten most common cancer types in the world, according to an observatory in 2018, with approximately 55000 new cases and 200000 deaths annually (1). It ranks tenth in worldwide absolute incidence: sixth in men and seventeenth in women (2). The worldwide Age Standardized Incidence Rate per year (ASR) is 9.6 per 100000 for males and 2.4 per 100000 for females (3).

Smoking is the most significant risk factor of BC, associated with 50-65% of male cases and 20-30% of female cases. The incidence of BC is reportedly directly associated with the duration of smoking, and the number of cigarettes smoked per day (4). Occupational factors are the second most important risk factor for BC (5).

Uroepithelial carcinoma originating from the bladder is the most common histologic type of cancer. Over 70% of cases are diagnosed at the non-muscle invasive stage and managed by minimally invasive local treatment. Unfortunately, this disease has a high recurrence rate and may require further treatment with more than one modality. In contrast, the muscle-invasive and metastatic stage of the disease requires multimodal treatment strategies, including surgical treatment and chemotherapy in addition to neoadjuvant, adjuvant or palliative care (6).

Cancer therapies that alter the immune status have gained prominence in oncology in recent years (7). Immunotherapy is often used to complement traditional cancer treatments such as surgery, chemotherapy, and radiation therapy. During clinical practice, it is used as a first-line treatment for some cancers (8) and involves the patient's immune system to modify or increase the defense mechanisms against the developing cancer cells (8). The first clinical application of immunotherapy was documented in the 1890s when William Coley first used a bacterial agent called Coley's toxin. Clinical trials showed minimal results. Importantly, this toxin provided the first compelling evidence of the potential to produce an antitumor response using the patient's immune system (8). Immunotherapy became part of standard cancer treatment in the mid-20th century, although it exhibited significant toxicity. Treatment with cell therapy and the development of bone marrow transplantation was initiated by Fritz Bach et al. in the 1960s, as well as the production, testing and approval of high doses of IL-2 (interleukin 2) for the treatment of metastatic kidney cancer and melanoma in clinical trials in the 1990s (9, 10). Several types of immunotherapies are currently used to treat cancer, including immune checkpoint inhibitors, T-cell transfer therapy, monoclonal antibodies, therapeutic vaccines, and immune system modulators.

Immunotherapy has an anti-cancer effect because it activates the immune response against cancer cells more specifically and strongly, thus killing them. In tumors, mutated or dysregulated proteins are processed into peptides, then loaded onto major histocompatibility complex I (MHCI) molecules to form immune complexes recognized by CD8+ T cells (11). Then cytotoxic T lymphocytes are activated (12), which not only kill cancer cells and inevitably cause some damage to normal cells, but may eventually attack any of the body's healthy or normal tissues or organs, leading to unpredictable side effects, also known as "immune-related adverse events (irAE)". Organ specificity, incidence, and severity of irAEs vary according to each agent and its dose, but also differ across tumor types (13). Immune-related adverse events include non-specific symptoms and damage to the skin and mucous membrane system, head and five sense organs, digestive system, cardiovascular system, respiratory system, endocrine system, blood system, neuropsychiatric system, bone and joint system, and immune system (14). Immunotherapy has benefited a significant proportion of BC patients and has even been able to cure cancer in some patients in combination with other drugs. This new treatment modality offers hope to cancer patients but emphasizes that the associated toxic side-effects are currently a challenge for effective clinical treatment (**Table 1**).

IMMUNOTHERAPY DRUGS AND SIDE EFFECTS

Non-Targeted Immunotherapy Drugs

Bacillus Calmette–Guerin

It is widely acknowledged that Everolimus (Afinitor) is an attenuated strain of Mycobacterium Bovis. Although it has been discovered for decades, its exact mechanism of action remains unknown (32). BCG is used as a vaccine and is now used stably in patients with carcinoma *in situ* or moderate or high non-muscle invasive BC (33). It has been shown that BCG can cause a massive release of cytokines and chemokines after attachment to tumor cells by fibronectin and then internalization into tumor cells (34). BCG also promotes tumor antigen presentation to cells of the immune system (35, 36), and induction of long-term adaptive immunity (32, 37). It has been shown that BCG treatment elicits an inflammatory response involving different immune cell subsets, including CD4+ and CD8+ lymphocytes (38, 39), natural killer (NK) cells (40), granulocytes (40, 41) and macrophages (42, 43), among other cell subsets. *In vitro* experiments have shown that integrin cross-linking of BCG leads to cell cycle arrest at the G1/S interface in proliferating cells of human urothelial carcinoma cells, resulting in a direct cytostatic effect on the cancer cell line (44).

BCG is currently the most common and important tool in treating and preventing different forms of superficial BC. In this regard, treatment with BCG after transurethral resection of bladder tumor (TUPRBT) reduces the risk of tumor recurrence or high-grade tumor development, and this is now standard practice in the treatment of non-muscle invasive bladder cancer (NMIBC, including carcinoma in situ, high-grade papillary tumors, and invasive plaque intrinsic tumors) (45). Indeed, BCG treatment is also associated with concomitant side effects. Currently, side effects such as fatigue, fever, mild lower urinary tract symptoms and frank hematuria have been reported in the literature after BCG intravesical infusion therapy for BC (46). Additional side-effects include infections such as granulomatous inflammation of the genitourinary tract (bladder, testes, or prostate), pneumonia, arthritis, and hepatitis. Indeed, tuberculosis may take years to be expressed clinically and often presents as local discomfort, recurrent fever, and night sweats. If the infection worsens, severe systemic manifestations such as high fever, hypotension, organ failure, or septic shock may be observed. Therefore, the BCG vaccine should be used in the prescribed concentration range as much as possible, which will not only increase its effectiveness but also reduce the side effects to some extent (47).

The mTOR Kinase Inhibitors

Studies on the use of the mTOR Kinase Inhibitors for BC are ongoing. An increasing body of evidence shows that these drugs act by binding to the tacrolimus binding protein 12 (FKBP-12) protein, forming a complex that inhibits mTOR activity. This phenomenon leads to cell cycle arrest and inhibition of angiogenesis, proliferation, and glucose delivery to cells (48). Angiogenesis is inhibited by downregulated expression of hypoxia-inducible factor 1, which reduces the levels of vascular endothelial growth factor (49). In 2016, the Food and Drug Administration (FDA) approved everolimus for adult patients with unresectable, locally advanced or metastatic disease with progressive neuroendocrine tumors of gastrointestinal or pulmonary origin (50). The most common side effects of this class of drugs include stomatitis, rash, fatigue, hyperglycemia, hyperlipidemia, and myelosuppression; most of these are mild and disappear with drug interruption or dose reduction.

TABLE 1 | List of side effects, indications and serious complications for immunotherapy for bladder cancer.

Compound	Target	Side effects	Serious Complications	Clinical Indications	Reference
BCG	Non-Target	Digestive, urinary, skeletal joint problems, and general symptoms.	Sepsis and pneumonia.	Carcinoma in situ, high-grade papillary tumors, and invasive plaque-proprious tumors.	(15)
The mTOR Kinase Inhibitors	Non-Target	Digestives, hematologic, dermatomycoses, endocrine problems, and general symptoms.	Cardiac insufficiency, respiratory failure and sepsis.	For adult patients with unresectable, locally advanced, or metastatic disease with progressive neuroendocrine tumors of gastrointestinal or pulmonary origin.	(16)
COX-2 Inhibitors	Non-Target	Digestive, cardiovascular system, urinary problems, and general symptoms.	Peptic ulcer.	Mainly used for the prevention of bladder cancer.	(17, 18)
Nivolumab	PD-1	Digestive, urinary, respiratory, dermatomycoses, endocrine problems, and general symptoms.	Infusion reaction, intestinal obstruction, urinary tract and infection, sepsis.	Locally advanced or metastatic uroepithelial carcinoma.	(19, 20)
Pembrolizumab	PD-1	Digestive, urinary, respiratory, dermatomycoses, endocrine, skeletal joint problems, and general symptoms.	Pneumonia and cardiac insufficiency.	BCG-non-responsive, high-risk, non-muscle-invasive bladder cancer patients (NMIBC) with carcinoma *in situ* (CIS) with or without papillary tumors who are not candidates for or have chosen not to undergo cystectomy.	(21–23)
Durvalimab	PD-L1	Digestive, urinary, skeletal joint problems, and general symptoms.	Peptic ulcer.	Patients with locally advanced or metastatic uroepithelial carcinoma.	(24, 25)
Atezolizumab	PD-L1	Digestive problems, urinary problems, immune problems, and general symptoms.	Pneumonia, drug hepatitis, colitis, intestinal obstruction, endocrine diseases, and pancreatitis.	Patients with locally advanced or metastatic urothelial carcinoma that experience exacerbations during or following platinum-containing chemotherapy, or within 12 months of receiving platinum-containing chemotherapy, either before (neoadjuvant) or after (adjuvant) surgical treatment.	(26–28)
Avelumab	PD-L1	Skeletal joint, endocrine, dermatomycoses, digestive, urinary, respiratory problems, and general symptoms.	Infusion reaction, pneumonia, colitis, drug hepatitis, nephritis, renal insufficiency, and respiratory failure.	Patients with locally advanced or metastatic uroepithelial carcinoma.	(29–31)
Ipilimumab	CTLA-4	Dermatomycoses, neurological, psychiatric and digestive problems.	Peptic ulcer.	–	
Tremelimumab	CTLA-4	–	–	–	
CAR-T	–	Hematologic problems and Immune problems.	–	–	

COX-2 Inhibitors

Cyclooxygenase inhibitors are compounds that have inhibitory effects on cyclooxygenase. Cyclooxygenase inhibitors include two major groups: nonspecific cyclooxygenase inhibitors, which can inhibit both COX-1 and COX-2, such as aspirin and specific COX-2 inhibitors, such as celecoxib. Interestingly, the Cyclooxygenase-2 (COX-2) inhibitor has been shown to exhibit chemopreventive activity against various cancers, including BC, by inhibiting the proliferation, migration, invasion, and epithelial-to-mesenchymal transition of BC cells. However, its mechanism of action is not fully understood (51). Common adverse reactions mainly involve the digestive, cardiovascular, and urinary systems. Other adverse reactions include systemic reactions, which are generally mild.

Targeted Immunotherapy Drugs

Immune checkpoints are molecules involved in maintaining immune homeostasis and therefore contribute to maintaining peripheral tolerance to their own molecules. The main immune checkpoint inhibitors include blockade of programmed cell death protein-1/programmed cell death protein ligand 1 (PD-1/PD-L1) and cytotoxic T cell antigen (CTLA4). The use of monoclonal antibodies that block co-inhibitory immune checkpoint molecules helps to increase T cell-specific immune responses and thus harness the immune system against tumors (52). Responsiveness to checkpoint inhibitors is key to treatment, but this does not necessarily mean that all patients have good outcomes since some can also experience drug side effects. Other immune cells can also play an important role in developing irAEs, including B cells, which can secrete antibodies to conduct toxicity (53, 54), and granulocytes, which secrete inflammatory mediators and cytokines (53, 55). Indeed, it should be borne in mind that the side effects of a drug may not significantly alter its effectiveness; however, the patient's quality of life may be affected during treatment. Overall, side effects associated with anti-PD-1/PD-L1 are less common and severe than with anti-CTLA-4

antibodies (56). The most typical manifestations involve the skin, gastrointestinal tract, liver, and endocrine system (57). Cutaneous toxicity is the most common irAE, although GI involvement is usually more clinically relevant because of its potential morbidity and management, requiring steroids and hospitalization (58). Other rarely reported irAEs include uveitis, conjunctivitis, neuropathy, myopathy, pancreatitis, pneumonia, hemocytopenia, and nephritis (57). Immune-related adverse events associated with a certain immune checkpoint inhibitor is usually consistent across tumor types (**Figure 1**).

PD-1/PD-L1

PD-1 and PD-L1 are important immune checkpoints that negatively modulate the immune system, impairing its response to antigens. PD-1 is expressed on the surface of activated T and B lymphocytes and macrophages, and PD-L1 on antigen-presenting cells (59). The binding of PD-1 and PD-L1 blocks the activation of T lymphocytes, thereby reducing the production of IL-2 (interleukin 2) and interferon-gamma (59). Anti-PD-1 and PD-L1 drugs can block either of these two molecules, preventing both from binding, thereby increasing the production of both cytokines (60).

Nivolumab

Nivolumab, a human monoclonal antibody of IgG4 type, was approved by the FDA in 2017 for use in advanced BC (61). The common complications are elevated lipase and amylase, fatigue, skin rash, dyspnea, neutropenia, and lymphopenia (62–64).

Pembrolizumab

Pembrolizumab is a humanized IgG4/kappa monoclonal antibody that can be used to treat various types of cancer. Approved by the FDA in 2019 for the treatment of BC, especially for advanced BC cases (21, 65), pembrolizumab may be used as a first-line treatment for uroepithelial cancer (66). Moreover, it can be used to treat patients with DNA repair defects (67), and the reported overall survival with pembrolizumab is significantly higher than with chemotherapy drugs (68). Importantly, Pembrolizumab has a better safety profile than other drugs, although it may cause immune-related adverse effects such as myocarditis and myasthenia gravis.

Durvalumab

Durvalumab is an IgG1k monoclonal antibody approved by the FDA to treat BC in 2017. Studies have shown that although Durvalumab has high activity in PD-L1-positive and negative patients, it exhibits relatively higher efficacy in patients with high PD-L1 expression (69).

Atezolizumab

Atezolizumab, a humanized IgG1 isotype monoclonal antibody (70), was the first PD-1/PD-L1 checkpoint inhibitor approved by the FDA and is often used in the second-line treatment of patients with advanced BC (71). Most treatment-related adverse events are mild to moderate, including fatigue, nausea, decreased appetite, pruritus, fever, diarrhea, rash, and arthralgia (26, 72).

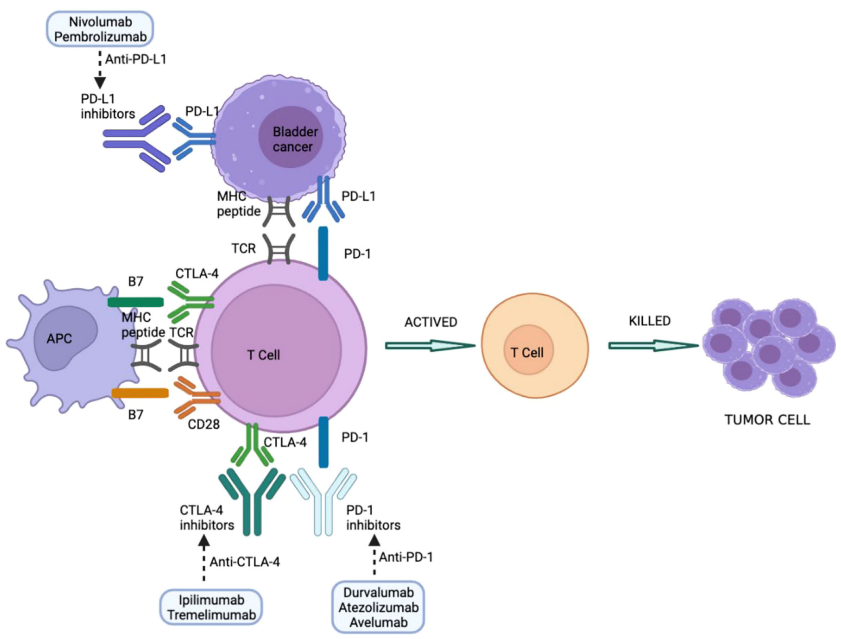

FIGURE 1 | Immune checkpoint inhibitors in BC treatment. PD-1/PD-L1 and CTLA-4 blockers interfere with suppression of checkpoint molecules of the immune system, leading to T-cell activation and tumor cell killing. CTLA-4, cytotoxic T-lymphocyte antigen 4; MHC, major histocompatibility complex; PD-1, programmed cell death-1; PD-L1, programmed cell death-1 ligand; TCR, T cell receptor; APC: Antigen-presenting cell.

Avelumab

Avelumab is also an IgG1 antibody that primarily targets PD-L1 and was approved by the FDA in 2017 for uroepithelial cancer (73). When combined with platinum-based drugs, Avelumab produces a sustained antitumor response in patients with advanced or present metastatic uroepithelial carcinoma (26). Patients may experience side effects such as fatigue, weakness, nausea, and infusion-related reactions (29).

Anti-CTLA-4 Antibodies

CTLA-4 is a surface molecule expressed by activated T cells that binds to B7.1 and B7.2 ligands expressed on B lymphocytes, dendritic cells, and macrophages (68). CTLA-4 is a co-stimulatory molecule necessary for the activation of T lymphocytes (68, 74, 75). It has been established to negatively regulate the immune system; nonetheless, the mechanism of its action is not fully understood. Given that CTLA-4 is structurally related to CD28, it has been suggested that CTLA-4 can compete with CD28 in terms of ligand binding. and another also suggested that it can directly signal all the way to the CTLA-4 cytoplasmic tail (76–78), and inhibition of CTLA-4 enhances the immune response.

Ipilimumab

Ipilimumab, originally developed by Bristol-Meyers Squibb as an anti-CTLA-4 monoclonal antibody for the treatment of melanoma, is also used in combination with nivolumab for the treatment of advanced kidney cancer and different types of metastatic colorectal cancer (79), with common side effects including toxicity in the dermal system, gastrointestinal tract, liver, and neurological and endocrine systems (80, 81). However, the efficacy of this drug in BC is largely unknown, warranting further studies.

Tremelimumab

Tremelimumab is a well-recognized humanized monoclonal antibody against CTLA-4, however, it has not been approved by the FDA for cancer treatment.

Chimeric Antigen Receptor Weight-Targeted T Cells

CAR-T is a novel precision-targeted therapy for the treatment of tumors. The Chimeric antigen receptor (CAR) is the core component of CAR-T, which gives T cells the ability to recognize tumor antigens in an HLA-independent manner, enabling them to recognize a broader range of target antigens than natural T-cell surface receptors (TCRs) (82). It is a highly promising immunotherapy approach that has yielded good results in clinical tumor treatment in recent years through optimization and improvement.

There are currently two FDA-approved CAR-T therapies: Kymriah (Tisagenlecleucel) and Yescarta (Axicabtagene ciloleucel). CAR-T is now predominantly used for the treatment of B-cell acute lymphoblastic leukemia (B-ALL) and diffuse large B-cell lymphoma (DLBCL) (83). Due to the complexity of BC and its location in the body, the treatment of solid tumors with CAR-T cells faces multiple obstacles, such as a harsh tumor microenvironment, on-tumor or off-tumor toxicity, and unpredictable antigen specificity (84). Notwithstanding that CAR-T is already approved to treat solid tumors such as BC, clinical trials on CAR-T cells for solid tumors are still being conducted on multiple fronts. CAR-T is also associated with serious adverse effects (85), mainly cytokine release syndrome (CRS) (86), immune effector cell-associated neurotoxic syndrome (ICANS) (87), infection, bone marrow suppression, phagocytic lymphohistiocytosis (HLH) (88), B-cell dysplasia, neurotoxicity (89), and disseminated intravascular coagulation (DIC) (90), and toxicity to other organs.

PREVENTION AND TREATMENT OF SIDE EFFECTS

The side effects of immune checkpoint inhibitors therapies are usually caused by the immune system attacking normal body parts in the same way it attacks cancer cells. Different types of immunotherapies can cause various side effects, many of which depend on the type of treatment, the tumor type and location, and the patient's general health condition. Immunotherapy side effects can be mild, moderate, or even life-threatening. Some side effects can resolve on their own within a certain time frame while others persist and worsen. In such cases, it should be considered to taper the dosage, discontinue, or change the medication. Indeed, prevention of the occurrence or worsening of side effects is essential for effective treatment of these patients population. At the end of immunotherapy, it is important to observe side effects, some of which may occur months or years later (91, 92). Side effects of immune checkpoint inhibitors therapies may affect the following parts of the body. (**Table 2**)

When an immunotherapy drug is given to the patients through a vein, it is called an infusion. Patients receiving infusions may experience different reactions, mainly including fever, chills, accompanied by nausea, vomiting, headache and peripheral discomfort. When a mild reaction is observed, the infusion rate can be slowed down, and attention can be paid to keeping the patients warm. In case of a severe reaction, the infusion should be immediately stopped, external cooling should be provided to pyrexial patients, and anti-allergy drugs should be prescribed if necessary (93–95).

Skin problems, like rash, itching and skin photosensitivity (72), are most common in people with BC. Skin problem caused by immunotherapy are usually not serious but can be significantly uncomfortable for the patients. For rashes, corticosteroid ointments or antibiotic ointments remain the mainstay of treatment, and oral medications may be required for severe cases. For dry skin, it is recommended to use a hypoallergenic, cream-based moisturizer to prevent skin dryness, try bath products that are gentle on the skin and shower with warm water. It is essential for patients complaining of itchy skin to avoid scented skin products and use topical steroids and oral antihistamines (96). Indeed, such patients should pay attention to hydration daily, avoiding contact with allergens and exposure to sunlight (97).

TABLE 2 | List of serious complications and brief prevention methods for bladder cancer.

Complications	Brief Prevention Methods
Infusion reaction	Strictly regulate infusion operation, closely observe patient infusion.
Sepsis	timely targeted treatment, avoid cross-infection.
Pneumonia	Improve resistance, avoid repeated infections.
Colitis	Avoid raw and cold diet, avoid repeated infections, and control with medication if necessary.
Intestinal obstruction	Medication to laxative, easy to digest diet, avoid strenuous exercise after meals.
Pancreatitis and peptic ulcer	Pay attention to dietary hygiene, inhibit gastric acid secretion, protect gastric mucosa.
Drug hepatitis	Use hepatotoxic drugs carefully, check liver function regularly, use liver protection drugs if necessary.
Renal insufficiency	Use nephrotoxic drugs carefully, check kidney function regularly.
Nephritis and urinary tract infection	Avoid holding urine, drink more water, strengthen nutrition.
Cardiac insufficiency	Absorb oxygen, control blood pressure, avoid emotional excitement, take oral vasoactive drugs if necessary.
Respiratory failure	Absorb oxygen, prevent respiratory tract infection, use ventilator if necessary.
Endocrine diseases	Pay attention to diet, strengthen exercise, use long-term maintenance medication if necessary.

General prevention: reasonable diet, pay attention to environmental hygiene, regular work and rest, avoid straining and staying up late, limit smoking and alcohol, strengthen exercise, and enhance their resistance.

Problems with the gastrointestinal tract are also some of the most common side effects related to immune checkpoint inhibitors therapies. These include colitis, diarrhea, swallowing problems, nausea and vomiting, and pain in the upper abdomen. Regular examination of abdominal signs, abdominal X-rays, abdominal ultrasound, CT, gastroscopy and enteroscopy can be used for diagnosis (98). The treatment regimen usually includes medications to inhibit hydrochloric acid and protect the digestive tract, such as proton pump inhibitors, and medications such as gastric mucosal protectors and hepatoprotective drugs can also be considered. Daily diet is carefully chosen by avoiding caffeine, alcohol, and spicy foods, eating less and more often, and regular monitoring of electrolyte levels, coupled with proper hydration and electrolyte supplementation to prevent further aggravation of the condition (99, 100).

Muscle, joint and bone problems can also occur in people who receive immune checkpoint inhibitors therapies. These can result in arthritis-type pain, swelling in joints, and muscle cramping, and even myasthenia gravis, manifest with limited range of motion and stiffness after inactivity or activity, swelling or pressure pain and redness or warmth at the joint. The diagnosis is usually made with X-rays, bone scans, CT, MRI and bone densitometry (101). Pain can be relieved with medications such as painkillers, corticosteroids, calcium tablets, vitamin D and antibiotics (102, 103). In addition, some physical therapies such as acupuncture, hot or cold compresses and massage can also be used to relieve pain (104, 105). It is worth mentioning that myasthenia gravis is a chronic autoimmune disease, the diagnosis is usually made by conducting the Tensilon test or a nerve conduction test. Acetylcholinesterase inhibitors such as neostigmine or pyridostigmine remain the mainstay of treatment of myasthenia gravis; immunosuppressive drugs such as prednisone or azathioprine also can be considered (106). Treatment with plasmapheresis and high doses of intravenous immunoglobulin may be required for cases presenting with sudden onset of symptoms (107). Adjunctive use of a ventilator may be required in cases of respiratory muscle weakness. For these problems, proper exercise, weight maintenance, and taking precautions to avoid falls are essential (102, 103).

In the urinary tract, renal inflammation and hematuria is more likely to occur in patients who with immune checkpoint inhibitors therapies compared to kidney damage and kidney failure. These can be diagnosed through complete blood count (CBC), creatinine, blood urea nitrogen, abdominal ultrasound, abdominal CT and ureteroscopy. The treatment mainly focuses on protecting kidney function, ensuring adequate rest, proper nutrition and strict control of blood pressure, blood lipids and blood sugar, coupled with management of major and minor symptoms (108–111).

The neurological side effects of immune checkpoint inhibitors therapies are mainly in the central and peripheral nervous system (112, 113), affecting your brain, senses, mind, and even movement. These are rare but can be serious side effects. A cranial CT or MRI would be a good choice for the diagnostic workup in patients with dizziness and headache combined with a history of severe illness. The treatment of neurological problems is based on neurotrophy and then, take appropriate treatment measures to deal with corresponding symptoms. For example, analgesics for headaches, anti-dizziness drugs for dizziness, etc. Although nerve damage and neurological symptoms are not preventable, most are manageable if detected early, and early treatment can also prevent symptoms from exacerbating.

Immunotherapy may cause changes in the number of blood cells and blood factors, which can lead to anemia, coagulation disorders and sepsis. It can be diagnosed with a CBC, clotting assays and blood protein tests. Anemia can be treated with blood transfusions or erythropoiesis-stimulating agents (ESAs), and a diet rich in iron, folic acid, and vitamin B12 can play a preventive role (114). Blood coagulation is a complex process involving a series of reactions involving platelets and clotting factors. Hemorrhage and thrombosis occur when the balance between clotting factors is disrupted (115). In the case of bleeding disorder, prompt supplementation of platelets, vitamin K and other pro-coagulant medications; A blood clot is a serious condition that needs treatment right away, the management of thrombosis consists of anticoagulation with warfarin or rivaroxaban, followed by thrombolytic therapy with urokinase or streptokinase. Besides, extra care should be taken during daily activities to avoid circumstances that may lead to bleeding and thrombosis (116, 117). Sepsis, on the other hand, requires the

selection of appropriate antibiotics, aggressive anti-infection treatment, increasing resistance, avoiding late nights and exertion, and avoiding the intake of unclean water and food.

Immune checkpoint inhibitors therapies may cause pneumonitis, which is inflammation of the lung that can cause a cough or trouble breathing. Pneumonitis is uncommon but may be serious. Inflammatory serum biomarkers, chest X-rays, contrast-enhanced CT, and pulmonary function tests are common diagnostic methods (118). The management involves aggressive treatment with anti-inflammatory drugs, coupled with symptomatic management to relieve respiratory spasms and alleviate wheezing (119, 120). In patients with pneumonia and pleural effusion, light exercise is recommended to accelerate resorption of inflammation. It is essential for patients with pulmonary vascular thrombosis to lie down to prevent dislodging of the thrombus that can block other blood vessels. The patient should refrain from smoking and exposure to secondhand smoke. Indeed, lots of fluids are required to keep hydrated, and exposure to irritants should be avoided to avoid exacerbating the cough (120–122).

The endocrine system controls the hormones that help the body regulate many important functions, like blood pressure, blood sugar, energy, and the ability to respond to stresses like infections and injuries (14, 123). The thyroid, adrenal, pancreatic, sexual gland is a vital part of the endocrine system, and it may be triggered to become either more or less productive by immune checkpoint inhibitor treatments. The diagnosis focuses on the examination of the corresponding glands and the hormones they secrete. To treat the above endocrine side effects, the patient's hormone levels should be assessed. If a decline is observed, treatment with hormone replacement therapy is indicated. Drugs that inhibit endocrine gland hormone release are prescribed if high levels are found. Given the insidious nature of these autoimmune events, the consequences are often ongoing and even permanent, requiring long-term hormone replacement therapy (107). Pay attention to exercise and healthy diet in daily life.

Immunotherapy may affect the heart and blood vessels. These side effects are rare but are often very serious and can be life-threatening. Includes cardiomyopathy, congestive heart failure (CHF), myocarditis, coronary artery disease, arrhythmias, heart valve damage, and pericardial disease. The clinical presentation usually consists of shortness of breath, dizziness, chest pain, edema, fatigue, etc. (124). Regular physical examinations heartbeat sounds, vascular murmurs, laboratory tests, cardiac enzyme profile, BNP, echocardiograms, chest X-rays, electrocardiograms, multi-gate acquisition scans (MUGA), cardiac MRI and angiograms can be used to diagnose heart problems. The treatment plan usually consists of cardio-protective drugs such as dexrazoxane (Zinecard) which help prevent cardiac problems induced by anthracyclines. Inotropes (digitalis), diuretics and hypertensive drugs should also be considered (125–128). Take care to avoid emotional excitement in daily life and have a light diet is necessary.

CONCLUSION

Immunotherapy is regarded as a promising and more effective therapeutic measure in the treatment of various types of cancer. However, the side effects of it are underestimated currently. The unpredictable occurrence of serious side effects not only causes serious health damage to patients, but also increases the medical burden to some extent. The clinical management of side effects in patients today is mainly empirical. Therefore, a uniform and systematic guideline to control the side effects of immunotherapy is necessary. Based on the insufficiency understanding on the side effects of immunotherapy, more follow-up data on the side effect is needed, as well as prospective, multicenter, large-scale trials on the preventive measures. Above all, further research on the molecular mechanisms and clinical efficacy of the side effects of immunotherapy is still urgent.

PROSPECT

Although immunotherapy developed and achieved widespread application in clinical cancer therapy, further research is necessary in immunotherapy for bladder cancer, especially in the systemic response, which may exert role in the development of side effects of immunotherapy. Furthermore, the genetic diversity of bladder cancer and epigenetic modification are also relevant to efficacy and side effects.

During recent years, researchers proposed new methods to improve the efficacy of immunotherapy and mitigate side effects, such as activation of thioredoxin, bacterial colony transplantation, and ferroptosis induction. At the same time, alternative therapeutic measures are beneficial in alleviating the symptoms of drug complications, such as rehabilitation therapy, Chinese acupuncture, and physiotherapy. In addition, combination or individualized treatments depending on the diversity of the patient is also a good choice. Hence, develop new methods to alleviate side effect would be an important subject in immunotherapy.

AUTHOR CONTRIBUTIONS

KL and SF searched for literature and wrote the first draft of this article. XZ edited tables and figures. JZ and GZ reviewed the manuscript and polished the grammar. All authors contributed to the article and approved the submitted version.

FUNDING

This work was supported by the National Natural Science Foundation of China (No. 81860456); The Jiangxi Natural Science Foundation (No. 20202BABL206031).

REFERENCES

1. Ferlay J, et al. *Global Cancer Observatory: Cancer Today* (2018). Available at: https://gco.iarc.fr/today (Accessed date 01 May 2019).
2. Brahmer J, Reckamp KL, Baas P, Crinò L, Eberhardt WE, Poddubskaya E, et al. Nivolumab Versus Docetaxel in Advanced Squamous-Cell Non-Small-Cell Lung Cancer. *N Engl J Med* (2015) 373(2):123–35. doi: 10.1056/NEJMoa1504627
3. Richters A, Aben KKH, Kiemeney L. The Global Burden of Urinary Bladder Cancer: An Update. *World J Urol* (2020) 38(8):1895–904. doi: 10.1007/s00345-019-02984-4
4. Kim HS, Seo HK. Immune Checkpoint Inhibitors for Urothelial Carcinoma. *Investig Clin Urol* (2018) 59(5):285–96. doi: 10.4111/icu.2018.59.5.285
5. Saginala K, Barsouk A, Aluru JS, Rawla P, Padala SA, Barsouk A. Epidemiology of Bladder Cancer. *Med Sci (Basel)* (2020) 8(1):5–15. doi: 10.3390/medsci8010015
6. Chien TM, Chan TC, Huang SK, Yeh BW, Li WM, Huang CN, et al. Role of Microtubule-Associated Protein 1b in Urothelial Carcinoma: Overexpression Predicts Poor Prognosis. *Cancers (Basel)* (2020) 12(3):630. doi: 10.3390/cancers12030630
7. AkgÜL A, Ahmed N, Raza A, Iqbal Z, Rafiq M, Rehman MA, et al. A Fractal Fractional Model for Cervical Cancer Due to Human Papillomavirus Infection. *Fractals* (2021) 29(05):2140015. doi: 10.1142/S0218348X21400156
8. Jagodinsky JC, Harari PM, Morris ZS. The Promise of Combining Radiation Therapy With Immunotherapy. *Int J Radiat Oncol Biol Phys* (2020) 108 (1):6–16. doi: 10.1016/j.ijrobp.2020.04.023
9. Fyfe GA, Fisher RI, Rosenberg SA, Sznol M, Parkinson DR, Louie AC. Long-Term Response Data for 255 Patients With Metastatic Renal Cell Carcinoma Treated With High-Dose Recombinant Interleukin-2 Therapy. *J Clin Oncol* (1996) 14(8):2410–1. doi: 10.1200/JCO.1996.14.8.2410
10. Atkins MB, Lotze MT, Dutcher JP, Fisher RI, Weiss G, Margolin K, et al. High-Dose Recombinant Interleukin 2 Therapy for Patients With Metastatic Melanoma: Analysis of 270 Patients Treated Between 1985 and 1993. *J Clin Oncol* (1999) 17(7):2105–16. doi: 10.1200/JCO.1999.17.7.2105
11. Havel JJ, Chowell D, Chan TA. The Evolving Landscape of Biomarkers for Checkpoint Inhibitor Immunotherapy. *Nat Rev Cancer* (2019) 19(3):133–50. doi: 10.1038/s41568-019-0116-x
12. Weber JS, Yang JC, Atkins MB, Disis ML. Toxicities of Immunotherapy for the Practitioner. *J Clin Oncol* (2015) 33(18):2092–9. doi: 10.1200/JCO.2014.60.0379
13. Marrone KA, Ying W, Naidoo J. Immune-Related Adverse Events From Immune Checkpoint Inhibitors. *Clin Pharmacol Ther* (2016) 100(3):242–51. doi: 10.1002/cpt.394
14. Michot JM, Bigenwald C, Champiat S, Collins M, Carbonnel F, Postel-Vinay S, et al. Immune-Related Adverse Events With Immune Checkpoint Blockade: A Comprehensive Review. *Eur J Cancer* (2016) 54:139–48. doi: 10.1016/j.ejca.2015.11.016
15. Pettenati C, Ingersoll MA. Mechanisms of BCG Immunotherapy and its Outlook for Bladder Cancer. *Nat Rev Urol* (2018) 15(10):615–25. doi: 10.1038/s41585-018-0055-4
16. Jurkowska K, Długosz A. Research on New Drugs in the Therapy of Bladder Cancer (BC). *Postępy Hig Med Dosw* (2018) 72:442–8. doi: 10.5604/01.3001.0012.0539
17. Eltze E, Wülfing C, Von Struensee D, Piechota H, Buerger H, Hertle L. Cox-2 and Her2/neu Co-Expression in Invasive Bladder Cancer. *Int J Oncol* (2005) 26(6):1525–31. doi: 10.3892/ijo.26.6.1525
18. Dhawan D, Jeffreys AB, Zheng R, Stewart JC, Knapp DW. Cyclooxygenase-2 Dependent and Independent Antitumor Effects Induced by Celecoxib in Urinary Bladder Cancer Cells. *Mol Cancer Ther* (2008) 7(4):897–904. doi: 10.1158/1535-7163.MCT-07-0313
19. Sharma P, Callahan MK, Bono P, Kim J, Spiliopoulou P, Calvo E, et al. Nivolumab Monotherapy in Recurrent Metastatic Urothelial Carcinoma (CheckMate 032): A Multicentre, Open-Label, Two-Stage, Multi-Arm, Phase 1/2 Trial. *Lancet Oncol* (2016) 17(11):1590–8. doi: 10.1016/S1470-2045(16)30496-X
20. Sharma P, Retz M, Siefker-Radtke A, Baron A, Necchi A, Bedke J, et al. Nivolumab in Metastatic Urothelial Carcinoma After Platinum Therapy (CheckMate 275): A Multicentre, Single-Arm, Phase 2 Trial. *Lancet Oncol* (2017) 18(3):312–22. doi: 10.1016/S1470-2045(17)30065-7
21. Bellmunt J, de Wit R, Vaughn DJ, Fradet Y, Lee JL, Fong L, et al. Pembrolizumab as Second-Line Therapy for Advanced Urothelial Carcinoma. *N Engl J Med* (2017) 376(11):1015–26. doi: 10.1056/NEJMoa1613683
22. Balar AV, Castellano D, O'Donnell PH, Grivas P, Vuky J, Powles T, et al. First-Line Pembrolizumab in Cisplatin-Ineligible Patients With Locally Advanced and Unresectable or Metastatic Urothelial Cancer (KEYNOTE-052): A Multicentre, Single-Arm, Phase 2 Study. *Lancet Oncol* (2017) 18 (11):1483–92. doi: 10.1016/S1470-2045(17)30616-2
23. Plimack ER, Bellmunt J, Gupta S, Berger R, Chow LQ, Juco J, et al. Safety and Activity of Pembrolizumab in Patients With Locally Advanced or Metastatic Urothelial Cancer (KEYNOTE-012): A Non-Randomised, Open-Label, Phase 1b Study. *Lancet Oncol* (2017) 18(2):212–20. doi: 10.1016/S1470-2045(17)30007-4
24. Massard C, Gordon MS, Sharma S, Rafii S, Wainberg ZA, Luke J, et al. Safety and Efficacy of Durvalumab (MEDI4736), an Anti-Programmed Cell Death Ligand-1 Immune Checkpoint Inhibitor, in Patients With Advanced Urothelial Bladder Cancer. *J Clin Oncol* (2016) 34(26):3119–25. doi: 10.1200/JCO.2016.67.9761
25. Powles T, O'Donnell PH, Massard C, Arkenau HT, Friedlander TW, Hoimes CJ, et al. Efficacy and Safety of Durvalumab in Locally Advanced or Metastatic Urothelial Carcinoma: Updated Results From a Phase 1/2 Open-Label Study. *JAMA Oncol* (2017) 3(9):e172411. doi: 10.1001/jamaoncol.2017.2411
26. Rosenberg JE, Hoffman-Censits J, Powles T, van der Heijden MS, Balar AV, Necchi A, et al. Atezolizumab in Patients With Locally Advanced and Metastatic Urothelial Carcinoma Who Have Progressed Following Treatment With Platinum-Based Chemotherapy: A Single-Arm, Multicentre, Phase 2 Trial. *Lancet* (2016) 387(10031):1909–20. doi: 10.1016/S0140-6736(16)00561-4
27. Powles T, Durán I, van der Heijden MS, Loriot Y, Vogelzang NJ, De Giorgi U, et al. Atezolizumab Versus Chemotherapy in Patients With Platinum-Treated Locally Advanced or Metastatic Urothelial Carcinoma (IMvigor211): A Multicentre, Open-Label, Phase 3 Randomised Controlled Trial. *Lancet* (2018) 391(10122):748–57. doi: 10.1016/S0140-6736(17)33297-X
28. Eckstein M, Erben P, Kriegmair MC, Worst TS, Weiß CA, Wirtz RM, et al. Performance of the Food and Drug Administration/EMA-Approved Programmed Cell Death Ligand-1 Assays in Urothelial Carcinoma With Emphasis on Therapy Stratification for First-Line Use of Atezolizumab and Pembrolizumab. *Eur J Cancer* (2019) 106:234–43. doi: 10.1016/j.ejca.2018.11.007
29. Apolo AB, Infante JR, Balmanoukian A, Patel MR, Wang D, Kelly K, et al. Avelumab, an Anti-Programmed Death-Ligand 1 Antibody, In Patients With Refractory Metastatic Urothelial Carcinoma: Results From a Multicenter, Phase Ib Study. *J Clin Oncol* (2017) 35(19):2117–24. doi: 10.1200/JCO.2016.71.6795
30. Patel MR, Ellerton J, Infante JR, Agrawal M, Gordon M, Aljumaily R, et al. Avelumab in Metastatic Urothelial Carcinoma After Platinum Failure (JAVELIN Solid Tumor): Pooled Results From Two Expansion Cohorts of an Open-Label, Phase 1 Trial. *Lancet Oncol* (2018) 19(1):51–64. doi: 10.1016/S1470-2045(17)30900-2
31. Powles T, Park SH, Voog E, Caserta C, Valderrama BP, Gurney H, et al. Avelumab Maintenance Therapy for Advanced or Metastatic Urothelial Carcinoma. *N Engl J Med* (2020) 383(13):1218–30. doi: 10.1056/NEJMoa2002788
32. Crispen PL, Kusmartsev S. Mechanisms of Immune Evasion in Bladder Cancer. *Cancer Immunol Immunother* (2020) 69(1):3–14. doi: 10.1007/s00262-019-02443-4
33. Farman M, Akgül A, Ahmad A, Imtiaz S. Analysis and Dynamical Behavior of Fractional-Order Cancer Model With Vaccine Strategy. *Math Methods Appl Sci* (2020) 43(7):4871–82. doi: 10.1002/mma.6240
34. Durek C, Brandau S, Ulmer AJ, Flad HD, Jocham D, Böhle A. Bacillus-Calmette-Guérin (BCG) and 3D Tumors: An in Vitro Model for the Study of Adhesion and Invasion. *J Urol* (1999) 162(2):600–5. doi: 10.1016/s0022-5347(05)68633-8
35. De Boer EC, De Jong WH, Steerenberg PA, Aarden LA, Tetteroo E, De Groot ER, et al. Induction of Urinary Interleukin-1 (IL-1), IL-2, IL-6, and Tumour Necrosis Factor During Intravesical Immunotherapy With Bacillus

Calmette-Guérin in Superficial Bladder Cancer. *Cancer Immunol Immunother* (1992) 34(5):306–12. doi: 10.1007/BF01741551
36. Luo Y, Chen X, O'Donnell MA. Mycobacterium Bovis Bacillus Calmette-Guérin (BCG) Induces Human CC- and CXC-Chemokines In Vitro and *In Vivo*. *Clin Exp Immunol* (2007) 147(2):370–8. doi: 10.1111/j.1365-2249.2006.03288.x
37. Kawai K, Miyazaki J, Joraku A, Nishiyama H, Akaza H. Bacillus Calmette-Guerin (BCG) Immunotherapy for Bladder Cancer: Current Understanding and Perspectives on Engineered BCG Vaccine. *Cancer Sci* (2013) 104(1):22–7. doi: 10.1111/cas.12075
38. Prescott S, James K, Hargreave TB, Chisholm GD, Smyth JF. Intravesical Evans Strain BCG Therapy: Quantitative Immunohistochemical Analysis of the Immune Response Within the Bladder Wall. *J Urol* (1992) 147(6):1636–42. doi: 10.1016/S0022-5347(17)37668-1
39. Ratliff TL, Ritchey JK, Yuan JJ, Andriole GL, Catalona WJ. T-Cell Subsets Required for Intravesical BCG Immunotherapy for Bladder Cancer. *J Urol* (1993) 150(3):1018–23. doi: 10.1016/S0022-5347(17)35678-1
40. Brandau S, Riemensberger J, Jacobsen M, Kemp D, Zhao W, Zhao X, et al. NK Cells Are Essential for Effective BCG Immunotherapy. *Int J Cancer* (2001) 92(5):697–702. doi: 10.1002/1097-0215(20010601)92:5<697::AID-IJC1245>3.0.CO;2-Z
41. Suttmann H, Riemensberger J, Bentien G, Schmaltz D, Stöckle M, Jocham D, et al. Neutrophil Granulocytes are Required for Effective Bacillus Calmette-Guérin Immunotherapy of Bladder Cancer and Orchestrate Local Immune Responses. *Cancer Res* (2006) 66(16):8250–7. doi: 10.1158/0008-5472.CAN-06-1416
42. Pryor K, Goddard J, Goldstein D, Stricker P, Russell P, Golovsky D, et al. Bacillus Calmette-Guerin (BCG) Enhances Monocyte- and Lymphocyte-Mediated Bladder Tumour Cell Killing. *Br J Cancer* (1995) 71(4):801–7. doi: 10.1038/bjc.1995.155
43. De Boer EC, De Jong WH, van der Meijden AP, Steerenberg PA, Witjes JA, Vegt PD, et al. Presence of Activated Lymphocytes in the Urine of Patients With Superficial Bladder Cancer After Intravesical Immunotherapy With Bacillus Calmette-Guérin. *Cancer Immunol Immunother* (1991) 33(6):411–6. doi: 10.1007/BF01741603
44. Chen F, Zhang G, Iwamoto Y, See WA. BCG Directly Induces Cell Cycle Arrest in Human Transitional Carcinoma Cell Lines as a Consequence of Integrin Cross-Linking. *BMC Urol* (2005) 5:8. doi: 10.1186/1471-2490-5-8
45. Zhang C, Berndt-Paetz M, Neuhaus J. Identification of Key Biomarkers in Bladder Cancer: Evidence From a Bioinformatics Analysis. *Diagn (Basel)* (2020) 10(2):66. doi: 10.3390/diagnostics10020066
46. Lockyer CR, Gillatt DA. BCG Immunotherapy for Superficial Bladder Cancer. *J R Soc Med* (2001) 94(3):119–23. doi: 10.1177/014107680109400305
47. Akgül A, Farman M, Ahmad A, Saleem MU. Bacillus Calmette Guerin (BCG) Immunotherapy for Bladder Cancer: A Control and Mathematical Analysis. *Int J Appl Comput Math* (2021) 7(6):254. doi: 10.1007/s40819-021-01191-3
48. Jurkowska K, Długosz A. Research on New Drugs in the Therapy of Bladder Cancer (BC) Postepy Hig. *Med Dosw* (2018) 72:442–8. doi: 10.5604/01.3001.0012.0539
49. Pinto-Leite R, Arantes-Rodrigues R, Sousa N, Oliveira PA, Santos L. mTOR Inhibitors in Urinary Bladder Cancer. *Tumour Biol* (2016) 37(9):11541–51. doi: 10.1007/s13277-016-5083-1
50. *Everolimus (Afinitor)*. Available at: https://www.fda.gov/drugs/resources-information-approved-drugs/everolimus-afinitor (Accessed February 26).
51. Liu X, Wu Y, Zhou Z, Huang M, Deng W, Wang Y, et al. Celecoxib Inhibits the Epithelial-to-Mesenchymal Transition in Bladder Cancer Via the miRNA-145/TGFBR2/Smad3 Axis. *Int J Mol Med* (2019) 44(2):683–93. doi: 10.3892/ijmm.2019.4241
52. Dunn GP, Bruce AT, Ikeda H, Old LJ, Schreiber RD. Cancer Immunoediting: From Immunosurveillance to Tumor Escape. *Nat Immunol* (2002) 3(11):991–8. doi: 10.1038/ni1102-991
53. Good-Jacobson KL, Szumilas CG, Chen L, Sharpe AH, Tomayko MM, Shlomchik MJ. PD-1 Regulates Germinal Center B Cell Survival and the Formation and Affinity of Long-Lived Plasma Cells. *Nat Immunol* (2010) 11(6):535–42. doi: 10.1038/ni.1877
54. Iwama S, De Remigis A, Callahan MK, Slovin SF, Wolchok JD, Caturegli P. Pituitary Expression of CTLA-4 Mediates Hypophysitis Secondary to Administration of CTLA-4 Blocking Antibody. *Sci Transl Med* (2014) 6(230):230ra45. doi: 10.1126/scitranslmed.3008002
55. Zitvogel L, Kroemer G. Targeting PD-1/PD-L1 Interactions for Cancer Immunotherapy. *Oncoimmunology* (2012) 1(8):1223–5. doi: 10.4161/onci.21335
56. Naidoo J, Page DB, Li BT, Connell LC, Schindler K, Lacouture ME, et al. Toxicities of the Anti-PD-1 and Anti-PD-L1 Immune Checkpoint Antibodies. *Ann Oncol* (2015) 26(12):2375–91. doi: 10.1093/annonc/mdv383
57. Callahan MK, Wolchok JD. At the Bedside: CTLA-4- and PD-1-Blocking Antibodies in Cancer Immunotherapy. *J Leukoc Biol* (2013) 94(1):41–53. doi: 10.1189/jlb.1212631
58. Weber JS, Postow M, Lao CD, Schadendorf D. Management of Adverse Events Following Treatment With Anti-Programmed Death-1 Agents. *Oncologist* (2016) 21(10):1230–40. doi: 10.1634/theoncologist.2016-0055
59. Rundo F, Spampinato C, Banna GL, Conoci S. Advanced Deep Learning Embedded Motion Radiomics Pipeline for Predicting Anti-PD-1/PD-L1 Immunotherapy Response in the Treatment of Bladder Cancer: Preliminary Results. *Electronics* (2019) 8:1134. doi: 10.3390/electronics8101134
60. Alsaab HO, Sau S, Alzhrani R, Tatiparti K, Bhise K, Kashaw SK, et al. PD-1 and PD-L1 Checkpoint Signaling Inhibition for Cancer Immunotherapy: Mechanism, Combinations, and Clinical Outcome. *Front Pharmacol* (2017) 8:561. doi: 10.3389/fphar.2017.00561
61. *Bristol-Myers Squibb Receives FDA Approval for Opdivo (Nivolumab) in Previously Treated Locally Advanced or Metastatic Urothelial Carcinoma* Available at: https://www.drugs.com/newdrugs/bristol-myers-squibb-receives-fda-approval-opdivo-nivolumab-previously-treated-locally-advanced-4484.html (Accessed on 20 January 2020).
62. Jain RK, Snyders T, Nandagopal L, Garje R, Zakharia Y, Gupta S. Immunotherapy Advances in Urothelial Carcinoma. *Curr Treat Opt Oncol* (2018) 19(12):79. doi: 10.1007/s11864-018-0598-x
63. Weber JS, Hodi FS, Wolchok JD, Topalian SL, Schadendorf D, Larkin J, et al. Safety Profile of Nivolumab Monotherapy: A Pooled Analysis of Patients With Advanced Melanoma. *J Clin Oncol* (2017) 35(7):785–92. doi: 10.1200/JCO.2015.66.1389
64. Larkin J, Lao CD, Urba WJ, McDermott DF, Horak C, Jiang J, et al. Efficacy and Safety of Nivolumab in Patients With BRAF V600 Mutant and BRAF Wild-Type Advanced Melanoma: A Pooled Analysis of 4 Clinical Trials. *JAMA Oncol* (2015) 1(4):433–40. doi: 10.1001/jamaoncol.2015.1184
65. Patterson K, Prabhu V, Xu R, Li H, Meng Y, Zarabi N, et al. Cost-Effectiveness of Pembrolizumab for Patients With Advanced, Unresectable, or Metastatic Urothelial Cancer Ineligible for Cisplatin-Based Therapy. *Eur Urol Oncol* (2019) 2(5):565–71. doi: 10.1016/j.euo.2018.09.009
66. Morsch R, Rose M, Maurer A, Cassataro MA, Braunschweig T, Knüchel R, et al. Therapeutic Implications of PD-L1 Expression in Bladder Cancer With Squamous Differentiation. *BMC Cancer* (2020) 20(1):230. doi: 10.1186/s12885-020-06727-2
67. Mancuso JG, Foulkes WD, Pollak MN. Cancer Immunoprevention: A Case Report Raising the Possibility of "Immuno-Interception". *Cancer Prev Res (Phila)* (2020) 13(4):351–6. doi: 10.1158/1940-6207.CAPR-19-0528
68. Farina MS, Lundgren KT, Bellmunt J. Immunotherapy in Urothelial Cancer: Recent Results and Future Perspectives. *Drugs* (2017) 77(10):1077–89. doi: 10.1007/s40265-017-0748-7
69. Zajac M, Boothman AM, Ben Y, Gupta A, Jin X, Mistry A, et al. Analytical Validation and Clinical Utility of an Immunohistochemical Programmed Death Ligand-1 Diagnostic Assay and Combined Tumor and Immune Cell Scoring Algorithm for Durvalumab in Urothelial Carcinoma. *Arch Pathol Lab Med* (2019) 143(6):722–31. doi: 10.5858/arpa.2017-0555-OA
70. Powles T, Eder JP, Fine GD, Braiteh FS, Loriot Y, Cruz C, et al. MPDL3280A (Anti-PD-L1) Treatment Leads to Clinical Activity in Metastatic Bladder Cancer. *Nature* (2014) 515(7528):558–62. doi: 10.1038/nature13904
71. *FDA Atezolizumab for Urothelial Carcinoma*. Available at: https://www.fda.gov/drugs/resources-information-approved-drugs/atezolizumab-urothelial-carcinoma (Accessed on 10 December 2019).
72. Teulings HE, Limpens J, Jansen SN, Zwinderman AH, Reitsma JB, Spuls PI, et al. Vitiligo-Like Depigmentation in Patients With Stage III-IV Melanoma

Receiving Immunotherapy and its Association With Survival: A Systematic Review and Meta-Analysis. *J Clin Oncol* (2015) 33(7):773–81. doi: 10.1200/JCO.2014.57.4756
73. *FDA FDA Approves Bavencio (Avelumab) for Metastatic Merkel Cell Carcinoma*. Available at: https://www.drugs.com/newdrugs/fda-approves-bavencio-avelumab-metastatic-merkel-cell-carcinoma-4502.html (Accessed on 10 December 2019).
74. Hojeij R, Domingos-Pereira S, Nkosi M, Gharbi D, Derré L, Schiller JT, et al. Immunogenic Human Papillomavirus Pseudovirus-Mediated Suicide-Gene Therapy for Bladder Cancer. *Int J Mol Sci* (2016) 17(7):1125. doi: 10.3390/ijms17071125
75. Schulz WA, Sørensen KD. Epigenetics of Urological Cancers. *Int J Mol Sci* (2019) 20(19):4775. doi: 10.3390/ijms20194775
76. Peggs KS, Quezada SA, Chambers CA, Korman AJ, Allison JP. Blockade of CTLA-4 on Both Effector and Regulatory T Cell Compartments Contributes to the Antitumor Activity of Anti-CTLA-4 Antibodies. *J Exp Med* (2009) 206 (8):1717–25. doi: 10.1084/jem.20082492
77. van der Merwe PA, Davis SJ. Molecular Interactions Mediating T Cell Antigen Recognition. *Annu Rev Immunol* (2003) 21:659–84. doi: 10.1146/annurev.immunol.21.120601.141036
78. Carreno BM, Bennett F, Chau TA, Ling V, Luxenberg D, Jussif J, et al. CTLA-4 (CD152) can Inhibit T Cell Activation by Two Different Mechanisms Depending on its Level of Cell Surface Expression. *J Immunol* (2000) 165(3):1352–6. doi: 10.4049/jimmunol.165.3.1352
79. *Yervoy Approval History*. Available at: https://www.drugs.com/history/yervoy.html (Accessed on 22 January 2020).
80. Weber JS, Kähler KC, Hauschild A. Management of Immune-Related Adverse Events and Kinetics of Response With Ipilimumab. *J Clin Oncol* (2012) 30(21):2691–7. doi: 10.1200/JCO.2012.41.6750
81. Bot I, Blank CU, Boogerd W, Brandsma D. Neurological Immune-Related Adverse Events of Ipilimumab. *Pract Neurol* (2013) 13(4):278–80. doi: 10.1136/practneurol-2012-000447
82. Sadelain M, Rivière I, Brentjens R. Targeting Tumours With Genetically Enhanced T Lymphocytes. *Nat Rev Cancer* (2003) 3(1):35–45. doi: 10.1038/nrc971
83. Fournier C, Martin F, Zitvogel L, Kroemer G, Galluzzi L, Apetoh L. Trial Watch: Adoptively Transferred Cells for Anticancer Immunotherapy. *Oncoimmunology* (2017) 6(11):e1363139. doi: 10.1080/2162402X.2017.1363139
84. Zhang H, Ye ZL, Yuan ZG, Luo ZQ, Jin HJ, Qian QJ. New Strategies for the Treatment of Solid Tumors With CAR-T Cells. *Int J Biol Sci* (2016) 12 (6):718–29. doi: 10.7150/ijbs.14405
85. Brudno JN, Kochenderfer JN. Toxicities of Chimeric Antigen Receptor T Cells: Recognition and Management. *Blood* (2016) 127(26):3321–30. doi: 10.1182/blood-2016-04-703751
86. Kochenderfer JN, Dudley ME, Feldman SA, Wilson WH, Spaner DE, Maric I, et al. B-Cell Depletion and Remissions of Malignancy Along With Cytokine-Associated Toxicity in a Clinical Trial of Anti-CD19 Chimeric-Antigen-Receptor-Transduced T Cells. *Blood* (2012) 119(12):2709–20. doi: 10.1182/blood-2011-10-384388
87. Locke FL, Neelapu SS, Bartlett NL, Siddiqi T, Chavez JC, Hosing CM, et al. Phase 1 Results of ZUMA-1: A Multicenter Study of KTE-C19 Anti-CD19 CAR T Cell Therapy in Refractory Aggressive Lymphoma. *Mol Ther* (2017) 25(1):285–95. doi: 10.1016/j.ymthe.2016.10.020
88. Neelapu SS, Locke FL, Bartlett NL, Lekakis LJ, Miklos DB, Jacobson CA, et al. Axicabtagene Ciloleucel CAR T-Cell Therapy in Refractory Large B-Cell Lymphoma. *N Engl J Med* (2017) 377(26):2531–44. doi: 10.1056/NEJMoa1707447
89. Turtle CJ, Hanafi LA, Berger C, Gooley TA, Cherian S, Hudecek M, et al. CD19 CAR-T Cells of Defined CD4+:CD8+ Composition in Adult B Cell ALL Patients. *J Clin Invest* (2016) 126(6):2123–38. doi: 10.1172/JCI85309
90. Davila ML, Riviere I, Wang X, Bartido S, Park J, Curran K, et al. Efficacy and Toxicity Management of 19-28z CAR T Cell Therapy in B Cell Acute Lymphoblastic Leukemia. *Sci Transl Med* (2014) 6(224):224ra25. doi: 10.1126/scitranslmed.3008226
91. Day D, Hansen AR. Immune-Related Adverse Events Associated With Immune Checkpoint Inhibitors. *BioDrugs* (2016) 30(6):571–84. doi: 10.1007/s40259-016-0204-3
92. Boutros C, Tarhini A, Routier E, Lambotte O, Ladurie FL, Carbonnel F, et al. Safety Profiles of Anti-CTLA-4 and Anti-PD-1 Antibodies Alone and in Combination. *Nat Rev Clin Oncol* (2016) 13(8):473–86. doi: 10.1038/nrclinonc.2016.58
93. Lenz HJ. Management and Preparedness for Infusion and Hypersensitivity Reactions. *Oncologist* (2007) 12(5):601–9. doi: 10.1634/theoncologist.12-5-601
94. Comer H, Cardwell K. Brentuximab Vedotin Infusion Reaction Management: A Case Study. *J Adv Pract Oncol* (2017) 8(6):626–9.
95. Roselló S, Blasco I, García Fabregat L, Cervantes A, Jordan K. Management of Infusion Reactions to Systemic Anticancer Therapy: ESMO Clinical Practice Guidelines. *Ann Oncol* (2017) 28(suppl_4):iv100–18. doi: 10.1093/annonc/mdx216
96. Muntyanu A, Netchiporouk E, Gerstein W, Gniadecki R, Litvinov IV. Cutaneous Immune-Related Adverse Events (irAEs) to Immune Checkpoint Inhibitors: A Dermatology Perspective on Management [Formula: See Text]. *J Cutan Med Surg* (2021) 25(1):59–76. doi: 10.1177/1203475420943260
97. Soliman YS, Hashim PW, Farberg AS, Goldenberg G. The Role of Diet in Preventing Photoaging and Treating Common Skin Conditions. *Cutis* (2019) 103(3):153–6.
98. Jackson P, Vigiola Cruz M. Intestinal Obstruction: Evaluation and Management. *Am Fam Phys* (2018) 98(6):362–7.
99. Whelan K, Schneider SM. Mechanisms, Prevention, and Management of Diarrhea in Enteral Nutrition. *Curr Opin Gastroenterol* (2011) 27(2):152–9. doi: 10.1097/MOG.0b013e32834353cb
100. Prichard DO, Bharucha AE. Recent Advances in Understanding and Managing Chronic Constipation. *F1000Res* (2018) 7:1640. doi: 10.12688/f1000research.15900.1
101. Lane JM, Russell L, Khan SN. Osteoporosis. *Clin Orthop Relat Res* (2000) 372):139–50. doi: 10.1097/00003086-200003000-00016
102. Spain L, Diem S, Larkin J. Management of Toxicities of Immune Checkpoint Inhibitors. *Cancer Treat Rev* (2016) 44:51–60. doi: 10.1016/j.ctrv.2016.02.001
103. Miller PD. Management of Severe Osteoporosis. *Expert Opin Pharmacother* (2016) 17(4):473–88. doi: 10.1517/14656566.2016.1124856
104. Zimmer L, Goldinger SM, Hofmann L, Loquai C, Ugurel S, Thomas I, et al. Neurological, Respiratory, Musculoskeletal, Cardiac and Ocular Side-Effects of Anti-PD-1 Therapy. *Eur J Cancer* (2016) 60:210–25. doi: 10.1016/j.ejca.2016.02.024
105. Cohen SP, Raja SN. Pathogenesis, Diagnosis, and Treatment of Lumbar Zygapophysial (Facet) Joint Pain. *Anesthesiology* (2007) 106(3):591–614. doi: 10.1097/00000542-200703000-00024
106. Makarious D, Horwood K, Coward JIG. Myasthenia Gravis: An Emerging Toxicity of Immune Checkpoint Inhibitors. *Eur J Cancer* (2017) 82:128–36. doi: 10.1016/j.ejca.2017.05.041
107. Haanen J, Carbonnel F, Robert C, Kerr KM, Peters S, Larkin J, et al. Management of Toxicities From Immunotherapy: ESMO Clinical Practice Guidelines for Diagnosis, Treatment and Follow-Up. *Ann Oncol* (2017) 28 (suppl_4):iv119–42. doi: 10.1093/annonc/mdx225
108. Foxman B. Urinary Tract Infection Syndromes: Occurrence, Recurrence, Bacteriology, Risk Factors, and Disease Burden. *Infect Dis Clin North Am* (2014) 28(1):1–13. doi: 10.1016/j.idc.2013.09.003
109. Avellino GJ, Bose S, Wang DS. Diagnosis and Management of Hematuria. *Surg Clin North Am* (2016) 96(3):503–15. doi: 10.1016/j.suc.2016.02.007
110. Stevens PE, Levin A. Evaluation and Management of Chronic Kidney Disease: Synopsis of the Kidney Disease: Improving Global Outcomes 2012 Clinical Practice Guideline. *Ann Intern Med* (2013) 158(11):825–30. doi: 10.7326/0003-4819-158-11-201306040-00007
111. Chenoweth CE, Gould CV, Saint S. Diagnosis, Management, and Prevention of Catheter-Associated Urinary Tract Infections. *Infect Dis Clin North Am* (2014) 28(1):105–19. doi: 10.1016/j.idc.2013.09.002
112. Wick W, Hertenstein A, Platten M. Neurological Sequelae of Cancer Immunotherapies and Targeted Therapies. *Lancet Oncol* (2016) 17(12): e529–41. doi: 10.1016/S1470-2045(16)30571-X
113. Wang ML, Rivlin M, Graham JG, Beredjiklian PK. Peripheral Nerve Injury, Scarring, and Recovery. *Connect Tissue Res* (2019) 60(1):3–9. doi: 10.1080/03008207.2018.1489381
114. Dan K. [Drug-Induced Anemia]. *Nihon Rinsho* (2008) 66(3):540–3.

115. Lisman T, Intagliata NM. Bleeding and Thrombosis in Patients With Liver Diseases. *Semin Thromb Hemost* (2020) 46(6):653–5. doi: 10.1055/s-0040-1715453
116. Johnstone C, Rich SE. Bleeding in Cancer Patients and its Treatment: A Review. *Ann Palliat Med* (2018) 7(2):265–73. doi: 10.21037/apm.2017.11.01
117. Moik F, Ay C. How I Manage Cancer-Associated Thrombosis. *Hamostaseologie* (2020) 40(1):38–46. doi: 10.1055/s-0039-3402806
118. Jany B, Welte T. Pleural Effusion in Adults-Etiology, Diagnosis, and Treatment. *Dtsch Arztebl Int* (2019) 116(21):377–86. doi: 10.3238/arztebl.2019.0377
119. Skřičková J. [Pneumonia in Immunocompromised Persons]. *Vnitr Lek* (2018) 63(11):786–95.
120. Beaudoin S, Gonzalez AV. Evaluation of the Patient With Pleural Effusion. *Cmaj* (2018) 190(10):E291–e295. doi: 10.1503/cmaj.170420
121. Stein PD. Acute Pulmonary Embolism. *Dis Mon* (1994) 40(9):467–523.
122. Perelas A, Silver RM, Arrossi AV, Highland KB. Systemic Sclerosis-Associated Interstitial Lung Disease. *Lancet Respir Med* (2020) 8(3):304–20. doi: 10.1016/S2213-2600(19)30480-1
123. Sznol M, Postow MA, Davies MJ, Pavlick AC, Plimack ER, Shaheen M, et al. Endocrine-Related Adverse Events Associated With Immune Checkpoint Blockade and Expert Insights on Their Management. *Cancer Treat Rev* (2017) 58:70–6. doi: 10.1016/j.ctrv.2017.06.002
124. Varricchi G, Marone G, Mercurio V, Galdiero MR, Bonaduce D, Tocchetti CG. Immune Checkpoint Inhibitors and Cardiac Toxicity: An Emerging Issue. *Curr Med Chem* (2018) 25(11):1327–39. doi: 10.2174/0929867324666170407125017
125. Brieler J, Breeden MA, Tucker J. Cardiomyopathy: An Overview. *Am Fam Phys* (2017) 96(10):640–6.
126. Figueroa MS, Peters JI. Congestive Heart Failure: Diagnosis, Pathophysiology, Therapy, and Implications for Respiratory Care. *Respir Care* (2006) 51(4):403–12.
127. Cooper LTJr. Myocarditis. *N Engl J Med* (2009) 360(15):1526–38. doi: 10.1056/NEJMra0800028
128. Zhang J, Zhang Q, Chen X, Zhang N. Management of Neoplastic Pericardial Disease. *Herz* (2020) 45(Suppl 1):46–51. doi: 10.1007/s00059-019-4833-4

Conflict of Interest: The authors declare that the research was conducted in the absence of any commercial or financial relationships that could be construed as a potential conflict of interest.

Publisher's Note: All claims expressed in this article are solely those of the authors and do not necessarily represent those of their affiliated organizations, or those of the publisher, the editors and the reviewers. Any product that may be evaluated in this article, or claim that may be made by its manufacturer, is not guaranteed or endorsed by the publisher.

frontiers | Frontiers in Oncology

REVIEW
published: 24 May 2022
doi: 10.3389/fonc.2022.877379

From Therapy Resistance to Targeted Therapies in Prostate Cancer

Filipa Moreira-Silva[1], *Rui Henrique*[1,2,3] *and Carmen Jerónimo*[1,3*]

[1] Cancer Biology and Epigenetics Group, Research Center of IPO Porto (CI-IPOP)/RISE@CI-IPOP (He-alth Research Network), Portuguese Oncology Institute of Porto (IPO Porto)/Porto Comprehensive Cancer Centre (Porto.CCC), Porto, Portugal, [2] Department of Pathology, Portuguese Oncology Institute of Porto (IPO Porto), Porto, Portugal, [3] Department of Pathology and Molecular Immunology, School of Medicine and Biomedical Sciences of the University of Porto (ICBAS-UP), Porto, Portugal

Prostate cancer (PCa) is the second most common malignancy among men worldwide. Although early-stage disease is curable, advanced stage PCa is mostly incurable and eventually becomes resistant to standard therapeutic options. Different genetic and epigenetic alterations are associated with the development of therapy resistant PCa, with specific players being particularly involved in this process. Therefore, identification and targeting of these molecules with selective inhibitors might result in anti-tumoral effects. Herein, we describe the mechanisms underlying therapy resistance in PCa, focusing on the most relevant molecules, aiming to enlighten the current state of targeted therapies in PCa. We suggest that selective drug targeting, either alone or in combination with standard treatment options, might improve therapeutic sensitivity of resistant PCa. Moreover, an individualized analysis of tumor biology in each PCa patient might improve treatment selection and therapeutic response, enabling better disease management.

Keywords: prostate cancer, castration-resistant prostate cancer, therapy resistance, targeted therapies, epigenetics

OPEN ACCESS

Edited by:
Bianca Nitzsche, Charité Universitätsmedizin Berlin, Germany

Reviewed by:
Remi Adelaiye-Ogala, University at Buffalo, United States
Guru Sonpavde, Dana–Farber Cancer Institute, United States

***Correspondence:**
Carmen Jerónimo
carmenjeronimo@ipoporto.min-saude.pt

Specialty section:
This article was submitted to Genitourinary Oncology, a section of the journal Frontiers in Oncology

Received: *16 February 2022*
Accepted: *25 April 2022*
Published: *24 May 2022*

Citation:
Moreira-Silva F, Henrique R and Jerónimo C (2022) From Therapy Resistance to Targeted Therapies in Prostate Cancer. Front. Oncol. 12:877379. doi: 10.3389/fonc.2022.877379

INTRODUCTION

Currently, prostate cancer (PCa) constitutes the second most common malignancy and the fifth leading cause of cancer-related death in men, worldwide (1). PCa is a highly heterogeneous disease (2), characterized by several genetic and epigenetic alterations (2, 3), some of which can be used to assist treatment decision-making (3). Localized disease arises from luminal cells' proliferation (2),

Abbreviations: AR, androgen receptor; AR-fl, androgen receptor full length; AR-V, androgen receptor variant; ADT, androgen-deprivation therapy; ARE, androgen-responsive elements; BET, bromodomain and extra-terminal motif; CAFs, cancer-associated fibroblasts; CRPC, castration resistant prostate cancer; DHT, dihydrotestosterone; DNMTs, DNA methyltransferases; EGF, epidermal growth factor; EMT, epithelial mesenchymal transition; EBRT, external beam radiotherapy; FGF, fibroblast growth factor; FDA, Food and Drug Administration; GR, glucocorticoid receptor; GF, growth factors; HATs, histone acetyltransferases; HDACs, histone deacetylases; HDMs, histone demethylases; HMTs, histone methyltransferases; IGF-1, insulin-like growth-factor-1; KGF, keratinocyte growth factor; LBD, ligand-binding domain; LHRH, luteinizing hormone-releasing hormone; MDSCs, myeloid-derived suppressor cells; NEPC, neuroendocrine prostate cancer; N.a., not applicable; PCa, Prostate cancer; PSA, prostate-specific antigen; RT, radiation therapy; RP, radical prostatectomy; RTK, receptor tyrosine kinase; T, testosterone; TF, transcript factors; TME, tumor microenvironment.

being characterized by a slow growth and hormone-responsiveness, more common in elderly men (3). At the time of diagnosis, 80% of all the tumors are confined to the prostate gland (2) and roughly 50% harbor the well-known gene fusion *TMPRSS2:ERG* (3–5), implicated in PI3K signaling pathway aberrant activation (3, 6), *AR* overexpression, *PTEN* loss (6) and deregulation of epigenetic players' encoding genes (3). Genetic alterations might also occur, specifically in *SPOP, TP53, ATM, MED12* and *FOXA1* genes (3). Furthermore, epigenetics also plays a role in prostate carcinogenesis, with DNA hypermethylation as one of the first alterations observed at low stages (7). Herein, one of the most well-known promotor's hypermethylated gene is the *GSTP1*, which occurs in 90% of the tumors (8). Interestingly, this alteration is also observed in 50% of the PCa precursor lesions, suggesting this as an early event in prostate carcinogenesis (8). Additionally, histone deacetylases (HDACs) overexpression frequently detected in high-grade disease, particularly HDAC1 and HDAC2, has been associated with increased cell proliferation (9).

In locally advanced PCa, tumor cells invade the extra-prostatic tissue and/or metastasize to regional lymph nodes, paving the way to metastatic dissemination at distant organs, most commonly to the bones, liver, and lungs (2). Several genome-wide copy-number alterations have been observed, particularly *MYC* overexpression and *PTEN* and *SMAD4* deletion, which drives genomic instability and tumor progression (3). Specific epigenetic alterations similarly drive PCa progression, including EZH2 overexpression (2), *RASSF1A* promoter methylation (10) and overall hypomethylation (11).

Eventually, in due course of disease, PCa becomes resistant to androgen-deprivation therapy (ADT) – castration resistant PCa (CRPC) – disclosing raising serum PSA levels and/or clinical/imagiological tumor progression despite testosterone castrate levels (12). Interestingly, alterations in *AR*, *TP53*, *PTEN*, *RB1*, *ETS2*, DNA repair and chromatin and histone modifying genes are commonly found in CRPC (13–15). Moreover, it is observed amplification of the AR co-activator *NCOA2* and deletion of the AR co-repressor *LATS2* (13, 15). Furthermore, high DNA methylation levels (15), and overexpression of HDAC1, HDAC2, HDCA3, EZH2 (16), G9a (17) and LSD1 (18) have also been associated with CRPC.

Approximately 17% of tumors from CRPC patients eventually become AR indifferent (19, 20), progressing to a neuroendocrine PCa (NEPC) state, that does not respond to hormone therapy (19). NEPC harbors several genetic alterations, including *TMPRSS2:ERG* fusion, *MYC* and *AKT* overexpression, *PTEN* and *RB1* loss, and *TP53* mutations (2, 12, 21, 22). Moreover, epigenetic alterations, such as DNA hypermethylation as well as EZH2 and bromodomain and extra-terminal motif (BET) proteins overexpression have been found in NEPC (12).

Standard of Care in Prostate Cancer Treatment

Clinical parameters and tumor stage are crucial for therapy decision making in PCa, with therapeutic recommendations varying for each stage (**Figure 1**) (23, 24). For localized disease, several possibilities exist, including active surveillance and curative-intent strategies (radical prostatectomy (RP), external beam radiotherapy (EBRT) and brachytherapy) (24, 25). Additionally, for the subset of high-risk localized PCa, neoadjuvant and concurrent ADT may be considered (25). Nevertheless, in approximately 30% of cases that undergo curative-intent treatment, disease progression develops, accompanied with lymph node invasion and/or metastatic dissemination. For these patients, ADT with luteinizing hormone-releasing hormone (LHRH) agonists, anti-androgens, or surgical castration is recommended (26–29). Initially, ADT typically leads to 90-95% decrease in circulating androgen levels,

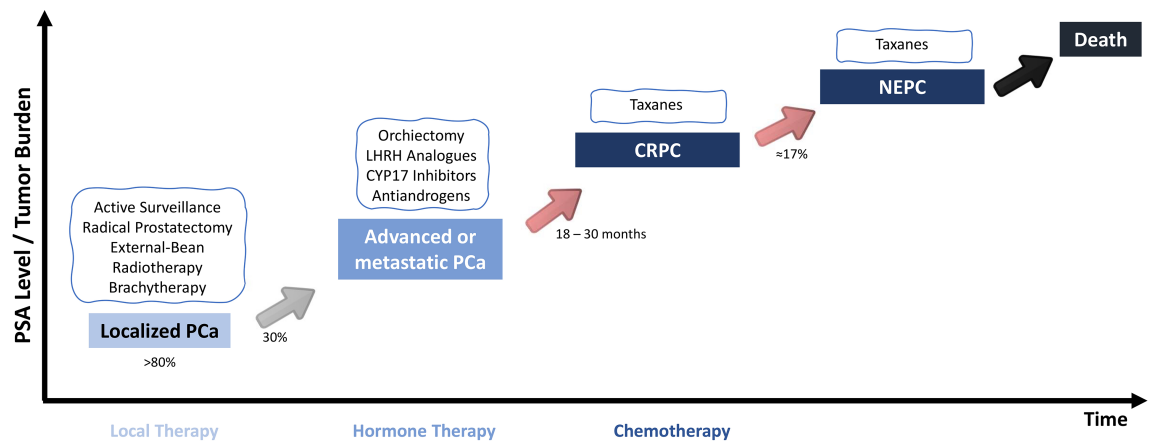

FIGURE 1 | Standard of care for the different PCa stages. For Localized PCa, RP is the interventional standard of care. On the other hand, for advanced and metastatic disease, ADT is the recommended treatment. However, nearly all patients stop responding ADT and progress to a CRPC, for which there are no effective treatment options. Moreover, about 17% of the patients with a castration-resistant form of the disease will develop neuroendocrine differentiation, which is independent of AR signaling pathway. PSA, prostate-specific antigen; PCa, prostate cancer; CRPC, castration-resistant prostate cancer; NEPC, neuroendocrine prostate cancer.

being complemented by a 50% decrease in intraprostatic dihydrotestosterone (DHT) and AR inhibition (30), impairing tumor cells' survival (26, 28). However, within 18-30 months, cancer cells eventually become resistant to the different castration strategies (31). For CRPC, although no curative options are available, docetaxel is recommended for disease management (25). Moreover, it was reported that patients might also benefit from bicalutamide and low dose corticosteroids, which were found to control PSA levels and improve symptoms, although no increase in overall survival was depicted (32). In the beginning of 2022, the Food and Drug Administration (FDA) approved the use of the novel Novartis Pluvicto™ - Lu^{177} vipivotide tetraxetan – for the treatment of progressive, PSMA-positive metastatic CRPC (33). This novel approach, in combination with the standard of care, decreased the death risk, improved overall survival and progression-free survival of these subset of patients (33). Neuroendocrine differentiation of tumor cells is observed in 17% of CRPC patients and only palliative options are proposed for this disease state (34).

Considering PCa disease progression, herein we intent to describe the mechanisms involved in therapy resistance in PCa, highlighting new potential drug targets.

Resistance Mechanisms

During treatment of advanced and metastatic PCa, most patients develop resistance to ADT (31, 35) and although this process is not fully understood, several mechanisms were reported to be involved in the acquisition of the castration-resistant state (**Figure 2**). Regardless of castrate levels of testosterone, tumor cells can proliferate due to clonal selection of cells with AR amplification (36). Thus, an enhanced number of receptors may bind to the vestigial androgens in circulation, maintaining AR signaling (36). Moreover, gain-of-function and point mutations in *AR* results in increased activation and decreased specificity, respectively, both resulting in tumor cell survival (37–39). Decreased AR specificity allows for growth factor-induced activation (39), through insulin-like growth-factor-1 (IGF-1), keratinocyte growth factor (KGF), epidermal growth factor (EGF) (37), and fibroblast growth factor (FGF) (40). Similarly, these growth factors also bind receptor tyrosine kinase (RTK), which can regulate AR activity (38, 40). RTK and their intracellular signaling pathways play an important role in CRPC cells' proliferation and, among these, the ERBB family (41), PI3K (5), ERK1/2 (42), Src (43), ROR-γ (44) and the glucocorticoid receptor (GR) (45) were found hyperactivated in CRPC (41, 46). Cytokines such as TNFα, IL-6 and IL-23 have been additionally suggested to modulate AR. TNFα was shown to bind to its receptor and activate NF-kB signaling pathway (47), whereas IL-6 was involved in MAPK cascades activation (48), both triggering AR signaling. Calcinotto *et al.* further reported that IL-23, secreted by myeloid-derived suppressor cells (MDSCs), activates the STAT3-RORγ pathway, by binding to IL-23R on tumor cell surface, culminating in AR

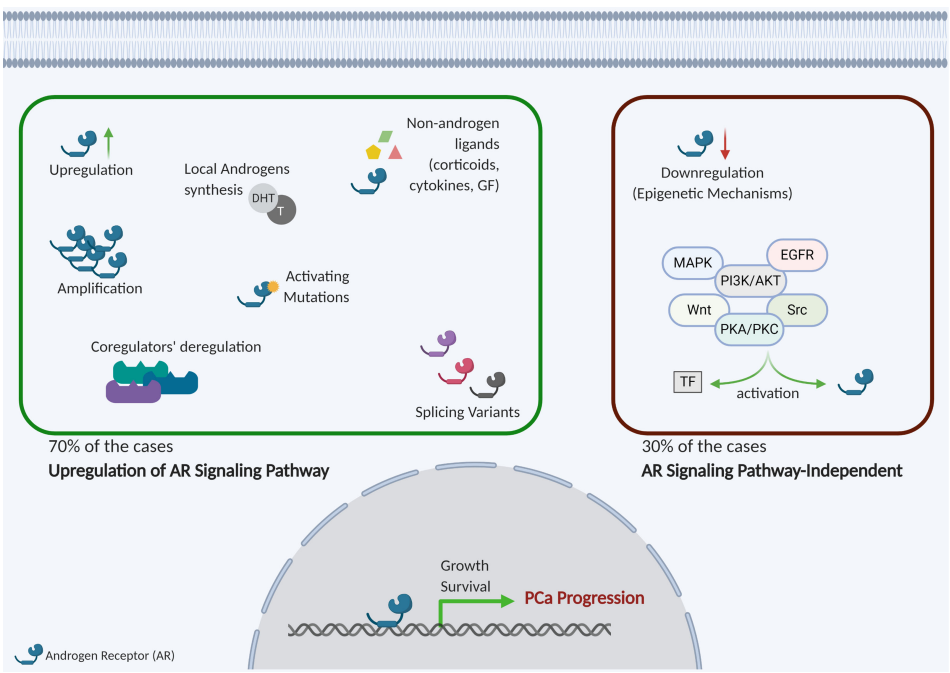

FIGURE 2 | Mechanisms of resistance to androgen deprivation therapy. The process underlying ADT resistance and CRPC development involve, in 70% of the cases, upregulation of AR signaling pathway. In this case, upregulation of AR expression, amplification or activating mutations, AR splice variants, promiscuous AR activation by non-androgen ligands and deregulation of AR coactivators and co-repressors is observed. On the other hand, in 30% of the cases there is AR expression downregulation and activation of other signaling pathways involved in cell survival and growth activation. AR, androgen receptor; T, testosterone; DHT, dihydrotestosterone; GF, growth factors: TF, transcript factors. Created with BioRender.com.

activation (49). Subsequently, AR binds to androgen-responsive elements (ARE) on DNA, and in association with different co-regulators, promotes gene expression (50). Importantly, when binding occurs in DNA repair genes' regulatory regions, especially of *PARP1*, *Ku-70*, *Ku-80* (51) and *TOP2B* (52), genomic rearrangements and DNA double stranded breaks may occur (53). The well-known *TMPRSS2:ERG* fusion can interact with the DNA repair protein and AR co-regulator PARP1, mediating transcription, invasion, and metastization (54). In AR-positive cells, GATA2, under the NOTCH family regulation, acts as an AR co-activator, maintaining AR signaling (55). Furthermore, different AR variants derived from alternative splicing have been shown to be involved in the acquisition of androgen-independent state (56). In CRPC, the most well described is the constitutively active AR-V7, which lacks the ligand-binding domain (LBD) and has an effective role in activating transcription (57). Epigenetic aberrations also contribute to post-ADT progression. In 30% of CRPC cases, *AR* expression might be completely lost and hypermethylation and histone post-translational modifications seem to be implicated in this process (2, 58, 59).

After resistance to first-line ADT, second generation anti-androgens (e.g., enzalutamide, abiraterone acetate) were found to improve survival of CRPC patients. Nonetheless, tumor cells eventually become resistant due to AR signaling reactivation (60). A specific kinase, AURKA, which is involved in chromosome instability, was found overexpressed in AR-positive CRPC cells (60). Kivinummi and colleagues showed that AURKA expression was directly targeted by androgens, with the AR specifically binding to the gene regulatory regions, resulting in reduced progression-free survival (60).

For patients harboring CRPC, taxane-based chemotherapy is the only therapeutic option which increases survival. However, patients eventually become resistant to docetaxel treatment (61). Cancer cells expressing *Mdr1* might be selected after therapy pressure, leading to decreased docetaxel intracellular intake (62). Moreover, alterations in microtubule-associated proteins' expression result in decreased docetaxel efficacy (63). Indeed, tubulin isoform βIII overexpression correlated with docetaxel resistance in CRPC (63, 64).

Although recently approved (33), approximately 1/3 of the PSMA-positive CRPC patients do not benefit from the Lu^{177} vipivotide tetraxetan PSMA-based targeting (65, 66). Several studies have already pinpointed the PSMA heterogenic expression, defect on DNA repair genes, clonal expansion of PSMA-negative cells and tumor heterogeneity as possible mechanism of resistance (66). A particular work reported, in a mouse model, that TP53-negative tumors were less responsive to treatment, compared to TP53 wild-type tumor-bearing mice, highlighting a potential resistance mechanism (65) and a need for assessing resistance in further studies.

Furthermore, tumor microenvironment (TME) has been shown to be an important driver of resistance to ADT and taxane-based chemotherapy. The stromal component might promote CRPC progression through vascularization, apoptosis inhibition and epithelial mesenchymal transition (EMT) promotion (67). Specifically, cancer-associated fibroblasts (CAFs) are known to stimulate mesenchymal phenotype through αSMA (68), and besides promoting cancer progression through EMT-related mechanisms, TGFβ-dependent activation leads to growth factor secretion and sustainment of cancer cells survival (69).

METHODS

A PubMed search was carried out, using the query (AR mutations OR AR variants OR γ-secretase inhibitor OR HERB inhibitor OR PI3K inhibitor OR AKT inhibitor OR mTOR inhibitor OR glucocorticoid receptor inhibitor OR ROR inhibitor OR IGFR inhibitor OR MAPK inhibitor OR AUKRA inhibitor OR Scr inhibitor OR MET inhibitor OR STAT3 inhibitor OR IL-23 antibody OR TOP2 inhibitor OR BET inhibitor OR HAT inhibitor OR HDAC inhibitor OR HMT inhibitor OR HDM inhibitor OR DNMT inhibitor) AND (prostate cancer), with the time interval from 2010 to 2022. Additionally, 23 research articles prior to 2010 covering relevant data were included. Only original research articles, written in English, and those including *in vitro* and/or *in vivo* pre-clinical studies reporting drug screening assays in prostate cancer were considered. The records were imported to the reference manager EndNote. Subsequently, all abstracts were critically evaluated and only those providing relevant information for the present topic were selected. Our aim was to address the recently reported targeted therapies and potential combinations that may improve disease management and care in PCa patients.

A summary of the methodology is provided in **Figure 3**.

TARGETED THERAPIES

Having in mind that the aforementioned molecular alterations may account for PCa therapy resistance, we focused on the development and pre-clinical screening of new and effective targeted therapies enabling Precision Medicine. Hence, we aimed to emphasize the current state of targeted therapies' screening in PCa, unveiling their potential clinical use.

Potential Targets for PCa Management

Because AR-dependent mechanisms are associated with 70% of ADT-resistant PCa cases (2), targeting the AR itself, its splicing variants or the associated co-regulators might have substantial therapeutic impact in CRPC. In the past few years, drug targeting of AR mutants, variants, and co-regulators has been shown to have anti-tumoral effects in AR-positive CRPC cells (**Table 1**). Galeterone, a CYP17A1 inhibitor, causes AR T878A mutant degradation and blocks transcription of AR target genes (70), whereas niclosamide induces AR-V7 protein degradation (75). This new AR target approach is under evaluation in clinical trials enrolling PCa patients (**Supplementary Table 1**). Nevertheless, for most of the described drugs, the anti-neoplastic effect was based on AR N-terminal blocking or AR splicing inhibition, ultimately impairing AR-driven PCa cell proliferation (**Table 1**

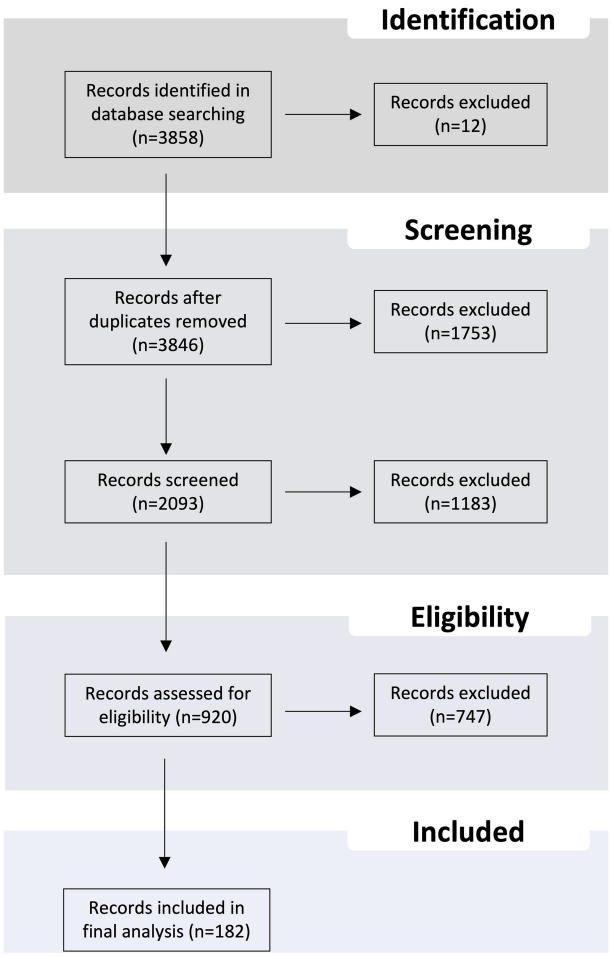

FIGURE 3 | Flux gram presenting the summary of the methodology used in this review.

and **Supplementary Table 1**). Additionally, indirect AR inhibition might be achieved by diminishing the activity of the positive co-regulators of the receptor transcription activity, such as GATA2 and ONECUT2 (**Table 1**), whose inhibition was reported to not only reduce cell proliferation (**Supplementary Table 1**), but also synergize with ADT agents (80, 81, 83) and docetaxel (82), displaying enhanced efficacy.

Conversely, 30% of the advanced and metastatic PCa cases progress due to AR bypass mechanisms, which allow tumor cells to survive in an AR-independent manner (2). As previously described, a significant proportion of the bypass is based on RTK intracellular signaling activation, that constitutes a putative therapy target in resistant PCa (2). Many of the existent pre-clinical studies target the HerbB family, PI3K, mTOR, Akt, GR, RORγ, IGFR, MAPK, Src and STAT3 (**Table 1** and **Supplementary Table 1**). Generally, drug treatment inhibited the specific target activity, reduced tumor cell proliferation and viability, and promoted apoptosis (**Supplementary Table 1**), displaying anti-tumoral effects both *in vitro* and *in vivo*.

Nonetheless, as reported for the drugs that target AR co-regulators, the most promising results were achieved when combining a targeted therapy with the standard therapy strategies. For example, the Akt inhibitor ipatasertib, under test in clinical studies in PCa (**Supplementary Table 1**), re-sensitized CRPC cells to antiandrogens, when combined with enzalutamide, inducing apoptosis, and leading to remarkable tumor cell growth inhibition, both *in vitro* and *in vivo* (114). Gefitinib (89), BEZ235 (110), RAD001 (124) or RU486 (131) were also reported to re-sensitize resistant cells to standard chemotherapy agents (**Supplementary Table 1**). Interestingly, CUDC-907 (101), CB-03-10 (130) and MP470 (135), in addition to selective RTK inhibition, were found to inhibit HDAC6, AR and EGFR, respectively. These drugs caused cytotoxic effects in resistant cells (**Supplementary Table 1**), indicating a possible benefit of targeting multiple pathways for management of resistant PCa.

Although most of the drugs listed in **Table 1** have demonstrated good therapeutic potential, in some cases a possible resistant mechanism was also identified. The PI3K inhibitor CUDC-907

TABLE 1 | Potential targets and drugs for the management of therapy resistant prostate cancer.

Target	Drug	Mechanism of action	Combination	References
AR mutations	Galeterone	AR T878A mutant degradation	N.a.	(70)
AR variants	EPI-506	Inhibits AR N-terminal domain	BEZ235 (PI3K/Akt inhibitor)	(71, 72)
	EPI-001		N.a.	(73, 74)
	Niclosamide	AR-V7 degradation	N.a.	(75)
	Thailanstatins	Inhibits AR splicing	N.a.	(76, 77)
	Peptidomimetic D2	Targets the transactive domain of AR-V	N.a.	(78)
	ONC201/TIC10	Targets AR-fl and AR-V7	Enzalutamide, docetaxel, everolimus (mTOR inhibitor)	(79)
Co-regulators	RO4929097	inhibits γ-secretase, impairing AR co-activator	Abiraterone	(75, 80)
	PF-3084014/PF-03084014/nirogacestat	GATA2 activity	Standard ADT, docetaxel	(80–82)
	DAPT/GSI-IX		Abiraterone	(80, 83, 84)
	BMS-708163/avagacestat		Enzalutamide	(80)
	CSRM617	inhibits ONECUT2 function	N.a.	(85)
Bypass Signaling	PKI 166	HerB1 and ErbB2 inhibitor	STI571 (PDGFR inhibitor), paclitaxel	(86–88)
	ZD1839/gefitinib		Enzalutamide, paclitaxel, ERK1/2 and PI3K inhibitors	(89–96)
	3BrQuin-SAHA & 3ClQuin-SAHA	EGFR inhibitor	N.a.	(97)
	Spautin-1		Standard ADT	(98)
	ZINC05463076 or ZINC2102846 or ZINC19901103		N.a.	(99)
	PD168393		N.a.	(100)
	CUDC-907	PI3K inhibitor	N.a.	(101)
	BAY1082439		N.a.	(102, 103)
	SF2523		N.a.	(104)
	LASSBio-2208		N.a.	(105)
	ZSTK474		N.a.	(106, 107)
	isorhamnetin		N.a.	(108)
	4-Acetylantroquinonol B		N.a.	(109)
	BEZ235/dactolisib	Dual PI3K and mTOR inhibitor	Docetaxel	(110–113)
	GDC-0068/Ipatasertib	AKT inhibitor	Enzalutamide	(114–116)
	MK-2206		N.a.	(117, 118)
	AZD5363		Standard ADT	(119–122)
	GNE-493		N.a.	(123)
	RAD001/everolimus	mTOR inhibitor	Docetaxel	(124–127)
	MK-2206	AKT and mTOR dual inhibitor	MK-8669	(128, 129)
	CB-03-10	Glucocorticoid receptor inhibitor	N.a.	(130)
	RU486/mifepristone		Docetaxel	(131–133)
	XY018	RORγ inhibitor	N.a.	(134)
	GSK805		N.a.	(134)
	SR2211		N.a.	(134)
	MP470/amuvatinib	RTK inhibitor	Erlotinib (EGFR inhibitor)	(135)
	GSK1838705A	IGFR1 inhibitor	N.a.	(136)
	NVP-AEW541		N.a.	(137)
	AZ12253801		N.a.	(138)
	PD325901/mirdametinib	MAPK/ERK inhibitor	N.a.	(139)
	U0126	MEK/ERK inhibitor	N.a.	(140)
	MLN8237/alisertib	AUKRA inhibitor	N.a.	(60)
	BMS-354825/dasatinib	Src inhibitor	BMS-754807 (IGF1 inhibitor)	(141–147)
	AZD0530/saracatinib		N.a.	(148, 149)
	SKI-606/bosutinib		N.a.	(150)
	BMS-777607	c-MET inhibitor	N.a.	(151, 152)
	GPB730	STAT3 inhibitor	Anti-CTLA-4	(153)
	Acacetin		N.a.	(154)
	GAP500/galiellalactone		Standard ADT	(155–157)
	EC-70124		N.a.	(158)
Cytokines	G23-8	Antibody against IL-23	Enzalutamide	(49)
DNA repair pathway	AZD-2281/olaparib	PARP inhibitor	N.a.	(159–162)
	ABT-888/veliparib		N.a.	(163, 164)
	AZD2461		N.a.	(165, 166)
	Rucaparib		N.a.	(167)
	VP-16/etoposide phosphate	TOP2 inhibitor	N.a.	(168)

N.a., not applicable; ADT, androgen deprivation therapy; AR-fl, androgen receptor full length; AR-V, androgen receptor variant.

resulted in increased phospo-ERK levels (101), whereas PD325901, by inhibiting the ERK pathway, induced hyperactivation of the pro-proliferative PI3K and hedgehog pathways (139). In both studies, compensatory signaling mechanisms were suggested as the cause of resistance, thus, reinforcing the benefit of combinatory strategies to enhance anti-tumoral effects.

Furthermore, the combination of standard radiation therapy and PARP inhibitors was shown to have a significant effect on tumor cells viability (**Table 1** and **Supplementary Table 1**). Specifically, veliparib (163) and rucaparib (167), two drugs under clinical investigation in PCa (**Supplementary Table 1**), were shown to re-sensitize CRPC cells to radiotherapy, impairing tumor cell growth. Moreover, this class of inhibitors similarly synergized with ADT agents (159, 160), AUKRA inhibitors (161) and epi-drugs (164, 165), with improved anti-neoplastic effects.

Targeting Epigenetics for PCa Treatment

Epigenetic alterations have been recognized as a hallmark of cancer (169), and since it comprises reversible modifications (59), there is a potential for drug targeting. FDA has approved two drugs that target epigenetic players, 5-azacytidine and 5-aza-2′-deoxycytidine, for myelodysplastic syndrome treatment (170). These two drugs, as DNA methyltransferases (DNMTs) inhibitors, are incorporated into DNA, inhibiting DNMT activity and decreasing global methylation levels (171, 172). Nevertheless, there is a potential for targeting the entire epigenetic machinery in cancer treatment, as we have previously reported (173). In therapy resistant PCa, histone acetyltransferases (HATs), HDACs, histone demethylases (HDMs), histone methyltransferases (HMTs), BET, and DNMTs inhibitors are currently under pre-clinical and clinical studies (**Table 2** and **Supplementary Table 2**), displaying anti-tumoral effects, mostly due to enzyme inhibition

TABLE 2 | Potential epigenetic targets and epi-drugs for the management of therapy resistant prostate cancer.

Target	Drug	Mechanism of action	Combination	References
BET	OTX015/MK-8628/birabresib	BRD2/3/4 inhibitor	N.a.	(174)
	JQ1	BRD4 inhibitor	N.a.	(175–182)
	GSK1210151A		N.a.	(180)
	Y08060		N.a.	(183)
	CPI-203		N.a.	(184)
	AZD5153		N.a.	(185)
	I-BET151		N.a.	(180)
	SF2523		N.a.	(104)
	WWL0245		N.a.	(186)
	I-BET762/molibresib	BET inhibitor	N.a.	(187)
	ZEN-3694		Enzalutamide	(188, 189)
	ABBV-744		N.a.	(190)
	Y06014		N.a.	(191)
	NEO2734		N.a.	(192)
	dBET6	BET protein degradation	N.a.	(175)
HAT	A-485	CBP/p300 inhibitor	N.a.	(193)
	CCS1477		N.a.	(194)
	Y08197		N.a.	(195)
	I-CBP112		A-485	(196)
HDAC	Trichostatin A/TSA	HDAC I and II inhibitor	Bortezomib (proteosome inhibitor), chemotherapy	(197–202)
	Panobinostat/LBH-589	Pan HDAC inhibitor	Hydralazine (DNMT inhibitor), RT, zoleronic acid	(203–208)
	Vorinostat/SAHA	HDAC I inhibitor	Bicalutamide, docetaxel	(209–212)
	MHY219		N.a.	(213, 214)
	Jazz90 & Jazz167	HDAC inhibitor	N.a.	(215, 216)
	CG200745		Docetaxel	(217)
	MHY4381		N.a.	(218)
	Valproic Acid/VPA		N.a.	(5, 17, 219, 220)
	A248		N.a.	(221)
	MPT0B451		N.a.	(222)
	2-75	HDAC 6 inhibitor	N.a.	(223)
HMT	GSK-343	EZH2 inhibitor	Standard ADT, metformin	(224)
	Tazemetostat/EPZ-6438		N.a.	(225)
	GSK-926		N.a.	(226)
	LG1980		N.a.	(227)
	GSK-126		N.a.	(228–231)
HDM	NCL1	LSD1 inhibitor	Docetaxel	(232, 233)
	HCI-2509		N.a.	(234)
DNMT	5-AZA-2'-deoxycytidine/decitabine	DNMT inhibitor	Sodium butyrate	(171, 235–240)
	5-azacytidine/azacytidine		Standard ADT	(172, 241)
	RG108		N.a.	(242)
	Hydralazine		Panabinostat	(204)

N.a., not applicable; ADT, androgen deprivation therapy; BET, Bromodomain and Extra-Terminal motif; HAT, histone acetyltransferase; HDAC, histone deacetylase; HMT, histone methyltransferase; HDM, histone demethylase; DNMT, DNA methyltransferase; RT, radiation therapy.

and gene expression reprograming (**Supplementary Table 2**). Interestingly, the most promising results were found when epi-drugs were combined with standard ADT compounds (188, 209, 224, 228, 229, 241, 243), docetaxel (175, 197, 210, 217, 234), radiation therapy (203) or other epi-drugs (196, 204, 235), suggesting an interplay between epigenetic and non-epigenetic targeting in PCa management.

Remarkably, BET inhibitors such as JQ1, GSK1210151A and I-BET151 were found to decrease AR-fl and AR-V7 expression and activity (**Supplementary Table 2**), demonstrating a potential to be used with both an epigenetic- and AR-targeting purpose. However, disadvantageous off-target effects were observed after JQ1 treatment. JQ1 was found to promote PCa cell invasion and metastatic potential due to FOXA1 inactivation in a BET-independent manner (176). Therefore, high *FOXA1* expression tumors are not suitable for JQ1 treatment (176), highlighting the importance of personalized strategies, based on tumor cell biology, for PCa management.

Notwithstanding all the work that has been accomplished in the epi-drug field, the role of different epigenetic enzymes in cancer, particularly PCa, and its potential targeting for a reprograming purpose remains largely unknow. Therefore, an investment in this field of research might contribute to improve the management of, not only therapy resistant PCa, but also other cancers displaying therapeutically relevant epigenetic modifications.

Immunotherapy-Based Therapies for PCa Management

PCa has long been described as a *"cold"* tumor, characterized by an immune-suppressive environment (244). However, in the last decade, several efforts have been made to overcome this feature. This includes the use of different immune therapies, alone or in combination with the standard of care (**Table 3** and **Supplementary Table 3**). Published data includes reports from clinical trials targeting PD-L1, PD-1, CTLA-4, and the approved cellular immunotherapy Sipuleucel-T (**Table 3**). Overall, immunotherapy did not significantly improve the survival of PCa patients, but the effect on PSA was promising (**Supplementary Table 3**). Interestingly, the most encouraging results were obtained by the combination of pembrolizumab (anti-PD-1 drug), with the ADT enzalutamide (246). These results highlight the need for pre-clinical *in vitro* studies aiming at understanding the molecular mechanisms behind the *"cold"* PCa microenvironment, paving the way to further studies of novel immune-based therapies.

TABLE 3 | Immunotherapy for the management of therapeutic resistant PCa.

Target	Drug	Mechanism of action	Combination	References
PD-L1	Atezolizumab	Inhibits PD-L1	Enzalutamide	(245)
PD-1	Pembrolizumab	Targets PD-1	Enzalutamide, docetaxel, prednisone	(246–251)
Cellular Therapy	Sipuleucel-T	Cellular immunotherapy	N.a.	(252)
CTLA-4	Ipilimumab	Inhibits CTLA-4	ADT	(253–256)
	Tremelimumab		Bicalutamide	(257)

N.a., not applicable; ADT, androgen deprivation therapy.

CONCLUSION

Herein, we described the mechanisms underlying the acquisition of therapy resistance in PCa, and potential targetable molecules, listing druggable targets in resistant disease and addressing pre-clinical studies describing the anti-tumoral effects of several drugs. We provided insight on innovative PCa treatments, to be exploited in pre-clinical studies and, if successful, in clinical trials, allowing for improved treatment of

CRPC patients. Although several targeted therapies are already under clinical trials in PCa, there is a need for a more personalized analysis of tumor cell biology, enabling the selection of the most suitable therapeutic strategy, improving the management of resistant disease.

AUTHOR CONTRIBUTIONS

Conceptualization, FM-S and CJ. Systematic review of literature, FM-S. Writing—original draft preparation, FM-S. Writing—review and editing, RH and CJ. Image editing, FM-S. Supervision, CJ. All authors have read and agreed to the published version of the manuscript.

FUNDING

CJ research is supported by the Research Center of Portuguese Oncology Institute of Porto (CI-IPOP-27-2016). FM-S contract was funded by Porto Comprehensive Cancer Center (Porto.CCC, Contract RNCCCP.CCC-CI-IPOP-LAB3-NORTE-01-0145-FEDER-072678).

SUPPLEMENTARY MATERIAL

The Supplementary Material for this article can be found online at: https://www.frontiersin.org/articles/10.3389/fonc.2022.877379/full#supplementary-material

REFERENCES

1. Sung H, Ferlay J, Siegel RL, Laversanne M, Soerjomataram I, Jemal A, et al. Global Cancer Statistics 2020: GLOBOCAN Estimates of Incidence and Mortality Worldwide for 36 Cancers in 185 Countries. *CA Cancer J Clin* (2021) 71(3):209–49. doi: 10.3322/caac.21660
2. Wang G, Zhao D, Spring DJ, DePinho RA. Genetics and Biology of Prostate Cancer. *Genes Dev* (2018) 32(17-18):1105–40. doi: 10.1101/gad.315739.118
3. Cancer Genome Atlas Research N. The Molecular Taxonomy of Primary Prostate Cancer. *Cell* (2015) 163(4):1011–25. doi: 10.1016/j.cell.2015.10.025
4. Mitchell T, Neal DE. The Genomic Evolution of Human Prostate Cancer. *Br J Cancer* (2015) 113(2):193–8. doi: 10.1038/bjc.2015.234
5. Taylor BS, Schultz N, Hieronymus H, Gopalan A, Xiao Y, Carver BS, et al. Integrative Genomic Profiling of Human Prostate Cancer. *Cancer Cell* (2010) 18(1):11–22. doi: 10.1016/j.ccr.2010.05.026
6. Carver BS, Tran J, Gopalan A, Chen Z, Shaikh S, Carracedo A, et al. Aberrant ERG Expression Cooperates With Loss of PTEN to Promote Cancer Progression in the Prostate. *Nat Genet* (2009) 41(5):619–24. doi: 10.1038/ng.370
7. Graca I, Pereira-Silva E, Henrique R, Packham G, Crabb SJ, Jeronimo C, et al. Epigenetic Modulators as Therapeutic Targets in Prostate Cancer. *Clin Epigenet* (2016) 8(1):98. doi: 10.1186/s13148-016-0264-8
8. Jerónimo C, Usadel H, Henrique R, Oliveira J, Lopes C, Nelson WG, et al. Quantitation of GSTP1 Methylation in non-Neoplastic Prostatic Tissue and Organ-Confined Prostate Adenocarcinoma. *J Natl Cancer Institute* (2001) 93(22):1747–52. doi: 10.1093/jnci/93.22.1747
9. Weichert W, Roske A, Gekeler V, Beckers T, Stephan C, Jung K, et al. Histone Deacetylases 1, 2 and 3 are Highly Expressed in Prostate Cancer and HDAC2 Expression is Associated With Shorter PSA Relapse Time After Radical Prostatectomy. *Br J Cancer* (2008) 98(3):604–10. doi: 10.1038/sj.bjc.6604199
10. Jerónimo C, Henrique R, Hoque MO, Mambo E, Ribeiro FR, Varzim G, et al. A Quantitative Promoter Methylation Profile of Prostate Cancer. *Clin Cancer Res: Off J Am Assoc Cancer Res* (2004) 10(24):8472–8. doi: 10.1158/1078-0432.CCR-04-0894
11. Yegnasubramanian S, Haffner MC, Zhang Y, Gurel B, Cornish TC, Wu Z, et al. DNA Hypomethylation Arises Later in Prostate Cancer Progression Than CpG Island Hypermethylation and Contributes to Metastatic Tumor Heterogeneity. *Cancer Res* (2008) 68(21):8954–67. doi: 10.1158/0008-5472.CAN-07-6088
12. Davies A, Conteduca V, Zoubeidi A, Beltran H. Biological Evolution of Castration-Resistant Prostate Cancer. *Eur Urol Focus* (2019) 5(2):147–54. doi: 10.1016/j.euf.2019.01.016
13. Grasso CS, Wu Y-M, Robinson DR, Cao X, Dhanasekaran SM, Khan AP, et al. The Mutational Landscape of Lethal Castration-Resistant Prostate Cancer. *Nature* (2012) 487(7406):239–43. doi: 10.1038/nature11125
14. Chan JSK, Sng MK, Teo ZQ, Chong HC, Twang JS, Tan NS. Targeting Nuclear Receptors in Cancer-Associated Fibroblasts as Concurrent Therapy to Inhibit Development of Chemoresistant Tumors. *Oncogene* (2018) 37 (2):160–73. doi: 10.1038/onc.2017.319
15. Friedlander TW, Roy R, Tomlins SA, Ngo VT, Kobayashi Y, Azameera A, et al. Common Structural and Epigenetic Changes in the Genome of Castration-Resistant Prostate Cancer. *Cancer Res* (2012) 72(3):616–25. doi: 10.1158/0008-5472.CAN-11-2079
16. Varambally S, Dhanasekaran SM, Zhou M, Barrette TR, Kumar-Sinha C, Sanda MG, et al. The Polycomb Group Protein EZH2 is Involved in Progression of Prostate Cancer. *Nature* (2002) 419(6907):624–9. doi: 10.1038/nature01075
17. Casciello F, Windloch K, Gannon F, Lee JS. Functional Role of G9a Histone Methyltransferase in Cancer. *Front Immunol* (2015) 6(487). doi: 10.3389/fimmu.2015.00487
18. Metzger E, Wissmann M, Yin N, Muller JM, Schneider R, Peters AH, et al. LSD1 Demethylates Repressive Histone Marks to Promote Androgen-Receptor-Dependent Transcription. *Nature* (2005) 437(7057):436–9. doi: 10.1038/nature04020
19. Conteduca V, Oromendia C, Eng KW, Bareja R, Sigouros M, Molina A, et al. Clinical Features of Neuroendocrine Prostate Cancer. *Eur J Cancer* (2019) 121:7–18. doi: 10.1016/j.ejca.2019.08.011
20. Beltran H, Prandi D, Mosquera JM, Benelli M, Puca L, Cyrta J, et al. Divergent Clonal Evolution of Castration-Resistant Neuroendocrine Prostate Cancer. *Nat Med* (2016) 22(3):298–305. doi: 10.1038/nm.4045
21. Vlachostergios PJ, Puca L, Beltran H. Emerging Variants of Castration-Resistant Prostate Cancer. *Curr Oncol Rep* (2017) 19(5):32–2. doi: 10.1007/s11912-017-0593-6
22. Nadal R, Schweizer M, Kryvenko ON, Epstein JI, Eisenberger MA. Small Cell Carcinoma of the Prostate. *Nat Rev Urol* (2014) 11(4):213–9. doi: 10.1038/nrurol.2014.21
23. Gillessen S, Attard G, Beer TM, Beltran H, Bossi A, Bristow R, et al. Management of Patients With Advanced Prostate Cancer: The Report of the Advanced Prostate Cancer Consensus Conference APCCC 2017. *Eur Urol* (2018) 73(2):178–211. doi: 10.1016/j.eururo.2017.06.002
24. Heidenreich A, Bastian PJ, Bellmunt J, Bolla M, Joniau S, van derKwast T, et al. EAU Guidelines on Prostate Cancer. Part II: Treatment of Advanced, Relapsing, and Castration-Resistant Prostate Cancer. *Eur Urol* (2014) 65 (2):467–79. doi: 10.1016/j.eururo.2013.11.002
25. Parker C, Castro E, Fizazi K, Heidenreich A, Ost P, Procopio G, et al. Prostate Cancer: ESMO Clinical Practice Guidelines for Diagnosis, Treatment and Follow-Up. *Ann Oncol* (2020) 31(9):1119–34. doi: 10.1016/j.annonc.2020.06.011
26. Cornford P, Bellmunt J, Bolla M, Briers E, De Santis M, Gross T, et al. EAU-ESTRO-SIOG Guidelines on Prostate Cancer. Part II: Treatment of Relapsing, Metastatic, and Castration-Resistant Prostate Cancer. *Eur Urol* (2017) 71(4):630–42. doi: 10.1016/j.eururo.2016.08.002
27. Ceder Y, Bjartell A, Culig Z, Rubin MA, Tomlins S, Visakorpi T. The Molecular Evolution of Castration-Resistant Prostate Cancer. *Eur Urol Focus* (2016) 2(5):506–13. doi: 10.1016/j.euf.2016.11.012

28. Parker C, Gillessen S, Heidenreich A, Horwich A. Cancer of the Prostate: ESMO Clinical Practice Guidelines for Diagnosis, Treatment and Follow-Up. *Ann Oncol* (2015) 26 Suppl 5:v69–77. doi: 10.1093/annonc/mdv222
29. Shore ND, Chowdhury S, Villers A, Klotz L, Siemens DR, Phung D, et al. Efficacy and Safety of Enzalutamide Versus Bicalutamide for Patients With Metastatic Prostate Cancer (TERRAIN): A Randomised, Double-Blind, Phase 2 Study. *Lancet Oncol* (2016) 17(2):153–63. doi: 10.1016/S1470-2045(15)00518-5
30. Obinata D, Takayama K, Takahashi S, Inoue S. Crosstalk of the Androgen Receptor With Transcriptional Collaborators: Potential Therapeutic Targets for Castration-Resistant Prostate Cancer. *Cancers* (2017) 9(3):22. doi: 10.3390/cancers9030022
31. Vellky JE, Ricke WA. Development and Prevalence of Castration-Resistant Prostate Cancer Subtypes. *Neoplasia* (2020) 22(11):566–75. doi: 10.1016/j.neo.2020.09.002
32. Venkitaraman R, Lorente D, Murthy V, Thomas K, Parker L, Ahiabor R, et al. A Randomised Phase 2 Trial of Dexamethasone Versus Prednisolone in Castration-Resistant Prostate Cancer. *Eur Urol* (2015) 67(4):673–9. doi: 10.1016/j.eururo.2014.10.004
33. Sartor O, de Bono J, Chi KN, Fizazi K, Herrmann K, Rahbar K, et al. Lutetium-177–PSMA-617 for Metastatic Castration-Resistant Prostate Cancer. *New Engl J Med* (2021) 385(12):1091–103. doi: 10.1056/NEJMoa2107322
34. Lowrance WT, Murad MH, Oh WK, Jarrard DF, Resnick MJ, Cookson MS. Castration-Resistant Prostate Cancer: AUA Guideline Amendment 2018. *J Urol* (2018) 200(6):1264–72. doi: 10.1016/j.juro.2018.07.090
35. Graca I, Sousa EJ, Costa-Pinheiro P, Vieira FQ, Torres-Ferreira J, Martins MG, et al. Anti-Neoplastic Properties of Hydralazine in Prostate Cancer. *Oncotarget* (2014) 5(15):5950–64. doi: 10.18632/oncotarget.1909
36. Visakorpi T, Hyytinen E, Koivisto P, Tanner M, Keinänen R, Palmberg C, et al. In Vivo Amplification of the Androgen Receptor Gene and Progression of Human Prostate Cancer. *Nat Genet* (1995) 9(4):401–6. doi: 10.1038/ng0495-401
37. Culig Z, Hobisch A, Cronauer MV, Radmayr C, Trapman J, Hittmair A, et al. Androgen Receptor Activation in Prostatic Tumor Cell Lines by Insulin-Like Growth Factor-I, Keratinocyte Growth Factor, and Epidermal Growth Factor. *Cancer Res* (1994) 54(20):5474–8. doi: 10.1159/000475232
38. Kaarbø M, Klokk TI, Saatcioglu F. Androgen Signaling and its Interactions With Other Signaling Pathways in Prostate Cancer. *BioEssays* (2007) 29 (12):1227–38. doi: 10.1002/bies.20676
39. Marcelli M, Ittmann M, Mariani S, Sutherland R, Nigam R, Murthy L, et al. Androgen Receptor Mutations in Prostate Cancer. *Cancer Res* (2000) 60 (4):944–9.
40. Bluemn EG, Coleman IM, Lucas JM, Coleman RT, Hernandez-Lopez S, Tharakan R, et al. Androgen Receptor Pathway-Independent Prostate Cancer Is Sustained Through FGF Signaling. *Cancer Cell* (2017) 32 (4):474–89.e6. doi: 10.1016/j.ccell.2017.09.003
41. Craft N, Shostak Y, Carey M, Sawyers CL. A Mechanism for Hormone-Independent Prostate Cancer Through Modulation of Androgen Receptor Signaling by the HER-2/Neu Tyrosine Kinase. *Nat Med* (1999) 5(3):280–5. doi: 10.1038/6495
42. Wang J, Kobayashi T, Floc'h N, Kinkade CW, Aytes A, Dankort D, et al. B-Raf Activation Cooperates With PTEN Loss to Drive C-Myc Expression in Advanced Prostate Cancer. *Cancer Res* (2012) 72(18):4765–76. doi: 10.1158/0008-5472.CAN-12-0820
43. Guo Z, Dai B, Jiang T, Xu K, Xie Y, Kim O, et al. Regulation of Androgen Receptor Activity by Tyrosine Phosphorylation. *Cancer Cell* (2007) 11(1):97. doi: 10.1016/j.ccr.2006.12.010
44. Wang J, Zou JX, Xue X, Cai D, Zhang Y, Duan Z, et al. ROR-γ Drives Androgen Receptor Expression and Represents a Therapeutic Target in Castration-Resistant Prostate Cancer. *Nat Med* (2016) 22(5):488–96. doi: 10.1038/nm.4070
45. Isikbay M, Otto K, Kregel S, Kach J, Cai Y, Vander Griend DJ, et al. Glucocorticoid Receptor Activity Contributes to Resistance to Androgen-Targeted Therapy in Prostate Cancer. *Horm Cancer* (2014) 5(2):72–89. doi: 10.1007/s12672-014-0173-2
46. Yeh S, Lin HK, Kang HY, Thin TH, Lin MF, Chang C. From HER2/Neu Signal Cascade to Androgen Receptor and its Coactivators: A Novel Pathway by Induction of Androgen Target Genes Through MAP Kinase in Prostate Cancer Cells. *Proc Natl Acad Sci U S A* (1999) 96(10):5458–63. doi: 10.1073/pnas.96.10.5458
47. Harada S, Keller ET, Fujimoto N, Koshida K, Namiki M, Matsumoto T, et al. Long-Term Exposure of Tumor Necrosis Factor α Causes Hypersensitivity to Androgen and Anti-Androgen Withdrawal Phenomenon in LNCaP Prostate Cancer Cells. *Prostate* (2001) 46 (4):319–26. doi: 10.1002/1097-0045(20010301)46:4<319::AID-PROS1039>3.0.CO;2-C
48. Lee SO, Lou W, Hou M, de Miguel F, Gerber L, Gao AC. Interleukin-6 Promotes Androgen-Independent Growth in LNCaP Human Prostate Cancer Cells. *Clin Cancer Res Off J Am Assoc Cancer Res* (2003) 9 (1):370–6. doi: 10.1016/j.mce.2011.05.033
49. Calcinotto A, Spataro C, Zagato E, Di Mitri D, Gil V, Crespo M, et al. IL-23 Secreted by Myeloid Cells Drives Castration-Resistant Prostate Cancer. *Nature* (2018) 559(7714):363–9. doi: 10.1038/s41586-018-0266-0
50. Feldman BJ, Feldman D. The Development of Androgen-Independent Prostate Cancer. *Nat Rev Cancer* (2001) 1(1):34–45. doi: 10.1038/35094009
51. Mayeur GL, Kung WJ, Martinez A, Izumiya C, Chen DJ, Kung HJ. Ku is a Novel Transcriptional Recycling Coactivator of the Androgen Receptor in Prostate Cancer Cells. *J Biol Chem* (2005) 280(11):10827–33. doi: 10.1074/jbc.M413336200
52. Haffner MC, Aryee MJ, Toubaji A, Esopi DM, Albadine R, Gurel B, et al. Androgen-Induced TOP2B-Mediated Double-Strand Breaks and Prostate Cancer Gene Rearrangements. *Nat Genet* (2010) 42(8):668–75. doi: 10.1038/ng.613
53. Lin C, Yang L, Tanasa B, Hutt K, Ju BG, Ohgi K, et al. Nuclear Receptor-Induced Chromosomal Proximity and DNA Breaks Underlie Specific Translocations in Cancer. *Cell* (2009) 139(6):1069–83. doi: 10.1016/j.cell.2009.11.030
54. Brenner JC, Ateeq B, Li Y, Yocum AK, Cao Q, Asangani IA, et al. Mechanistic Rationale for Inhibition of Poly(ADP-Ribose) Polymerase in ETS Gene Fusion-Positive Prostate Cancer. *Cancer Cell* (2011) 19(5):664–78. doi: 10.1016/j.ccr.2011.04.010
55. Wu D, Sunkel B, Chen Z, Liu X, Ye Z, Li Q, et al. Three-Tiered Role of the Pioneer Factor GATA2 in Promoting Androgen-Dependent Gene Expression in Prostate Cancer. *Nucleic Acids Res* (2014) 42(6):3607–22. doi: 10.1093/nar/gkt1382
56. Tepper CG, Boucher DL, Ryan PE, Ma A-H, Xia L, Lee L-F, et al. Characterization of a Novel Androgen Receptor Mutation in a Relapsed CWR22 Prostate Cancer Xenograft and Cell Line. *Cancer Res* (2002) 62 (22):6606–14.
57. Hu R, Lu C, Mostaghel EA, Yegnasubramanian S, Gurel M, Tannahill C, et al. Distinct Transcriptional Programs Mediated by the Ligand-Dependent Full-Length Androgen Receptor and its Splice Variants in Castration-Resistant Prostate Cancer. *Cancer Res* (2012) 72(14):3457–62. doi: 10.1158/0008-5472.CAN-11-3892
58. Jarrard DF, Kinoshita H, Shi Y, Sandefur C, Hoff D, Meisner LF, et al. Methylation of the Androgen Receptor Promoter CpG Island is Associated With Loss of Androgen Receptor Expression in Prostate Cancer Cells. *Cancer Res* (1998) 58(23):5310–4.
59. Jeronimo C, Bastian PJ, Bjartell A, Carbone GM, Catto JW, Clark SJ, et al. Epigenetics in Prostate Cancer: Biologic and Clinical Relevance. *Eur Urol* (2011) 60(4):753–66. doi: 10.1016/j.eururo.2011.06.035
60. Kivinummi K, Urbanucci A, Leinonen K, Tammela TLJ, Annala M, Isaacs WB, et al. The Expression of AURKA is Androgen Regulated in Castration-Resistant Prostate Cancer. *Sci Rep* (2017) 7(1):17978. doi: 10.1038/s41598-017-18210-3
61. Madan RA, Pal SK, Sartor O, Dahut WL. Overcoming Chemotherapy Resistance in Prostate Cancer. *Clin Cancer Res Off J Am Assoc Cancer Res* (2011) 17(12):3892–902. doi: 10.1158/1078-0432.CCR-10-2654
62. Kartner N, Riordan JR, Ling V. Cell Surface P-Glycoprotein Associated With Multidrug Resistance in Mammalian Cell Lines. *Science* (1983) 221 (4617):1285–8. doi: 10.1126/science.6137059
63. Terry S, Ploussard G, Allory Y, Nicolaiew N, Boissière-Michot F, Maillé P, et al. Increased Expression of Class III Beta-Tubulin in Castration-Resistant Human Prostate Cancer. *Br J Cancer* (2009) 101(6):951–6. doi: 10.1038/sj.bjc.6605245

64. Ploussard G, Terry S, Maillé P, Allory Y, Sirab N, Kheuang L, et al. Class III Beta-Tubulin Expression Predicts Prostate Tumor Aggressiveness and Patient Response to Docetaxel-Based Chemotherapy. *Cancer Res* (2010) 70 (22):9253–64. doi: 10.1158/0008-5472.CAN-10-1447
65. Stuparu AD, Capri JR, Meyer CAL, Le TM, Evans-Axelsson SL, Current K, et al. Mechanisms of Resistance to Prostate-Specific Membrane Antigen-Targeted Radioligand Therapy in a Mouse Model of Prostate Cancer. *J Nucl Med* (2021) 62(7):989–95. doi: 10.2967/jnumed.120.256263
66. Cao J, Chen Y, Hu M, Zhang W. (177)Lu-PSMA-RLT of Metastatic Castration-Resistant Prostate Cancer: Limitations and Improvements. *Ann Nucl Med* (2021) 35(8):861–70. doi: 10.1007/s12149-021-01649-w
67. Toivanen R, Mohan A, Shen MM. Basal Progenitors Contribute to Repair of the Prostate Epithelium Following Induced Luminal Anoikis. *Stem Cell Rep* (2016) 6(5):660–7. doi: 10.1016/j.stemcr.2016.03.007
68. Zhu ML, Kyprianou N. Role of Androgens and the Androgen Receptor in Epithelial-Mesenchymal Transition and Invasion of Prostate Cancer Cells. *FASEB J* (2010) 24(3):769–77. doi: 10.1096/fj.09-136994
69. Ting HJ, Deep G, Jain AK, Cimic A, Sirintrapun J, Romero LM, et al. Silibinin Prevents Prostate Cancer Cell-Mediated Differentiation of Naïve Fibroblasts Into Cancer-Associated Fibroblast Phenotype by Targeting TGF β2. *Mol Carcinog* (2015) 54(9):730–41. doi: 10.1002/mc.22135
70. Yu Z, Cai C, Gao S, Simon NI, Shen HC, Balk SP. Galeterone Prevents Androgen Receptor Binding to Chromatin and Enhances Degradation of Mutant Androgen Receptor. *Clin Cancer Res Off J Am Assoc Cancer Res* (2014) 20(15):4075–85. doi: 10.1158/1078-0432.CCR-14-0292
71. Yang YC, Banuelos CA, Mawji NR, Wang J, Kato M, Haile S, et al. Targeting Androgen Receptor Activation Function-1 With EPI to Overcome Resistance Mechanisms in Castration-Resistant Prostate Cancer. *Clin Cancer Res* (2016) 22(17):4466–77. doi: 10.1158/1078-0432.CCR-15-2901
72. Kato M, Banuelos CA, Imamura Y, Leung JK, Caley DP, Wang J, et al. Cotargeting Androgen Receptor Splice Variants and mTOR Signaling Pathway for the Treatment of Castration-Resistant Prostate Cancer. *Clin Cancer Res Off J Am Assoc Cancer Res* (2016) 22(11):2744–54. doi: 10.1158/1078-0432.CCR-15-2119
73. Myung J-K, Banuelos CA, Fernandez JG, Mawji NR, Wang J, Tien AH, et al. An Androgen Receptor N-Terminal Domain Antagonist for Treating Prostate Cancer. *J Clin Invest* (2013) 123(7):2948–60. doi: 10.1172/JCI66398
74. Andersen RJ, Mawji NR, Wang J, Wang G, Haile S, Myung JK, et al. Regression of Castrate-Recurrent Prostate Cancer by a Small-Molecule Inhibitor of the Amino-Terminus Domain of the Androgen Receptor. *Cancer Cell* (2010) 17(6):535–46. doi: 10.1016/j.ccr.2010.04.027
75. Liu X, Biswas S, Berg MG, Antapli CM, Xie F, Wang Q, et al. Niclosamide Inhibits Androgen Receptor Variants Expression and Overcomes Enzalutamide Resistance in Castration-Resistant Prostate Cancer. *Clin Cancer Res Off J Am Assoc Cancer Res* (2014) 20(12):3198–210. doi: 10.1158/1078-0432.CCR-13-3296
76. Liu X, Biswas S, Berg MG, Antapli CM, Xie F, Wang Q, et al. Genomics-Guided Discovery of Thailanstatins A, B, and C As pre-mRNA Splicing Inhibitors and Antiproliferative Agents From Burkholderia Thailandensis MSMB43. *J Natural Prod* (2013) 76(4):685–93. doi: 10.1021/np300913h
77. Wang B, Lo UG, Wu K, Kapur P, Liu X, Huang J, et al. Developing New Targeting Strategy for Androgen Receptor Variants in Castration Resistant Prostate Cancer. *Int J Cancer* (2017) 141(10):2121–30. doi: 10.1002/ijc.30893
78. Ravindranathan P, Lee TK, Yang L, Centenera MM, Butler L, Tilley WD, et al. Peptidomimetic Targeting of Critical Androgen Receptor-Coregulator Interactions in Prostate Cancer. *Nat Commun* (2013) 4:1923. doi: 10.1038/ncomms2912
79. Lev A, Lulla AR, Ross BC, Ralff MD, Makhov PB, Dicker DT, et al. ONC201 Targets AR and AR-V7 Signaling, Reduces PSA, and Synergizes With Everolimus in Prostate Cancer. *Mol Cancer Res* (2018) 16(5):754–66. doi: 10.1158/1541-7786.MCR-17-0614
80. Du Z, Li L, Sun W, Wang X, Zhang Y, Chen Z, et al. Systematic Evaluation for the Influences of the SOX17/Notch Receptor Family Members on Reversing Enzalutamide Resistance in Castration-Resistant Prostate Cancer Cells. *Front Oncol* (2021) 11:607291. doi: 10.3389/fonc.2021.607291
81. Du Z, Li L, Sun W, Zhu P, Cheng S, Yang X, et al. HepaCAM Inhibits the Malignant Behavior of Castration-Resistant Prostate Cancer Cells by Downregulating Notch Signaling and PF-3084014 (a γ-Secretase Inhibitor) Partly Reverses the Resistance of Refractory Prostate Cancer to Docetaxel and Enzalutamide *In Vitro*. *Int J Oncol* (2018) 53(1):99–112. doi: 10.3892/ijo.2018.4370
82. Cui D, Dai J, Keller JM, Mizokami A, Xia S, Keller ET, et al. Notch Pathway Inhibition Using PF-03084014, a γ-Secretase Inhibitor (GSI), Enhances the Antitumor Effect of Docetaxel in Prostate Cancer. *Clin Cancer Res* (2015) 21 (20):4619. doi: 10.1158/1078-0432.CCR-15-0242
83. Rice MA, Hsu EC, Aslan M, Ghoochani A, Su A, Stoyanova T, et al. Loss of Notch1 Activity Inhibits Prostate Cancer Growth and Metastasis and Sensitizes Prostate Cancer Cells to Antiandrogen Therapies. *Mol Cancer Ther* (2019) 18(7):1230–42. doi: 10.1158/1535-7163.MCT-18-0804
84. Cui J, Wang Y, Dong B, Qin L, Wang C, Zhou P, et al. Pharmacological Inhibition of the Notch Pathway Enhances the Efficacy of Androgen Deprivation Therapy for Prostate Cancer. *Int J Cancer* (2018) 143(3):645–56. doi: 10.1002/ijc.31346
85. Rotinen M, You S, Yang J, Coetzee SG, Reis-Sobreiro M, Huang WC, et al. ONECUT2 is a Targetable Master Regulator of Lethal Prostate Cancer That Suppresses the Androgen Axis. *Nat Med* (2018) 24(12):1887–98. doi: 10.1038/s41591-018-0241-1
86. Mellinghoff IK, Tran C, Sawyers CL. Growth Inhibitory Effects of the Dual ErbB1/ErbB2 Tyrosine Kinase Inhibitor PKI-166 on Human Prostate Cancer Xenografts. *Cancer Res* (2002) 62(18):5254–9.
87. Kim SJ, Uehara H, Yazici S, Langley RR, He J, Tsan R, et al. Simultaneous Blockade of Platelet-Derived Growth Factor-Receptor and Epidermal Growth Factor-Receptor Signaling and Systemic Administration of Paclitaxel as Therapy for Human Prostate Cancer Metastasis in Bone of Nude Mice. *Cancer Res* (2004) 64(12):4201–8. doi: 10.1158/0008-5472.CAN-03-3763
88. Kim SJ, Uehara H, Karashima T, Shepherd DL, Killion JJ, Fidler IJ, et al. Blockade of Epidermal Growth Factor Receptor Signaling in Tumor Cells and Tumor-Associated Endothelial Cells for Therapy of Androgen-Independent Human Prostate Cancer Growing in the Bone of Nude Mice. *Clin Cancer Res* (2003) 9(3):1200–10. doi: 10.1016/S0002-9440(10)64253-8
89. Sirotnak FM, She Y, Lee F, Chen J, Scher HI. Studies With CWR22 Xenografts in Nude Mice Suggest That ZD1839 may Have a Role in the Treatment of Both Androgen-Dependent and Androgen-Independent Human Prostate Cancer. *Clin Cancer Res* (2002) 8(12):3870–6.
90. Moasser MM, Basso A, Averbuch SD, Rosen N. The Tyrosine Kinase Inhibitor ZD1839 ("Iressa") Inhibits HER2-Driven Signaling and Suppresses the Growth of HER2-Overexpressing Tumor Cells. *Cancer Res* (2001) 61(19):7184–8.
91. Formento P, Hannoun-Levi JM, Fischel JL, Magné N, Etienne-Grimaldi MC, Milano G. Dual HER 1-2 Targeting of Hormone-Refractory Prostate Cancer by ZD1839 and Trastuzumab. *Eur J Cancer* (2004) 40(18):2837–44. doi: 10.1016/j.ejca.2004.07.033
92. Sgambato A, Camerini A, Faraglia B, Ardito R, Bianchino G, Spada D, et al. Targeted Inhibition of the Epidermal Growth Factor Receptor-Tyrosine Kinase by ZD1839 ('Iressa') Induces Cell-Cycle Arrest and Inhibits Proliferation in Prostate Cancer Cells. *J Cell Physiol* (2004) 201(1):97–105. doi: 10.1002/jcp.20045
93. Festuccia C, Muzi P, Millimaggi D, Biordi L, Gravina GL, Speca S, et al. Molecular Aspects of Gefitinib Antiproliferative and Pro-Apoptotic Effects in PTEN-Positive and PTEN-Negative Prostate Cancer Cell Lines. *Endocr Relat Cancer* (2005) 12(4):983–98. doi: 10.1677/erc.1.00986
94. Bonaccorsi L, Marchiani S, Muratori M, Forti G, Baldi E. Gefitinib ('Iressa', ZD1839) Inhibits EGF-Induced Invasion in Prostate Cancer Cells by Suppressing PI3 K/AKT Activation. *J Cancer Res Clin Oncol* (2004) 130 (10):604–14. doi: 10.1007/s00432-004-0581-8
95. Vicentini C, Festuccia C, Gravina GL, Angelucci A, Marronaro A, Bologna M. Prostate Cancer Cell Proliferation is Strongly Reduced by the Epidermal Growth Factor Receptor Tyrosine Kinase Inhibitor ZD1839 *In Vitro* on Human Cell Lines and Primary Cultures. *J Cancer Res Clin Oncol* (2003) 129 (3):165–74. doi: 10.1007/s00432-003-0420-3
96. Angelucci A, Gravina GL, Rucci N, Millimaggi D, Festuccia C, Muzi P, et al. Suppression of EGF-R Signaling Reduces the Incidence of Prostate Cancer Metastasis in Nude Mice. *Endocr Relat Cancer* (2006) 13(1):197–210. doi: 10.1677/erc.1.01100

97. Goehringer N, Biersack B, Peng Y, Schobert R, Herling M, Ma A, et al. Anticancer Activity and Mechanisms of Action of New Chimeric EGFR/HDAC-Inhibitors. *Int J Mol Sci* (2021) 22(16) 22(16): 8432. doi: 10.3390/ijms22168432
98. Liao Y, Guo Z, Xia X, Liu Y, Huang C, Jiang L, et al. Inhibition of EGFR Signaling With Spautin-1 Represents a Novel Therapeutics for Prostate Cancer. *J Exp Clin Cancer Res* (2019) 38(1):157. doi: 10.1186/s13046-019-1165-4
99. Zhi Y, Wu X, Shen W, Wang Y, Zhou X, He P, et al. Synthesis and Pharmacological Evaluation of Novel Epidermal Growth Factor Receptor Inhibitors Against Prostate Tumor Cells. *Oncol Lett* (2018) 16(5):6522–30. doi: 10.3892/ol.2018.9438
100. Pu YS, Hsieh MW, Wang CW, Liu GY, Huang CY, Lin CC, et al. Epidermal Growth Factor Receptor Inhibitor (PD168393) Potentiates Cytotoxic Effects of Paclitaxel Against Androgen-Independent Prostate Cancer Cells. *Biochem Pharmacol* (2006) 71(6):751–60. doi: 10.1016/j.bcp.2005.12.009
101. Hu C, Xia H, Bai S, Zhao J, Edwards H, Li X, et al. CUDC-907, a Novel Dual PI3K and HDAC Inhibitor, in Prostate Cancer: Antitumour Activity and Molecular Mechanism of Action. *J Cell Mol Med* (2020) 24(13):7239–53. doi: 10.1111/jcmm.15281
102. Zou Y, Qi Z, Guo W, Zhang L, Ruscetti M, Shenoy T, et al. Cotargeting the Cell-Intrinsic and Microenvironment Pathways of Prostate Cancer by PI3Kα/β/δ Inhibitor Bay1082439. *Mol Cancer Ther* (2018) 17(10):2091–9. doi: 10.1158/1535-7163.MCT-18-0038
103. Qi Z, Xu Z, Zhang L, Zou Y, Li J, Yan W, et al. Overcoming Resistance to Immune Checkpoint Therapy in PTEN-Null Prostate Cancer by Intermittent Anti-PI3Kα/β/δ Treatment. *Nat Commun* (2022) 13(1):182. doi: 10.1038/s41467-021-27833-0
104. Shen G, Jiang M, Pu J. Dual Inhibition of BRD4 and PI3K by SF2523 Suppresses Human Prostate Cancer Cell Growth In Vitro and *In Vivo*. *Biochem Biophys Res Commun* (2018) 495(1):567–73. doi: 10.1016/j.bbrc.2017.11.062
105. Guerra FS, Rodrigues DA, Fraga CAM, Fernandes PD. Novel Single Inhibitor of HDAC6/8 and Dual Inhibitor of PI3K/HDAC6 as Potential Alternative Treatments for Prostate Cancer. *Pharmaceut (Basel)* (2021) 14(5):387. doi: 10.3390/ph14050387
106. Zhao W, Guo W, Zhou Q, Ma SN, Wang R, Qiu Y, et al. *In Vitro* Antimetastatic Effect of Phosphatidylinositol 3-Kinase Inhibitor ZSTK474 on Prostate Cancer PC3 Cells. *Int J Mol Sci* (2013) 14(7):13577–91. doi: 10.3390/ijms140713577
107. Liu J, Tan X, Zhao W, Liu J, Xing X, Fan G, et al. *In Vitro* and *In Vivo* Antimetastatic Effects of ZSTK474 on Prostate Cancer DU145 Cells. *Curr Cancer Drug Targets* (2019) 19(4):321–9. doi: 10.2174/1568009618666180911101310
108. Cai F, Zhang Y, Li J, Huang S, Gao R. Isorhamnetin Inhibited the Proliferation and Metastasis of Androgen-Independent Prostate Cancer Cells by Targeting the Mitochondrion-Dependent Intrinsic Apoptotic and PI3K/Akt/mTOR Pathway. *Biosci Rep* (2020) 40(3):BSR20192826. doi: 10.1042/BSR20192826
109. Huang TF, Wang SW, Lai YW, Liu SC, Chen YJ, Hsueh TY, et al. 4-Acetylantroquinonol B Suppresses Prostate Cancer Growth and Angiogenesis via a VEGF/PI3K/ERK/mTOR-Dependent Signaling Pathway in Subcutaneous Xenograft and *In Vivo* Angiogenesis Models. *Int J Mol Sci* (2022) 23(3):1446. doi: 10.3390/ijms23031446
110. Yasumizu Y, Miyajima A, Kosaka T, Miyazaki Y, Kikuchi E, Oya M. Dual PI3K/mTOR Inhibitor NVP-BEZ235 Sensitizes Docetaxel in Castration Resistant Prostate Cancer. *J Urol* (2014) 191(1):227–34. doi: 10.1016/j.juro.2013.07.101
111. Potiron VA, Abderrahmani R, Giang E, Chiavassa S, Di Tomaso E, Maira SM, et al. Radiosensitization of Prostate Cancer Cells by the Dual PI3K/mTOR Inhibitor BEZ235 Under Normoxic and Hypoxic Conditions. *Radiother Oncol* (2013) 106(1):138–46. doi: 10.1016/j.radonc.2012.11.014
112. Hong SW, Shin JS, Moon JH, Kim YS, Lee J, Choi EK, et al. NVP-BEZ235, a Dual PI3K/mTOR Inhibitor, Induces Cell Death Through Alternate Routes in Prostate Cancer Cells Depending on the PTEN Genotype. *Apoptosis* (2014) 19(5):895–904. doi: 10.1007/s10495-014-0973-4
113. Carver BS, Chapinski C, Wongvipat J, Hieronymus H, Chen Y, Chandarlapaty S, et al. Reciprocal Feedback Regulation of PI3K and Androgen Receptor Signaling in PTEN-Deficient Prostate Cancer. *Cancer Cell* (2011) 19(5):575–86. doi: 10.1016/j.ccr.2011.04.008
114. Adelaiye-Ogala R, Gryder BE, Nguyen YTM, Alilin AN, Grayson AR, Bajwa W, et al. Targeting the PI3K/AKT Pathway Overcomes Enzalutamide Resistance by Inhibiting Induction of the Glucocorticoid Receptor. *Mol Cancer Ther* (2020) 19(7):1436–47. doi: 10.1158/1535-7163.MCT-19-0936
115. Sun L, Huang Y, Liu Y, Zhao Y, He X, Zhang L, et al. Ipatasertib, a Novel Akt Inhibitor, Induces Transcription Factor FoxO3a and NF-κb Directly Regulates PUMA-Dependent Apoptosis. *Cell Death Dis* (2018) 9(9):911. doi: 10.1038/s41419-018-0943-9
116. Lin J, Sampath D, Nannini MA, Lee BB, Degtyarev M, Oeh J, et al. Targeting Activated Akt With GDC-0068, a Novel Selective Akt Inhibitor That is Efficacious in Multiple Tumor Models. *Clin Cancer Res* (2013) 19(7):1760–72. doi: 10.1158/1078-0432.CCR-12-3072
117. Tee SS, Suster I, Truong S, Jeong S, Eskandari R, DiGialleonardo V, et al. Targeted AKT Inhibition in Prostate Cancer Cells and Spheroids Reduces Aerobic Glycolysis and Generation of Hyperpolarized [1-(13)C] Lactate. *Mol Cancer Res* (2018) 16(3):453–60. doi: 10.1158/1541-7786.MCR-17-0458
118. Al-Saffar NMS, Troy H, Wong TeFong A-C, Paravati R, Jackson LE, Gowan S, et al. Metabolic Biomarkers of Response to the AKT Inhibitor MK-2206 in Pre-Clinical Models of Human Colorectal and Prostate Carcinoma. *Br J Cancer* (2018) 119(9):1118–28. doi: 10.1038/s41416-018-0242-3
119. De Velasco MA, Kura Y, Yoshikawa K, Nishio K, Davies BR, Uemura H, et al. Efficacy of Targeted AKT Inhibition in Genetically Engineered Mouse Models of PTEN-Deficient Prostate Cancer. *Oncotarget* (2016) 7(13):15959–76. doi: 10.18632/oncotarget.7557
120. Lamoureux F, Thomas C, Crafter C, Kumano M, Zhang F, Davies BR, et al. Blocked Autophagy Using Lysosomotropic Agents Sensitizes Resistant Prostate Tumor Cells to the Novel Akt Inhibitor AZD5363. *Clin Cancer Res* (2013) 19(4):833–44. doi: 10.1158/1078-0432.CCR-12-3114
121. Marques RB, Aghai A, de Ridder CMA, Stuurman D, Hoeben S, Boer A, et al. High Efficacy of Combination Therapy Using PI3K/AKT Inhibitors With Androgen Deprivation in Prostate Cancer Preclinical Models. *Eur Urol* (2015) 67(6):1177–85. doi: 10.1016/j.eururo.2014.08.053
122. Thomas C, Lamoureux F, Crafter C, Davies BR, Beraldi E, Fazli L, et al. Synergistic Targeting of PI3K/AKT Pathway and Androgen Receptor Axis Significantly Delays Castration-Resistant Prostate Cancer Progression In Vivo. *Mol Cancer Ther* (2013) 12(11):2342–55. doi: 10.1158/1535-7163.MCT-13-0032
123. Jin L, Zhang W, Yao MY, Tian Y, Xue BX, Tao W. GNE-493 Inhibits Prostate Cancer Cell Growth *via* Akt-mTOR-Dependent and -Independent Mechanisms. *Cell Death Discovery* (2022) 8(1):120. doi: 10.1038/s41420-022-00911-y
124. Morgan TM, Pitts TE, Gross TS, Poliachik SL, Vessella RL, Corey E. RAD001 (Everolimus) Inhibits Growth of Prostate Cancer in the Bone and the Inhibitory Effects are Increased by Combination With Docetaxel and Zoledronic Acid. *Prostate* (2008) 68(8):861–71. doi: 10.1002/pros.20752
125. Alshaker H, Wang Q, Kawano Y, Arafat T, Böhler T, Winkler M, et al. Everolimus (RAD001) Sensitizes Prostate Cancer Cells to Docetaxel by Down-Regulation of HIF-1α and Sphingosine Kinase 1. *Oncotarget* (2016) 7(49):80943–56. doi: 10.18632/oncotarget.13115
126. Schayowitz A, Sabnis G, Goloubeva O, Njar VC, Brodie AM. Prolonging Hormone Sensitivity in Prostate Cancer Xenografts Through Dual Inhibition of AR and mTOR. *Br J Cancer* (2010) 103(7):1001–7. doi: 10.1038/sj.bjc.6605882
127. Alshaker H, Wang Q, Böhler T, Mills R, Winkler M, Arafat T, et al. Combination of RAD001 (Everolimus) and Docetaxel Reduces Prostate and Breast Cancer Cell VEGF Production and Tumour Vascularisation Independently of Sphingosine-Kinase-1. *Sci Rep* (2017) 7(1):3493. doi: 10.1038/s41598-017-03728-3
128. Zhang W, Haines BB, Efferson C, Zhu J, Ware C, Kunii K, et al. Evidence of mTOR Activation by an AKT-Independent Mechanism Provides Support for the Combined Treatment of PTEN-Deficient Prostate Tumors With mTOR and AKT Inhibitors. *Transl Oncol* (2012) 5(6):422–9. doi: 10.1593/tlo.12241
129. Floc'h N, Kinkade CW, Kobayashi T, Aytes A, Lefebvre C, Mitrofanova A, et al. Dual Targeting of the Akt/mTOR Signaling Pathway Inhibits Castration-Resistant Prostate Cancer in a Genetically Engineered Mouse

Model. *Cancer Res* (2012) 72(17):4483–93. doi: 10.1158/0008-5472.CAN-12-0283

130. Rosette C, Agan FJ, Rosette N, Mazzetti A, Moro L, Gerloni M. The Dual Androgen Receptor and Glucocorticoid Receptor Antagonist CB-03-10 as Potential Treatment for Tumors That Have Acquired GR-Mediated Resistance to AR Blockade. *Mol Cancer Ther* (2020) 19(11):2256–66. doi: 10.1158/1535-7163.MCT-19-1137
131. Kroon J, Puhr M, Buijs JT, van derHorst G, Hemmer DM, Marijt KA, et al. Glucocorticoid Receptor Antagonism Reverts Docetaxel Resistance in Human Prostate Cancer. *Endocrine-Related Cancer* (2016) 23(1):35–45. doi: 10.1530/ERC-15-0343
132. Yan TZ, Jin FS, Xie LP, Li LC. Relationship Between Glucocorticoid Receptor Signal Pathway and Androgen-Independent Prostate Cancer. *Urol Int* (2008) 81(2):228–33. doi: 10.1159/000144067
133. El Etreby MF, Liang Y, Johnson MH, Lewis RW. Antitumor Activity of Mifepristone in the Human LNCaP, LNCaP-C4, and LNCaP-C4-2 Prostate Cancer Models in Nude Mice. *Prostate* (2000) 42(2):99–106. doi: 10.1002/(SICI)1097-0045(20000201)42:2<99::AID-PROS3>3.0.CO;2-I
134. Gao M, Guo L, Wang H, Huang J, Han F, Xiang S, et al. Orphan Nuclear Receptor Rorγ Confers Doxorubicin Resistance in Prostate Cancer. *Cell Biol Int* (2020) 44(10):2170–6. doi: 10.1002/cbin.11411
135. Qi W, Cooke LS, Stejskal A, Riley C, Croce KD, Saldanha JW, et al. MP470, a Novel Receptor Tyrosine Kinase Inhibitor, in Combination With Erlotinib Inhibits the HER Family/PI3K/Akt Pathway and Tumor Growth in Prostate Cancer. *BMC Cancer* (2009) 9:142. doi: 10.1186/1471-2407-9-142
136. Zhou F, Chen X, Fan S, Tai S, Jiang C, Zhang Y, et al. GSK1838705A, an Insulin-Like Growth Factor-1 Receptor/Insulin Receptor Inhibitor, Induces Apoptosis and Reduces Viability of Docetaxel-Resistant Prostate Cancer Cells Both In Vitro and *In Vivo*. *Oncol Targets Ther* (2015) 8:753–60. doi: 10.2147/OTT.S79105
137. Isebaert SF, Swinnen JV, McBride WH, Haustermans KM. Insulin-Like Growth Factor-Type 1 Receptor Inhibitor NVP-AEW541 Enhances Radiosensitivity of PTEN Wild-Type But Not PTEN-Deficient Human Prostate Cancer Cells. *Int J Radiat Oncol Biol Phys* (2011) 81(1):239–47. doi: 10.1016/j.ijrobp.2011.03.030
138. Chitnis MM, Lodhia KA, Aleksic T, Gao S, Protheroe AS, Macaulay VM. IGF-1R Inhibition Enhances Radiosensitivity and Delays Double-Strand Break Repair by Both non-Homologous End-Joining and Homologous Recombination. *Oncogene* (2014) 33(45):5262–73. doi: 10.1038/onc.2013.460
139. Gioeli D, Wunderlich W, Sebolt-Leopold J, Bekiranov S, Wulfkuhle JD, Petricoin EF3rd, et al. Compensatory Pathways Induced by MEK Inhibition are Effective Drug Targets for Combination Therapy Against Castration-Resistant Prostate Cancer. *Mol Cancer Ther* (2011) 10(9):1581–90. doi: 10.1158/1535-7163.MCT-10-1033
140. Ciccarelli C, Di Rocco A, Gravina GL, Mauro A, Festuccia C, Del Fattore A, et al. Disruption of MEK/ERK/c-Myc Signaling Radiosensitizes Prostate Cancer Cells In Vitro and *In Vivo*. *J Cancer Res Clin Oncol* (2018) 144 (9):1685–99. doi: 10.1007/s00432-018-2696-3
141. Dayyani F, Parikh NU, Varkaris AS, Song JH, Moorthy S, Chatterji T, et al. Combined Inhibition of IGF-1r/IR and Src Family Kinases Enhances Antitumor Effects in Prostate Cancer by Decreasing Activated Survival Pathways. *PLos One* (2012) 7(12):e51189. doi: 10.1371/journal.pone.0051189
142. Park SI, Zhang J, Phillips KA, Araujo JC, Najjar AM, Volgin AY, et al. Targeting SRC Family Kinases Inhibits Growth and Lymph Node Metastases of Prostate Cancer in an Orthotopic Nude Mouse Model. *Cancer Res* (2008) 68(9):3323–33. doi: 10.1158/0008-5472.CAN-07-2997
143. Nam S, Kim D, Cheng JQ, Zhang S, Lee JH, Buettner R, et al. Action of the Src Family Kinase Inhibitor, Dasatinib (BMS-354825), on Human Prostate Cancer Cells. *Cancer Res* (2005) 65(20):9185–9. doi: 10.1158/0008-5472.CAN-05-1731
144. Rice L, Lepler S, Pampo C, Siemann DW. Impact of the SRC Inhibitor Dasatinib on the Metastatic Phenotype of Human Prostate Cancer Cells. *Clin Exp Metastasis* (2012) 29(2):133–42. doi: 10.1007/s10585-011-9436-2
145. Liu Y, Karaca M, Zhang Z, Gioeli D, Earp HS, Whang YE, et al. Dasatinib Inhibits Site-Specific Tyrosine Phosphorylation of Androgen Receptor by Ack1 and Src Kinases. *Oncogene* (2010) 29(22):3208–16. doi: 10.1038/onc.2010.103
146. Chakraborty G, Patail NK, Hirani R, Nandakumar S, Mazzu YZ, Yoshikawa Y, et al. Attenuation of SRC Kinase Activity Augments PARP Inhibitor-Mediated Synthetic Lethality in BRCA2-Altered Prostate Tumors. *Clin Cancer Res* (2021) 27(6):1792–806. doi: 10.1158/1078-0432.CCR-20-2483
147. Araujo JC, Poblenz A, Corn P, Parikh NU, Starbuck MW, Thompson JT, et al. Dasatinib Inhibits Both Osteoclast Activation and Prostate Cancer PC-3-Cell-Induced Osteoclast Formation. *Cancer Biol Ther* (2009) 8(22):2153–9. doi: 10.4161/cbt.8.22.9770
148. Chang YM, Bai L, Liu S, Yang JC, Kung HJ, Evans CP. Src Family Kinase Oncogenic Potential and Pathways in Prostate Cancer as Revealed by AZD0530. *Oncogene* (2008) 27(49):6365–75. doi: 10.1038/onc.2008.250
149. Yang JC, Bai L, Yap S, Gao AC, Kung HJ, Evans CP, et al. Effect of the Specific Src Family Kinase Inhibitor Saracatinib on Osteolytic Lesions Using the PC-3 Bone Model. *Mol Cancer Ther* (2010) 9(6):1629–37. doi: 10.1158/1535-7163.MCT-09-1058
150. Rabbani SA, Valentino ML, Arakelian A, Ali S, Boschelli F. SKI-606 (Bosutinib) Blocks Prostate Cancer Invasion, Growth, and Metastasis *In Vitro* and *In Vivo* Through Regulation of Genes Involved in Cancer Growth and Skeletal Metastasis. *Mol Cancer Ther* (2010) 9(5):1147–57. doi: 10.1158/1535-7163.MCT-09-0962
151. Dai Y, Siemann DW. BMS-777607, a Small-Molecule Met Kinase Inhibitor, Suppresses Hepatocyte Growth Factor-Stimulated Prostate Cancer Metastatic Phenotype In Vitro. *Mol Cancer Ther* (2010) 9(6):1554–61. doi: 10.1158/1535-7163.MCT-10-0359
152. Dai Y, Siemann DW. Constitutively Active C-Met Kinase in PC-3 Cells is Autocrine-Independent and can be Blocked by the Met Kinase Inhibitor BMS-777607. *BMC Cancer* (2012) 12:198. doi: 10.1186/1471-2407-12-198
153. Witt K, Evans-Axelsson S, Lundqvist A, Johansson M, Bjartell A, Hellsten R. Inhibition of STAT3 Augments Antitumor Efficacy of Anti-CTLA-4 Treatment Against Prostate Cancer. *Cancer Immunol Immunother* (2021) 70(11):3155–66. doi: 10.1007/s00262-021-02915-6
154. Yun S, Lee YJ, Choi J, Kim ND, Han DC, Kwon BM. Acacetin Inhibits the Growth of STAT3-Activated DU145 Prostate Cancer Cells by Directly Binding to Signal Transducer and Activator of Transcription 3 (Stat3). *Molecules* (2021) 26(20):6204. doi: 10.3390/molecules26206204
155. Canesin G, Maggio V, Palominos M, Stiehm A, Contreras HR, Castellón EA, et al. STAT3 Inhibition With Galiellalactone Effectively Targets the Prostate Cancer Stem-Like Cell Population. *Sci Rep* (2020) 10(1):13958. doi: 10.1038/s41598-020-70948-5
156. Canesin G, Evans-Axelsson S, Hellsten R, Sterner O, Krzyzanowska A, Andersson T, et al. The STAT3 Inhibitor Galiellalactone Effectively Reduces Tumor Growth and Metastatic Spread in an Orthotopic Xenograft Mouse Model of Prostate Cancer. *Eur Urol* (2016) 69(3):400–4. doi: 10.1016/j.eururo.2015.06.016
157. Thaper D, Vahid S, Kaur R, Kumar S, Nouruzi S, Bishop JL, et al. Galiellalactone Inhibits the STAT3/AR Signaling Axis and Suppresses Enzalutamide-Resistant Prostate Cancer. *Sci Rep* (2018) 8(1):17307. doi: 10.1038/s41598-018-35612-z
158. Civenni G, Longoni N, Costales P, Dallavalle C, García Inclán C, Albino D, et al. EC-70124, a Novel Glycosylated Indolocarbazole Multikinase Inhibitor, Reverts Tumorigenic and Stem Cell Properties in Prostate Cancer by Inhibiting STAT3 and NF-κb. *Mol Cancer Ther* (2016) 15(5):806–18. doi: 10.1158/1535-7163.MCT-15-0791
159. Feiersinger GE, Trattnig K, Leitner PD, Guggenberger F, Oberhuber A, Peer S, et al. Olaparib is Effective in Combination With, and as Maintenance Therapy After, First-Line Endocrine Therapy in Prostate Cancer Cells. *Mol Oncol* (2018) 12(4):561–76. doi: 10.1002/1878-0261.12185
160. Li L, Karanika S, Yang G, Wang J, Park S, Broom BM, et al. Androgen Receptor Inhibitor-Induced "BRCAness" and PARP Inhibition are Synthetically Lethal for Castration-Resistant Prostate Cancer. *Sci Signaling* (2017) 10(480):eaam7479. doi: 10.1126/scisignal.aam7479
161. Zhang W, Liu B, Wu W, Li L, Broom BM, Basourakos SP, et al. Targeting the MYCN-PARP-DNA Damage Response Pathway in Neuroendocrine Prostate Cancer. *Clin Cancer Res* (2018) 24(3):696–707. doi: 10.1158/1078-0432.CCR-17-1872
162. Gani C, Coackley C, Kumareswaran R, Schütze C, Krause M, Zafarana G, et al. *In Vivo* Studies of the PARP Inhibitor, AZD-2281, in Combination

With Fractionated Radiotherapy: An Exploration of the Therapeutic Ratio. *Radiother Oncol* (2015) 116(3):486–94. doi: 10.1016/j.radonc.2015.08.003
163. Barreto-Andrade JC, Efimova EV, Mauceri HJ, Beckett MA, Sutton HG, Darga TE, et al. Response of Human Prostate Cancer Cells and Tumors to Combining PARP Inhibition With Ionizing Radiation. *Mol Cancer Ther* (2011) 10(7):1185–93. doi: 10.1158/1535-7163.MCT-11-0061
164. Yin L, Liu Y, Peng Y, Peng Y, Yu X, Gao Y, et al. PARP Inhibitor Veliparib and HDAC Inhibitor SAHA Synergistically Co-Target the UHRF1/BRCA1 DNA Damage Repair Complex in Prostate Cancer Cells. *J Exp Clin Cancer Res* (2018) 37(1):153. doi: 10.1186/s13046-018-0810-7
165. Sargazi S, Saravani R, Zavar Reza J, Jaliani HZ, Mirinejad S, Rezaei Z, et al. Induction of Apoptosis and Modulation of Homologous Recombination DNA Repair Pathway in Prostate Cancer Cells by the Combination of AZD2461 and Valproic Acid. *Excli J* (2019) 18:485–98. doi: 10.17179/excli2019-1098
166. Sargazi S, Saravani R, Zavar Reza J, Zarei Jaliani H, Galavi H, Moudi M, et al. Novel Poly(Adenosine Diphosphate-Ribose) Polymerase (PARP) Inhibitor, AZD2461, Down-Regulates VEGF and Induces Apoptosis in Prostate Cancer Cells. *Iran BioMed J* (2019) 23(5):312–23. doi: 10.29252/ibj.23.5.2
167. Chatterjee P, Choudhary GS, Sharma A, Singh K, Heston WD, Ciezki J, et al. PARP Inhibition Sensitizes to Low Dose-Rate Radiation TMPRSS2-ERG Fusion Gene-Expressing and PTEN-Deficient Prostate Cancer Cells. *PLos One* (2013) 8(4):e60408. doi: 10.1371/journal.pone.0060408
168. Cattrini C, Capaia M, Boccardo F, Barboro P. Etoposide and Topoisomerase II Inhibition for Aggressive Prostate Cancer: Data From a Translational Study. *Cancer Treat Res Commun* (2020) 25:100221. doi: 10.1016/j.ctarc.2020.100221
169. Hanahan D, Robert A. Weinberg, Hallmarks of Cancer: The Next Generation. *Cell* (2011) 144(5):646–74. doi: 10.1016/j.cell.2011.02.013
170. Naveja JJ, Dueñas-González A, Medina-Franco JL. Chapter 12 - Drug Repurposing for Epigenetic Targets Guided by Computational Methods. In: JL Medina-Franco, editor. *Epi-Informatics*. Boston: Academic Press (2016). p. 327–57.
171. Cheng H, Tang S, Lian X, Meng H, Gu X, Jiang J, et al. The Differential Antitumor Activity of 5-Aza-2'-Deoxycytidine in Prostate Cancer DU145, 22RV1, and LNCaP Cells. *J Cancer* (2021) 12(18):5593–604. doi: 10.7150/jca.56709
172. Gravina GL, Marampon F, Sanità P, Mancini A, Colapietro A, Scarsella L, et al. Increased Expression and Activity of P75ntr are Crucial Events in Azacitidine-Induced Cell Death in Prostate Cancer. *Oncol Rep* (2016) 36 (1):125–30. doi: 10.3892/or.2016.4832
173. Moreira-Silva F, Camilo V, Gaspar V, Mano JF, Henrique R, Jeronimo C. Repurposing Old Drugs Into New Epigenetic Inhibitors: Promising Candidates for Cancer Treatment? *Pharmaceutics* (2020) 12(5):410. doi: 10.3390/pharmaceutics12050410
174. Civenni G, Bosotti R, Timpanaro A, Vàzquez R, Merulla J, Pandit S, et al. Epigenetic Control of Mitochondrial Fission Enables Self-Renewal of Stem-Like Tumor Cells in Human Prostate Cancer. *Cell Metab* (2019) 30(2):303–18.e6. doi: 10.1016/j.cmet.2019.05.004
175. Bauer K, Berghoff AS, Preusser M, Heller G, Zielinski CC, Valent P, et al. Degradation of BRD4 - a Promising Treatment Approach Not Only for Hematologic But Also for Solid Cancer. *Am J Cancer Res* (2021) 11(2):530–45.
176. Wang L, Xu M, Kao CY, Tsai SY, Tsai MJ. Small Molecule JQ1 Promotes Prostate Cancer Invasion *via* BET-Independent Inactivation of FOXA1. *J Clin Invest* (2020) 130(4):1782–92. doi: 10.1172/JCI126327
177. Chan SC, Selth LA, Li Y, Nyquist MD, Miao L, Bradner JE, et al. Targeting Chromatin Binding Regulation of Constitutively Active AR Variants to Overcome Prostate Cancer Resistance to Endocrine-Based Therapies. *Nucleic Acids Res* (2015) 43(12):5880–97. doi: 10.1093/nar/gkv262
178. Tan Y, Wang L, Du Y, Liu X, Chen Z, Weng X, et al. Inhibition of BRD4 Suppresses Tumor Growth in Prostate Cancer *via* the Enhancement of FOXO1 Expression. *Int J Oncol* (2018) 53(6):2503–17. doi: 10.3892/ijo.2018.4577
179. Gao L, Schwartzman J, Gibbs A, Lisac R, Kleinschmidt R, Wilmot B, et al. Androgen Receptor Promotes Ligand-Independent Prostate Cancer Progression Through C-Myc Upregulation. *PLos One* (2013) 8(5):e63563. doi: 10.1371/journal.pone.0063563
180. Welti J, Sharp A, Yuan W, Dolling D, Nava Rodrigues D, Figueiredo I, et al. Targeting Bromodomain and Extra-Terminal (BET) Family Proteins in Castration-Resistant Prostate Cancer (CRPC). *Clin Cancer Res* (2018) 24 (13):3149–62. doi: 10.1158/1078-0432.CCR-17-3571
181. Mao W, Ghasemzadeh A, Freeman ZT, Obradovic A, Chaimowitz MG, Nirschl TR, et al. Immunogenicity of Prostate Cancer is Augmented by BET Bromodomain Inhibition. *J Immunother Cancer* (2019) 7(1):277–7. doi: 10.1186/s40425-019-0758-y
182. Liu K, Zhou Z, Gao H, Yang F, Qian Y, Jin H, et al. JQ1, a BET-Bromodomain Inhibitor, Inhibits Human Cancer Growth and Suppresses PD-L1 Expression. *Cell Biol Int* (2019) 43(6):642–50. doi: 10.1002/cbin.11139
183. Xiang Q, Zhang Y, Li J, Xue X, Wang C, Song M, et al. Y08060: A Selective BET Inhibitor for Treatment of Prostate Cancer. *ACS Med Chem Lett* (2018) 9(3):262–7. doi: 10.1021/acsmedchemlett.8b00003
184. Xu X, Zhu X, Liu F, Lu W, Wang Y, Yu J. The Effects of Histone Crotonylation and Bromodomain Protein 4 on Prostate Cancer Cell Lines. *Trans Androl Urol* (2021) 10(2):900–14. doi: 10.21037/tau-21-53
185. Shen G, Chen J, Zhou Y, Wang Z, Ma Z, Xu C, et al. AZD5153 Inhibits Prostate Cancer Cell Growth in Vitro and in Vivo. *Cell Physiol Biochem* (2018) 50(2):798–809. doi: 10.1159/000494244
186. Hu R, Wang WL, Yang YY, Hu XT, Wang QW, Zuo WQ, et al. Identification of a Selective BRD4 PROTAC With Potent Antiproliferative Effects in AR-Positive Prostate Cancer Based on a Dual BET/PLK1 Inhibitor. *Eur J Med Chem* (2022) 227:113922. doi: 10.1016/j.ejmech.2021.113922
187. Attwell S CE, Jahagirdar R, Kharenko O, Norek K, Tsujikawa L, Calosing C, et al. (2015). The Clinical Candidate ZEN-3694, a Novel BET Bromodomain Inhibitor, is Efficacious in the Treatment of a Variety of Solid Tumor and Hematological Malignancies, Alone or in Combination With Several Standard of Care and Targeted Therapies, in: Molecular Targets And Cancer Therapeutics, John B, Hynes veterans memorial Convention center Boston, MA.
188. Kim D-H, Sun D, Storck WK, Welker Leng K, Jenkins C, Coleman DJ, et al. BET Bromodomain Inhibition Blocks an AR-Repressed, E2F1-Activated Treatment-Emergent Neuroendocrine Prostate Cancer Lineage Plasticity Program. *Clin Cancer Res* (2021) 27(17):4923. doi: 10.1158/1078-0432.CCR-20-4968
189. Faivre EJ, Wilcox D, Lin X, Hessler P, Torrent M, He W, et al. Exploitation of Castration-Resistant Prostate Cancer Transcription Factor Dependencies by the Novel BET Inhibitor ABBV-075. *Mol Cancer Res* (2017) 15(1):35–44. doi: 10.1158/1541-7786.MCR-16-0221
190. Faivre EJ, McDaniel KF, Albert DH, Mantena SR, Plotnik JP, Wilcox D, et al. Selective Inhibition of the BD2 Bromodomain of BET Proteins in Prostate Cancer. *Nature* (2020) 578(7794):306–10. doi: 10.1038/s41586-020-1930-8
191. Wu TB, et al. Y06014 is a Selective BET Inhibitor for the Treatment of Prostate Cancer. *Acta Pharmacol Sin* (2021) 42(12):2120–31. doi: 10.1038/s41401-021-00614-7
192. Yan Y, Ma J, Wang D, Lin D, Pang X, Wang S, et al. The Novel BET-CBP/p300 Dual Inhibitor NEO2734 is Active in SPOP Mutant and Wild-Type Prostate Cancer. *EMBO Mol Med* (2019) 11(11):e10659–9. doi: 10.15252/emmm.201910659
193. Lasko LM, Jakob CG, Edalji RP, Qiu W, Montgomery D, Digiammarino EL, et al. Discovery of a Selective Catalytic P300/CBP Inhibitor That Targets Lineage-Specific Tumours. *Nature* (2017) 550(7674):128–32. doi: 10.1038/nature24028
194. Welti J, Sharp A, Brooks N, Yuan W, McNair C, Chand SN, et al. Targeting the P300/CBP Axis in Lethal Prostate Cancer. *Cancer Discovery* (2021) 11 (5):1118–37. doi: 10.1158/2159-8290.CD-20-0751
195. Zou LJ, Xiang QP, Xue XQ, Zhang C, Li CC, Wang C, et al. Y08197 is a Novel and Selective CBP/EP300 Bromodomain Inhibitor for the Treatment of Prostate Cancer. *Acta Pharmacol Sin* (2019) 40(11):1436–47. doi: 10.1038/s41401-019-0237-5
196. Zucconi BE, Makofske JL, Meyers DJ, Hwang Y, Wu M, Kuroda MI, et al. Combination Targeting of the Bromodomain and Acetyltransferase Active Site of P300/CBP. *Biochemistry* (2019) 58(16):2133–43. doi: 10.1021/acs.biochem.9b00160

197. Kiliccioglu I, Konac E, Varol N, Gurocak S, Yucel Bilen C. Apoptotic Effects of Proteasome and Histone Deacetylase Inhibitors in Prostate Cancer Cell Lines. *Genet Mol Res* (2014) 13(2):3721–31. doi: 10.4238/2014.May.9.17
198. Zhang H, Zhao X, Liu H, Jin H, Ji Y. Trichostatin A Inhibits Proliferation of PC3 Prostate Cancer Cells by Disrupting the EGFR Pathway. *Oncol Lett* (2019) 18(1):687–93. doi: 10.3892/ol.2019.10384
199. Wang X, Xu J, Wang H, Wu L, Yuan W, Du J, et al. Trichostatin A, a Histone Deacetylase Inhibitor, Reverses Epithelial-Mesenchymal Transition in Colorectal Cancer SW480 and Prostate Cancer PC3 Cells. *Biochem Biophys Res Commun* (2015) 456(1):320–6. doi: 10.1016/j.bbrc.2014.11.079
200. Zhu S, Li Y, Zhao L, Hou P, Shangguan C, Yao R, et al. TSA-Induced JMJD2B Downregulation is Associated With Cyclin B1-Dependent Survivin Degradation and Apoptosis in LNCap Cells. *J Cell Biochem* (2012) 113 (7):2375–82. doi: 10.1002/jcb.24109
201. Pulukuri SM, Gorantla B, Knost JA, Rao JS. Frequent Loss of Cystatin E/M Expression Implicated in the Progression of Prostate Cancer. *Oncogene* (2009) 28(31):2829–38. doi: 10.1038/onc.2009.134
202. Xu Q, Liu X, Zhu S, Hu X, Niu H, Zhang X, et al. Hyper-Acetylation Contributes to the Sensitivity of Chemo-Resistant Prostate Cancer Cells to Histone Deacetylase Inhibitor Trichostatin A. *J Cell Mol Med* (2018) 22 (3):1909–22. doi: 10.1111/jcmm.13475
203. Xiao W, Graham PH, Hao J, Chang L, Ni J, Power CA, et al. Combination Therapy With the Histone Deacetylase Inhibitor LBH589 and Radiation is an Effective Regimen for Prostate Cancer Cells. *PLos One* (2013) 8(8):e74253. doi: 10.1371/journal.pone.0074253
204. Pacheco MB, Camilo V, Lopes N, Moreira-Silva F, Correia MP, Henrique R, et al. Hydralazine and Panobinostat Attenuate Malignant Properties of Prostate Cancer Cell Lines. *Pharmaceut (Basel)* (2021) 14(7):670. doi: 10.3390/ph14070670
205. Chen E, Liu N, Zhao Y, Tang M, Ou L, Wu X, et al. Panobinostat Reverses HepaCAM Gene Expression and Suppresses Proliferation by Increasing Histone Acetylation in Prostate Cancer. *Gene* (2021) 808:145977. doi: 10.1016/j.gene.2021.145977
206. Pettazzoni P, Pizzimenti S, Toaldo C, Sotomayor P, Tagliavacca L, Liu S, et al. Induction of Cell Cycle Arrest and DNA Damage by the HDAC Inhibitor Panobinostat (LBH589) and the Lipid Peroxidation End Product 4-Hydroxynonenal in Prostate Cancer Cells. *Free Radic Biol Med* (2011) 50 (2):313–22. doi: 10.1016/j.freeradbiomed.2010.11.011
207. Chuang MJ, Wu ST, Tang SH, Lai XM, Lai HC, Hsu KH, et al. The HDAC Inhibitor LBH589 Induces ERK-Dependent Prometaphase Arrest in Prostate Cancer *via* HDAC6 Inactivation and Down-Regulation. *PLos One* (2013) 8 (9):e73401. doi: 10.1371/journal.pone.0073401
208. Bruzzese F, Pucci B, Milone MR, Ciardiello C, Franco R, Chianese MI, et al. Panobinostat Synergizes With Zoledronic Acid in Prostate Cancer and Multiple Myeloma Models by Increasing ROS and Modulating Mevalonate and P38-MAPK Pathways. *Cell Death Dis* (2013) 4(10):e878. doi: 10.1038/cddis.2013.406
209. Marrocco DL, Tilley WD, Bianco-Miotto T, Evdokiou A, Scher HI, Rifkind RA, et al. Suberoylanilide Hydroxamic Acid (Vorinostat) Represses Androgen Receptor Expression and Acts Synergistically With an Androgen Receptor Antagonist to Inhibit Prostate Cancer Cell Proliferation. *Mol Cancer Ther* (2007) 6(1):51–60. doi: 10.1158/1535-7163.MCT-06-0144
210. Park SE, Kim HG, Kim DE, Jung YJ, Kim Y, Jeong SY, et al. Combination Treatment With Docetaxel and Histone Deacetylase Inhibitors Downregulates Androgen Receptor Signaling in Castration-Resistant Prostate Cancer. *Invest New Drugs* (2018) 36(2):195–205. doi: 10.1007/s10637-017-0529-x
211. Wang L, Zou X, Berger AD, Twiss C, Peng Y, Li Y, et al. Increased Expression of Histone Deacetylaces (HDACs) and Inhibition of Prostate Cancer Growth and Invasion by HDAC Inhibitor SAHA. *Am J Transl Res* (2009) 1(1):62–71.
212. Shi XY, Ding W, Li TQ, Zhang YX, Zhao SC. Histone Deacetylase (HDAC) Inhibitor, Suberoylanilide Hydroxamic Acid (SAHA), Induces Apoptosis in Prostate Cancer Cell Lines *via* the Akt/FOXO3a Signaling Pathway. *Med Sci Monit* (2017) 23:5793–802. doi: 10.12659/MSM.904597
213. Patra N, De U, Kim TH, Lee YJ, Ahn MY, Kim ND, et al. A Novel Histone Deacetylase (HDAC) Inhibitor MHY219 Induces Apoptosis *via* Up-Regulation of Androgen Receptor Expression in Human Prostate Cancer Cells. *BioMed Pharmacother* (2013) 67(5):407–15. doi: 10.1016/j.biopha.2013.01.006
214. De U, Kundu S, Patra N, Ahn MY, Ahn JH, Son JY, et al. A New Histone Deacetylase Inhibitor, MHY219, Inhibits the Migration of Human Prostate Cancer Cells *via* HDAC1. *Biomol Ther (Seoul)* (2015) 23(5):434–41. doi: 10.4062/biomolther.2015.026
215. Rana Z, Diermeier S, Walsh FP, Hanif M, Hartinger CG, Rosengren RJ, et al. Anti-Proliferative, Anti-Angiogenic and Safety Profiles of Novel HDAC Inhibitors for the Treatment of Metastatic Castration-Resistant Prostate Cancer. *Pharmaceut (Basel)* (2021) 14(10):1020. doi: 10.3390/ph14101020
216. Rana Z, Tyndall JDA, Hanif M, Hartinger CG, Rosengren RJ. Cytostatic Action of Novel Histone Deacetylase Inhibitors in Androgen Receptor-Null Prostate Cancer Cells. *Pharmaceut (Basel)* (2021) 14(2):103. doi: 10.3390/ph14020103
217. Hwang JJ, Kim YS, Kim T, Kim MJ, Jeong IG, Lee JH, et al. A Novel Histone Deacetylase Inhibitor, CG200745, Potentiates Anticancer Effect of Docetaxel in Prostate Cancer *via* Decreasing Mcl-1 and Bcl-XL. *Invest New Drugs* (2012) 30(4):1434–42. doi: 10.1007/s10637-011-9718-1
218. Richa S, Dey P, Park C, Yang J, Son JY, Park JH, et al. A New Histone Deacetylase Inhibitor, MHY4381, Induces Apoptosis *via* Generation of Reactive Oxygen Species in Human Prostate Cancer Cells. *Biomol Ther (Seoul)* (2020) 28(2):184–94. doi: 10.4062/biomolther.2019.074
219. Qi G, Lu G, Yu J, Zhao Y, Wang C, Zhang H, et al. Up-Regulation of TIF1γ by Valproic Acid Inhibits the Epithelial Mesenchymal Transition in Prostate Carcinoma Through TGF-β/Smad Signaling Pathway. *Eur J Pharmacol* (2019) 860:172551. doi: 10.1016/j.ejphar.2019.172551
220. Makarević J, Rutz J, Juengel E, Maxeiner S, Tsaur I, Chun FK, et al. Influence of the HDAC Inhibitor Valproic Acid on the Growth and Proliferation of Temsirolimus-Resistant Prostate Cancer Cells *In Vitro*. *Cancers (Basel)* (2019) 11(4):566. doi: 10.3390/cancers11040566
221. Choi ES, Han G, Park SK, Lee K, Kim HJ, Cho SD, et al. A248, a Novel Synthetic HDAC Inhibitor, Induces Apoptosis Through the Inhibition of Specificity Protein 1 and its Downstream Proteins in Human Prostate Cancer Cells. *Mol Med Rep* (2013) 8(1):195–200. doi: 10.3892/mmr.2013.1481
222. Wu YW, Hsu KC, Lee HY, Huang TC, Lin TE, Chen YL, et al. A Novel Dual HDAC6 and Tubulin Inhibitor, MPT0B451, Displays Anti-Tumor Ability in Human Cancer Cells in Vitro and in Vivo. *Front Pharmacol* (2018) 9:205. doi: 10.3389/fphar.2018.00205
223. Hu WY, Xu L, Chen B, Ou S, Muzzarelli KM, Hu DP, et al. Targeting Prostate Cancer Cells With Enzalutamide-HDAC Inhibitor Hybrid Drug 2-75. *Prostate* (2019) 79(10):1166–79. doi: 10.1002/pros.23832
224. Kim J, Lee Y, Lu X, Song B, Fong KW, Cao Q, et al. Polycomb- and Methylation-Independent Roles of EZH2 as a Transcription Activator. *Cell Rep* (2018) 25(10):2808–2820.e4. doi: 10.1016/j.celrep.2018.11.035
225. Morel KL, Sheahan AV, Burkhart DL, Baca SC, Boufaied N, Liu Y, et al. EZH2 Inhibition Activates a dsRNA-STING-Interferon Stress Axis That Potentiates Response to PD-1 Checkpoint Blockade in Prostate Cancer. *Nat Cancer* (2021) 2(4):444–56. doi: 10.1038/s43018-021-00185-w
226. Verma SK, Tian X, LaFrance LV, Duquenne C, Suarez DP, Newlander KA, et al. Identification of Potent, Selective, Cell-Active Inhibitors of the Histone Lysine Methyltransferase Ezh2. *ACS Med Chem Lett* (2012) 3(12):1091–6. doi: 10.1021/ml3003346
227. Li X, Gera L, Zhang S, Chen Y, Lou L, Wilson LM, et al. Pharmacological Inhibition of Noncanonical EED-EZH2 Signaling Overcomes Chemoresistance in Prostate Cancer. *Theranostics* (2021) 11(14):6873–90. doi: 10.7150/thno.49235
228. Bai Y, Zhang Z, Cheng L, Wang R, Chen X, Kong Y, et al. Inhibition of Enhancer of Zeste Homolog 2 (EZH2) Overcomes Enzalutamide Resistance in Castration-Resistant Prostate Cancer. *J Biol Chem* (2019) 294(25):9911–23. doi: 10.1074/jbc.RA119.008152
229. Shankar E, Franco D, Iqbal O, Moreton S, Kanwal R, Gupta S. Dual Targeting of EZH2 and Androgen Receptor as a Novel Therapy for Castration-Resistant Prostate Cancer. *Toxicol Appl Pharmacol* (2020) 404:115200. doi: 10.1016/j.taap.2020.115200
230. Kong Y, Zhang Y, Mao F, Zhang Z, Li Z, Wang R, et al. Inhibition of EZH2 Enhances the Antitumor Efficacy of Metformin in Prostate Cancer. *Mol Cancer Ther* (2020) 19(12):2490–501. doi: 10.1158/1535-7163.MCT-19-0874

231. Wu C, Jin X, Yang J, Yang Y, He Y, Ding L, et al. Inhibition of EZH2 by Chemo- and Radiotherapy Agents and Small Molecule Inhibitors Induces Cell Death in Castration-Resistant Prostate Cancer. *Oncotarget* (2016) 7 (3):3440–52. doi: 10.18632/oncotarget.6497
232. Etani T, Naiki T, Naiki-Ito A, Suzuki T, Iida K, Nozaki S, et al. NCL1, A Highly Selective Lysine-Specific Demethylase 1 Inhibitor, Suppresses Castration-Resistant Prostate Cancer Growth *via* Regulation of Apoptosis and Autophagy. *J Clin Med* (2019) 8(4):442. doi: 10.3390/jcm8040442
233. Etani T, Suzuki T, Naiki T, Naiki-Ito A, Ando R, Iida K, et al. NCL1, a Highly Selective Lysine-Specific Demethylase 1 Inhibitor, Suppresses Prostate Cancer Without Adverse Effect. *Oncotarget* (2015) 6(5):2865–78. doi: 10.18632/oncotarget.3067
234. Gupta S, Weston A, Bearrs J, Thode T, Neiss A, Soldi R, et al. Reversible Lysine-Specific Demethylase 1 Antagonist HCI-2509 Inhibits Growth and Decreases C-MYC in Castration- and Docetaxel-Resistant Prostate Cancer Cells. *Prostate Cancer Prostatic Dis* (2016) 19(4):349–57. doi: 10.1038/pcan.2016.21
235. Fialova B, Luzna P, Gursky J, Langova K, Kolar Z, Trtkova KS. Epigenetic Modulation of AR Gene Expression in Prostate Cancer DU145 Cells With the Combination of Sodium Butyrate and 5'-Aza-2'-Deoxycytidine. *Oncol Rep* (2016) 36(4):2365–74. doi: 10.3892/or.2016.5000
236. Liu T, Qiu X, Zhao X, Yang R, Lian H, Qu F, et al. Hypermethylation of the SPARC Promoter and its Prognostic Value for Prostate Cancer. *Oncol Rep* (2018) 39(2):659–66. doi: 10.3892/or.2017.6121
237. Wang X, Gao H, Ren L, Gu J, Zhang Y, Zhang Y. Demethylation of the miR-146a Promoter by 5-Aza-2'-Deoxycytidine Correlates With Delayed Progression of Castration-Resistant Prostate Cancer. *BMC Cancer* (2014) 14:308. doi: 10.1186/1471-2407-14-308
238. Tian J, Lee SO, Liang L, Luo J, Huang CK, Li L, et al. Targeting the Unique Methylation Pattern of Androgen Receptor (AR) Promoter in Prostate Stem/Progenitor Cells With 5-Aza-2'-Deoxycytidine (5-AZA) Leads to Suppressed Prostate Tumorigenesis. *J Biol Chem* (2012) 287(47):39954–66. doi: 10.1074/jbc.M112.395574
239. Patra A, Deb M, Dahiya R, Patra SK. 5-Aza-2'-Deoxycytidine Stress Response and Apoptosis in Prostate Cancer. *Clin Epigenet* (2011) 2 (2):339–48. doi: 10.1007/s13148-010-0019-x
240. Chiam K, Centenera MM, Butler LM, Tilley WD, Bianco-Miotto T. GSTP1 DNA Methylation and Expression Status is Indicative of 5-Aza-2'-Deoxycytidine Efficacy in Human Prostate Cancer Cells. *PLos One* (2011) 6(9):e25634. doi: 10.1371/journal.pone.0025634
241. Gravina GL, Marampon F, Di Staso M, Bonfili P, Vitturini A, Jannini EA, et al. 5-Azacitidine Restores and Amplifies the Bicalutamide Response on Preclinical Models of Androgen Receptor Expressing or Deficient Prostate Tumors. *Prostate* (2010) 70(11):1166–78. doi: 10.1002/pros.21151
242. Graça I, Sousa EJ, Baptista T, Almeida M, Ramalho-Carvalho J, Palmeira C, et al. Anti-Tumoral Effect of the non-Nucleoside DNMT Inhibitor RG108 in Human Prostate Cancer Cells. *Curr Pharm Design* (2014) 20(11):1803–11. doi: 10.2174/13816128113199990516
243. Chou YW, Chaturvedi NK, Ouyang S, Lin FF, Kaushik D, Wang J, et al. Histone Deacetylase Inhibitor Valproic Acid Suppresses the Growth and Increases the Androgen Responsiveness of Prostate Cancer Cells. *Cancer Lett* (2011) 311(2):177–86. doi: 10.1016/j.canlet.2011.07.015
244. Stultz J, Fong L. How to Turn Up the Heat on the Cold Immune Microenvironment of Metastatic Prostate Cancer. *Prostate Cancer Prostatic Dis* (2021) 24(3):697–717. doi: 10.1038/s41391-021-00340-5
245. Powles T, Yuen KC, Gillessen S, Kadel EE, Rathkopf D, Matsubara N, et al. Atezolizumab With Enzalutamide Versus Enzalutamide Alone in Metastatic Castration-Resistant Prostate Cancer: A Randomized Phase 3 Trial. *Nat Med* (2022) 28(1):144–53. doi: 10.1038/s41591-021-01600-6
246. Graff JN, Beer TM, Alumkal JJ, Slottke RE, Redmond WL, Thomas GV, et al. A Phase II Single-Arm Study of Pembrolizumab With Enzalutamide in Men With Metastatic Castration-Resistant Prostate Cancer Progressing on Enzalutamide Alone. *J ImmunoTher Cancer* (2020) 8(2):e000642. doi: 10.1136/jitc-2020-000642
247. Hansen AR, Massard C, Ott PA, Haas NB, Lopez JS, Ejadi S, et al. Pembrolizumab for Advanced Prostate Adenocarcinoma: Findings of the KEYNOTE-028 Study. *Ann Oncol* (2018) 29(8):1807–13. doi: 10.1093/annonc/mdy232
248. Graff JN, Alumkal JJ, Drake CG, Thomas GV, Redmond WL, Farhad M, et al. Early Evidence of Anti-PD-1 Activity in Enzalutamide-Resistant Prostate Cancer. *Oncotarget* (2016) 7(33):52810–7. doi: 10.18632/oncotarget.10547
249. Antonarakis ES, Piulats JM, Gross-Goupil M, Goh J, Ojamaa K, Hoimes CJ, et al. Pembrolizumab for Treatment-Refractory Metastatic Castration-Resistant Prostate Cancer: Multicohort, Open-Label Phase II KEYNOTE-199 Study. *J Clin Oncol* (2020) 38(5):395–405. doi: 10.1200/JCO.19.01638
250. Yu EY, Kolinsky MP, Berry WR, Retz M, Mourey L, Piulats JM, et al. Pembrolizumab Plus Docetaxel and Prednisone in Patients With Metastatic Castration-Resistant Prostate Cancer: Long-Term Results From the Phase 1b/2 KEYNOTE-365 Cohort B Study. *Eur Urol* (2022) S0302-2838(22)01665–7. doi: 10.1016/j.eururo.2022.02.023
251. Lin H, Liu Q, Zeng X, Yu W, Xu G. Pembrolizumab With or Without Enzalutamide in Selected Populations of Men With Previously Untreated Metastatic Castration-Resistant Prostate Cancer Harbouring Programmed Cell Death Ligand-1 Staining: A Retrospective Study. *BMC Cancer* (2021) 21 (1):399. doi: 10.1186/s12885-021-08156-1
252. Kantoff PW, Higano CS, Shore ND, Berger ER, Small EJ, Penson DF, et al. Sipuleucel-T Immunotherapy for Castration-Resistant Prostate Cancer. *N Engl J Med* (2010) 363(5):411–22. doi: 10.1056/NEJMoa1001294
253. Kwon ED, Drake CG, Scher HI, Fizazi K, Bossi A, van denEertwegh AJ, et al. Ipilimumab Versus Placebo After Radiotherapy in Patients With Metastatic Castration-Resistant Prostate Cancer That had Progressed After Docetaxel Chemotherapy (CA184-043): A Multicentre, Randomised, Double-Blind, Phase 3 Trial. *Lancet Oncol* (2014) 15(7):700–12. doi: 10.1016/S1470-2045(14)70189-5
254. Beer TM, Kwon ED, Drake CG, Fizazi K, Logothetis C, Gravis G, et al. Randomized, Double-Blind, Phase III Trial of Ipilimumab Versus Placebo in Asymptomatic or Minimally Symptomatic Patients With Metastatic Chemotherapy-Naive Castration-Resistant Prostate Cancer. *J Clin Oncol* (2017) 35(1):40–7. doi: 10.1200/JCO.2016.69.1584
255. Tollefson M, Karnes RJ, Thompson RH, Granberg C, Hillman D, Breau R, et al. 668 A RANDOMIZED PHASE II STUDY OF IPILIMUMAB WITH ANDROGEN ABLATION COMPARED WITH ANDROGEN ABLATION ALONE IN PATIENTS WITH ADVANCED PROSTATE CANCER. *J Urol* (2010) 183(4S):e261–1. doi: 10.1016/j.juro.2010.02.1055
256. Slovin SF, Higano CS, Hamid O, Tejwani S, Harzstark A, Alumkal JJ, et al. Ipilimumab Alone or in Combination With Radiotherapy in Metastatic Castration-Resistant Prostate Cancer: Results From an Open-Label, Multicenter Phase I/II Study. *Ann Oncol* (2013) 24(7):1813–21. doi: 10.1093/annonc/mdt107
257. McNeel DG, Smith HA, Eickhoff JC, Lang JM, Staab MJ, Wilding G, et al. Phase I Trial of Tremelimumab in Combination With Short-Term Androgen Deprivation in Patients With PSA-Recurrent Prostate Cancer. *Cancer Immunol Immunother* (2012) 61(7):1137–47. doi: 10.1007/s00262-011-1193-1

Conflict of Interest: The authors declare that the research was conducted in the absence of any commercial or financial relationships that could be construed as a potential conflict of interest.

Advantages of publishing in Frontiers

OPEN ACCESS
Articles are free to read for greatest visibility and readership

FAST PUBLICATION
Around 90 days from submission to decision

HIGH QUALITY PEER-REVIEW
Rigorous, collaborative, and constructive peer-review

TRANSPARENT PEER-REVIEW
Editors and reviewers acknowledged by name on published articles

Frontiers
Avenue du Tribunal-Fédéral 34
1005 Lausanne | Switzerland

Visit us: www.frontiersin.org
Contact us: frontiersin.org/about/contact

REPRODUCIBILITY OF RESEARCH
Support open data and methods to enhance research reproducibility

DIGITAL PUBLISHING
Articles designed for optimal readership across devices

FOLLOW US
@frontiersin

IMPACT METRICS
Advanced article metrics track visibility across digital media

EXTENSIVE PROMOTION
Marketing and promotion of impactful research

LOOP RESEARCH NETWORK
Our network increases your article's readership